STRUCTURAL EVOLUTION AND NEOTECTONICS OF THE RHINE-BRESSE TRANSFER ZONE

Inauguraldissertation

zur

Erlangung der Würde eines Doktors der Philosophie

vorgelegt der

Philosophisch-Naturwissenschaftlichen Fakultät der Universität Basel

von

Herfried Madritsch

aus

Lienz, Österreich

Basel, Juni 2008

Genehmigt von der Philosophisch-Naturwissenschaftlichen Fakultät auf Antrag von

Prof. Dr. Olivier Bellier
Centre Européen de Recherche et d'Enseignement des Géosciences de l´Environnement, Aix-en-Provence

Prof. Dr. Olivier Fabbri
UMR Chrono-Environnement, Universitè de Franche Comté

Prof. Dr. Olivier Lacombe
Laboratoire de Tectonique, Université Pierre et Marie Curie - Paris VI

PD. Dr. Jon Mosar
Département de géosciences, Université de Fribourg

PD. Dr. Frank Preusser
Institut für Geologie, Universität Bern

Prof. Dr. Stefan Schmid
Institut für Geologie und Paläontologie, Universität Basel

Prof. Dr. Stefan Schmid
(Fakultätsverantwortlicher)

Basel Juni, 2008

Basel, 24. Juni 2008

Prof. Dr. Hans-Peter Hauri
(Dekan der Philosophisch-Naturwissenschaftlichen Fakultät)

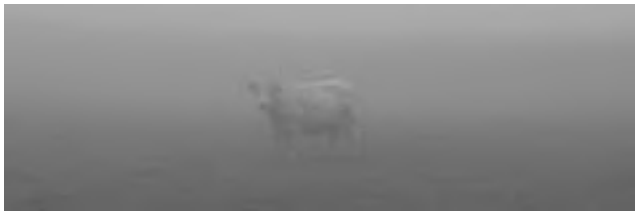

“It’s a dirty job but someone has to do it”

Faith no more 1985

Abstract:

This thesis was carried out within the framework of the international EUCOR-URGENT project and represents a joint study (co-tutelle) between the Universities of Basel and Besançon. It is devoted to the structural evolution and present-day tectonic activity of the region of Franche Comté in Eastern France, a region that is located at the intersection between the Jura fold-and-thrust belt representing the front of Alpine shortening and the immediately adjacent northwestern foreland, characterized by the intra-continental Rhine-Bresse Transfer Zone (RBTZ).

The formation of the RBTZ, that forms a central segment of the Paleogene European Cenozoic Rift System, involved the extensional reactivation of the Late Paleozoic Burgundy Trough System. Substantial extension occurred in Eo-Oligocene times and was achieved by ENE-WSW striking normal faults that are highly oblique to the dominant strike of the Rhine and Bresse grabens. Fission track data suggest that basement reactivation also contributed to the Eo-Oligocene exhumation of the Late Paleozoic La Serre Horst in the context of rifting. Basement reactivation in connection with the formation of the RBTZ resulted in complex fault patterns and local stress field perturbations, especially in the surroundings of the pre-existing Paleozoic horst structure.

During Late Miocene to Early Pliocene times the northwestern most segment of the thin-skinned Jura fold-and-thrust belt, the Besançon Zone, encroached onto the RBTZ. Moreover, NW-SE directed foreland compression caused thick-skinned, transpressive reactivation of the RBTZ that started by Late Pliocene times at the earliest. Present-day seismicity in the RBTZ indicates that thick-skinned tectonics are still active and may reflect ongoing tectonic underplating in the northwestern Alpine foreland.

Post-Pliocene relative rock uplift is recorded along the RBTZ by differential erosion of the Middle Pliocene Sundgau-Forêt de Chaux Gravels on a regional scale. Uplifted remnants of this gravel plain, identified by heavy mineral analyses, permitted to determine a latest Pliocene to recent minimum regional rock uplift rate of 0.05 +/- 0.02 mm/yr. A reconstruction of the Plio-Pleistocene drainage basin evolution of the Ognon and Doubs Rivers revealed that this relative rock uplift is still ongoing and most likely partly driven by the inversion of the RBTZ. Pleistocene folding near Besançon is evident from differentially up warped paleo-meanders along the Citadelle Anticline. This deformation is apparently enhanced by the bedrock incision of the Doubs River and associated with higher local uplift rates of 0.17 +/- 0.03 mm/yr.

The results of this study vividly illustrate the dynamic processes that control the progressive evolution of continental collisional forelands. It appears that while the evolution of the RBTZ was largely controlled by the reactivation of pre-existing structures, its present tectonic activity is to some extent also controlled by surface processes and involves positive feedbacks between large-scale uplift, enhanced erosion and active deformation.

Résumé:

Cette thèse a été réalisée dans le cadre du projet international EUCOR-URGENT et résulte d'une collaboration (co-tutelle) entre les universités de Bâle et de Franche-Comté. Elle est dédiée à l'évolution structurale et à l'activité tectonique actuelle de la Franche-Comté, région de l'est de la France, à l'intersection entre le front de l'orogène alpin et son avant-pays situé au nord-ouest. Le secteur d'étude est donc caractérisé par le front nord-occidental de la chaîne du Jura, plissée au Néogène, et un segment clé du système de rift cénozoïque ouest-européen, la zone de transfert fossé rhénan-fossé bressan (RTBZ) datant du Paléogène.

La formation au Paléogène de la RTBZ a induit une réactivation en extension du système de grabens fini-paléozoïques (*Burgundy Through System*). Une extension importante s'est produite à l'Eocène-Oligocène par le biais de failles normales ENE-WSW fortement obliques sur la direction dominante des fossés bressan et rhénan. Les données de traces de fission suggèrent que la réactivation du socle a également contribué à l'exhumation du massif fini-paléozoïque de la Serre à cette même époque (Eocène-Oligocène). Plus généralement, cette réactivation du socle, en parallèle avec la formation de la RTBZ, a induit des réseaux de failles à géométrie complexe et des perturbations locales des champs de contraintes, surtout à proximité des structures de horsts paléozoïques pré-existants.

Au cours du Miocène supérieur à Pléistocène inférieur, le segment le plus au nord-ouest de la chaîne plissée du Jura, nouvellement défini comme étant la zone de Besançon, s'est individualisé aux dépens de la RTBZ. De plus, et au plus tôt à partir du Pliocène supérieur, une compression dans l'avant-pays selon la direction NW-SE a induit une réactivation transpressive de type "thick-skinned" de la RTBZ. La sismicité actuelle dans la RTBZ montre que la tectonique de type "thick-skinned" est toujours active et qu'elle pourrait en fait être une conséquence d'un sous-plaquage tectonique (*underplating*) en cours dans l'avant-pays nord-ouest alpin.

L'érosion différentielle des cailloutis du Sundgau-Forêt de Chaux, plus récente que 2,9 Ma, plaide pour un soulèvement régional relatif le long de la RTBZ postérieurement au Pliocène. Les restes de cailloutis soulevés, identifiés grâce à des analyses de minéraux lourds, ont permis de mettre en évidence un soulèvement régional caractérisé, pour la période allant du Pliocène terminal à l'époque récente, par un taux minimal de 0,05 +/- 0,02 mm/an. Une reconstruction de l'évolution des bassins drainés par les rivières Ognon et Doubs montre que ce soulèvement est encore actif et qu'il serait en partie causé par l'inversion tectonique le long de la RTBZ. A proximité de Besançon, une phase de plissement pléistocène est démontrée par un soulèvement et un début de flambage des terrasses alluviales recoupant l'anticlinal de la Citadelle. Cette phase de plissement semble contrôlée, voire amplifiée, par l'incision causée par le Doubs. La déformation associée à cette érosion est caractérisée par des taux de soulèvement localement forts atteignant 0,17 +/- 0,03mm/an.

Les résultats de cette étude illustrent clairement les processus dynamiques qui contrôlent l'évolution graduelle des avant-pays de chaînes de collision. Il apparaît que, alors que l'évolution de la RTBZ est largement influencée par la réactivation de structures préexistantes, son activité tectonique actuelle est dans une certaine mesure contrôlée par des processus de surface et implique des interactions entre des soulèvements régionaux et des déformations actives amplifiées par l'érosion.

Thesis Organisation

This thesis is organized into a series of individual chapters. Four of them (chapters 2-5) will be published in international peer reviewed journals and have been, or, in case of chapter 5, will be submitted soon. Chapter 1 introduces the general topic covered by this thesis while chapter 6 will provide a summary of all the chapters. The contributions of the individual co-authors to the articles submitted in co-authorship will be specified below.

Chapter 1:

Introduction

This chapter defines the objectives and basic research questions to be addressed by this thesis. A regional geological overview is provided, as well as an outline of the general methodological approach.

Chapter 2:

Multiple fault reactivation within the intra-continental Rhine-Bresse Transfer Zone (La Serre Horst, Eastern France)

by

Herfried Madritsch, Alexandre Kounov, Stefan M. Schmid & Olivier Fabbri

Submitted to *Tectonophysics*

This chapter comprises a study that examines the exhumation history of the Late Paleozoic La Serre Horst and its relation to the structural evolution of the intra-continental Rhine-Bresse Transfer Zone that was active during Eo-Oligocene times. Thus, this chapter largely concentrates on the pre-Neogene evolution of the working area. This is crucial for understanding the later (Neogene to recent) deformation history, which is largely controlled by the reactivation of pre-existing fault patterns. The chapter results from a close cooperation with Dr. A. Kounov (Basel) and combines subsurface and brittle tectonic field investigations of the first author with Fission-Track dating from the Palaeozoic basement by Dr. Kounov.

The first author carried out all the fieldwork, as well as the analysis of the paleostress data and the subsurface data. He assisted with fission track sampling and the interpretation of the fission track ages. He wrote the main part of a first version of the manuscript. Dr. Kounov author carried out the actual fission track dating and contributed to the discussion of the data in text and figures. The third and fourth authors (Profs. S.M. Schmid from Basel and O. Fabbri from Besançon), in their function as thesis supervisors, helped with the discussions of the data and the preparation of the final version of the manuscript.

Chapter 3:

Interactions between thin- and thick-skinned tectonics
at the north western front of the Jura fold-and-thrust belt (Eastern France)

by

Herfried Madritsch, Stefan M. Schmid & Olivier Fabbri

Tectonics in press

This chapter is devoted to the structural and temporal interactions of different deformation styles that characterize the north western front of the Alpine orogen that propagated far north and into the working area in Miocene to recent times. Based on field work and subsurface data a new tectonic map was compiled and complemented by regional cross sections. Extensive paleostress analysis provides constraints on the kinematics of deformation and - along with geomorphic and geophysical data – spatial and temporal relationships between the different styles of deformation. Some of these deformation processes are still ongoing at present. Hence this chapter also discusses the neotectonic scenario and is relevant for seismic hazard assessment.

The first author carried out all the field work, as well as the paleostress analysis. He also performed the compilation and interpretation of the subsurface data and he compiled existing seismological data. Hence the main results presented, i.e. the development of the new tectonic map and the construction of the cross sections, are entirely the result of his own research efforts. The second and third authors (the thesis supervisors) provided logistical and advisory scientific help. They also assisted with the preparation of the final manuscript.

Chapter 4

Incision boosted buckling:
Field evidence from an active fold at the front of the Jura Mountains (Eastern France)

by

Herfried Madritsch, Frank Preusser, Olivier Fabbri, Fritz Schlunegger, Vincent Bichet
& Stefan M. Schmid

Submitted to *Geology*

This process-orientated chapter provides evidence for Pleistocene folding within the internal Jura Mountains for the first time by integrating structural field observations, geophysical subsurface investigations, regional paleo-topographic reconstructions and dating by Optical Stimulated Luminescence (OSL) of alluvial deposits.

The first author wrote a first version of the manuscript. He carried out most of the fieldwork. Furthermore he was responsible for OSL and heavy mineral sampling, including sample preparation in the laboratory. He also assisted the geophysical and geodetic campaigns and interpreted the data. The

second author (PD Frank Preusser, Bern) carried out the OSL-measurements, wrote the related appendix chapter and assisted in the writing process. The third author (Prof. Fabbri, Besançon) coordinated the geo-electrical campaigns and assisted the field work. The fourth author (Prof. Fritz Schlunegger, Bern) proposed a concept for the manuscript and assisted the writing processes. The fifth author (Dr. Vincent Bichet, Besançon) coordinated and carried out the geodetic measurements. The sixth author (Prof. Stefan M. Schmid, Basel) revised a final version of the manuscript.

Chapter 5:

Feedbacks between uplift, erosion and active deformation:
Geomorphic constraints from the north western front of the Jura fold-and-thrust belt

by

Herfried Madritsch, Olivier Fabbri, Eva-Maria. Hagedorn,
Frank Preusser, Stefan M. Schmid and Peter A. Ziegler

In preparation

This chapter represents a synthesis of the geomorphic investigations that were carried out during this study. It presents evidence for Post-Pliocene differential rock uplift throughout the Rhine-Bresse Transfer Zone based on paleo-topographic reconstructions and the revised analyses of alluvial terrace and drainage systems.

The first author developed the concept regarding the investigation methods. He wrote the manuscript and carried out all the field work and the Digital Elevation Model (DEM) analyses. He was also responsible for OSL and heavy mineral sampling including sample preparation. The second author (Prof. O. Fabbri, Besançon) assisted field work and provided logistical help. The third author (Dr. Eva-Maria Hagedorn, Leverkusen) carried out heavy mineral analyses and assisted the first author with the interpretation of these results. Fourth, fifth and sixth author (PD Frank Preusser, Bern; Prof. Stefan, M. Schmid, Basel; Prof. Dr. Peter Ziegler, Basel) helped during the writing process and provided the necessary knowledge on the geology of surrounding areas.

Chapter 6

Summary and conclusions

This chapter is a summary of the combined results of the thesis and outlines future research perspectives.

Content

Chapter 1
Introduction

1. Thesis motivation and objectives

This PhD study was carried out within the framework of the international EUCOR-URGENT project launched by Prof. Ziegler (Basel) and financed through a grant (ELTEM) provided to Basel University by the Staatssekretariat für Bildung und Forschung (Bern). The general goal of the EUCOR-URGENT project, and also the present PhD work, is a better understanding of the tectonic evolution of the Upper Rhine Graben and adjacent areas, with a particular focus on the neotectonic activity and associated hazards. In 1356 this densely populated region witnessed the famous earthquake of Basel, one of the strongest historical earthquakes of western central Europe (Mayer-Rosa and Cadiot, 1979).

This thesis represents a joint study (Co-Tutelle) between the Universities of Basel and Franche Comté (Besançon). It is devoted to the structural and kinematic evolution of the intracontinental Rhine-Bresse Transfer Zone that is part of the European Cenozoic Rift System and stretches for about 200km throughout the entire district of Franche Comté in Eastern France. From a geodynamic point of view this region represents a key area, as it also comprises the northwestern front of the Jura fold-and-thrust belt and therefore represents the intersection between the Alpine orogen and its adjacent foreland.

While neighboring areas, such as the Southern Upper Rhine Graben, have been intensively investigated during the last 50 years the tectonic evolution of the Rhine-Bresse Transfer Zone and the adjacent front of the Jura fold-and-thrust belt are still poorly understood. Especially the role of Paleozoic structures for the structural and kinematic Cenozoic evolution of the area is a matter of long-lasting scientific debates (Laubscher, 1970; Illies, 1972; Bergerat, 1977; Lacombe et al., 1993; Schumacher, 2002; Ustaszewski and Schmid, 2007).

The present tectonic activity (neotectonics) of the region is defined by low seismicity, which makes any seismotectonic characterization difficult (Kastrup et al., 2004). Mid- to short term geodetic surveying indicates very slow vertical and horizontal deformation rates, close to the error margin inherent to the current GPS technology (Tesauro et al., 2005). Nevertheless, the area received increased attention after the 4.8 M_L earthquake of Rigney NE of Besançon that took place on 23rd February 2004 and that still marks one of the strongest seismic events in the wider area during the last couple of years (Baer et al., 2005). Beyond this, the earthquake revealed a significant difference in the mode of tectonic faulting (thrusting to transpression) in comparison with earthquakes from the well-studied Southern Upper Rhine Graben area (strike slip and/or transtension; (Plenefisch and Bonjer, 1997; Kastrup et al., 2004; Baer et al., 2005)). This observation gave rise to new considerations and

hypotheses regarding the present day tectonics and geodynamics of the area that were tested during this investigation.

Accordingly, the aims of this study can be summed up in terms of the following three main scientific questions:

1) How did the Rhine-Bresse Transfer Zone evolve during deformations that took place during the geological past? Thereby the analysis of the role of structural inheritance of pre-existing Paleozoic basement faults during repeated reactivations is of particular relevance for better understanding the neotectonic scenario.

2) How did the Paleogene fault system of the Rhine-Bresse Transfer Zone react to the Neogene change in the stress field that occurred throughout the northwestern Alpine foreland in response to the Alpine collision? Thereby the styles of foreland deformations, in particular the questions after past or present thick- vs. thin-skinned deformations and possible interactions between these two contrasting styles, are of particular interest.

3) What is the style and faulting mode of the present-day neotectonic activity in the area west of Basel, and does it differ from that of the better-known areas around east, north or south of Basel? The existing seismotectonic and geodetic dataset so far can only poorly define the neotectonic activity in the Rhine Bresse Transfer Zone, hence tectonic geomorphology is more capable for better constraining active deformation throughout the area. In this context the thesis searches after the driving force of active tectonics and attempts to establish rates of active deformation.

These questions were addressed using a multidisciplinary and integrative approach that combines structural, geophysical, geochronological, sedimentological and geomorphic methods. This approach required intense scientific cooperation with a multinational team of specialists from the Universities of Basel, Besançon and Bern.

The results of this thesis yield new implications regarding the regional geology and neotectonics of the area. Furthermore the thesis contributes to a better overall understanding of geological processes that occur during the progressive tectonic evolution in the forelands of continental collisional orogens. It addresses a wide range of topics such as structural inheritance and fault reactivation, interactions of thick- and thin-skinned tectonics in foreland settings, coupling between active deformation and erosion and controls on alluvial terrace formation. In answering the research questions outlined above, this study also represents an important contribution for future investigations concerning seismic hazard assessment and the planning of nuclear waste disposal sites in the surroundings of the working area.

2. Methodological approach

In order to solve the defined research questions outlined above a multidisciplinary research approach was adopted.

Subsurface analysis: This analysis was carried out throughout the study area by compiling geological logs of exploration wells and by interpreting seismic reflection data that became available to an academic institution for the first time.

Structural field work: Extensive own field work was combined with a close and detailed analysis of existing geological maps. The results of this approach allowed to develop a new tectonic map of the study, area complemented by several regional structural cross sections that also integrated the analysis of the subsurface data.

Paleostress analysis: The kinematic and structural evolution of the area throughout the Cenozoic was revealed and characterized by the extensive analysis of the manifestations of brittle deformation (fault slip data) allowing for paleostress and paleo-kinematic reconstructions. Newly available fission track ages from the Paleozoic basement and its cover, cropping out in the La Serre Horst, were also integrated into this analysis of the tectonic evolution of the working area.

Quantitative geomorphology, heavy mineral analysis and dating by optical stimulated luminescence dating (OLS): Digital elevation models were used to study the geomorphology of the area, focusing on the Mid-Pliocene to Pleistocene drainage pattern evolution and incision history. Terrace mapping in the field was complemented by heavy mineral analysis and OSL-dating. The resulting paleo-topographic reconstructions and revised terrace maps, together with a compilation of seismological data allowed to better constrain the most recent tectonic activity of the area.

3. Tectonic Setting

The study area is located in Eastern France where the northwestern front of Alpine orogen, formed by the Mio- Pliocene Jura fold-and-thrust belt, meets the adjacent only weakly or non-deformed foreland, pre-structured by the European Cenozoic Rift System (ECRIS) that formed in Eo- Oligocene times (Figure 1).

The European Cenozoic Rift System dissects the European continent over a distance of approximately 1100 km, from the North Sea coast to the western Mediterranean (Ziegler, 1992). The Upper Rhine Graben (URG) and the Bresse Graben (BG) represent the central segments of this rift system (Fig. 1). Both are kinematically interconnected by the approximately 200km long ENE-WSW striking intra- continental Rhine-Bresse-Transfer Zone (RBTZ). The northern part of the RBTZ cuts

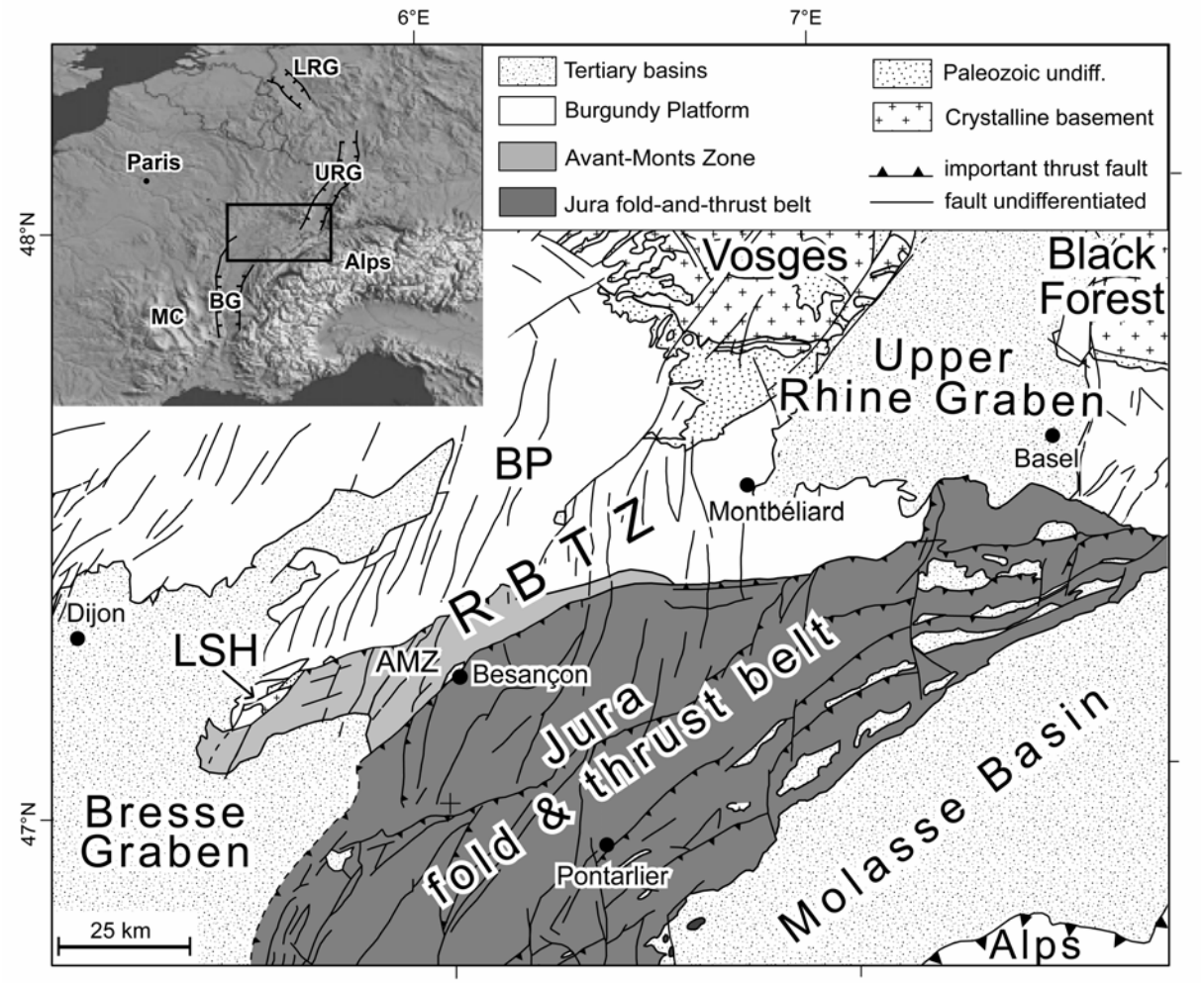

Figure 1: Tectonic map of the study area (after (Chauve et al., 1980)). AMZ: Avant-Monts Zone; BG: Bresse Graben; BP: Burgundy Platform; LRG: Lower Rhine Graben; LSH: La Serre Horst; MC: Massif Central; RBTZ: Rhine-Bresse Transfer Zone; URG: Upper Rhine Graben

through the autochthonous Mesozoic sediments of the Burgundy Platform (BP) and is flanked to the northeast by the crystalline Vosges Massif. Many authors suggested that the RBTZ transferred crustal extension between Rhine and Bresse Graben in a sinistral strike-slip or transtensive manner during the main stage of rifting in the Eo-Oligocene (Laubscher, 1970; Illies, 1972; Contini and Theobald, 1974; Bergerat and Chorowicz, 1981; Lacombe et al., 1993).

To the south the RBTZ is bordered, and partially overridden, by the thin-skinned Neogene Jura fold-and-thrust belt. Its formation is widely accepted to have resulted from “distant push” (Laubscher, 1961) induced by Late Miocene crustal shortening and nappe stacking in the external crystalline massifs of the Central Alps. Large scale thin-skinned decoupling of the Mesozoic sedimentary cover along a décollement horizon running along Mid to Late Triassic evaporites enabled the propagation of the thrust front towards the distal foreland in the northwest (Burkhard, 1990; Schmid et al., 1996).

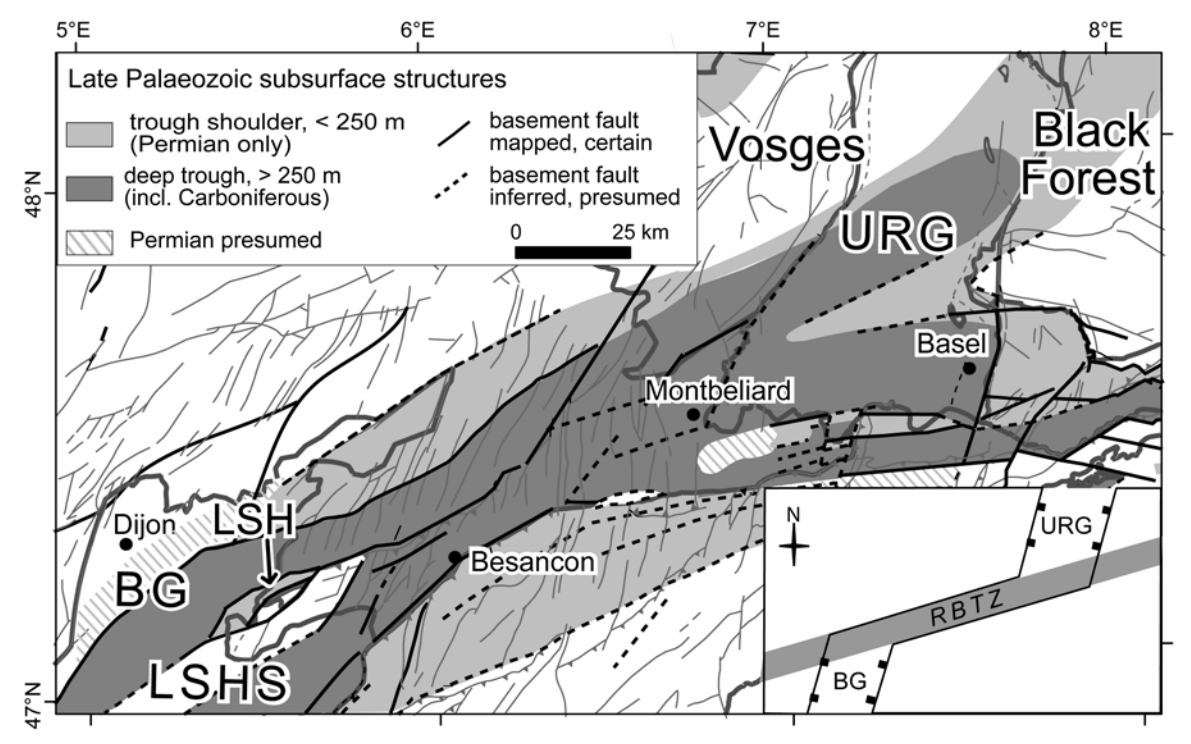

Figure 2: Subsurface map of the Rhine-Bresse Transfer Zone showing the Late Paleozoic Burgundy Trough System. (modified from (Debrand-Passard and Courbouleix, 1984; Ustaszewski et al., 2005). BG: Bresse Graben; LSH: La Serre Horst; LSHS: La Serre Horst Structure; RBTZ: Rhine-Bresse Transfer Zone; URG: Upper Rhine Graben.

The main deformation phase of the fold-and-thrust belt is suggested to have lasted from Late Miocene to Early Pliocene times according to most authors (Laubscher, 1987) but the question if thin-skinned tectonics completely terminated by the Early Pliocene is still a matter of ongoing scientific debate (Mosar, 1999; Becker, 2000; Nivière and Winter, 2000; Ustaszewski and Schmid, 2007).

The Cenozoic tectonic evolution of the area has been inferred to be largely controlled by pre-existing Paleozoic structures by many authors (Laubscher, 1970; Bergerat, 1977; Ziegler, 1992; Lacombe et al., 1993; Schumacher, 2002). The evolution of the Eo-Oligocene RBTZ is suggested to have been controlled by the Late Paleozoic Burgundy Trough system (Figure 2). This roughly ENE-WSW striking Permo-Carboniferous graben system extends over a distance of about 300 km from the northern parts of the Massif Central through the Bresse Graben into the area of the RBTZ, and then further to Basel where it links with the Permo-Carboniferous graben system of Northern Switzerland and Southern Germany (Boigk and Schöneich, 1970; Debrand-Passard and Courbouleix, 1984; Diebold and Noack, 1997). The NE-SW striking La Serre Horst (LSH) (Coromina and Fabbri, 2004) is part of a larger basement high within this Burgundy Trough, referred to as the La Serre Horst Structure (LSHS in Fig. 2) and located at the transition between the Bresse Graben and the RBTZ. Mesozoic rocks cover most of the Late Paleozoic structures throughout the RBTZ. Exposures of Paleozoic rocks

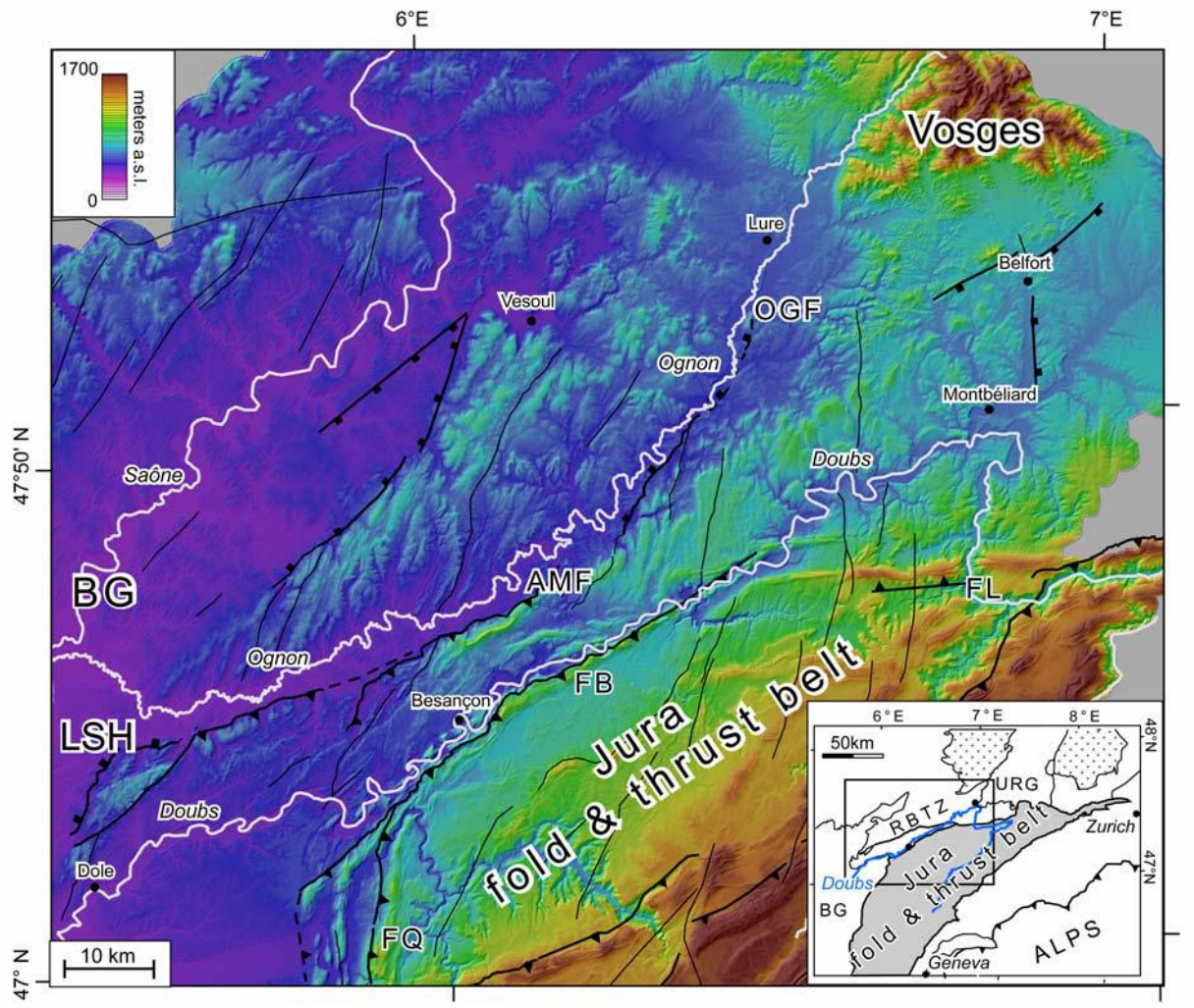

Figure 3: Shaded digital elevation model of the study area (horizontal resolution 50 m). AMF: Avant-Monts Fault; BG: Bresse Graben; FB: Faisceau Bisontin; FL: Faisceau du Lomont; FQ: Faisceau de Quingey; LSH: La Serre Horst; OGF: Ognon Fault; RBTZ: Rhine-Bresse Transfer Zone; URG: Upper Rhine Graben.

are restricted to the LSH. Therefore this area represents a key location to study the influence of Paleozoic basement structures on the Cenozoic structural evolution of the region.

4. Geomorphic Setting

The geomorphology of the study area was shaped and controlled by tectonic and surface processes and is illustrated by the digital elevation model of Franche Comté (50m horizontal resolution) which was available for this study (Fig. 3).

Throughout the study area topographic relief is closely related to tectonic structures. The overall structural and morphological trend of the region strikes ENE-WSW. The fault-related folds along

important deformation fronts, such as the Avant-Monts Fault or the Lomont, Bisontin and Quingey Faisceaux, are expressed in the form of distinct morphological ridges. Furthermore, the La Serre Horst with its outcrops of Paleozoic rocks forms a topographic high.

The region is characterized by two major drainage basins that are oriented roughly parallel to the structural trend. The Doubs River and its tributaries represent the major drainage system of the Jura fold-and-thrust belt. West of the city of Montbéliard the lower reach of the Doubs River follows the deformation front of the Faisceau Bisontin and deeply incised into the limestone bedrock. The Ognon River and its tributaries further north drain the Vosges Mountains. The lower and highly sinuous reach of the Ognon River occupies a broad valley with a wide alluvial plane. Along its upper segment the Ognon valley runs parallel to the prominent NE-SW striking Ognon Fault. Further downstream the river course bends slightly towards the west and parallels the Avant-Monts fault. Both rivers finally drain into the Saône River, which flows southwards and along the Bresse Graben into the Rhône River.

5. Seismicity and present day tectonic activity

Scenario and intensity of present day tectonic activity (Neotectonics) of the study area are yet poorly constrained. Seismicity in the northern Alpine foreland is low to intermediate (Kastrup et al., 2004). The RBTZ shows a significantly lower activity in comparison to the Rhine Graben area (Figure 4), hence the present day stress field is rather ill defined by earthquake fault plane solutions (Kastrup et al., 2004; Baer et al., 2007) (Figure 4). Interestingly, and in contrast to the neighboring Rhine Graben area characterized by deformation by strike-slip or transtension, the earthquakes observed within the RBTZ also reveal pure to oblique thrust faulting mechanisms (Plenefisch and Bonjer, 1997; Lopes Cardozo and Granet, 2003; Baer et al., 2005). This hints towards a different mode of active deformation.

Despite very low vertical and horizontal present day displacement rates throughout the region (Tesauro et al., 2005) evidence for ongoing deformation throughout the area is provided by pioneer studies in tectonic geomorphology (Dreyfuss and Glangeaud, 1950; Liniger, 1967; Theobald et al., 1977; Campy, 1984). However, recent studies applying modern techniques based on digital elevation models and absolute dating methods are so far completely lacking throughout the area of the RBTZ.

Moreover, the tectonic style associated with the most recent (post-Pliocene) shortening has so far been discussed controversially. Some authors argued that present day tectonic activity simply represents the most recent stage of ongoing thin-skinned Jura folding and thrusting (Nivière and Winter, 2000; Müller et al., 2002). Other workers inferred a switch towards thick-skinned tectonics that involve reactivation of pre-existing structures that are rooted in the crystalline basement (Giamboni et al., 2004; Ustaszewski and Schmid, 2007). The question whether thin-skinned, thick-

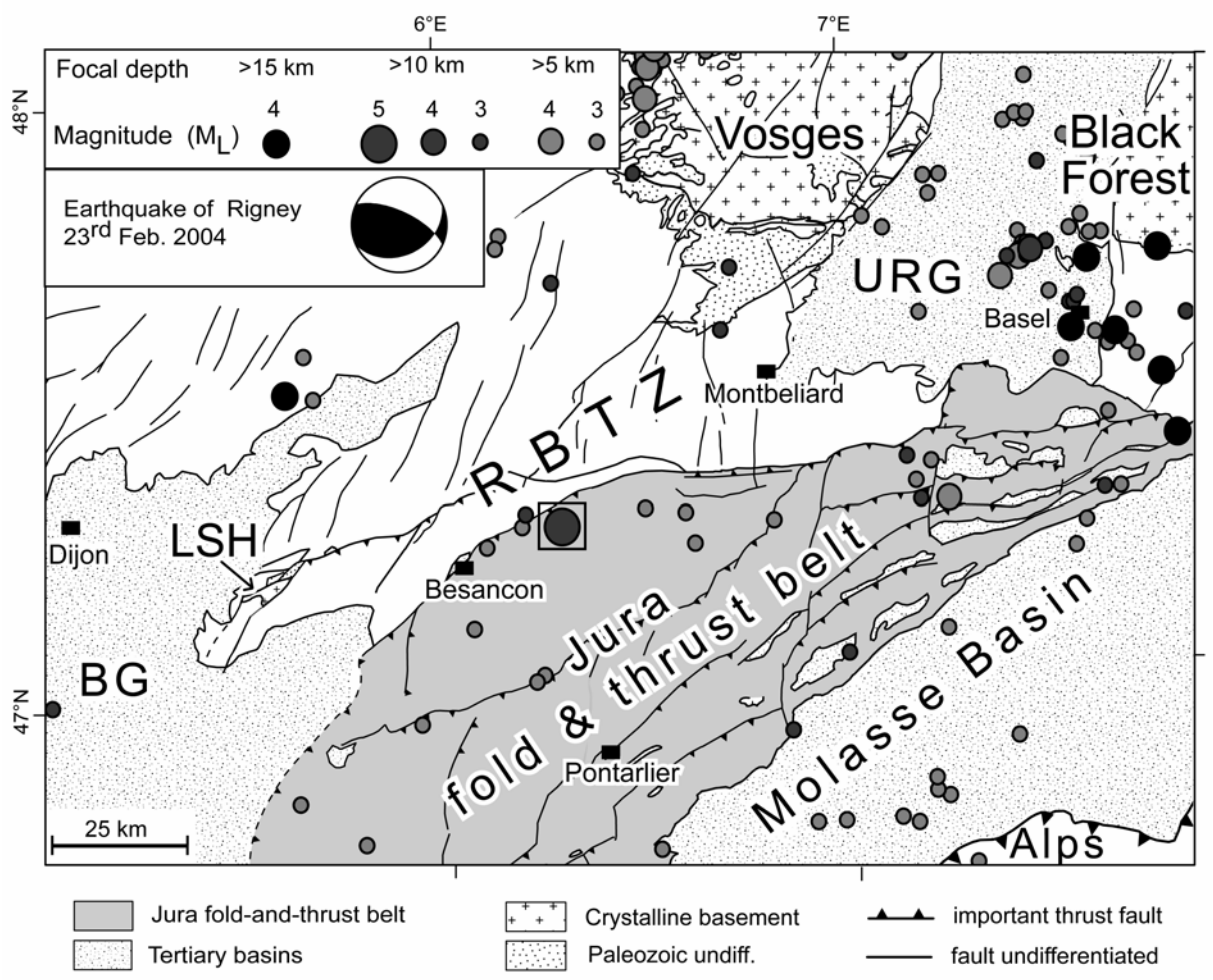

Figure 4: Instrumentally recorded earthquakes (M_L > 3) throughout the Rhine-Bresse Transfer Zone and surrounding areas from 1980 to present (source: Réseau National de Surveillence Sismique (RéNaSS, 2007)). Focal mechanism of the Rigney earthquake (marked by the square) based on full waveform moment tensor inversion taken from (Baer et al., 2005). Tectonic units after (Chauve et al. 1980). BG: Bresse Graben; LSH: La Serre Horst; RBTZ: Rhine-Bresse Transfer Zone; URG: Upper Rhine Graben.

skinned, or a combination of both modes are active at present is of prime importance for any seismic hazard assessment.

References:

Baer, M. et al., 2007. Earthquakes in Switzerland and surrounding regions during 2006. Swiss Journal of Geosciences, 100: 517-528.

Baer, M. et al., 2005. Earthquakes in Switzerland and surrounding regions during 2004. Eclogae geol. Helv., 98(3): 407-418.

Becker, A., 2000. The Jura Mountains - an active foreland fold-and-thrust belt? Tectonophysics, 321: 381-406.

Bergerat, F., 1977. La fraturaction de l'avant-pays jurassien entre les fossés de la Saône et du Rhin. Analyse et essai d'interpretation dynamique. Revue de Géographie physique et de Géologie dynamique (2), 14(4): 325-338.

Bergerat, F. and Chorowicz, J., 1981. Etude des images Landsat de la zone tranformante Rhin-Saône (France). Geologische Rundschau, 70(1): 354-367.

Boigk, H. and Schöneich, H., 1970. Die Tiefenlage der Permbasis im nördlichen Teil des Oberrheingrabens. In: J.H. Illies and S. Mueller (Editors), Graben Problems. Proceedings of an International Rift Symposium held in Karlsruhe 1968, International Upper Mantle Project. E. Schweitzerbart'sche, Stuttgart, pp. 45-55.

Burkhard, M., 1990. Aspects of the large-scale Miocene deformation in the most external part of the Swiss Alps (Subalpine Molasse to Jura fold belt). Eclogae Geologicae Helvetiae, 83(3): 559-583.

Campy, M., 1984. Signification dynamique et climatique des formations et terrasses fluviatiles dans un environnement de moyenne montagne. Bulletin de l'Association française pour l'Etude du Quaternaire, 1: 87-92.

Chauve, P., Enay, R., Fluck, P. and Sittler, C., 1980. L'Est de la France (Vosges, Fossé Rhénan, Bresse, Jura). Annales scientifiques de l'Université de Besançon, 4(1): 3-80.

Contini, D. and Theobald, N., 1974. Relations entre le Fossé rhenan et le Fossé de la Saône. Tectonique des régions sous vosgiennes et prejurrassiennes. In: J.H. Illies and K. Fuchs (Editors), Approaches to Taphrogenesis. Sc. Report., Stuttgart, pp. 310-321.

Coromina, G. and Fabbri, O., 2004. Late Palaeozoic NE-SW ductile-brittle extension in the La Serre horst, eastern France. Comptes Rendus Geosciences, 336(1): 75-84.

Debrand-Passard, S. and Courbouleix, S. (Editors), 1984. Synthèse Géologique du Sud-Est de la France, volume 2: Atlas comprenant 64 planches en couleurs. Mémoire du Bureau de recherches géologiques et minières, 126. BRGM, 614 pp.

Diebold, P. and Noack, T., 1997. Late Palaeozoic troughs and Tertiary Structures in the eastern Folded Jura. In: O.A. Pfiffner, P. Lehner, P. Heitzmann, S. Mueller and A. Steck (Editors), Deep structure of the Swiss Alps. Results of NRP 20. Birkhäuser, pp. 59-63.

Dreyfuss, M. and Glangeaud, L., 1950. La valée de Doubs et l'évolution morphotectonique de la région bisontine. Annales scientifiques de l'Université de Besançon, 5: 2.

Giamboni, M., Ustaszewski, K., Schmid, S.M., Schumacher, M.E. and Wetzel, A., 2004. Plio-Pleistocene Transpressional Reactivation of Paleozoic and Paleogene Structures in the Rhine-Bresse transform Zone (northern Switzerland and eastern France). International Journal of Earth Sciences, 93(2): 207–223, DOI: 10.1007/s00531-003-0375-2.

Illies, J.H., 1972. The Rhinegraben rift system - plate tectonics and transform faulting. Geophysical Surv., 1: 27-60.

Kastrup, U. et al., 2004. Stress field variations in the Swiss Alps and the northern Alpine foreland derived from inversion of fault plane solutions. J. Geophys. Res., 109(B01402): doi:10.1029/2003JB002550.

Lacombe, O., Angelier, J., Byrne, D. and Dupin, J., 1993. Eocene-Oligocene tectonics and kinematics of the Rhine-Saone continental transform zone (Eastern France). Tectonics, 12(4): 874-888.

Laubscher, H., 1961. Die Fernschubhypothese der Jurafaltung. Eclogae Geologicae Helvetiae, 54(1): 222-282.

Laubscher, H., 1970. Grundsätzliches zur Tektonik des Rheingrabens. In: J.H. Illies and S. Mueller (Editors), Graben Problems. Proceedings of an International Rift Symposium held in Karlsruhe 1968, International Upper Mantle Project. E. Schweitzerbart'sche, Stuttgart, pp. 79-86.

Laubscher, H., 1987. Die tektonische Entwicklung der Nordschweiz. Eclogae Geologicae Helvetiae, 80: 287-303.

Liniger, H., 1967. Pliozän und Tektonik des Jura Gebirges. Eclogae Geol Helv, 60(2): 407-490.

Lopes Cardozo, G.G.O. and Granet, M., 2003. New insight in the tectonics of the southern Rhine Graben-Jura region using local earthquake seismology. Tectonics, 22(6): 1078, doi:10.1029/ 2002TC001442.

Mayer-Rosa, D. and Cadiot, B., 1979. Review of the 1356 Basel earthquake: basic data. Tectonophysics, 53: 325-333.

Müller, W.H., Naef, H. and Graf, H.R. (Editors), 2002. Geologische Entwicklung der Nordschweiz, Neotektonik und Langzeitszenarien, Zürcher Weinland. NAGRA Technischer Bericht, 99-08. NAGRA, Wettingen, 226 pp.

Mosar, J., 1999. Present-day and future tectonic underplating in the western Swiss Alps: reconciliation of basement/wrench-faulting and décollement folding of the Jura and Molasse basin in the Alpine foreland. Earth and Planetary Science Letters, 173: 143-155.

Nivière, B. and Winter, T., 2000. Pleistocene northwards fold propagation of the Jura within the southern Upper Rhine Graben: seismotectonic implications. Global and Planetary Change, 27: 263–288.

Plenefisch, T. and Bonjer, K., 1997. The stress field in the Rhine Graben area inferred from earthquake focal mechanisms and estimation of frictional parameters. Tectonophysics, 275: 71-97.

RéNaSS, R.N.d.S.S., 2007. Réseau National de Surveillance Sismique, http://renass.u-strasbg.fr/. In: E.e.O.d.S.d.l.T.d. Strasbourg (Editor).

Schmid, S.M., Pfiffner, O.A., Froitzheim, N., Schönborn, G. and Kissling, E., 1996. Geophysical-geological transect and tectonic evolution of the Swiss-Italian Alps. Tectonics, 15: 1036-1064.

Schumacher, M.E., 2002. Upper Rhine Graben: Role of preexisting structures during rift evolution. Tectonics, 21(1): 6-1-6-17.

Tesauro, M., Hollenstein, C., Egli, R., Geiger, A. and Kahle, H.-G., 2005. Continuous GPS and broad-scale deformation across the Rhine Graben and the Alps. International Journal of Earth Sciences, 94: 525-537.

Theobald, N., Vogt, H. and Wittmann, O., 1977. Néotectonique de la partie méridionale du bloc rhénan. Bull. B.R.G.M., 2(4): 121-140.

Ustaszewski, K. and Schmid, S.M., 2007. Latest Pliocene to recent thick-skinned tectonics at the Upper Rhine Graben - Jura Mountains junction. Swiss Journal of Geosciences, 100(2): 293-312.

Ustaszewski, K., Schumacher, M.E., Schmid, S.M. and Nieuwland, D., 2005. Fault reactivation in brittle-viscous wrench systems - dynamically scaled analogue models and application to the Rhine-Bresse Transfer Zone. Quaternary Science Reviews, 24(3-4): 363-380, doi:10.1016/j.quascirev.2004.03.015.

Ziegler, P.A., 1992. European Cenozoic rift system. Tectonophysics, 208: 91-111.

Chapter 2

Multiple fault reactivation within the intra-continental Rhine-Bresse Transfer Zone (La Serre Horst, eastern France)

by

Herfried Madritsch, Alexandre Kounov, Stefan M. Schmid and Olivier Fabbri

submitted to *Tectonophysics*

Abstract:

Thermochronological, structural and kinematic data demonstrate the influence of Late Paleozoic basement structures, such as the Burgundy Trough and the La Serre Horst, on the localization and evolution of the Eo-Oligocene Rhine-Bresse Transfer zone (RBTZ), a major segment of the European Cenozoic Rift system.

Zircon and apatite fission track data indicate that the Paleozoic crystalline basement and its Permo-Triassic cover, exposed in the La Serre Horst, experienced a Middle Jurassic to Early Cretaceous heating event which was followed by two distinct periods of cooling. A first cooling event occurred in the Early Cretaceous and is probably related to thermal relaxation. A second one, at 38 to 32 Ma, is interpreted to reflect reactivation of the La Serre Horst during the Eo-Oligocene rifting and associated formation of the RBTZ.

Eo-Oligocene basement fault reactivation in connection with the formation of the RBTZ resulted in a complex fault pattern and local stress field perturbations in the surroundings of the pre-existing Paleozoic horst structure. Kinematic analyses indicate a NW-SE directed extension throughout the western part of the RBTZ. Substantial extension occurred in Eo-Oligocene times and was achieved by ENE-WSW striking normal faults trending highly oblique to the dominant strike of the Rhine and Bresse Graben rifts. Such normal faults are typically associated with extensional flexures. These ENE-WSW striking major faults are oriented parallel to pre-existing Paleozoic basement faults which formed in the context of the formation of the Late Paleozoic Burgundy Trough and the La Serre Horst; localization of the RBTZ was hence controlled by structural inheritance of pre-existing basement structures. Due to this inheritance reactivation of Paleozoic structures in the RBTZ is of extensional rather than of strike-slip character. This demonstrates that the RBTZ forms a separate oblique graben segment within the European Cenozoic Rift System rather than a sinistral strike slip transfer zone supposedly connecting Rhine and Bresse Graben structures.

Keywords: *fault reactivation, fission-track dating, paleostress analysis, La Serre Horst, Rhine-Bresse Transfer Zone, France*

2.1 Introduction and objectives

The influence of Paleozoic basement discontinuities on the Cenozoic structural evolution of the northwestern Alpine foreland in general and the formation and evolution of the European Rift System in particular has been widely discussed by numerous authors (Laubscher, 1970; Illies, 1981; Ziegler, 1992; Lacombe et al. 1993; Schumacher, 2002; Dèzes et al., 2004; Michon and Sokoutis, 2005). This contribution addresses the evolution of the intra-continental Rhine-Bresse Transfer Zone (RBTZ), a central segment of the European Cenozoic Rift System, and discusses reactivation of pre-existing Paleozoic basement structures during its formation. Several authors proposed that Eo-Oligocene crustal extension, responsible for the opening of the Rhine and Bresse Graben, was transferred along the Rhine-Bresse Transfer Zone (RBTZ) by sinistrally transtensive reactivation of an ENE-WSW striking, pre-existing Paleozoic basement fault system (e.g. Laubscher, 1970; Illies, 1972; Contini and Theobald, 1974; Bergerat, 1977; Bergerat and Chorowicz, 1981; Lacombe et al., 1993). This concept is based on map interpretation and kinematic studies on brittle deformation of the Mesozoic cover, but also inspired by analogue and numerical modelling (Elmohandes, 1981; Lacombe et al., 1993; Ustaszewski et al., 2005b). However, direct field evidence in support of reactivation of Paleozoic basement faults during the Eo-Oligocene formation of the RBTZ is still scarce. Moreover, the subsurface structures within the Paleozoic basement underlying the area of the RBTZ are still poorly known. Hence, the so far proposed models regarding transfer zone formation by structural inheritance appear very simplified in view of the complex fault geometries.

This study aims to fill some of these gaps by combining fission track data from the Paleozoic basement with extensive analyses of structural and subsurface data. The latter are based on seismic reflection data that became available to academic institutions for the first time. The investigation focuses on the La Serre Horst (LSH) that is located in the western part of the RBTZ and which contains the only outcrop of Paleozoic granites and overlying Permian deposits found between the French Massif Central and the Vosges Mountains crystalline basement complexes (Figure 1). Similarly to these two much larger basement complexes, the LSH presently forms a topographic high. Our combined dataset will allow constraining the exhumation history of the Paleozoic horst in order to clarify its influence on fault geometries and kinematics of the Cenozoic Rhine-Bresse Transfer Zone.

2.2 Geological setting

The roughly N-S striking European Cenozoic Rift System (ECRIS) dissects Western Europe from the North Sea to the western Mediterranean over a distance of about 1100 km (inset Figure 1) (Ziegler, 1992; Dèzes et al., 2004). The Upper Rhine Graben (URG), together with the Bresse Graben (BG), represent the central segments of this rift system (Figure 1). They are connected by the

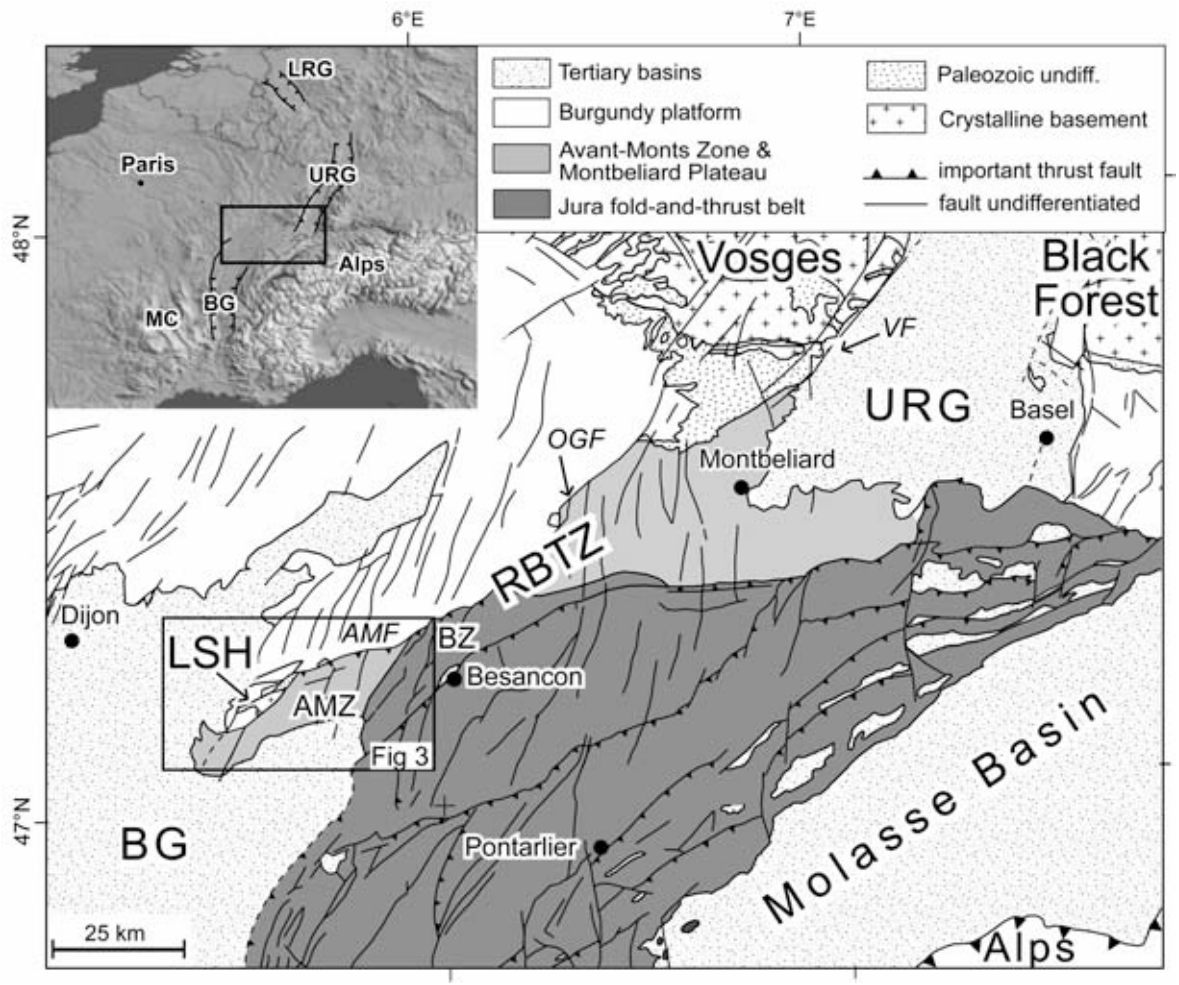

Figure 1: Geological setting of the study area. The Rhine-Bresse Transfer Zone (RBTZ) is a segment of the European Cenozoic Rift system (inset) located between the Rhine and Bresse Graben. The La Serre Horst (LSH) forms an isolated crystalline massif at the western termination of the RBTZ. The tectonic units are drawn as defined in Madritsch et al. (2008 in press). AMF: Avant-Monts Fault; AMZ: Avant-Monts Zone; BG: Bresse Graben; BZ: Besançon Zone; MC: Massif Central; LSH: La Serre Horst; LRG: Lower Rhine Graben; OGF: Ognon Fault; RBTZ: Rhine-Bresse Transfer Zone; URG: Upper Rhine Graben; VF: Vosges Fault.

approximately 200km long ENE-WSW striking intra-continental Rhine-Bresse-Transfer Zone (RBTZ). The northern part of the RBTZ cuts through the autochthonous Mesozoic sediments of the Burgundy Platform and is flanked to the northeast by the crystalline Vosges Mountains. To the south the RBTZ is bordered, and partially overthrust, by the thin-skinned Neogene Jura fold-and-thrust belt (Madritsch et al., 2008 in press).

The sedimentary record of the Southern Upper Rhine Graben suggests that the formation of ECRIS started in Middle (42.5 Ma, Lutetian; Berger et al., 2005; Hinsken et al., 2007) to Late Eocene times (36 Ma, Late Priabonian, Sissingh, 1998). Mechanisms controlling the development of ECRIS have been debated for a long time and the proposed models range from hot-spot driven active rifting (Neugebauer, 1978) to passive rifting, the latter being possibly induced by collisional foreland

splitting (Dèzes et al., 2004; Sengör, 1976), back-arc extension (Jowett, 1991) or slab-pull (Merle and Michon, 2001). Many authors suggested that during the main stage of rifting in the Eo-Oligocene, the RBTZ transferred crustal extension between the Rhine and Bresse Graben (Laubscher, 1970; Illies, 1972; Contini and Theobald, 1974; Bergerat and Chorowicz, 1981) and different kinematic models were evoked (Bergerat, 1977; Lacombe et al., (1993); see discussion).

The southern URG as well as the RBTZ were affected by large-scale differential uplift after the main phase of rifting. This uplift probably started in the Early Miocene (Aquitanian, Berger et al., 2005) but is well constrained only for the Middle Miocene (Burdigalian, Schumacher, 2002; Ziegler and Dèzes, 2007). From Early to Middle Miocene times the axis of the uplift apparently shifted NW-ward (Schumacher, 2002). This has been interpreted as reflecting the outward migration of the Alpine flexural fore-bulge (Laubscher, 1992; Schumacher, 2002) or as being the effect of collision-related compressional deformation involving lithospheric folding (Dèzes et al., 2004; Bourgeois et al., 2007; Ziegler and Dèzes, 2007). The lithospheric folding model for the uplift of the Vosges-Black Forest arch is compatible with the configuration of the Moho discontinuity, which forms an anticlinal structure that extends from the northern Massif Central towards the Bohemian Massif, culminating beneath the southern parts of the Upper Rhine Graben. The uplift not only led to exhumation of the southern URG rift shoulders and the southern parts of the graben fill, but apparently also affected the RBTZ. In the RBTZ area the locally preserved remnants of Oligocene sediments testify to former rift-related depocenters (Chauve et al., 1983; Dreyfuss and Kuntz, 1969) (Figure 1). However, the majority of them were removed during post-Oligocene phases of erosion.

Crustal shortening and nappe stacking in the external crystalline massifs of the Central Alps during the Late Miocene induced the formation of the thin-skinned Jura fold-and-thrust belt (Laubscher 1972; Burkhard, 1990; Schmid et al., 1996). By the Early Pliocene its northwestern-most segment, the Besançon Zone (Figure 1), encroached onto the RBTZ (Madritsch et al., 2008 in press). Subsequently, further stress build-up in response to ongoing Alpine collision caused thick-skinned reactivation of the RBTZ at the northern margin of the Jura fold-and-thrust belt. This is associated with partial inversion of former Paleozoic and Paleogene basement faults that formed by extension or transtension. Such inversion during compressional to dextrally transpressive deformation is well documented from seismic reflection data throughout the Avant-Monts Zone (Figure 1) (Madritsch et al., 2008 in press) and also reported from the easternmost part of the RBTZ (Giamboni et al., 2004; Rotstein et al. 2005; Ustaszewski and Schmid, 2007). Present day low to medium seismicity of the area implies that thick-skinned tectonics is probably still ongoing (Ustaszewski and Schmid, 2007; Madritsch et al., 2008 in press).

According to many authors the RBTZ formed during Eo-Oligocene by structural inheritance and reactivation of the Late Paleozoic Burgundy Trough (Laubscher, 1970; Illies, 1972; Ziegler, 1992; Schumacher, 2002; Ustaszewski et al., 2005a) (Figure 2). This roughly ENE-WSW striking Permo-

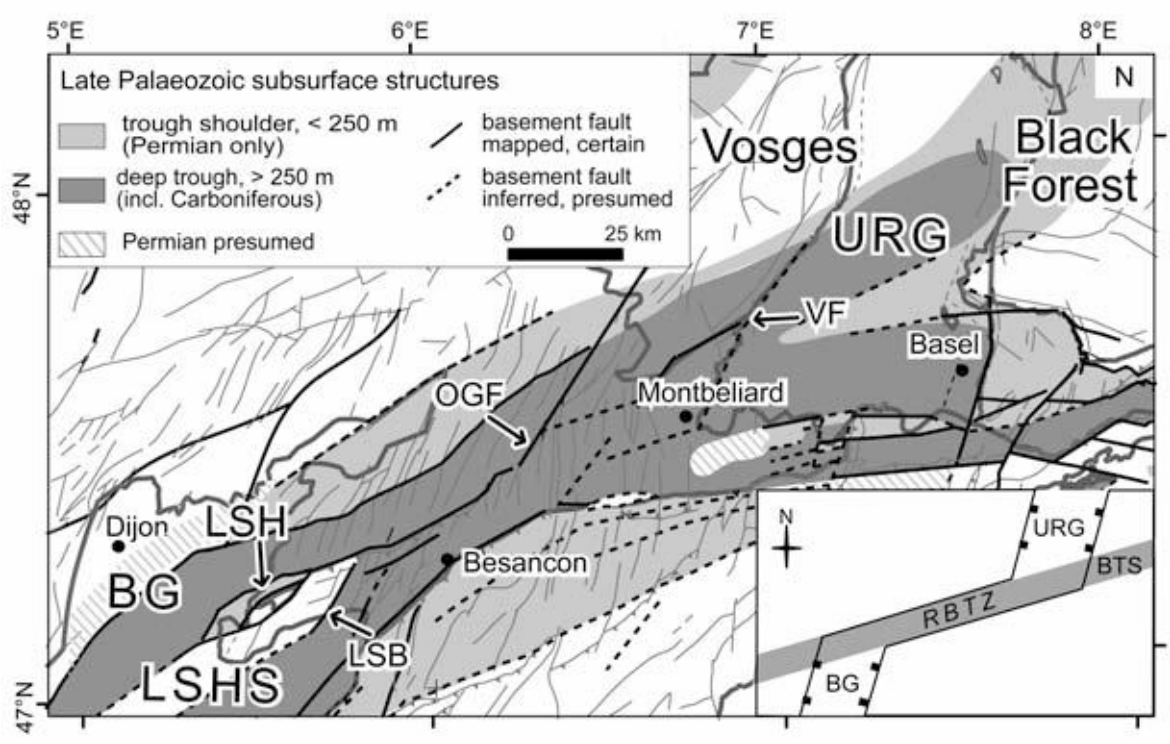

Figure 2: Subsurface map of the Rhine-Bresse Transfer Zone (RBTZ), modified after Debrand-Passard and Coubrouleix (1984) and Ustaszewski et al. (2005a, b). The Eo-Oligocene RBTZ parallels the Late Paleozoic Burgundy Trough system (see sketch in the lower right). Thick grey lines depict the borders of Tertiary basins. BG: Bresse Graben; BTS: Burgundy Trough System; LSB: La Serre Border Fault; LSH: La Serre Horst; LSHS: La Serre Horst Structure; OGF: Ognon Fault; RBTZ: Rhine-Bresse Transfer Zone; URG: Upper Rhine Graben; VF: Vosges Fault.

Carboniferous graben system extends over a distance of about 300 km from the northern parts of the Massif Central through the Bresse Graben into the area of the RBTZ and further to Basel where it links with the Permo-Carboniferous graben system of Northern Switzerland and Southern Germany (Boigk and Schöneich, 1970; Debrand-Passard and Courbouleix, 1984; Bergerat et al., 1990; Diebold and Naef, 1990; Ziegler et al., 2004). The northern and southern boundaries of the Burgundy Trough are poorly constrained. Most authors report an approximate width of about 50 km (Figure 2) (e.g. Debrand-Passard and Courbouleix, 1984; Ziegler et al., 2004). Deep wells in the central part of the transfer zone document graben depths of over 800 meters and indicate that graben formation already in Late Carboniferous times (Chauve et al., 1983). The formation of the Burgundy Trough was probably related to the activity along a dextrally transtensive trans-European shear zone and was also accompanied by volcanism (Ziegler, 1986; Schumacher, 2002; McCann et al. 2006).

The NE-SW striking La Serre Horst (LSH) (Figure 1, 3, 4) is part of a larger basement high within the Burgundy Trough, referred to as the La Serre Horst Structure (LSHS in Figure 2). This basement high is located at the transition between the northern Bresse Graben and the RBTZ. To the

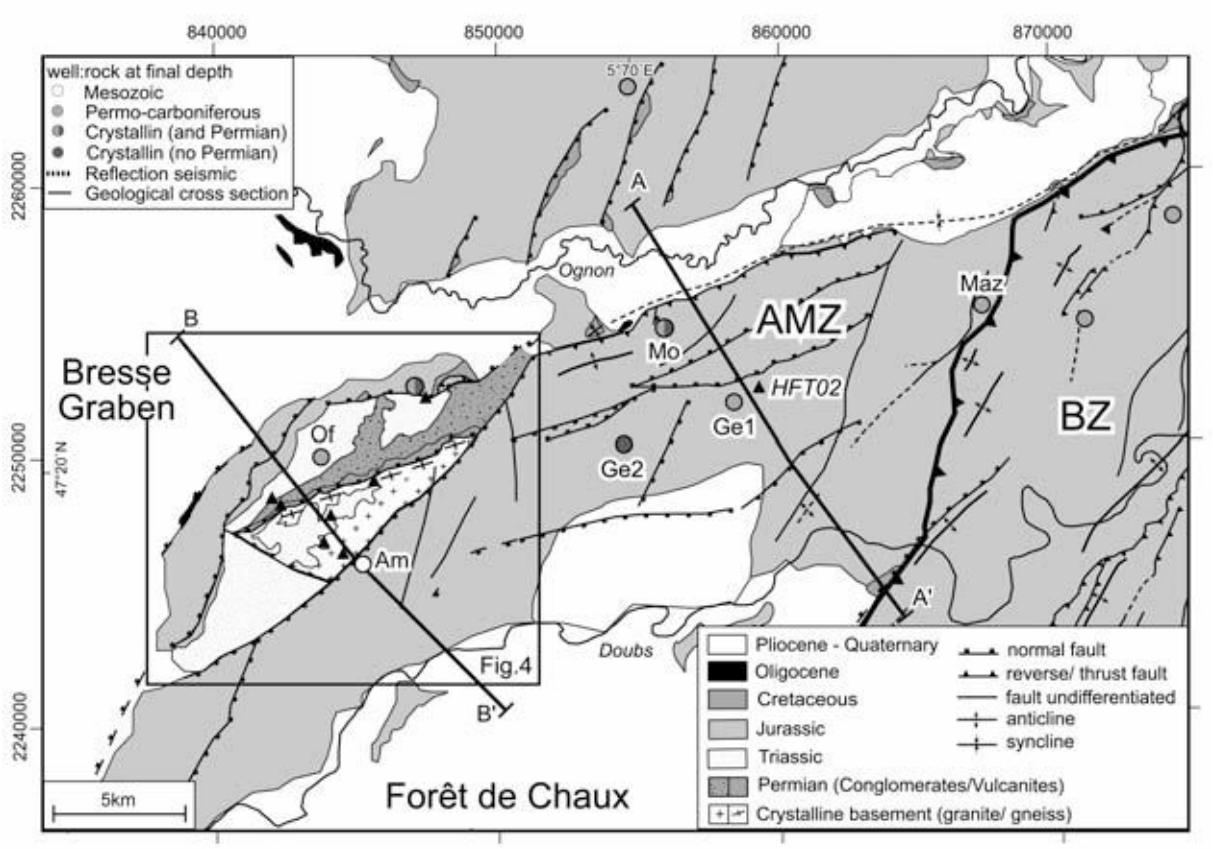

Figure 3: Geological map of the study area, indicating the location of wells (Figure 7) and geological cross sections (Figure 15). Triangles mark the location of fission track samples from the La Serre Horst and its surroundings (see Figures 4 and 5 for details). The thick black line marks the front of the Besançon Zone that is part of the thin-skinned Jura fold-and-thrust belt. AF: Arne Fault; AMF: Avant-Monts Fault; AMZ: Avant-Monts Zone; BZ: Besançon Zone.

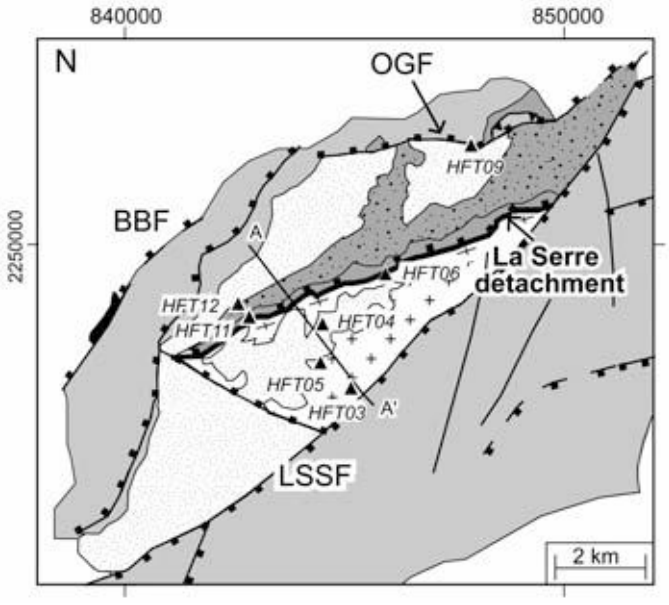

Figure 4: Detail geological map of the La Serre Horst, showing the location of fission track samples (see Figure 3 for location of sample HFT02); ages are given Table 1 and Fig 5; legend as in Figure 3. BBF: Bresse Border Fault; LSSF: La Serre Southern Fault, OGF: Ognon Fault.

southwest the La Serre Horst Structure connects with the Sennecey high of the northern central Bresse Graben (Rat, 1976; Bergerat et al., 1990; Rocher et al., 2003). While Mesozoic sediments cover most of the Paleozoic La Serre Horst Structure, Paleozoic rocks are only exposed in the LSH (Morre and Thiebaut, 1961; Chauve et al., 1983; Coromina and Fabbri, 2004) (Figure 1, 3, 4). In the LSH a ductile to brittle low-angle fault zone separates a Late Devonian to Early Carboniferous granite in the foot wall (U-Pb age 362±12 Ma (Morre-Biot and Storet, 1967) from Permian volcanics and conglomerates in the hanging-wall (Coromina and Fabbri, 2004) (Figure 5). In this study this low angle detachment fault, called La Serre Median Fault Zone in Coromina & Fabbri (2004), will be referred here to as the La Serre Detachment (Figures 4, 5). The fault zone shows a top-to- the-NE sense of shear and is sealed by Lower Triassic sandstones of the Buntsandstein formation. This suggests that activity along this fault was restricted to Late Paleozoic times (Coromina and Fabbri, 2004). The northern limit of the LSH is formed by a NNW-dipping high-angle normal fault of Permian age, also delimiting the La Serre Horst Structure (Figure 2) and post-dating the La Serre Detachment. To the southeast the LSH is bound by the high-angle La Serre Southern Fault (LSSF) (Coromina and Fabbri, 2004) (Figures 3, 4, 5) that separates it from the subsurface extent of the La Serre Horst Structure (Figure 2).

2.3. Fission track analysis

2.3.1. Methodology

The samples for zircon and apatite fission track dating were collected along a NW-SE striking profile across the La Serre Horst (Figures 4, 5, Table 1). The samples include Late Paleozoic granites and gneisses and Permian to Early Triassic volcanics, conglomerates and sandstones. A Liassic claystone sample was also collected from the Mesozoic cover of the La Serre Horst about 12 km east of the main traverse (sample HFT02, see Figure 3 for location).

Sample preparation followed the routine technique described in Seward (1989). Etching of the apatite grains used 7% HNO_3 at 21°C for 50 seconds. Zircon grains were etched in an eutectic mixture of KOH and NaOH at 220°C for between 9 and 15 h. Irradiation was carried out at the OSU facility, Oregon State University Radiation Center, USA. Microscopic analysis was completed at Basel University using an optical microscope with a Kinetek computer-driven stage (Dumitru, 1995).

All ages were determined (analyst: A. Kounov) using the zeta approach (Hurford and Green, 1983) with a zeta value of 332±7 for apatite (CN5 standard glass) and 122±2 for zircon (CN1 standard glass) (Table 1). Ages are reported as central ages (Galbraith and Laslett, 1993) with a 2σ error (Table 1). The magnification used was x1250 for apatite and x1600 (dry objective) for zircon. Horizontal confined track lengths in apatite grains were measured at a magnification of x1250. Fission track etch pit diameters (Dpar) were measured at a magnification of x2500 in order to estimate the compositional

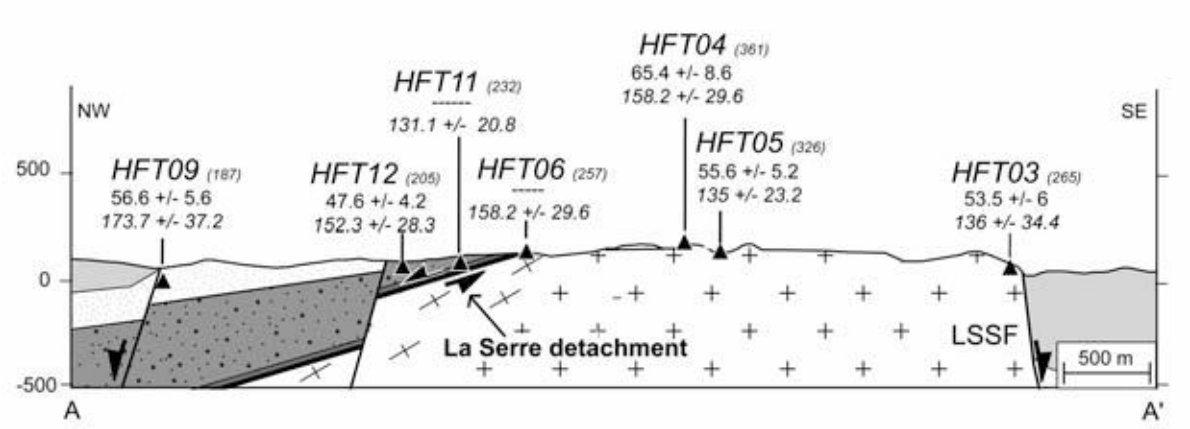

Figure 5: Cross-section across the La Serre Horst showing the fission track ages (Central ages for apatite and zircon, the latter being given in italic letters; see also Table 1). Legend according to Figure 3. LSSF: La Serre Southern Fault.

influence on fission track annealing (Carlson et al., 1999).The magnification used was x1250 for apatite and x1600 (dry objective) for zircon. Horizontal confined track lengths in apatite grains were measured at a magnification of x1250. Fission track etch pit diameters (Dpar) were measured at a magnification of x2500 in order to estimate the compositional influence on fission track annealing (Carlson et al., 1999).

The temperatures at which fission tracks in apatite and zircon minerals partially anneal (i.e. partial isotopic resetting) are not clearly defined. The temperature range within which partial track annealing occurs is known as partial annealing zone (PAZ). The effective closure of the system lies within this zone and is dependent on the overall cooling rates and the kinetic properties of the minerals. The specific partial annealing zone for apatite lies between 60°C and 110°C (Green and Duddy, 1989; Corrigan, 1993). Unfortunately our knowledge of zircon annealing is not as advanced as that of apatite and wide-ranging values for the temperature bounds for the partial annealing zone of zircon have been published. Yamada et al. (1995) suggest temperature limits of 170°C - ~390°C whereas Tagami and Dumitru (1996) and Tagami et al. (1998) suggested temperature limits of 230°C - ~310°C. Brandon et al. (1998) argued that for old zircons, with relatively high density of α-damages, the partial annealing zone could move to lower temperatures by about 50 to 100°C. Considering the relatively high amount

Table 1: Sample details and results of zircon and apatite fission-track dating (refer to Figures 3 and 4 for sample locations). All ages are central ages (Galbraith, 1981). $\lambda D = 1.55125 \times 10^{-10}$. A geometry factor of 0.5 was used. Zeta = 332 ±7 for CN5/apatite and 122 ±2 for CN1/zircon. Irradiations were performed at the OSU facility, Oregon State University Radiation Center, USA. $P(\chi^2)$ is the probability of obtaining χ^2 values for ν degrees of freedom where ν= number of crystals -1. ρd, ρs and ρi represent the standard, sample spontaneous and induced track densities respectively. Dpar: mean track pit length; MTL: mean track length; N: Number of measurements; Std. Dev.: standard deviation; All numbers in brackets are numbers of measurements

Sample	Coordinates X / Y	Alt. m. a.s.l.	Lithology	Age	Mineral	N	ρd x10^6 cm-2	ρs x10^6 cm-2	ρi x10^6 cm-2	P(χ2) (%)	U. conc. (ppm)	Central age (±2σ)Ma	MTL(±2σ) µm	Std. Dev.(N) µm	Dpar µm
	859444 /	280	marls	Toarcian	zircon	3	3.640	25.644	2.459	49	274	***226.9***			
HFT02	2252492						(2659)	-219	-21			***±104.4***			
		265	granite	Paleozoic	apatite	20	15.397	1.838	8.590	0	69	**53.5**		2.59	1.93
HFT03	44133 / 224636						(8099)	(1156)	(5403)			**±6.0**	12.68 (±0.25)	(104)	
					zircon	5	3.591	22.764	3.607	65	440	***136.4***			
							-2659	-486	-77			***±34.4***			
	843388 /	361	sandstone	Lower Triassic	apatite	20	1.350	1.115	3.611	0	33	**65.4**		2.38	1.98
HFT04	2248022						(8099)	(748)	(2423)			**±8.6**	12.15 (±0.25)	(91)	
					zircon	8	3.541	23.217	3.124	90	346	***158.2***			
							(2659)	(48)	(141)			***±29.6***			
	843239 /	326	granite	Paleozoic	apatite	20	1.461	1.314	5.715	58	50	**55.6**		2.4	1.83
HFT05	2246759						(8099)	(783)	(3406)			**±5.2**	12.10 (±0.23)	(1069)	
					zircon	8	3.516	23.888	3.747	100	424	***135***			
							(2659)	(11229	(176)			***±23.2***			
		257	granite	Paleozoic	zircon	12	3.442	18.073	2.859	88	360	***131.1***			
HFT06	44226 / 224931						(26599	(13349	(211)			***±20.8***			
	847000 /	187	sandstone	Lower Triassic	apatite	20	1.318	0.890	3.431	74	34	**56.6**		2.37	1.89
HFT09	2252114						-8099	-714	-2752			**±5.6**	12.50 (±0.23)	(103)	
					zircon	7	3.318	23.601	2.706	97	317	***173.7***			
							(2659)	(907)	(104)			***±37.2***			
		232	rhyolithe	Permian?	zircon	7	3.269	20.323	2.550	95	304	***156.6***			
HFT11	41585 / 224823						(2659)	(781)	(98)			***±34.6***			
	841315 /	205	conglomerate	Permian	apatite	20	1.429	0.981	4.874	97	45	**47.6**		2.64	1.86
HFT12	2248413						(8099)	(923)	(4586)			**±4.2**	12.89 (±0.26)	(101)	
					zircon	9	3.195	20.888	2.634	100	332	***152.3***			
							(2659)	(1134)	(143)			***±28.4***			

of α-damage accumulated in the crystal lattice of the analysed samples, given the high protolith age (Variscan or older), we suggest temperature bounds for the zircon partial annealing zone (ZPAZ) that are located between 160 and 270°C. Thereby we follow a summary given by Brandon et al. (1998) concerning the thermal stability of naturally α-damaged zircons. Accordingly we use a value of 230°C for positioning the ZFT central age in a temperature (T) vs. time (t) thermal history path (e.g. in Figure 13).

2.3.2. Results

Zircon:

Eight samples from magmatic and sedimentary rocks were dated by the zircon FT method (Table 1). Due to the bad quality (metamictisation) of the zircon minerals in the samples analysed, only three to twelve datable grains were found per sample. Zircon central ages range from 227±104 Ma to 131±21 Ma (Table 1). All samples passed the χ^2 test and have FT ages younger than their stratigraphic ages, indicating that they were affected by temperatures higher than 160°C after their deposition or formation. The only exception is the Liassic sample HFT02, from which only three grains could be dated; it has a central age that overlaps with the age of deposition, given its large 2σ error.

Apatite:

Five zircon FT dated samples were also be used for apatite FT analysis (Table 1). Apatite fission track central ages range between 65±9 Ma and 48±44 Ma. Three out of the five analysed samples (HFT05, HFT09 and HFT12) passed the χ^2 test. The samples have mean track lengths between 12.10 and 12.89 μm, with a standard deviation of 2.37 – 2.648 μm (Table 1). The Dpar values of the analysed samples range between 1.83 and 1.98 μm.

2.4. Subsurface Analysis

The analysed seismic data cover an area east of the La Serre Horst known as the Avant-Monts Zone (AMZ in Figure1, Figure6, Chauve et al., 1980; Madritsch et al., 2008 in press). The geological logs of deep wells (Figure 7, see Figures 3 and 6b for location) were obtained from BRGM (Bureau de Recherches Géologiques et Minières, Dijon office) and seismic reflection sections (see Figure 6b for their locations) were provided by Gaz de France. All seismic data have been commercially processed and were received for interpretation in form of paper copies.

Seismic velocity analyses of the area were carried out based on correlations between two-way travel time and stratigraphic logging in 4 deep wells (Figure 7), as well as from seismic check-shot information from the surroundings of the wells. Whilst high velocities characterise Early Jurassic clays (6000 m/sec), the evaporitic Middle and Late Triassic sediments exhibit low velocities (2700-3400 m/sec). The interval velocity for the entire Mesozoic succession is in the range of 4000-4400 m/sec. Because similar values were obtained from the different wells and appear to be constant throughout the area of investigation, they were used for an approximate depth conversion of the seismic lines.

The Mesozoic series are characterized by continuous high amplitude reflections in the seismic lines (Figure 8). Along most of the examined lines four distinct reflectors are evident and were calibrated by correlations with the logs of deep wells located close to the trace of the lines (Figure 6b). In the profiles of Figure 8 the uppermost reflector L is within Early Jurassic clays (Liassic). Reflector K represents the top of the Late Triassic Keuper Formation. Reflector M marks the boundary between Late and Middle Triassic lithologies (top of the Muschelkalk Formation). The lowermost, continuous, high amplitude reflections at about 300 and 450 msec TWT mark the top and base of the Early Triassic Buntsandstein Formation. The depth of the base-Mesozoic reflector B is contoured in Figure 6a. Permian and Carboniferous sediments have been recorded in several wells drilled in the RBTZ area (Figure 7) and are characterized by discontinuous reflections (P) with rather chaotic seismic character. Some inclined P-reflections are indicative for an angular unconformity between Permo-Carboniferous sediments and overlying Mesozoic sediments (Figures 8b and 8c). The contact between the Permo-Carboniferous deposits and the crystalline basement does not give rise to a clear reflector and thus is very difficult to define. In the vicinity of the LSH, the crystalline basement was reached by the Mo and Ge2 wells (Figures 3, 6b, 7) (Morre and Thiébaut, 1961) that are located near Line 1 (Figure 8a) and Line 3 (Figure 8c), respectively.

The seismic interpretations of a dense network of 10 seismic sections (Figure 6b), combined with the borehole data (Figure 7) and the available 1: 50'000 geological maps (Chauve et al., 1983; Dreyfuss and Kuntz, 1969), allowed for the construction of a subsurface map at the level of the B-reflector, corresponding to the base of the Mesozoic series; the resulting contour map is given in two-way-travel-time (TWT) in Figure 6a. It illustrates the complex Post-Paleozoic fault pattern adjacent to the La Serre Horst.

The NNE-SSW striking faults in the study area (Figure 6) mostly represent sub-vertical normal faults (Figure 8a, b, c) and are oriented sub-parallel to the border faults of the Eo-Oligocene Bresse Graben. The La Serre Southern Fault (Coromina and Fabbri, 2004) shows a slightly different (NE-SW) strike (see LSSF in Figure 4, 5, 6) and produces a vertical offset of ~500 meters. Paleozoic rocks are exposed in the La Serre Horst, i.e. in the footwall of the La Serre Southern Fault. Farther to the SE and in the hanging wall of the LSSF (Figures 6, 8a), however, they are covered by a thick succession of Mesozoic sediments, but were penetrated by well Ge2 (Morre and Thiebaut, 1961; Chauve et al., 1983) (Figure 7, 8a). The base-Mesozoic boundary is well displayed in the seismic profiles

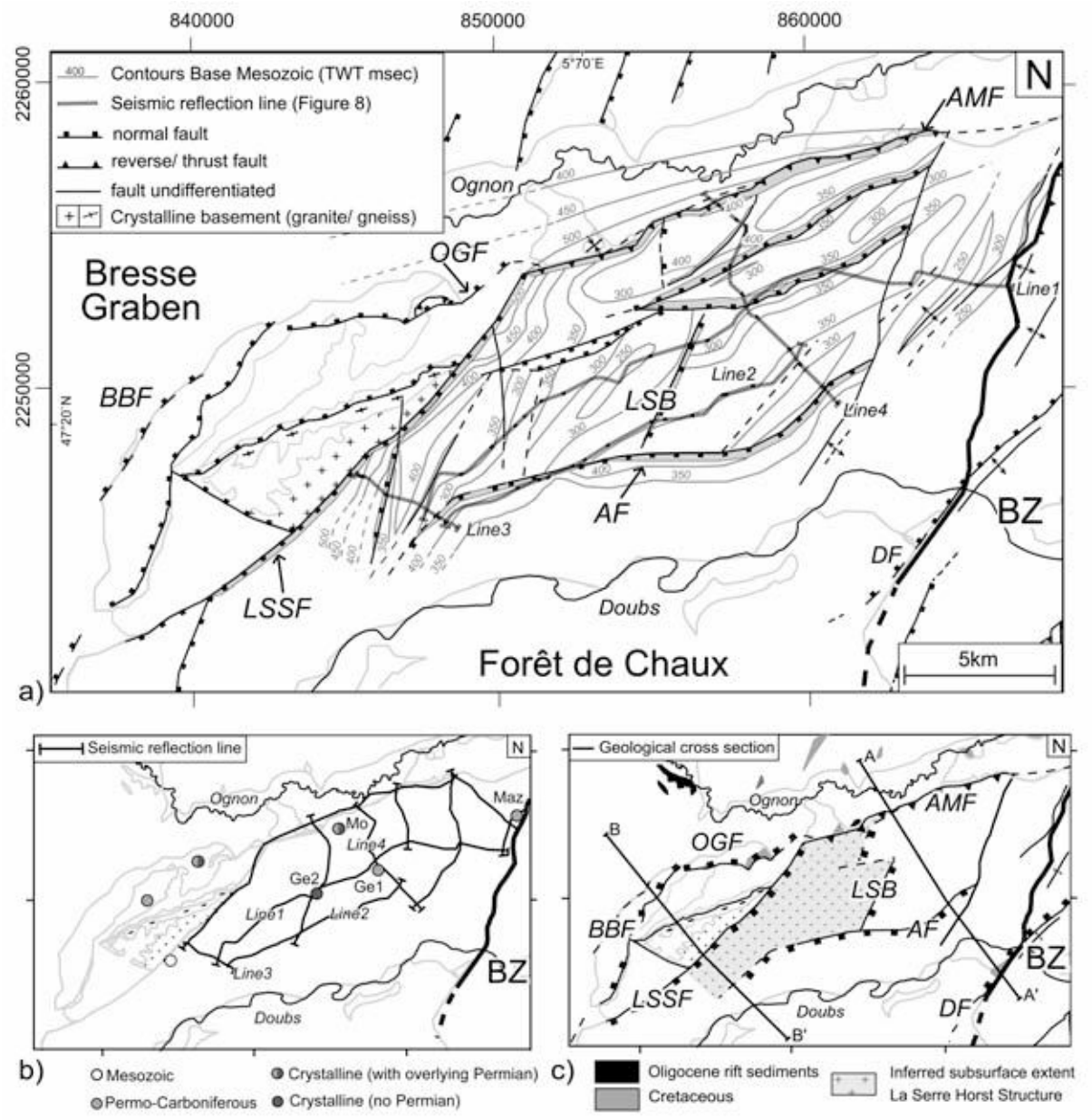

Figure 6: Subsurface data from the Avant Monts Zone.

a) Base Mesozoic subsurface map of the Avant-Monts Zone based on seismic reflection data. Contour lines are given in terms of two-way travel times (msec). Grey shades along fault traces mark fault heaves. The seismic lines shown in Figure 8 are also displayed.

b) Array of seismic reflection lines and deep wells (see Figure 7 for well logs) used for interpretation.

c) Simplified structural interpretation, showing the subsurface extent of the La Serre Horst Structure, location of outcrops of Cretaceous and Oligocene strata marking Paleogene depocenters, and, location of the structural cross-sections depicted in Figure 15. AMF: Avant-Monts Fault; BZ: Besançon Zone; BBF: Bresse Border Fault, DF: Doubs Fault; LSB: La Serre Border Fault; LSSF: La Serre Southern Fault; OGF: Ognon Fault.

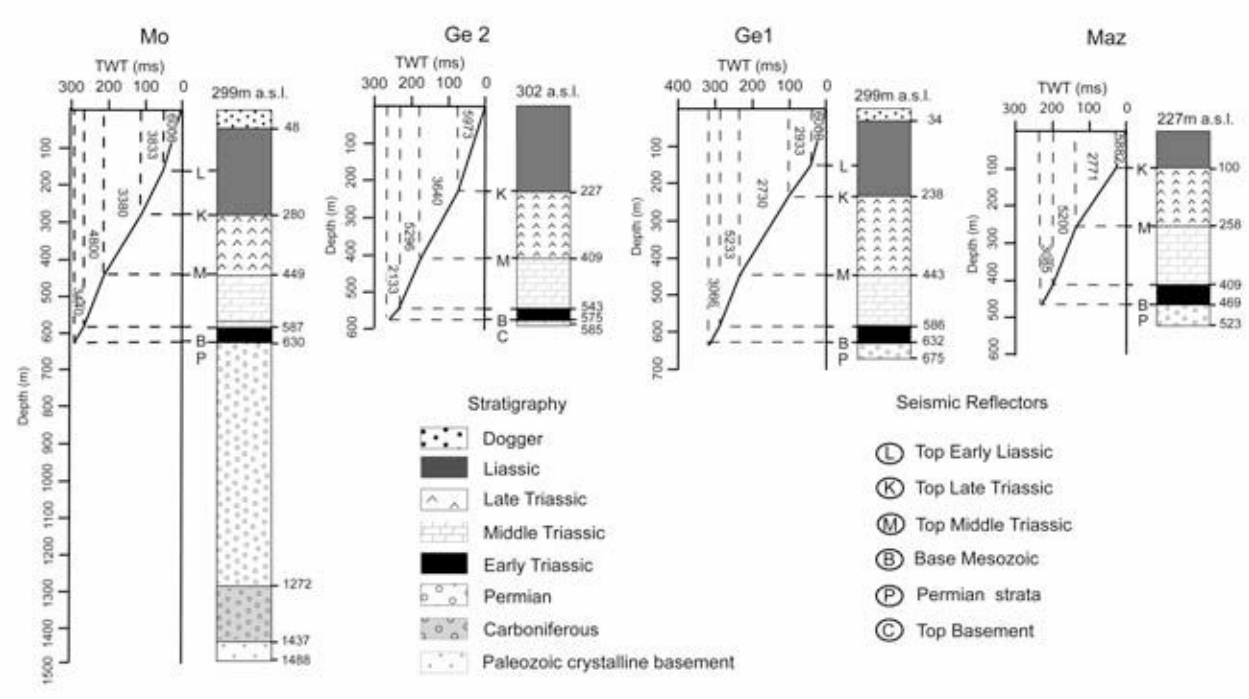

Figure 7: Lithological logs of 4 deep wells from the Avant-Monts Zone, showing seismic interval velocities determined by correlation between seismic reflectors and depth of related stratigraphic horizons (see Figures 3 and 6b for location). Note the position of the seismic reflectors outlined in Figure 8.

(Figure 8a, b). Its inclination to the NW, inferred from the subsurface map (Figure 6a), indicates that the hanging-wall was slightly tilted towards the La Serre Southern Fault.

The ENE-WSW striking set of faults runs parallel to the Late Paleozoic Burgundy Trough system (Figure 2, 6). The most prominent faults of this set are the Ognon, Avant-Monts and Arne faults (OGF, AMF and AF, indicated in Figure 6a) that delimit the La Serre Horst Structure (Figure 2) to the north and south, respectively. Generally these faults show more gentle dips and greater vertical offsets than the NNE-SSE striking ones (Figure 6, 8b, d).

Most of the above-described faults represent pre-existing Late Paleozoic faults that were reactivated during the Cenozoic. This reactivation can be inferred from the seismic sections depicted in Figure 8. In the central part of Lines 1 and 2 (Figures 8a, 8b, locations in Figure 6a) the Mesozoic sediments form several gentle flexures. Slight flexuring of the Mesozoic is visible above the NNE-SSW striking eastern border fault (LSB) of the La Serre Horst Structure (Figure 6a, inset of Figure 8a featuring a detail). Flexuring is much more pronounced above the ENE-WSW-striking normal faults (e.g. the Arne Fault Figures 8b, d) where reactivation clearly appears to be extensional (Figures 8a, b, c). Some of the Cenozoic normal faults have been reactivated in a compressive to transpressive mode during a later stage of deformation.

The best example for later inversion is the Avant-Monts Fault (AMF in Figures 6a, 6c, Figure 8d).

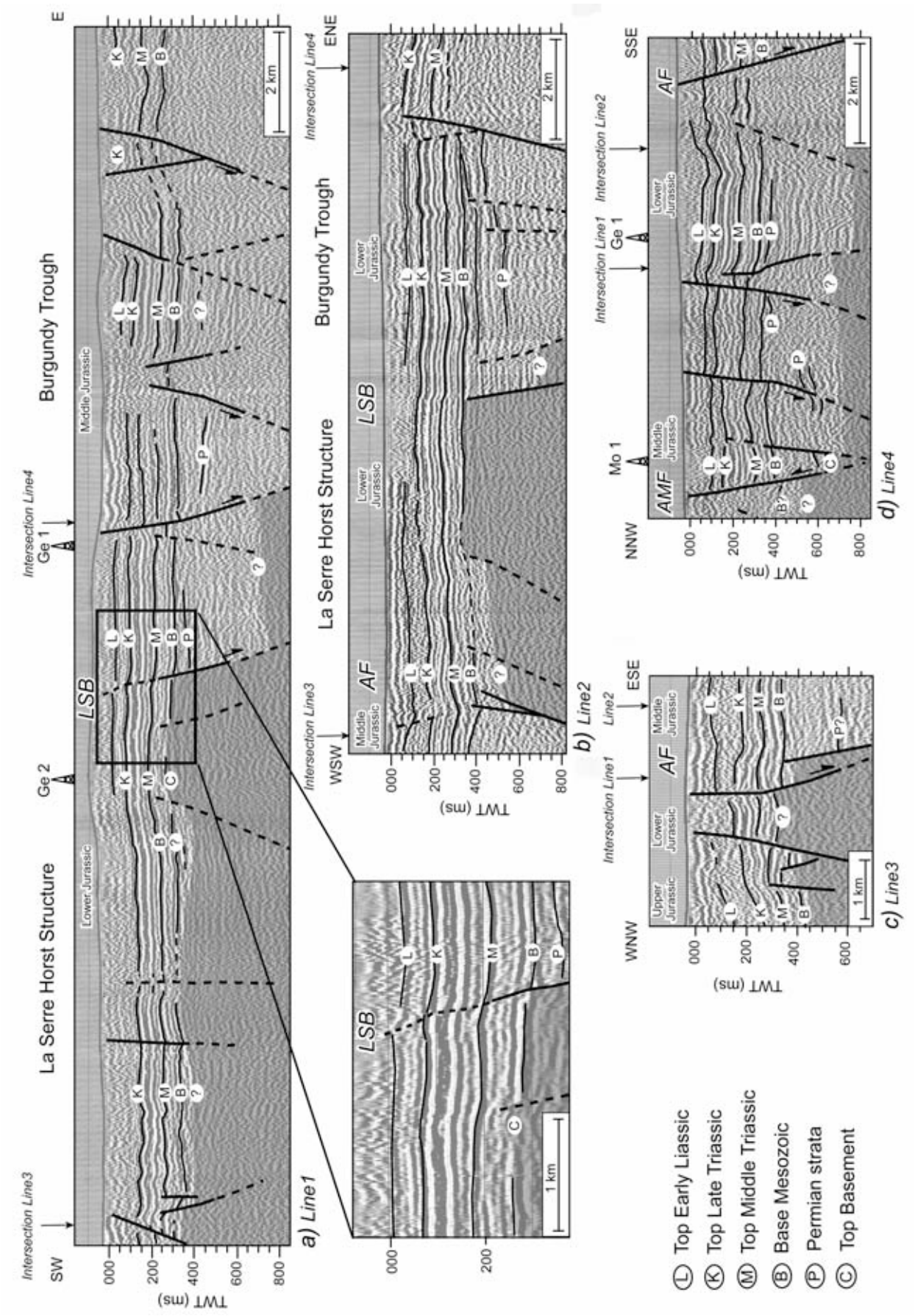
a) Line1
b) Line2
c) Line3
d) Line4
La Serre Horst Structure
Burgundy Trough
LSB
AF
AMF
Ge 1
Ge 2
Mo 1
Intersection Line1
Intersection Line2
Intersection Line3
Intersection Line4
SW
E
WSW
ENE
WNW
ESE
NNW
SSE
Lower Jurassic
Middle Jurassic
Upper Jurassic
TWT (ms)
2 km
1 km
Ⓛ Top Early Liassic
Ⓚ Top Late Triassic
Ⓜ Top Middle Triassic
Ⓑ Base Mesozoic
Ⓟ Permian strata
Ⓒ Top Basement

This fault represents a steep reverse fault that is closely related to an adjacent and ENE-WSW-oriented Cenozoic graben (Figure 8d). This indicates that the Avant-Monts Fault most probably represents an inverted normal fault.

2.5. Brittle deformation and paleostress analysis

2.5.1. Methodology

To assess the kinematic history of post-Jurassic brittle deformation of the RBTZ and possible influences of the LSH we applied a combined kinematic-dynamic paleostress determination based on fault slip data analysis (Angelier and Mechler, 1977; Marrett and Allmendinger, 1990; Pfiffner and Burkhard, 1987).

Analyses were carried out at 56 different sites throughout the entire RBTZ giving more than 2400 fault slip measurements within the data set. Measurements were predominantly carried out on Middle (Bajocian) to Latest Jurassic limestones (Sequanian) and locally on Late Paleozoic granites (sites 48, 49), Permian conglomerates and volcanics (site 47), as well as the Middle Triassic Muschelkalk formation (site 8) (see Table 2). Slickolites are the most frequent slip indicators found. Calcite slickenfibres and lunate fractures (Petit, 1987) were only occasionally found. The kinematic indicators were given quality marks ranging from 1 (excellent) to 3 (poor) (Table 2). Different stages of brittle deformation were detected by overprinting relationships between different striae within one and the same fault plane, or alternatively, by crosscutting relationships between different fault sets (Figure 9).

Figure 8: Selected seismic reflection lines through the Avant-Monts Zone. See Figure 6b for the location of the lines and to Figure 7 for well logs and stratigraphic identification of seismic reflectors. AF: Arne Fault; AMF: Avant-Monts Fault; LSB: La Serre Border Fault.

a) Line1, crossing the subsurface border of the La Serre Horst Structure that is documented by boreholes Ge1 and Ge2 and that appears to be slightly reactivated, as is indicated by the flexure of the overlying Mesozoic strata (see inset).

b) Line 2, paralleling Line1, but also crossing the Arne Fault in the western part of the section, were a pronounced extensional flexure is developed.

c) Line 3, extending from the La Serre Southern Fault, not displayed on the section, all the way across the Arne Fault

d) Line 4, displaying the Avant-Monts Fault, a steep reverse fault that emerges out of a Paleogene/ Late Paleozoic graben and is inferred to have formed by inversion of a former normal fault. The southern part of this section crosses the Arne Fault.

The field data were processed with the Windows-based computer program TectonicsFP (Reiter and Acs, 1996-2000). Data sets from each locality were first separated into homogeneous subsets, based on overprinting and/or or crosscutting criteria observed in the field (Figure 9, 10a). In addition, we applied the pole projection plot (Meschede and Decker, 1993) and the p-t axes method (Marrett and Allmendinger, 1990) in order to graphically test the fault sets for kinematic homogeneity (Figure 10b). Thus, kinematically incompatible fault-striation pairs could be detected within a given subset and be reconsidered as part of another subset, taking also into account the quality of the slip indicators.

In addition to the kinematic analyses based on the p-t axes method (Marrett and Allmendinger, 1990) we also applied the dynamic Right-Dihedra method (Angelier and Mechler, 1977; Pfiffner and Burkhard, 1987) (Figure 10c). While the first method is purely descriptive and calculates the principal axes of incremental strain (Marrett and Peacock, 1999), the latter permits to estimate the orientation of the principal axes of stress ($\sigma1 > \sigma2 > \sigma3$) (Angelier, 1989).

All paleostress methods rely on several assumptions, the most important ones being that (i) slip observed on a fault plane is parallel to the maximum resolved shear stress (Wallace, 1951), (ii) movement on a fault occurred under a homogenous state of stress and (iii) faults do not mechanically interact with each other. The Right-Dihedra method is the most simple paleostress analysis and does not calculate a stress ratio. It is also considered as most robust and especially suited for areas undergoing poly-phase brittle deformation (Angelier, 1989). This method only yields an estimation of the possible orientation of the principal stress axes with the most likely orientation computed at point maxima of superimposed compressional and tensional dihedras, calculated for each fault slip pair (Angelier and Mechler, 1977; Pfiffner and Burkhard, 1987) (Figure 10c). Therefore the Right-Dihedra method considers also movement along possibly pre-existing, reactivated fault planes that are not ideally oriented in respect to a theoretical best-fit reduced stress tensor calculated when applying Direct Inversion methods (Angelier, 1990). Comparative studies have shown that the Right-Dihedra method is less sensitive to highly asymmetric fault plane associations, common in tectonic settings of polyphase brittle deformation (Meschede and Decker, 1993). Comparison of our results obtained by using the kinematic p-t axes with those yielded by the Right-Dihedra method revealed similar results regarding the orientation of incremental strain and the principal stress axes, respectively (Figure 10b and 10c).

Figure 9: Examples of crosscutting and overprinting criteria of brittle structures, allowing to distinguish distinct deformation stages and to establish a relative chronology. Stereographic, equal area, lower hemisphere projections of the fault slip data are also shown (circles, squares and triangles indicate $\sigma1$, $\sigma2$, and $\sigma3$, respectively.

a) Crosscutting generations of normal faults.

b) Steep strike-slip faults indicating ENE-WSW shortening and crosscutting older normal faults.

c) Strike-slip slickoliths overprinting a former normal fault.

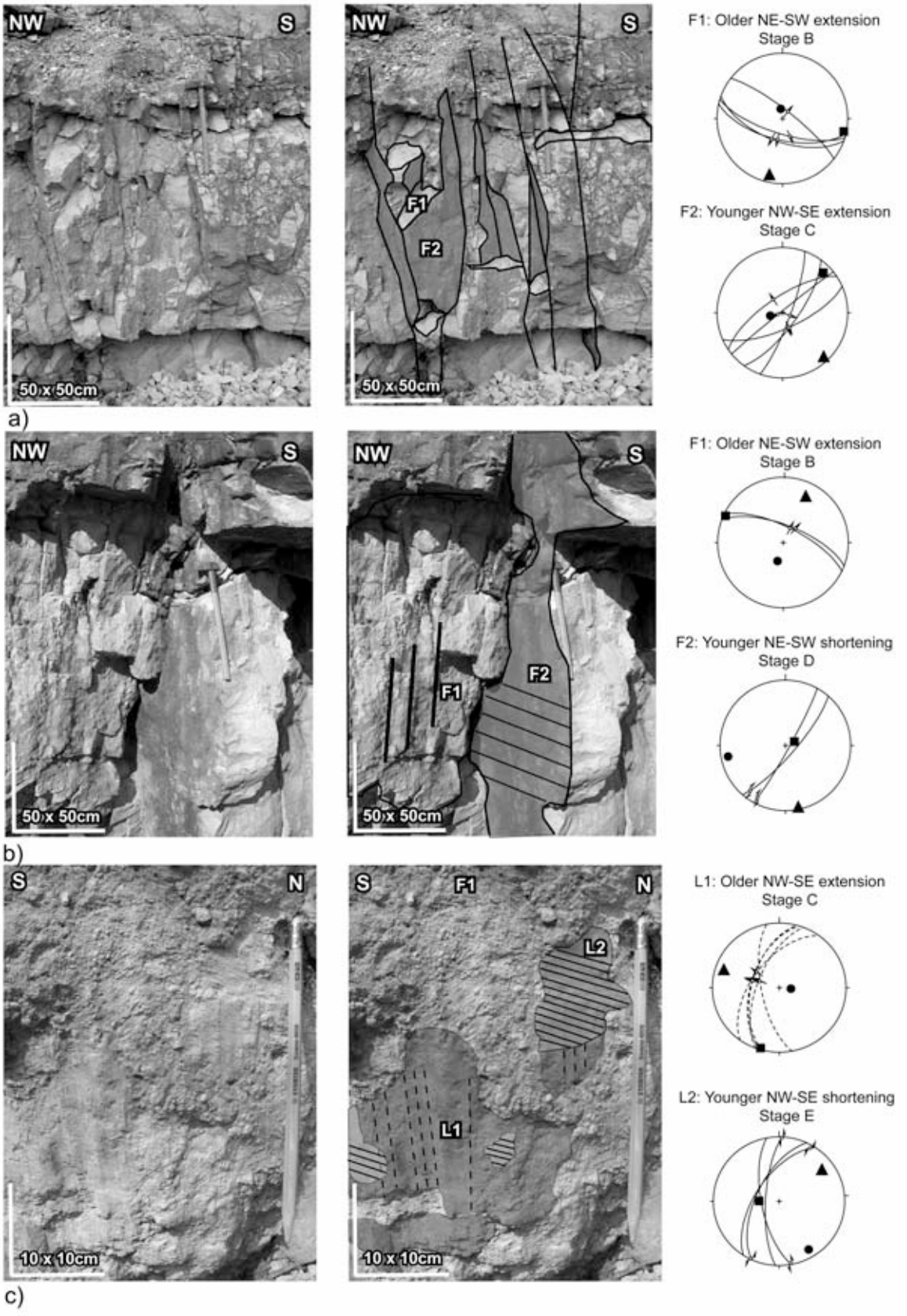
NW
S
50 x 50cm
F1
F2
a)
F1: Older NE-SW extension
Stage B
F2: Younger NW-SE extension
Stage C
b)
F2: Younger NE-SW shortening
Stage D
S
N
10 x 10cm
L1
L2
c)
L1: Older NW-SE extension
Stage C
L2: Younger NW-SE shortening
Stage E

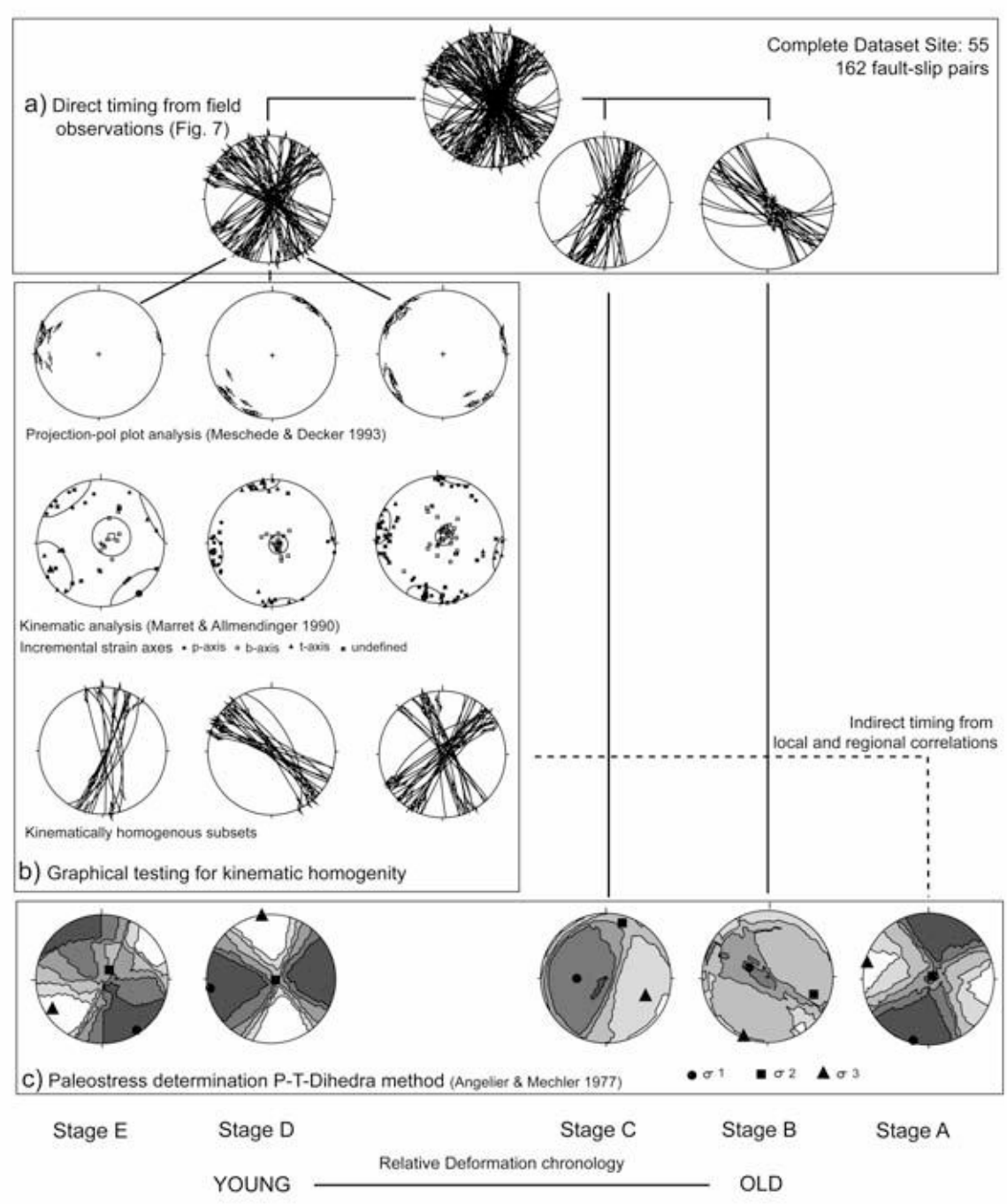

Figure 10: Processing of fault-slip data. Fault slip data shown as stereographic, equal area, lower hemisphere projection

a) Field observations provide the first order criteria for separating the dataset into different deformation events.

b) Graphical tests applied for further separating the remaining dataset into homogenous subsets prior to paleostress analysis.

c) Paleostress analysis using the Right-Dihedra method, as applied to kinematically homogenous subsets in order to estimate the principal stress axis orientations ($\sigma 3 < \sigma 2 < \sigma 1$).

2.5.2. Results

Five different post-Jurassic stages of brittle deformation are distinguished in the RBTZ (stages A to E, Figure 11 and Table 2; stereographic lower hemisphere equal area projections of fault slip data are shown in the appendix of this chapter). Their relative chronology is established by the observation of crosscutting and overprinting structural criteria, and additionally supported by comparison with previous studies from neighbouring areas (Bergerat, 1987; Larroque and Laurent, 1988; Lacombe et al., 1990; Lacombe et al., 1993; Homberg et al., 2002; Rocher et al., 2003; Ustaszewski et al., 2005a) (Figure 9, 10).

The arrows in Figure 11 indicate the azimuth of the axis of either the maximum (σ1) or the minimum (σ3) principal stress, as derived from the Right-Dihedra paleostress analysis for each site during contractional or extensional deformation stages, respectively (Figure 10c). In addition, contoured projections of all tensors (σ1 as circles, σ3 as triangles) obtained for a particular phase are shown. From the orientation of σ1 and σ3 the tectonic regime of the deformation stage can be inferred.

The oldest (Stage A) deformation event is manifested by strike slip faults related to NNE-SSW-directed shortening, (Figure 9, 11b). These faults are commonly reactivated or crosscut by NW-SE or NNE-SSW striking normal faults. The latter define younger events associated with NE-SW (Stage B) and NW-SE (Stage C) directed extension (Figure 11c, d).

NE-SW extension is defined by dip-slip and oblique-slip along NW-SE striking normal faults (Stage B, Figure11) and is almost exclusively restricted to the area around the northern border of the Bresse Graben (BG) and the La Serre Horst (LSH). The NW-SE directed extension (Stage C, Figure11) is constrained by NNE-SSW striking normal faults and is detected throughout the entire RBTZ. The stress tensor related to Stage C shows a systematic change in orientation of the minimum axis of horizontal stress (σ3) throughout the studied area (Figure 11d). The axis of maximum horizontal tension σ3 is oriented WNW-ESE in the eastern part of the study area and progressively rotates into a NW-SE, locally even into a NNW-SSE, orientation in the western part including the LSH area. NW-SE striking normal faults that accommodated NE-SW (Stage B) extension are often overprinted by N-S striking normal faults associated with NW-SE extension of Stage C (e.g. sites 53, 55, 41; see also Figure9a). However, relative overprinting criteria between these two deformation

Table 2: Results of the paleostress analyses based on the Right-Dihedra method (stereographic lower hemisphere equal area projections of fault slip data are shown in the appendix of this chapter). Numbers and letters refer to locations and deformation stages, respectively, as given in Figure 11. σ1, 2, 3: maximum, intermediate and minimum axis of principal stress; Azi.: azimuth; pl.: plunge; N: number of measured faults considered for paleostress calculation; n: number of faults with no indication of slip direction; Q: Quality remark (1: excellent; 2: good; 3: poor); Rot.: Datasets that were inferred to be tilted and were back-rotated prior to paleostress calculation.

Site	Location	X	Y	Age	Stage	σ1		σ2		σ3		N	n	Q	Rot
						Azi.	pl.	Azi.	pl.	Azi.	pl.				
1	ColombiereFontaine	928370	2281073	Sequanien	1 a	29	2	176	88	299	1	22	2	1	
					1 e	335	5	160	85	65	0	14	0	1	
2	Longevelle	926463	2281522	Sequanien	2 a	33	3	275	83	124	6	7	1	2	
					2 c	89	68	189	4	280	21	10	0	1	
					2 e	149	9	292	79	58	6	26	2	1	
3	LongevelleWest	923433	2281634	Sequanien	3 c	329	73	195	12	103	12	4	0	3	x
					3 e	159	5	272	77	68	12	28	1	1	
4	Anteuil	917598	2273891	Bathonien	4 c	279	60	178	6	85	29	16	1	2	
					4 d	47	8	164	74	315	14	13	1	2	
					4 e	184	1	276	76	94	14	36	3	1	
5	Clerval	914680	2273779	Bajocien	5 a	25	4	250	84	115	4	16	1	2	x
					5 c	243	58	4	19	104	26	3	0	2	x
					5 e	170	3	272	75	79	15	23	5	1	
6	L'Hopital St.Lieffroy	912212	2275014	Sequanien	6 a	215	1	34	89	125	0	15	2	2	
					6 c	250	58	355	9	90	30	4	0	1	
					6 e	322	0	53	87	232	3	21	1	1	
7	Soye	913222	2279839	Callovien	7 a	5	1	99	77	275	15	21	1	1	x
					7 e	334	3	100	85	244	4	10	0	1	
8	Vellechevreux	915862	2290580	Middle Triassic	8 a	21	1	286	75	112	15	26	4	2	
					8 e	155	2	258	80	65	10	5	1	2	
9	Vergranne	904581	2280288	Bathonien	9 a	14	0	112	88	284	2	37	11	1	
					9 b	45	64	150	7	224	24	9	7	3	
					9 c	93	54	242	32	341	15	6	0	2	
					9 e	122	7	349	80	213	7	22	8	1	
10	Romain	904581	2280288	Bathonien	10 a	202	5	94	75	293	14	8	3	3	
					10 e	333	1	73	85	243	5	41	6	1	
11	Villersexel	909436	2292712	Middle Triassic	11 c	258	80	71	10	161	1	7	0	1	
12	Aillevans	906601	2296221	Bajocien	12 b	154	50	301	35	43	17	6	0	1	
					12 e	151	5	25	81	242	7	24	3	2	
13	Bonnal	902334	2286785	Argovien	13 d	261	7	20	75	169	13	15	5	2	
14	Cognieres	896726	2285000	Sequanien	14 d	49	1	282	88	139	2	29	0	1	
					14 e	165	13	11	75	257	6	14	0	1	
15	Ormenans	897288	2274789	Sequanien	15 a	218	2	119	78	308	12	14	3	2	
					15 e	349	2	94	82	258	8	20	5	1	
16	Battenans les Mines	898858	2276809	Bajocien	16 a	14	10	133	69	281	18	8	2	2	
					16 e	163	2	33	87	253	3	9	3	3	
17	Rougemontot	897056	2273189	Bajocien	17 c	238	63	355	13	90	24	7	3	3	x
18	Baume-les-Dames	901103	2268729	Bajocien	18 c	343	7	215	78	74	9	6	0	2	x
					18 d	23	4	140	80	293	9	12	2	2	x
					18 e	344	8	193	81	74	4	14	0	1	x
19	Champlive	895267	2262445	Bajocien	19 d	231	0	138	82	321	8	10	0	1	
20	Rigney	891000	2273891	Sequanien	20 c	97	70	217	10	310	17	6	2	2	
					20 e	154	4	292	85	64	4	16	9	2	
21	Traitiefontaine	884495	2275013	Sequanien	21 c	224	66	10	20	105	12	16	1	2	
					21 d	34	3	155	85	304	4	12	2	2	
					21 e	313	2	138	88	43	0	7	5	2	
22	Marchaux	885618	2265475	Bathonien	22 c	102	63	204	6	297	26	21	7	2	
					22 d	33	2	310	83	123	8	38	13	2	
					22 e	307	5	64	79	216	10	43	13	2	
23	Thise	882570	2260539	Bathonien	23 b	335	71	146	19	237	3	7	3	2	
24	Besancon	896165	2259079	Bathonien	24 a	181	2	333	87	90	1	28	1	1	
					24 c	23	69	202	21	292	0	12	4	1	
					24 e	310	3	172	86	41	3	27	7	1	
25	Tallenay	879221	2262109	Bajocien	25 c	349	64	202	22	107	13	7	1	1	x
26	Devecey	875967	2262445	Bajocien	26 c	228	69	48	21	318	0	5	0	1	x
27	Auxon-Dessus	875743	2262333	Bajocien	27 c	115	80	250	7	341	7	9	4	2	x
					27 e	138	6	241	65	45	24	17	0	2	
28	Besancon-Temis	876865	2256723	Bajocien	28 a	203	8	327	76	112	11	15	2	1	
					28 d	258	7	41	81	167	5	9	1	2	
					28 e	139	5	36	68	231	21	36	11	1	
29	Beure	878099	2252458	Sequanien	29 a	188	3	309	83	98	6	17	2	1	
					29 e	144	7	282	80	53	7	39	9	1	
30	Busy	874733	2247858	Bajocien	30 a	187	3	283	68	96	22	13	2	2	x
					30 b	360	71	106	5	197	18	6	0	1	x
					30 c	57	72	226	18	317	3	25	8	1	x
					30 e	320	14	228	9	106	73	28	0	1	
31	Bussieres	870356	2246736	Bajocien	31 b	250	65	151	4	59	25	10	0	1	
					31 e	141	1	288	89	51	1	13	3	2	

Site	Location	X	Y	Age	Stage	σ1		σ2		σ3		N	n	Q	Rot.
						Azi.	pl.	Azi.	pl.	Azi.	pl.				
32	Quiney	870693	2239788	Bathonien	32 c	157	76	6	12	275	7	8	0	1	
					32 e	132	6	16	77	224	12	47	0	1	
33	Pointvillers	870132	2236637	Portlandien	33 b	36	78	281	5	190	11	5	0	1	
					33 e	306	11	117	79	216	2	34	2	1	
34	Pin	865868	2265924	Sequanien	34 d	254	7	79	83	344	1	16	0	3	
					34 e	169	1	30	88	259	1	11	4	2	
35	Chemaudin	869683	2251673	Bathonien	35 a	196	10	324	74	104	13	22	9	1	
					35 c	277	88	34	1	124	2	9	2	2	
					35 e	112	7	339	80	203	7	44	7	2	
36	Rouset Fluans	864477	2247181	Sequanien	36 d	228	2	32	87	137	1	7	2	2	
37	StVit East	865082	2248531	Bathonien	37 a	178	6	32	83	268	4	13	7	3	
					37 b	245	55	142	9	46	34	8	0	1	
					37 e	126	2	13	86	216	4	24	11	2	
38	StVit West	861106	2247349	Bajocien	38 c	221	82	50	8	320	1	13	2	1	
39	Avrigney	859725	2266975	Sequanien	39 c	296	53	204	1	113	37	28	0	1	
40	Marnay	857676	2261435	Rauracien	40 a	198	7	45	82	288	4	22	1	1	
					40 e	325	15	115	73	233	8	20	8	1	
41	Ranchot	837564	2244604	Bathonien	41 b	230	58	138	1	47	32	15	7	1	
					41 c	55	83	186	5	277	5	17	7	1	
					41 d	255	3	41	86	165	2	29	9	2	
					41 e	150	2	311	88	60	1	8	4	1	
42	Monteplain	855656	2244379	Callovien	42 b	206	56	302	4	35	34	4	0	1	
					42 c	185	61	72	12	336	26	8	2	2	
					42 d	71	6	330	63	164	27	13	0	2	
					42 e	167	12	5	76	256	3	31	4	2	
43	Taxenne	853637	2252571	Bajocien	43 b	216	84	109	2	19	6	9	4	3	x
					43 c	147	74	249	4	340	16	7	x	1	x
					43 e	295	13	171	65	30	19	14	5	1	x
44	Gendrey	852178	2251000	Bathonien	44 c	339	82	237	2	147	8	6	1	1	
					44 e	118	2	223	82	28	7	75	28	3	
45	Montagney	852290	2258967	Sequanien	45 b	125	64	278	23	12	11	30	6	1	
					45 c	316	67	215	4	123	23	39	5	1	
					45 e	299	5	45	74	208	15	12	2	3	
46	Brans	845366	2252501	Bajocien	46 b	189	60	325	22	63	19	9	1	2	x
					46 c	59	61	192	21	289	20	7	0	2	x
47	Moissey	843650	2249429	Permian Vulcanite	47 a	355	5	161	85	265	1	12	3	1	
					47 b	78	71	311	12	218	15	13	2	1	
					47 d	58	2	255	8	148	1	13	4	3	
					47 e	333	7	181	82	64	4	27	7	2	
48	Bois deMalange	847016	2248868	Paleozoic Granite	48 c	18	59	218	29	123	9	5	2	3	
49	Forret de la Serre	844772	2247072	Paleozoic Granite	49 b	133	39	341	48	234	14	13	6	3	
					49 e	330	7	81	71	238	17	18	8	1	
50	Orchamp	849709	2243594	Bathonien	50 c	149	56	54	3	322	34	6	0	2	
					50 d	236	5	20	83	146	4	13	1	2	
					50 e	327	1	220	88	57	2	36	20	1	
51	Amange	844435	2246175	Bajocien	51 b	219	66	114	7	21	23	9	2	1	x
					51 c	120	71	233	8	326	17	10	3	1	
					51 e	340	7	82	61	246	28	15	6	2	
52	Jouhe	839834	2242920	Bajocien	52 c	217	54	24	35	118	7	6	2	2	x
					52 d	63	14	228	75	332	4	6	2	2	
					52 e	151	5	260	76	60	13	12	6	1	
53	Authume	839385	2239778	Bathonien	53 b	171	61	272	6	5	28	12	6	2	
					53 c	250	73	35	15	128	10	28	9	1	
					53 d	69	2	322	83	159	6	22	6	2	
					53 e	152	6	31	78	243	10	35	18	1	
54	Mont Roland	837702	2239442	Bathonien	54 c	287	56	27	7	122	33	23	10	1	
					54 c	247	4	142	76	338	13	17	7	3	
					54 d	56	51	308	14	208	35	12	6	2	
					54 e	156	5	45	75	247	14	26	12	1	
55	Monniere	837702	2238544	Bajocien	55 a	194	5	52	84	284	4	32	15	1	
					55 b	296	65	111	25	202	2	23	8	1	
					55 c	268	54	16	12	114	34	37	7	1	
					55 d	261	5	103	84	351	2	19	2	2	
					55 e	140	10	25	68	234	20	18	3	1	
56	Dampiere	834224	2234180	Sequanien	56 a	185	5	51	83	276	5	14	1	2	
					56 b	216	49	102	20	358	34	8	4	2	
					56 c	139	70	46	1	316	20	16	6	1	
					56 d	46	1	189	88	316	1	10	1	1	
					56 e	148	6	51	52	243	37	20	3	1	

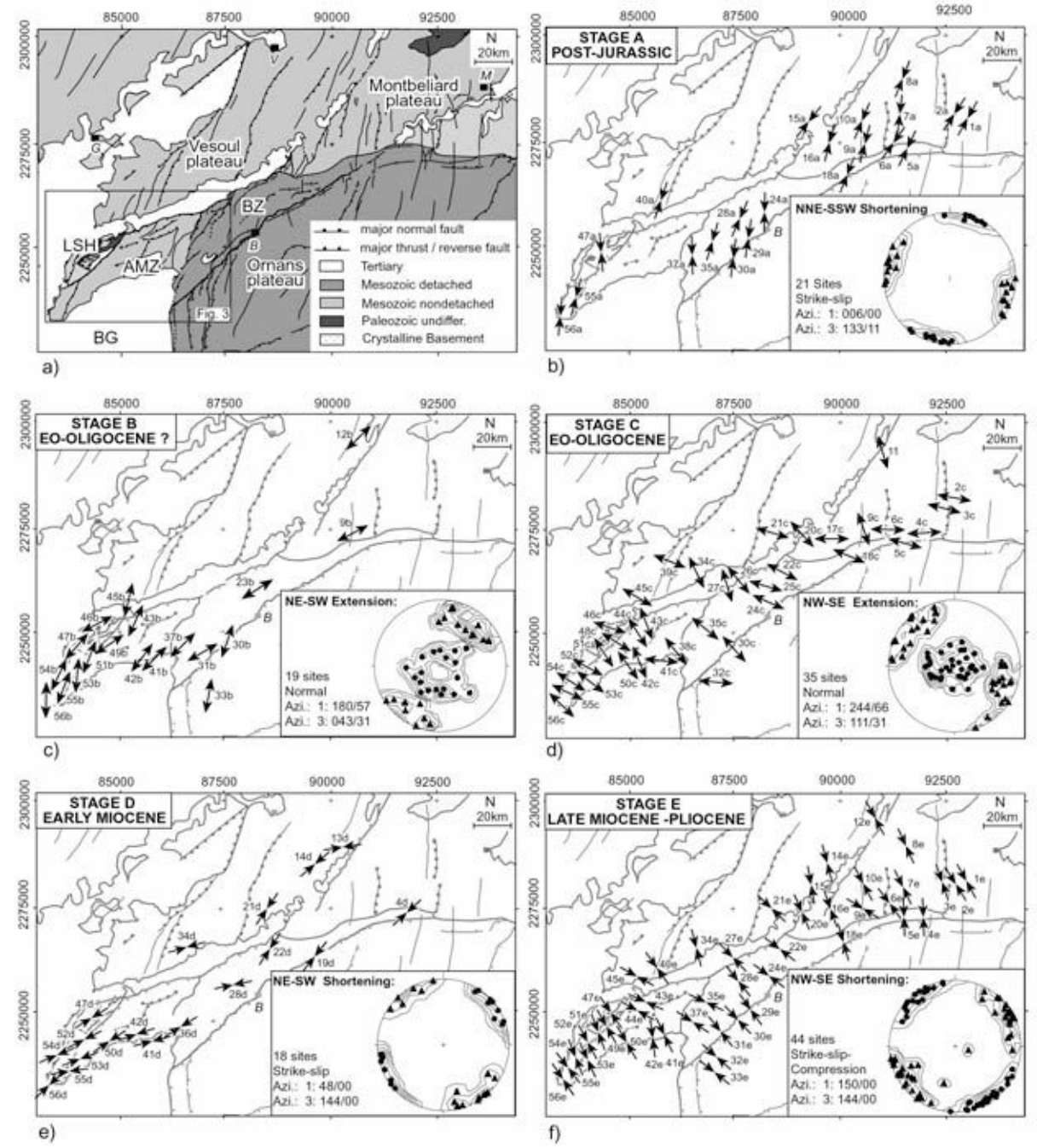

Figure 11: Paleostress maps for the Rhine-Bresse Transfer Zone displayed for 5 different deformation stages. Convergent and divergent arrow pairs indicate the orientation of maximum (σ1) and minimum (σ3) axis of principal stress, respectively, as obtained using the Right-Dihedra method. Insets show contoured equal area lower hemisphere projections of the calculated tensors with circles indicating σ1 and triangles indicating σ3.
a) Tectonic map of the area (tectonic units after Madritsch et al. 2008 submitted). b) Post-Jurassic NNE-SSW shortening. c) NE-SW extension of presumed Eo-Oligocene age, occurring around the La Serre Horst. d) NW-SE extension of Eo-Oligocene age. Note the systematic deflection of the extension direction. e) ENE-WSW shortening, postdating the two extensional deformation phases. f) NW-SE shortening representing the youngest deformation stage recorded.

stages cannot be detected at all sites. All three of these sets of normal faults are clearly overprinted by a fourth deformation event, representing a phase of NE-SW-oriented shortening (Stage D, Figure 11e). The associated fault set is characterized by strike-slip faulting, implying a sub-horizontally oriented direction of maximum principal stress σ1 (e.g. sites 9, 10, 41, 45, 53, 54. 55 Figure 9b).

The latest observed deformation stage (Stage E) represents a NW-SE directed shortening event (Figure 11f) and is, in contrast to Stage D faulting, recorded in almost all the investigated sites (Table 2). In the field it is manifested by strike-slip reactivation of pre-existing NNE-SSW and WNW-ESE striking normal faults (Figure 9c), as well as by newly formed thrust faults along the north western front of the thin-skinned Jura fold-and-thrust belt (Madritsch et al., 2008 in press).

2.6. Data Interpretation and discussion

2.6.1. Timing of exhumation of the La Serre Horst

The combination of fission track analysis with structural data allows constraining the thermal and tectonic evolution of the La Serre Horst (LSH) since the Paleozoic and in the context of the evolution of the European Cenozoic rift system (Figure12). The crystallization age of the La Serre two-mica granite is 362±12 Ma (U-Pb) according to Morre-Biot and Storet (1967). As discussed by Coromina and Fabbri (2004), this Late Devonian to Early Carboniferous age is significantly older than the ages reported more recently for similar Late Variscan granitic intrusions in the Vosges Mountains (Schaltegger et al., 1996) and the Black Forest (357±10 Ma to 325±5 Ma; Echtler and Chauvet, 1991-1992). The La Serre Granite possesses a magmatic foliation that grades into a mylonitic foliation near the La Serre Detachment. This indicates that the exhumation of the granite and the surrounding metamorphic Variscan basement along the La Serre Detachment under NE-SW-directed extension occurred during or shortly after granite intrusion (Coromina and Fabbri, 2004). The granite that is located in the footwall of this detachment may therefore be interpreted as part of a Late Paleozoic metamorphic core complex, similar to those described from the Massif Central (Echtler and Malavielle, 1990). This type of crustal extension is also observed in the southern Black Forest and the Vosges Mountains and is possibly related to magmatic underplating and/or orogenic collapse (Eisbacher et al., 1989; Echtler and Chauvet, 1991-1992; Rey et al, 1991-1992). According to these authors extension started by Middle-to Late Carboniferous times (330-310 Ma). Following these lines of reasoning, the radiometric dating of the granite (362±12 Ma), performed in the 1960'ies and possessing a large error, appears questionable (Figure 12). A much younger age of 317 +/- 5 Ma is indeed indicated by more recent U-Th/Pb monazite EMPA dating (Choulon et al., 2007 unpublished data) which appears more realistic regarding the geodynamic context (Figure 12).

Extension was still ongoing in Late Carboniferous and Permian times, but along high angle normal faults. This later stage of extension led to the formation of the Burgundy Trough and the La Serre Horst Structure (LSHS in Figure 2). The La Serre Horst (LSH in Figure 2), i.e. the outcropping part of the LSHS also comprises parts of the earlier formed (Carboniferous) core complex. However, the observation that Early Permian conglomerates (295-275 Ma) are affected by brittle deformation along the La Serre Detachment (Coromina and Fabbri, 2004) suggests that low-angle faulting and core complex formation were still ongoing during the formation of the La Serre Horst. Therefore low- and high-angle normal faulting must have at least partly occurred simultaneously. Both processes have terminated sometime before the Early Triassic, as is shown by the Lower Triassic sediments of of the Buntsandstein formation that seal Paleozoic basement and non-metamorphosed Permian graben sediments (Figure 5, 12). This can also be inferred from the seismic sections (Figure 8a, b), and moreover, can be seen elsewhere in Western Europe (Ziegler, 1990; Ziegler et al., 2004; McCann et al., 2006). The further Mesozoic thermo-tectonic evolution of the study area was revealed through our zircon and apatite fission-track thermochronological data.

The zircon fission track analyses of the Variscan basement of the La Serre Horst and its Permian to Lower Triassic cover indicate that these rocks have experienced a substantial amount of annealing, as is indicated by the reduction of the central ages with respect of their emplacement or deposition ages (Figure 13). Sample HFT02, a Toarcian (Liassic) claystone, is the only exception (Figure 3; Table 1). This sample experienced only little, if any, annealing and remained at shallower depth compared to the other samples since its deposition. Hence, it will not be used in the following discussion on the thermal evolution of the area. Among the three analysed zircon grains from this sample two central ages are older than stratigraphic age and one is overlapping within the 2σ error.

Unfortunately, it is very difficult to estimate the exact temperatures at which the zircon fission tracks in the analyzed samples were annealed. The large range of single grain and central ages alike (Figure 13 and Table 1) obtained for the analysed samples could be explained by the different degree of annealing which zircon fission tracks experienced at temperatures probably below the upper temperature limit of the partial annealing zone (270° C). This suggestion agrees with the reported maximum temperatures of 200-250 °C, which the Mesozoic sedimentary cover and underlying basement from the URG area have experienced (Brockamp and Zuther, 1983; Surma et al., 2003; Timar-Geng et al., 2004).

The high P ($\chi^{2)}$) values obtained from the analysed samples (higher than 5%) and the respective absence of extra-Poissonian variation of the single grain age distribution does not indicate that they belong to the single age population (see Green, 1981) but is rather a consequence of poor statistic due to the low number of counted tracks. Therefore we conclude that the large spread in single grain ages is related to the different track retentivities of the individual grains within a given sample. Moreover, a

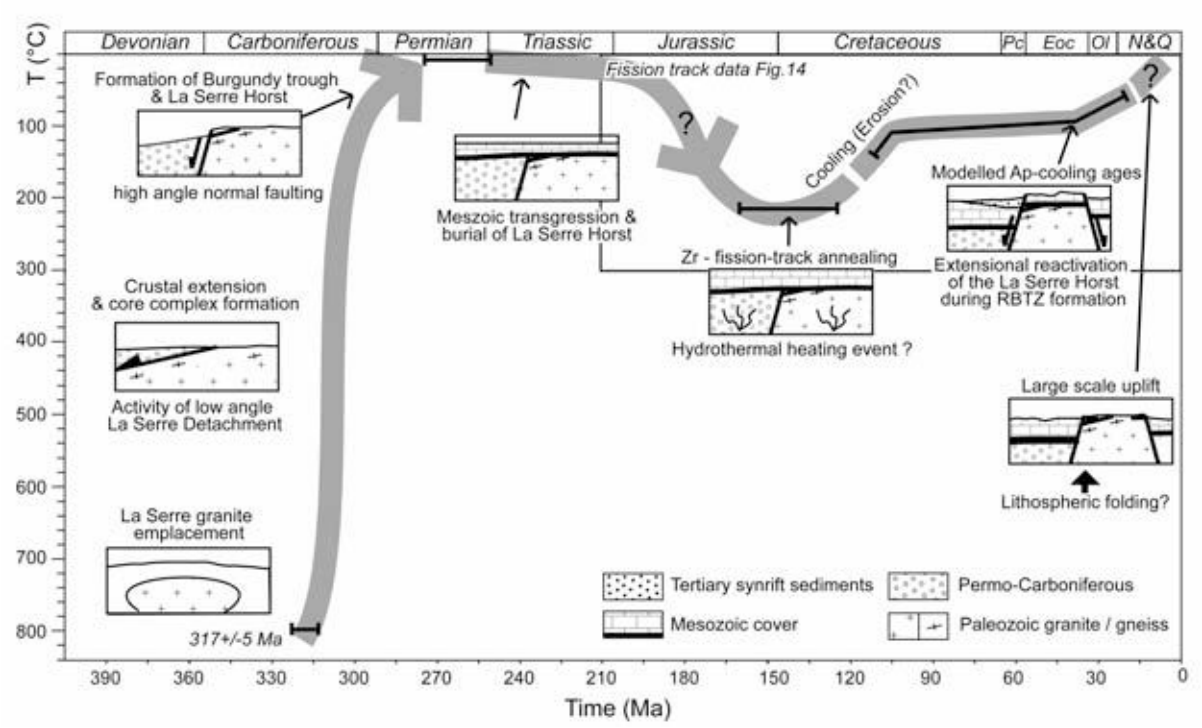

Figure 12: Exhumation history of the La Serre Horst as inferred from fission track and structural data.

relation between lithology and FT ages is also observed. The three granite samples show younger ages (between 131±21 and 136±34 Ma) when compared to the sedimentary and volcanic samples (between 152±28 and 173±37 Ma, again excluding sample HFT02). Although the annealing characteristics of zircon are still poorly understood, the distinct annealing behaviour was probably related to variable amounts of accumulated α-damage and/or compositional variations. The exact timing of the heating event that led to the annealing of the analysed samples is also difficult to be determined. We suggest that this event is most probably of Late Jurassic – Early Cretaceous age (Figure 12). This is the time span for which the zircon single grain age distribution shows a maximum (130 - 160 Ma, Figure 13), possibly implying that the temperature obtained within ZPAZ was a maximum during this period of time. On the other hand, the younger ages commonly attributed to the granite samples probably date final cooling to the temperatures below ZPAZ (see Fügenschuh and Schmid, 2003). After 110 Ma the analysed samples already reached temperatures that are within the apatite partial annealing zone (less than 110° C), as is indicated by the apatite single grains that reach ages up to 110 Ma (Figure 13).

A maximum thickness of 1300m has been estimated from well data (Fleury et al., 1982; Chauve et al., 1983) for the Mesozoic strata presently preserved in the studied area. The total maximum thickness of the Mesozoic sediments, including eventually eroded parts, is estimated to range between 2200-2500m, based on the fission track analyses along the crystalline flanks of the Southern Upper Rhine Graben (Timar-Geng et al., 2006) and the southern French Massif Central (Barbarand et al., 2001).

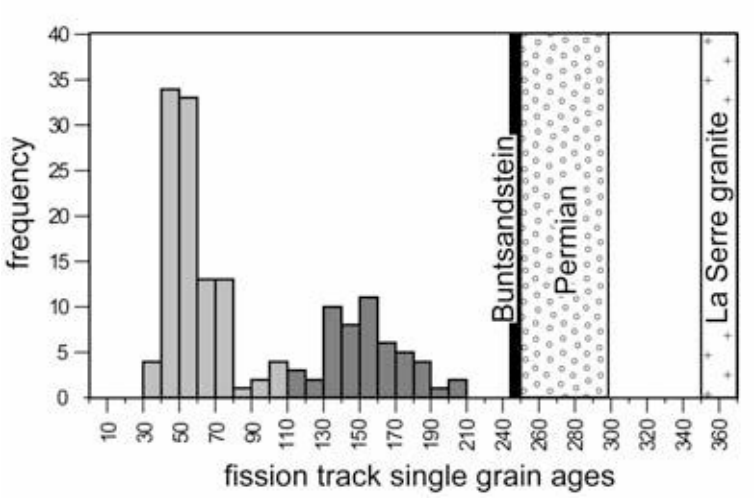

Figure 13: Frequency distribution of the apatite (light grey) and zircon (dark gray) single-grain ages from the analysed samples. Also shown are the ages of emplacement or deposition, respectively, for the samples (compare Table 1). Note that sample HFT02 is not considered.

Therefore, we assume that during this heating event the rocks analyzed in this study were at a maximum depth between 1300 and 2500m. This implies that our FT results indicate an anomalously high thermal gradient that cannot be explained by burial alone. There are no previous studies concerning the thermal evolution of our working area during Jurassic and earliest Cretaceous times, but a similar elevated thermal gradient, presumably due to hydrothermal fluid activity during the Jurassic and Early Cretaceous, was reported for the Variscan basement and its Mesozoic cover from the French Massif Central (Macquar, 1984; Lancelot et al., 1995) and from NW Switzerland, including the area of the Southern Upper Rhine Graben (Wetzel et al., 2003; Timar-Geng et al., 2004). Interestingly, although the thermal pulse is reported as being related to hydrothermal fluid migration, it apparently affected a large area comprising the entire central part of the European Cenozoic Rift System (Timar-Geng et al. 2005). Wetzel et al. (2003) tentatively relate such hydrothermal processes (from Sinemurian to Oxfordian times) to a tectonically induced enhanced subsidence during crustal extension of the continental margin of the Alpine Tethys.

The later thermal evolution of the La Serre Horst is constrained by apatite fission track data. The analysed samples have relatively short mean track lengths (between 12.10 and 12.89 µm; Table 1) with broad and often bimodal distributions (Figure 13). Broad track length distributions, combined with shorter mean lengths, suggest that the samples experienced a complex thermal history and that they spent a significant amount of time within the PAZ for apatite (Gleadow et al., 1986). We modelled the apatite fission track data in order to quantify timing and amount of cooling experienced by the samples analysed as they remained within the apatite PAZ (Figure 13). Modelling of the apatite ages and the track length distribution data was completed with the Monte Trax program of Gallagher (Gallagher, 1995), using an initial track length of 16.3 µm. A composition of Durango apatite was used with the Laslett model when running modelling programs.

The Zircon FT central ages, combined with the thermal evolution modelled on the basis of the apatite data, reveal a thermal history that is characterized by two distinct periods of cooling since Late

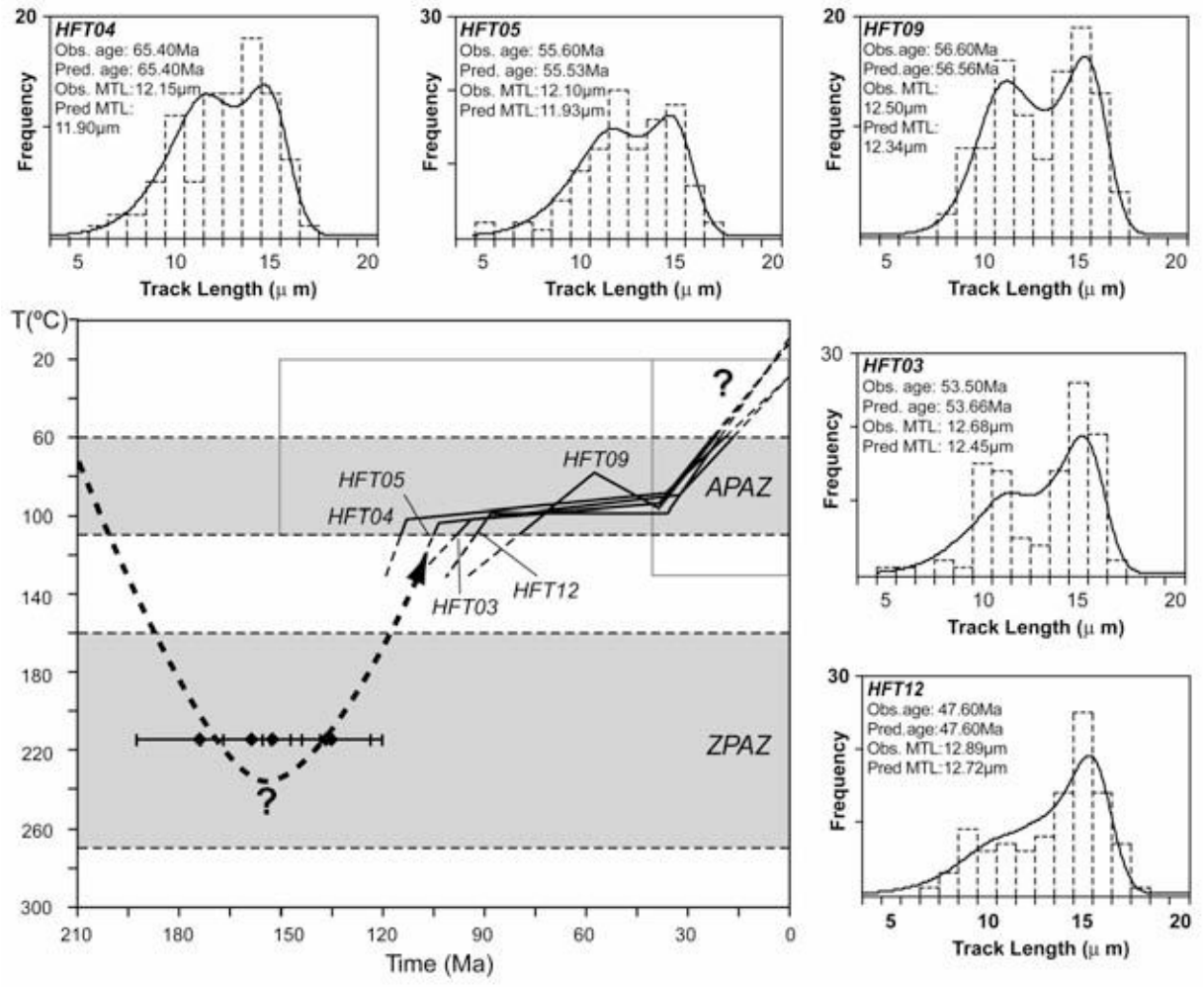

Figure 14: Modelled thermal history and comparison between observed and predicted fission track parameters for the individual FT samples from the La Serre Horst. The upper left corner of the model diagrams compares the observed ages with those predicted by the model; also given are the observed and predicted mean track lengths (MTL). The thick black lines in the model diagrams represent the best-fit model. The apatite partial annealing zone lies within the temperature limits assigned by Laslett et al. (1987).
The dashed segments of the thermal histories at temperatures lower than 60 °C only indicate a possible continuation of the thermal history because the annealing model is not sufficiently sensitive below 60 °C. The modelled T–t paths are extended into the zircon partial annealing zone (Brandon et al., 1998) where the black diamonds represent the zircon FT ages for the modelled samples. See Figures 3, 4, 5 and Table 1 for more details on the samples.

Jurassic times (Figure 14). A first cooling event occurred during the Early Cretaceous (Figure 12 & 14) and is probably related to thermal relaxation after hydrothermal activity in the area ceased. Some of this cooling could also be attributed to erosional denudation, as is suggested by the presence of intra-Cretaceous unconformities in the area (Chauve et al., 1983). This cooling was followed by a Late Cretaceous to Early Cenozoic period of relative quiescence for which only extremely slow cooling

rates are inferred within the 100° to 90 °C temperature range (Figures 12, 14). The only exception to this is sample HFT09, which still experienced relative cooling to temperature of less than 80 °C during this same period of time (Figure 14). The modelling of the data predicts that a relatively high geothermal gradient was maintained all the way to the Early Paleogene. However, it must be pointed out that relative variations in the temperatures estimated by the modelling in the order of ±30°C need to be considered in order to allow for the dependency of the track annealing process on the apatite composition, in particular the Cl/F ratio (Green et al., 1985; Green et al., 1986; Burtner et al., 1994).

A second, well-pronounced and relatively fast cooling event started some 38 to 32 Ma ago (Figure 14). Since the start of this cooling event coincides rather well with the onset of syn-rift deposition in the URG (Mid to Late Eocene 42.5-36 Ma, Berger *et al.*, 2005; Hinsken *et al.*, 2007) it is interpreted as a consequence of accelerated erosion in the La Serre Horst Structure due to extension and rift shoulder uplift (Dèzes *et al.*, 2004; Ziegler and Dèzes, 2007). Eocene to Oligocene cooling related to rifting was also suggested by Timar-Geng et al. (2005), based on apatite fission track modelling on crystalline samples from the flanks of the Southern Upper Rhine Graben. Most importantly, this second cooling event indicates that the La Serre Horst, already formed in Permian times, was substantially reactivated during Eo-Oligocene rifting; hence it must be considered an active horst structure also during this tectonic phase. Sample HFT09, collected near to the main border fault delimiting the La Serre massif to the north, namely the Ognon Fault (Figure 4), shows some late heating with its temperature maximum being attained at about 38 Ma (Figure 14). This heating could possibly be related to hot fluids circulating along the fault that was active during that time.

In summary, the fission track data presented in this study show that substantial exhumation of the La Serre Horst Structure started during Cenozoic rifting, i.e. before the end of the Oligocene (~23 Ma). However the fission track data do not constrain the timing of final exhumation of the rocks to the earth's surface (Figure 12, 14). This last cooling event was probably driven by large-scale Early Miocene uplift of the northwestern Alpine foreland due to lithospheric deformation (Dèzes *et al.*, 2004; Bourgeois *et al.*, 2007; Ziegler and Dèzes, 2007) induced by the Alpine collision (Figure 12). Thick-skinned dextrally transpressive reactivation of the Rhine-Bresse Transfer Zone in Early Pliocene to recent times (Madritsch et al., 2008 in press) could also have contributed to the final exhumation of the La Serre Horst that forms a restraining bend in such a dextrally transpressive tectonic setting.

2.6.2. Structural grain of the western Rhine-Bresse Transfer Zone

We now interpret and discuss the relationship between the Late Paleozoic Burgundy Trough and La Serre Horst Structure (Figure 2) and the post-Jurassic fault pattern recorded in the Mesozoic cover. Our interpretation is based on the base-Mesozoic (B reflector) contour map presented in Figure 6a and

two interpretative structural cross-sections given in Figure 15. The latter were constructed using existing geological maps (Bonte, 1975; Chauve et al., 1983; Chauve et al., 1979; Dreyfuss and Kuntz, 1969, 1970), complemented by our own field measurements, as well as by the available seismic and well data.

The Ognon Graben parallels the present-day valley of the Ognon River NNE of the La Serre Horst Structure and represents a small Paleogene depocenter as shown by Oligocene synrift sediments (Chauve et al., 1983) (Figures 3, 6c 15a). It strikes ENE-WSW and merges with the northern end of the Bresse Graben further to the west (Figure 15b). In map view the location of the southern border fault of the Ognon Graben can only be traced in the north eastern-most part of the study area, where it is delimited by the NE-SW striking Ognon Fault (OGF in Figure 1). Along this fault remnants of Oligocene rift sediments are also reported (Dreyfuss and Théobald, 1972). The Ognon Fault can be traced further to the north into the Vosges Mountains (Figure 1, 2), where it follows a major Paleozoic lineament (Ruhland, 1959). This indicates that the Ognon Normal Fault, in the sense of a Cenozoic-age normal fault, probably reactivated a Paleozoic basement fault. South-westward we suspect that both faults bend and run further west along the ENE-WSW oriented Ognon Valley (Figure 6, 15a). Near its western termination it delimits the La Serre Horst and finally merges with eastern Bresse Graben Border Fault BBF (Figures 1, 3, 6, 15a, b). The Avant-Monts Fault (AMF in Figures 1, 3, 6, 8d, 8, 15a) represents a steep south-dipping reverse fault, as is evident from the seismic reflection data. It runs parallel to the Ognon Graben and the south-dipping Ognon Fault in the area between La Serre Southern Fault (LSSF in Figure 6, Figure 15b) and the western segment of the Ognon Fault. The base Mesozoic subsurface map (Figure 6a) reveals that the Avant-Monts Fault also borders an ENE-striking Paleogene graben. Therefore the Avant-Monts Fault most likely developed by inversion of a Paleogene normal fault and its presumed Late Paleozoic precursor.

The Arne Normal Fault (Chauve et al., 1983) (AF in Figures 6, 8b, d, 15a, b) strikes ENE-WSW and is interpreted as the southern boundary of the La Serre Horst Structure. Most probably it also represents a Paleozoic fault that was reactivated in extensional mode during Cenozoic rifting (Figures 8b, c, d, 15b). Together with the southerly adjacent Doubs Normal Fault (DF in Figures 6 & 15a) it forms the small ENE-WSW striking Doubs Graben that merges with the main Bresse Graben in the area of the Forêt de Chaux (Figure 6a, 15a, b). Like the Ognon Fault, the Arne Fault and the Doubs Fault are marked by extensional flexures in the Mesozoic cover (Figure 8b, d, 15a). Remnants of Cretaceous sediments are preserved in the core of the flexure along the Doubs Fault (Figures 3, 6c, 15a) (Chauve et al., 1979). The Doubs Fault also marks the front of the thin-skinned Jura fold-and-thrust belt (Figures 3, 15a). Further to the east it is overridden by the thrust sheets of the Besançon Zone, which is part of the Jura-fold-and-thrust belt (Figure 1, 3) and thus cannot be traced towards the southern Upper Rhine Graben (Madritsch et al., 2008 in press). Based on these observations and interpretations we conclude that the La Serre Horst, first formed during the Late Paleozoic, was reactivated during Early Cenozoic extension when it represented a structural high between two

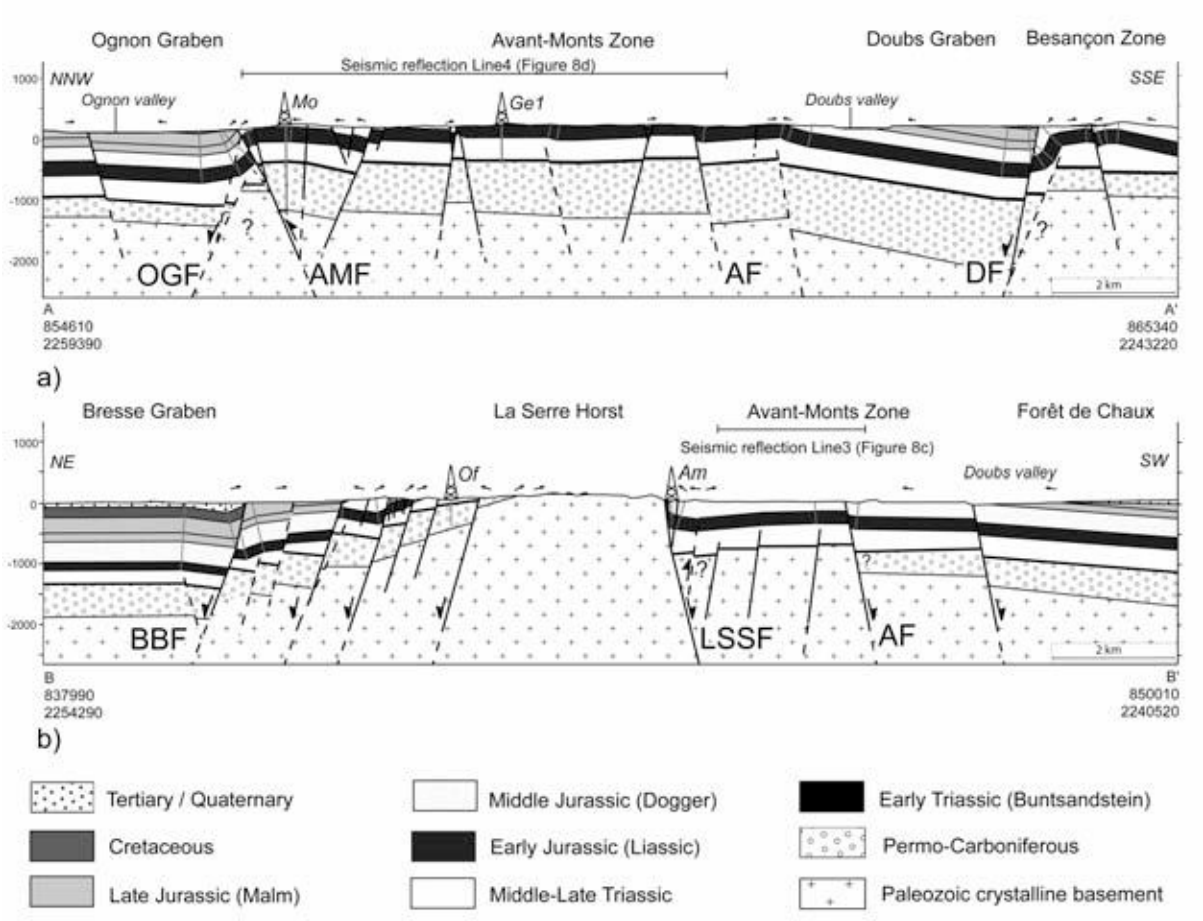

Figure 15: Interpretative geological cross sections. See Figures 3 and 6c for the location of the cross sections. For the exact location of the wells, see Figures 3 and 6b; locations of seismic reflection lines are indicated in Figure 6b. AF: Arnes Fault; AMF: Avant-Monts Fault; BBF: Bresse Border Fault; DF: Doubs Fault; LSSF: La Serre Southern Fault; OGF: Ognon Fault. a) Cross section across the Avant-Monts Zone b) Cross section across the La Serre Horst.

Paleogene grabens (the Ognon and Doubs grabens Figure 15a). These grabens are bounded by ENE-WSE striking normal faults that caused extensional flexures within the Mesozoic cover (Figure 15a), similar to those reported from the southern Upper Rhine Graben (Ustaszewski et al., 2005a; Ford et al., 2007). These ENE-WSW striking normal faults follow the Late Paleozoic Burgundy Trough System and are highly oblique to the faults bordering the Upper Rhine and Bresse grabens. This reveals their inherited character (Figure 2). Most importantly, the inferred extension perpendicular to the strike of these normal faults, i.e. in a NNW-SSE direction, is in agreement with the paleostress data (Figure 11d Stage C).

2.6.3. The kinematics of Cenozoic deformation

Based on our paleostress analysis the following Post-Jurassic stages of deformation in the area of the RBTZ can be constrained (Figure 11):

The earliest deformation stage (Stage A in Figure 11b) implies NNE-SSW-directed shortening, as recorded throughout the entire European platform (Bergerat, 1987; Dèzes et al., 2004). Most of the previous authors interpreted this event to be of Early Eocene age and related it to the Pyrenean orogeny (Bergerat, 1987; Lacombe et al., 1993; Rocher et al., 2003; Dèzes et al., 2004). Michon and Merle (2005) however suggested a Latest Cretaceous to Early Paleocene age for this stage and related it to a phase of intra-plate compression, that is evidenced by the development of a regionally recognized erosional unconformity throughout the northwestern Alpine foreland (Ziegler, 1990). Concerning the area of the southern Upper Rhine Graben, Schumacher (2002) proposed that σ1 was N-S oriented during this phase of intra-continental compression, and subsequently rotated clockwise to a NNE-SSW orientation during late Middle to Late Eocene times. Rifting presumably initiated under the latter stress field orientation (Dèzes et al., 2004).

Two extensional stages (Stages B and C in Figure11c, d) followed this earlier shortening in the area of the La Serre Horst. NE-SW extension during stage B is recorded only locally (Figure 11c) and we attribute it to local Eo-Oligocene-age stress field perturbations around the La Serre Horst, as will be discussed below. However, it has to be noted that the NE-SW extension has also been reported from adjacent regions by previous studies, and interpreted differently. In the internal Jura fold-and-thrust belt the NE-SW extension was reported locally by Homberg et al. (2002) who inferred a maximum Cretaceous age for this deformation event. In the Burgundy area the NE-SW extension was attributed to a Late Mesozoic deformation phase, which predates N-S shortening related to Pyrenean orogeny (Lacombe et al., 1990). The latter interpretation was mostly based on correlations with the Swabian and Francian Jura (Bergerat, 1985). In the eastern Paris basin Coulon and Frizon De Lammotte (1989) made contradicting interpretations and suggested a Latest Oligocene age for the NE-SW directed extension event.

Ustaszewski et al. (2005a), on the other hand, reported similar extension directions related to the opening of the southern Upper Rhine Graben and occurring only in the vicinity of major ENE-WSW striking flexures. These authors suggested that this N-S to NE-SW extension was simultaneous with the widely recognized predominant WNW-ESE extension of Eo-Oligocene age. Based on these findings, and also because clear overprinting criteria between stage B and stage C deformations are scarce, we do not favour the idea of the existence of separate stage of NE-SW directed extension for our working area. Deciphering a relative chronology between the local NE-SW (Stage B) and the widely recognized Stage C extension event (Figure 11c and 11d) from crosscutting observations was only possible at some localities. In the absence of stratigraphic criteria, such overprinting criteria must be taken with caution. In summary, we favor simultaneous Eo-Oligocene activity of Stage B and Stage

C normal faulting during an overall NW-SE directed extension related to the Paleogene rifting. The fact that NE-SW oriented σ3-axes are detected exclusively around the La Serre Horst (Figure 11c) suggests that it rather reflects a local stress field perturbation during the formation of the Upper Rhine and Bresse grabens, due to the rheological heterogeneities induced by the pre-existing La Serre Horst.

The more widely observed Stage C NW-SE extension (Figure 11d) is interpreted to reflect the main extensional phase that led to the opening of the Upper Rhine and Bresse grabens in Late Eocene to Oligocene times (Bergerat, 1987; Hinsken et al., 2007; Rocher et al., 2003; Schumacher, 2002; Ziegler, 1992). The observation that extension in the Rhine-Bresse Transfer Zone (RBTZ) is predominantly NW-SE orientated is in agreement with previous studies on brittle deformation that applied Direct Inversion paleostress methods (Bergerat, 1987; Lacombe et al., 1993). Assuming the overall orientation of the axis of minimum horizontal stress (σ3) to be indeed roughly E-W-oriented during the evolution of the rest of the European rift system (Bergerat, 1987; Lacombe et al., 1993; Michon and Merle, 2001; Schumacher, 2002; Ustaszewski et al., 2005a), the paleostress pattern in the RBTZ must be considered as perturbed, as was outlined by Lacombe et al. (1993). This perturbation is most distinct around the La Serre Horst where the extension direction even deviates from the regional trend by up to 80 degrees (see stage C data in Figure 11d).

The NE-SW oriented stage D shortening associated to strike-slip faulting (Figure11e) clearly post-dates Paleogene extension during stages B and C. This compressional event has also been reported from the Burgundy area (Lacombe et al., 1990), the northern Bresse Graben (Rocher et al., 2003) and the eastern parts of the European platform (Bergerat, 1987). We share the interpretation of Bergerat (1987) and Schumacher (2002), that this event is of Aquitanian age and that it marks the build-up of collision-related stresses in the northern Alpine foreland. Similar to what was observed in the northern Bresse Graben area (Rocher et al., 2003), this event represented a permutation between σ2 and σ1 throughout the RBTZ, while the orientation of σ3 remained approximately constant.

Stage E deformation, representing the last stage of deformation, is characterized by roughly NW-SE directed shortening (Figure 11f). It is interpreted to reflect Late Miocene to recent compression related to Alpine collision processes. Such a deformation propagated far northward into the distal foreland of the Alps (Rocher et al., 2004). At first the compression was restricted to the Mesozoic cover, when the formation of the thin-skinned Jura fold-and-thrust belt initiated and when the northwestern-most segment of this decoupled cover, the Besançon Zone, encroached onto the RBTZ (Madritsch et al., 2008 in press). From the Early Pliocene onwards, however, this compression also affected the underlying crystalline basement and induced thick-skinned reactivation of pre-existing basement faults related to the formation of the RBTZ in particular and the southern Upper Rhine Graben in general (see also Giamboni et al., 2004; Rotstein et al., 2005; Ustaszewski and Schmid, 2007; Madritsch et al., 2008 in press). In our study area this style of deformation is typically expressed by the steeply dipping Avant-Monts reverse fault (AMF), which represents an inversion of the Paleogene-age Avant-Monts Normal Fault. The reverse movement along the AMF was accompanied

by the reactivation of La Serre Southern Fault and the Ognon Normal Fault, leading to partial inversion of the RBTZ in a regime of dextral transpression (Madritsch et al., 2008 in press).

2.6.4. Strike-slip dominated transform zone or oblique graben?

Finally we also discuss our combined dataset in the light of the tectonic concept of the so-called Rhine-Bresse Transfer Zone (or Rhine-Sâone Transform Zone; Bergerat and Chorowicz, (1981)). Two distinct kinematic models for the formation of the RBTZ were proposed (Figure 16). A first one by Bergerat (1977) suggested that E-W extension in the Rhine- and Bresse grabens occurred under a dominant N-S compression and was transferred along the RBTZ by pure strike-slip reactivation of an ENE-WSW striking basement fault system (Figure 16a). Lacombe et al. (1993) modified this concept and suggested that the RBTZ formed by sinistrally transtensional reactivation of a ENE-WSW striking basement fault systems under overall E-W extension (Figure 16b, see also Figure 2). Thereby NW-SE extension within the RBTZ is regarded as reflecting local stress (and strain) perturbations within the sedimentary cover under crustal-scale E-W directed extension during the formation of the European Cenozoic Rift System (e.g. Lacombe et al. 1993). A large-scale, deep-seated wrench fault, reactivating the pre-existing Paleozoic ENE-WSW striking fault system could cause such perturbations at shallow depth. However, the available data do not point towards reactivation of such wrench fault at great crustal depth.

In any case, our data do not support the idea that the RBTZ represents a distinct intra-continental transform zone dominated by strike slip tectonics (Figure 16a). Instead, following Hinsken et al. (2007), we propose that the RBTZ represents an inherited and oblique graben segment within the European Cenozoic Rift System, which is also dominated by extension (Figure 16c). We share this conclusion based on the following lines of evidence:

1) The fission track analyses show that the Late Paleozoic La Serre Horst was reactivated during the Eo-Oligocene formation of the RBTZ (Figure 12, 14). This requires a substantial amount of extension and pleads against a pure strike-slip mode of deformation within the RBTZ.

2) Subsurface data show that basement reactivation was mainly extensional and led to the formation of major ENE-WSW striking normal faults, the most notable examples being the Ognon, Avant-Monts, Arnes and Doubs faults that all feature distinctive extensional flexures (Figure 8, 15 a, b). These faults are parallel to the ENE-WSW aligned Paleogene graben and horst structures that are oriented highly oblique to the overall trend of the European Cenozoic Rift System. The fact that these faults also parallel the Late Paleozoic Burgundy Trough and the La Serre Horst emphasizes their inherited character.

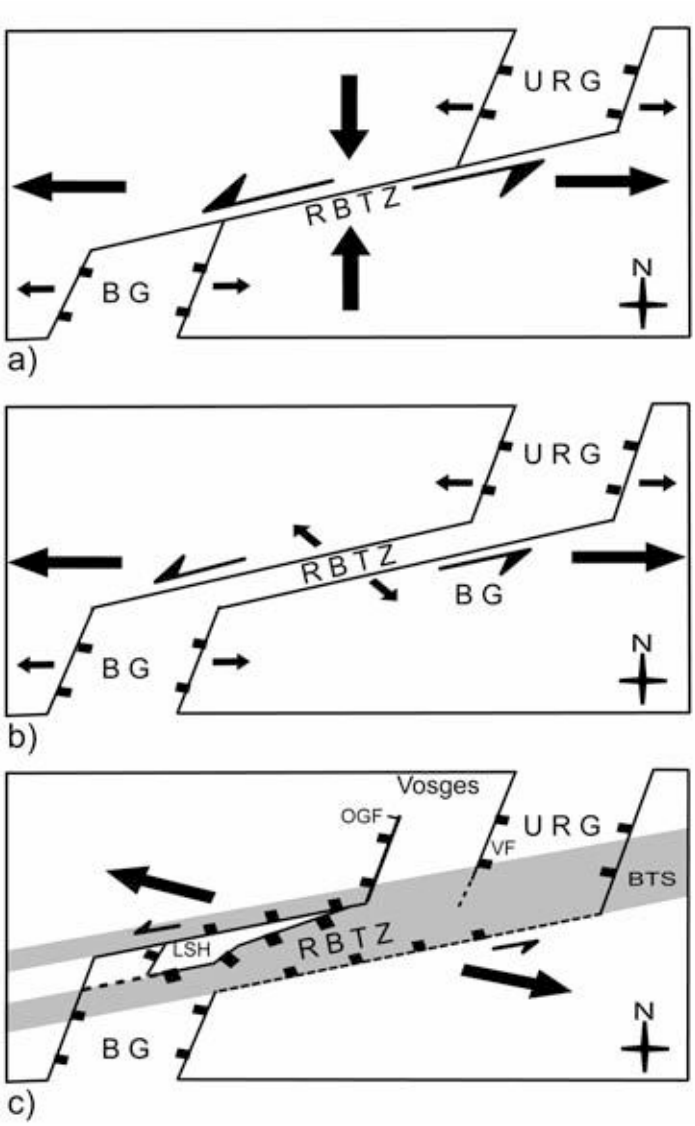

Figure 16: Comparison of genetic and kinematic models for the formation of the Rhine-Bresse Transfer Zone: a) N-S compression resulting in E-W extension along the Rhine and Bresse graben and formation of the RBTZ by pure strike-slip reactivation of a pre-existing basement fault (Bergerat, 1977). b) Overall E-W extension causes sinistral transtensive reactivation of a basement fault that leads to stress pertubations with σ3 trending NW-SE in the RBTZ (Lacombe et al., 1993). c) Overall NW-SE extension leads to the oblique extensional reactivation of the Burgundy Trough and La Serre Horst with a minor sinistral transtensive strike-slip component (this study). BG: Bresse graben; BTS: Burgundy Trough System; LSH: La Serre Horst; OGF: Ognon Fault; RBTZ: Rhine-Bresse Transfer Zone; URG: Upper Rhine Graben; VF: Vosges Fault

3) Individual major ENE-WSW striking normal faults that are part of the fault set characterizing the Rhine-Bresse Transfer Zone cannot be directly interconnected to each other across the area between the Upper Rhine and the Bresse grabens. For example, the Ognon Fault that reactivated a Paleozoic normal fault cannot be traced into the Southern Upper Rhine Graben itself, but instead bends eastward into a NE-oriented strike and runs into the Vosges mountains (Ruhland, 1959). Hence, the Ognon Normal Fault is not capable to transfer extension from the Bresse Graben to the Southern Upper Rhine Graben by sinistral or sinistrally transtensional movement. This is further supported by the observations of Ford et al. (2007), who found that the western border fault of the Upper Rhine Graben (Vosges Fault), which represents the most likely candidate to form the eastern connection of the Ognon Fault, does not connect into the RBTZ but rather dies out east to the city of Montbéliard (Figure 1, 2).

4) At the outcrop scale dip-slip normal faults are dominant throughout the area. When applying the simple but robust P-T Dihedra method, the results of the paleostress analysis regarding stage C deformation (Figure 11d) indicate that the axis of minimum horizontal stress, and therefore the direction of extension, is slightly oblique to the structural grain of the RBTZ striking NW-SE. These results are in line with the structural observations and also confirm other studies that applied Direct Inversion methods (e.g. Lacombe et. al 1993).

2.7. Conclusions

The combined results of surface and subsurface structural analyses, paleostress determinations and thermochronological dating shed new light on the multiple reactivation of Late Paleozoic basement structures and its control on fault geometries and kinematics throughout the area of the Rhine-Bresse Transfer Zone (RBTZ).

The zircon fission track data from the La Serre Horst document a Middle Jurassic to Early Cretaceous heating event at temperatures that probably were not higher than 200-250 °C. Furthermore, the zircon FT ages, when combined with modeling of the apatite FT data, reveal a thermal history that shows two distinct periods of cooling. A first cooling event, probably related to thermal relaxation, occurred in the Early Cretaceous and was followed by extremely slow cooling at a high geothermal gradient until the end of the Eocene. A second rapid cooling event initiated at around 38 to 32 Ma and is interpreted to reflect significant extensional reactivation of the La Serre Horst during Eo-Oligocene rifting. This period also represents the main stage of the RBTZ formation and was associated with substantial uplift and erosion. Neogene to present final exhumation of the La Serre Horst is related to compression-induced uplift and erosion driven by the Alpine collision. This collision included an Early to Middle Miocene differential uplift of the area induced by lithospheric deformation, involving Early Pliocene to recent and probably largely thick-skinned compression and/or transpression, once more reactivating the multiply pre-structured RBTZ.

Subsurface analysis confirms that the structural grain of the RBTZ is defined by the reactivation of Late Paleozoic basement structures, namely the Burgundy Trough System. Together with the reactivation of typical NNE-SSE striking normal fault set, oriented parallel to the Rhine and Bresse grabens, a second major normal ENE-WSW striking fault set formed. This second fault set predominantly accommodated NW-SE directed extension, rather than sinistral strike-slip motion. This led to the formation of two small ENE-WSW striking Paleogene grabens located north and south of the reactivated La Serre Horst.

On a larger scale the results of this study confirm the view that the RBTZ formed by structural inheritance from pre-existing Late Paleozoic basement structures. We propose that Paleogene

reactivation produced a separate oblique graben segment within the European Cenozoic Rift system in the form of the RBTZ, which hence does not represent a strike-slip dominated transform zone.

Acknowledgments:

This project was funded by ELTEM and carried out within the framework of the EUCOR URGENT project. The authors are indebted to Gaz de France for the authorization to analyze and publish seismic reflection data. The authors would furthermore like to thank H. Dresmann, S. Hinsken, K. Ustaszewski and P. A. Ziegler for discussions on the data and comments on earlier versions of the manuscript. Our thanks also go to the entire past and present EUCOR-URGENT team at the Geological Institute at Basel University.

References:

Angelier, J., 1989. From orientation to magnitudes in paleostress determinations using fault slip data. Journal of Structural Geology 11, 37-50.

Angelier, J. 1990. Inversion of field data in fault tectonics to obtain the regional stress - III. A new rapid direct inversion method by analytical means. Geophysical Journal International 103, 363-376.

Angelier, J., Mechler, P., 1977. Sur une méthode graphique de recherche des contraintes principales également utilisable en tectonique et en seismologie: la méthode des dièdres droits. Bull. Soc. géol. France 19, 1309-1318.

Barbarand, J., Lucazeau, F., Pagel, M., and Sérrane, O., 2001. Burial and exhumation history of the south eastern Massif Central (France) constrained by apatite fission-track thermochronology. Tectonophysics 335, 275-290.

Berger, J.P., Reichenbacher, B., Becker, D., Grimm, M., Grimm, K., Picot, L., Storni, A., Pirkenseer, C., Derer, C., Schaefer, A., 2005, Paleogeography of the Upper Rhine Graben (URG) and the Swiss Molasse Basin (SMB) from Eocene to Pliocene. International Journal of Earth Sciences 94, 697-710.

Bergerat, F., 1977. La fraturaction de l'avant-pays jurassien entre les fossés de la Saône et du Rhin. Analyse et essai d'interpretation dynamique. Revue de Géographie physique et de Géologie dynamique (2) 14, 325-338.

Bergerat, F., 1985. Deformations cassantes et champs de constrainte tertiares de la platforme carbonatée européene. Thèse de Doctorat-es-Sciences, Mém. Sci. Terre, Univ.P. et M. Curie, No. 85-87, Paris 315 pp.

Bergerat, 1987. Stress Fields in the European Platform at the time of Africa-Eurasia Collision. Tectonics 6, 99-132.

Bergerat, F., Chorowicz, J., 1981. Etude des images Landsat de la zone tranformante Rhin-Saône (France). Geologische Rundschau 70, 354-367.

Bergerat, F., Mugnier, J.L., Guellec, S., Truffert, C., Cazes, M., Damotte, B., Roure, F., 1990. Extensional tectonics and subsidence of the Bresse basin. An interpretation from ECORS data. In: Roure, F., Heitzmann, P., Polino, R. (eds)., Deep Structure of the Alps 1, pp. 145-156, Vol. spec. Soc. Geol. It. Zürich, Mémoire de la Société géologique de la Suisse.

Boigk, H., Schöneich, H., 1970. Die Tiefenlage der Permbasis im nördlichen Teil des Oberrheingrabens. In: Illies, J.H., Mueller, S. (eds.), Graben Problems. Proceedings of an International Rift Symposium held in Karlsruhe 1968, International Upper Mantle Project. pp. 45-55, Stuttgart, E. Schweitzerbart'sche.

Bonte, A., 1975. Carte géolog. France (1/50000), feuille Quingey, XXXIII-24, BRGM.

Bourgeois, O., Ford, M., Diraison, C., Le Carlier de Veslud, M., Gerbault, R., Pik, N., 2007. Separation of rifting and lithospheric folding signatures in the NW-Alpine foreland. International Journal of Earth Sciences, 96, 1003-1031.

Burkhard, M., 1990. Aspects of the large-scale Miocene deformation in the most external part of the Swiss Alps (Subalpine Molasse to Jura fold belt). Eclogae Geologicae Helvetiae 83, 559-583.

Brandon, M.T., Roden-Tice, M.K., Garver, J.I., 1998 Late Cenozoic exhumation of the Cascadia accretionary wedge in the Olympic Mountains, northwest Washington State. GSA Bulletin 110, 985-1009.

Brockamp, O., Zuther, M., 1983. Das Uranvorkommen Müllenbach/Baden-Baden, eine epigenetisch-hydrothermale Imrägnationslagerstätte in Sedimenten des Oberkarbon, Teil II. Das Nebengestein. Neus Jahrb. Mineral. Abh. 148, 22-33.

Burtner, L.R., Nigrini, A., Donelik, R.A., 1994. Thermochronology of Lower cretaceous source rocks in the Idaho-Wyoming thrust belt. AAPG Bulletin 78, 1613-1636.

Carlson, D.W., Donelick, R.A., Ketcham, R.A., 1999. Variability of apatite fission-track annealing kinetics, I. Experimental results. American Mineralogist 84, 1213-1223.

Chauve, P., Campy, M., Pernin, C., Morre-Biot, N., 1983. Carte géolog. France (1/50000), feuille Pesmes, XXXII-23, BRGM.

Chauve, P., Enay, R., Fluck, P., Sittler, C., 1980. L'Est de la France (Vosges, Fossé Rhénan, Bresse, Jura). Annales scientifiques de l'Université de Besançon 4, 3-80.

Chauve, P., Kerrien, Y., Pernin, C., 1979. Carte géolog. France (1/50000), feuille Dole XXXII-24, BRGM.

Choulet, F., Faure, M., Fabbri O., 2007. The Autun Shear zone: age, kinematics, significance and regional correlations. In: "Mechanism of Variscan Orogeny : A modern view on orogenic research", Proceedings Special Meeting of the French and Czech Geological Societies, Géologie de la France, 2, p. 82.

Contini, D., Theobald, N., 1974. Relations entre le fossé rhénan et le fossé de la Sâone. Tectonique des régions sous-vosgiennes et préjurassiennes. In: Illies, J. H., Fuchs, K. (eds.), Approaches to Taphrogenesis, Sci. Rep. 8, pp. 309-321, Stuttgart.

Coromina, G., Fabbri, O., 2004. Late Palaeozoic NE-SW ductile-brittle extension in the La Serre horst, eastern France. Comptes Rendus Geosciences 336, 75-84.

Corrigan, J.D., 1993. Apatite fission-track analysis of Oligocene strata in South Texas, USA; testing annealing models. Chemical Geology 104, 227-249.

Coulon, M., Frizon De Lamotte, D., 1988. Les extensions céneozoiques dans l'Est du bassin de Paris. C. R. Acad. Sc. Paris 307, 1111-1119.

Debrand-Passard, S., Courbouleix, S., 1984. Synthèse Géologique du Sud-Est de la France, volume 2. Atlas comprenant 64 planches en couleurs, Mémoire du Bureau de recherches géologiques et minières, Volume 126, BRGM, 614.

Dèzes, P., Schmid, S.M., Ziegler, P.A., 2004. Evolution of the European Cenozoic Rift System. interaction of the Alpine and Pyrenean orogens with their foreland lithosphere. Tectonophysics 389, 1-33.

Diebold, P., Naef, H., 1990. Der Nordschweizer Permokarbontrog. Nagra informiert 2, 29-36.

Dreyfuss, M., Kuntz, G., 1969. Carte géolog. France (1/50000), feuille Besançon, XXXII-23, BRGM.

Dreyfuss, M., Kuntz, G., 1970. Carte géolog. France (1/50000), feuille Gy, XXXIII-22, BRGM.

Dreyfuss, M., Théobald, N., 1972. Carte géolog. France (1/50000), feuille Baume-les-Dames, XXXIV-22, BRGM.

Dumitru, T.A., 1995. A new computer automated microscope stage system for fission track analysis. Nuclear Tracks Radiation Measurements 21, 575-580.

Echtler, H., Malavielle, J., 1990. Extensional basement uplift and Stephano-Permian collapse basin in a late Variscian metamorphic core complex (Montagne Noire, Southern Massif Central). Tectonophysics 177, 125-138.

Echtler, H.P., Chauvet, A., 1991-1992. Carboniferous convergence and subsequent crustal extension in the southern Schwarzwald (SW Germany). Geodinamica Acta 5, 37-49.

Eisbacher, G., Lüschen, E., Wickert, F., 1989. Crustal scale thrusting and extension in the Hercynian Schwarzwald and Vosges, Central Europe. Tectonics 8, 1-21.

Elmohandes, S.-E., 1981. The Central European Graben System. Rifting imitated by Clay Modelling. Tectonophysics 73, 69-78.

Ford, M., Le Carlier de Veslud, C., Bourgeois, O., 2007. Kinematic and geometric analysis of fault related folds in a rift setting. The Dannemarie basin, Upper Rhine Graben, France. Journal of Structural Geology 29, 1811-1830.

Fügenschuh, B., Schmid, S.M., 2003. Late stages of deformation and exhumation of an orogen constrained by fission-track data. A case study in the Western Alps. Geol. Soc. Am. Bull. 115, 1425-1440.

Galbraith, R.F., Laslett, G.M., 1993. Statistical models for mixed fission-track ages. Nuclear Tracks and Radiation Measurements 21, 459-470.

Gallagher, K., 1995. Evolving temperature histories from apatite fission-track data. Earth and Planetary Sciences Letters 136, 421-435.

Giamboni, M., Ustaszewski, K., Schmid, S.M., Schumacher, M.E., Wetzel, A., 2004. Plio-Pleistocene Transpressional Reactivation of Paleozoic and Paleogene Structures in the Rhine-Bresse transform Zone (northern Switzerland and eastern France). International Journal of Earth Sciences 93, 207–223, DOI. 10.1007/s00531-003-0375-2.

Gleadow, A.J.W., Duddy, I.R., Green, P.F., Hegarty, K.A., 1986. Fission track length in the apatite annealing zone and interpretation of mixed ages. Earth and planetary Science Letters 78, 245-254.

Green, P.F., 1981. A new look at statistics in fission track dating. Nuclear Tracks and Radiation Measurements 5, 77-86.

Green, P.F., Duddy, I.R., 1989. Some comments on paleotemperature estimation from apatite fission track analysis. Journal of Petroleum Geology 12, 111-114.

Green, P.F., Duddy, I.R., Gleadow, A.J.W., Tingate, P.R., 1985. Fission-track annealing in apatite, track length measurements and the form of the Arrhenius plot. Nuclear Tracks and Radiation Measurements 10, 323-328.

Green, P.F., Duddy, I.R., Gleadow, A.J.W., Tingate, P.R., Laslett, G.M., 1986. Thermal annealing of fission tracks in apatite, 1. A qualitative description. Chemical Geology 59, 237-253.

Hinsken, S., Ustaszewski, K., Wetzel, A., 2007. Graben width controlling syn-rift sedimentation. the Palaeogene southern Upper Rhine Graben as an example. International Journal of Earth Sciences 96, 979-1002.

Homberg, C., Bergerat, F., Philippe, Y., Lacombe, O., Angelier, J., 2002. Structural inheritance and cenozoic stress fields in the Jura fold-and-thrust belt (France). Tectonophysics 357, 137– 158.

Hurford, A.J., Green, P.F., 1983. The zeta age calibration of fission-track dating. Chemical Geology 41, 285-317.

Illies, J.H., 1972. The Rhinegraben rift system - plate tectonics and transform faulting. Geophysical Surv. 1, 27-60.

Illies, J. H., 1981. Mechanism of Graben formation. Tectonophysics 73, 249-266.

Jowett, E.C., 1991. Post-collisional formation of the Alpine foreland rifts. Annales Geological Society of Poland 61, 37-59.

Lacombe, O., Angelier, J., Byrne, D., Dupin, J., 1993. Eocene-Oligocene tectonics and kinematics of the Rhine-Saone continental transform zone (Eastern France). Tectonics 12, 874-888.

Lacombe, O., Angelier, J., Laurent, P., Bergerat, F., Tourneret, C., 1990. Joint analyses of calcite twins and fault slips as a key for deciphering polyphase tectonics. Burgundy as a case study. Tectonophysics 182, 279-300.

Lancelot, J., Briqueu, L., Respaut, J.P., Clauer, N., 1995. Géochimie isotopique des systèmes U- Pb/Pb- Pb et évolution polyphasée des gîtes d'uranium du Lodévois et du sud du Massif central. Chron. Rech. Min. 521, 3-18.

Larroque, J., Laurent, P., 1988. Evolution of the stress field pattern in the south of the Rhine Graben from the Eocene to the present. Tectonophysics 148, 41-58.

Laubscher, H., 1970. Grundsätzliches zur Tektonik des Rheingrabens. In: Illies, J.H., Mueller, S. (eds.), Graben Problems. Proceedings of an International Rift Symposium held in Karlsruhe 1968, International Upper Mantle Project, pp.79-86, Stuttgart, E. Schweitzerbart'sche.

Laubscher, H., 1972. Some overall aspects of Jura dynamics. American Journal of Science 272, 293-304.

Laubscher, H., 1992. Jura kinematics and the Molasse Basin. Eclogae Geologicae Helvetiae 85, 653-675.

Macquar, J.-C., 1984. Minéralisation triasiques en Pb, Zn, Ba (Cu, Fe) du Bassin subalpin. typologie, chronologie, contrôles et modèles. In: Debrand-Passard, S., Courbouleix, S.M.J., L. (eds.), Synthèse géologique du Sud-Est de la France- stratigraphie et paléogéographie, Mém. Bur. Rech. Géol. Min 125, 112-118.

Madritsch, H., Schmid, S.M., Fabbri, O., 2008. Interactions of thin- and thick-skinned tectonics along the northwestern front of the Jura fold-and-thrust-belt (Eastern France). Tectonics submitted.

Marrett, R., Allmendinger, R.W., 1990. Kinematic analysis of fault-slip data. Journal of Structural Geology 12, 973-986.

Marrett, R., Peacock, D.C.P., 1999, Strain and stress. Journal of Structural Geology, 21, 1057-1063.

McCann, T., Pascal, C., Timmerman, M.J., Krzywiec, P., López-Gómez, J., Wetzel, A., Krawczyk, C.M., Rieke, H., Lamarche, J., 2006. Post-Variscan (end Carboniferous-Early Permian) basin evolution in Western and Central Europe. In: Gee, D.G., Stephenson, R.A. (eds.), European Lithosphere Dynamics, Geological Society of London Memoirs, 32, pp. 355-388.

Merle, O., Michon, L., 2001. The formation of the West European rift: A new model as exemplified by the Massif Central area: Bull. Soc. Geol. France 172, 213-221.

Meschede, M., Decker, K., 1993. Störungsflächenanalyse entlang des Nordrandes der Ostalpen - ein methodischer Vergleich. Z. dt. Geol. Ges. 144, 419-433.

Michon, L., Merle, O., 2001. The evolution of the Massif Central Rift: spatio-temporal distribution of the volcanism. Bull. Soc. Geol. France 172, 69-80.

Michon, L., Merle, O., 2005. Discussion on "Evolution of the European Cenozoic Rift System: interaction of the Alpine and Pyrenean orogens with their foreland lithosphere by P. Dèzes, S.M. Schmid, P.A. Ziegler, Tectonophysics 389 (2004) 1-33. Tectonophysics. 401, 251-256.

Michon, L., Sokoutis, D., 2005. Interaction between structural inheritance and extension direction during graben formation: An experimental approach. Tectonophysics 409, 125-146.

Morre, N., Thiébaut, J., 1961. Etude pétrographique des roches cristallines decouvertes par sondage profonds entre Vosges et Morvan. Annales scientifiques de l'Univeristé de Besançon 14, 73-83.

Morre-Biot, N., Storet, J., 1967. Sur l'âge absolu du granite de la Serre (Jura). C. R. Acad. Sc. Paris 265, 1869-1870.

Neugebauer, H.J., 1978. Crustal doming and mechanism of rifting: Part 1, Rift formation. Tectonophysics 45, 159-186.

Petit, J.P., 1987. Criteria for the sense of movement on fault surfaces in brittle rocks. Journal of Structural Geology 9, 597-608.

Pfiffner, O.A., Burkhard, M., 1987. Determination of paleo-stress axes orientations from fault, twin and earthquake data. Annales Tectonicae, 1, 48-57.

Rat, P., 1976. Structures et phases de structuration dans les plateaux bourguignons et le Nord Ouest du fossé bressan (France). Geologische Rundschau 65, 101-126.

Reiter, F., Acs, P., 1996-2000. TectonicsFP. Computer Software for Structural Geology, version 2.0 PR. http://www.tectonicsfp.com/.

Rey, P., Burg, J.-P., Caron, J.-M., 1991-1992. Middle and Late Carboniferous extension in the Variscian Belt: structural and petrological evidences from the Vosges massif (Eastern France). Geodinamica Acta 5, 17-36.

Rocher, M., Chevalier, F., Petit, C., Guiraud, M., 2003. Tectonics of the Northern Bresse region (France) during the Alpine cycle. Geodinamica Acta 16, 131-147.

Rocher, M., M. Cushing, F. Leimeille, Y. Lozac'h, J. Angelier, 2004. Intraplate paleostresses reconstructed with calcite twinning and faulting: improved method and application to the eastern Paris Basin (Lorraine, France), Tectonophysics 387, 1-21.

Rotstein, Y., Schaming, M., Rousse, S., 2005. Structure and Tertiary Tectonic history of the Mulhouse High, Upper Rhine Graben: Block faulting modified by changes in the Alpine stress regime. Tectonics 24, TC1012 doi:10.1029/2004TC001654.

Ruhland, M., 1959. Une dislocation majeure du socle Vosgien dans la haute Vallée de l' Ognon. Bull. Serv. Carte Géol. Als. Lorr. 12, 61-64.

Schaltegger, U., Schneider, J.L., Maurin, J.C., Corfu, F., 1996. Precise U-Pb chronometry of 345-340 Ma old magmatism related to syn-convergence extension in the southern Vosges (Central Variscian Belt). Earth and Planetary Science Letters 144, 403-419.

Schmid, S.M., Pfiffner, O.A., Froitzheim, N., Schönborn, G., Kissling, E., 1996. Geophysical-geological transect and tectonic evolution of the Swiss-Italian Alps. Tectonics 15, 1036-1064.

Schumacher, M.E., 2002, Upper Rhine Graben: Role of preexisting structures during rift evolution. Tectonics 21(1), 6-1-6-17.

Sengör, A.M.C., 1976. Collision of irregular continental margins: implications for foreland deformation of Alpine-type orogens. Geology 4, 779-782.

Seward, D., 1989. Cenozoic basin histories determined by fission track dating of basement granites, South New Island, Zealand. Chemical Geology 79, 31-48.

Sissingh, W., 1998. Comparative Tertiary stratigraphy of the Rhine Graben, Bresse Graben and Molasse Basin: correlation of Alpine foreland events. Tectonophysics 300, 249-284.

Surma, F., Geraud, Y., Pourcelot, L., Gauthier-Lafaye, F., Clavaud, J.B., Zamora, M., Lespinasse, M., Cathelineau, M., 2003. Microstructures d'un grès affecté par une faille normale; anisotropie de connectivité et de pérméabilite. Bull. Soc. Géol France 174, 295-303.

Tagami, T., Dumitru, T.A., 1996. Provenance and history of the Franciscan accretionary complex: Constraints from zircon fission track thermochronology. J. Geophys. Res. 101, 8345-8255.

Tagami, T., Galbraith, R.F., Yamada, R., Laslett, G.M., 1998. Revised annealing kinetics of fission tracks in zircon and geological implications. In: Van den Haute, P., de Corte, F. (eds.), Advances in Fission-Track Geochronology. Solid Earth Sci. Libr. Kluwer Acad., Norwell, Mass., Volume 10, pp. 99-112.

Timar-Geng, Z., Fügenschuh, B., Schaltegger, U., and Wetzel, A., 2004. The impact of the Jurassic hydrothermal activity on zircon fission track data from the southern Upper Rhine Graben area. Schweizerische Mineralogische und Petrographische Mitteilungen, 84: 257-269.

Timar-Geng, Z., Fügenschuh, B., Wetzel, A., Dresmann, H. 2006. Low-temperature thermochronology of the flanks of the southern Upper Rhine Graben. Int J Earth Sci 95: 685-702.

Ustaszewski, K., Schmid, S.M., 2007. Latest Pliocene to recent thick-skinned tectonics at the Upper Rhine Graben - Jura Mountains junction. Swiss Journal of Geosciences 100, 293-312.

Ustaszewski, K., Schumacher, M.E., Schmid, S.M., 2005a. Simultaneous normal faulting and extensional flexuring during rifting - an example from the southernmost Upper Rhine Graben. International Journal of Earth Sciences 94, 680-669.

Ustaszewski, K., Schumacher, M.E., Schmid, S.M., Nieuwland, D., 2005b. Fault reactivation in brittle-viscous wrench systems - dynamically scaled analogue models and application to the Rhine-Bresse Transfer Zone. Quaternary Science Reviews 24, 363-380.

Wetzel, A., Allenbach, R., Allia, V., 2003. Reactivated basement structures affecting the sedimentary facies in a tectonically "quiescent" epicontinental Basin: an example from NW Switzerland. Sedimentary Geology 157, 153-172.

Wallace, R.E., 1951. Geometry of shearing stress and relation to faulting. J. Geol. 59, 118-130.

Yamada, R., Tagami, T., Nishimura, S., Ito, H., 1995. Annealing kinetics of fission tracks in zircon: an experimental study. Chemical Geology 122, 249-248.

Ziegler, P., Dèzes, P., 2007. Cenozoic uplift of Variscian Massifs in the foreland of the Alpine foreland: Timing and controlling mechanisms. Global and Planetary Change 58, 237-269.

Ziegler, P., 1986. Geodynamic model for the Paleozoic crustal consolidation of Western and Central Europe. Tectonophysics 126, 303-328.

Ziegler, P.A., 1990. Geological Atlas of Western and Central Europe. Den Haag, Shell Internationale Petroleum Maatschappij B.V., 1-238.

Ziegler, P.A., 1992. European Cenozoic rift system. Tectonophysics 208, 91-111.

Ziegler, P.A., Schumacher, M.E., Dèzes, P., van Wees, J.-D., Cloetingh, S., 2004. Post-Variscan evolution of the lithosphere in the Rhine Graben area: constraints from subsidence modelling. In: Wilson, M. (ed.), Permo-Carboniferous magmatism and rifting in Europe, Volume 223. Geological Society of London Special Publications, Geological Society, pp. 289-317.

Appendix:

Stereographic lower hemisphere equal area projections of fault slip data. Numbers refer to Table 2 and Figure 10.

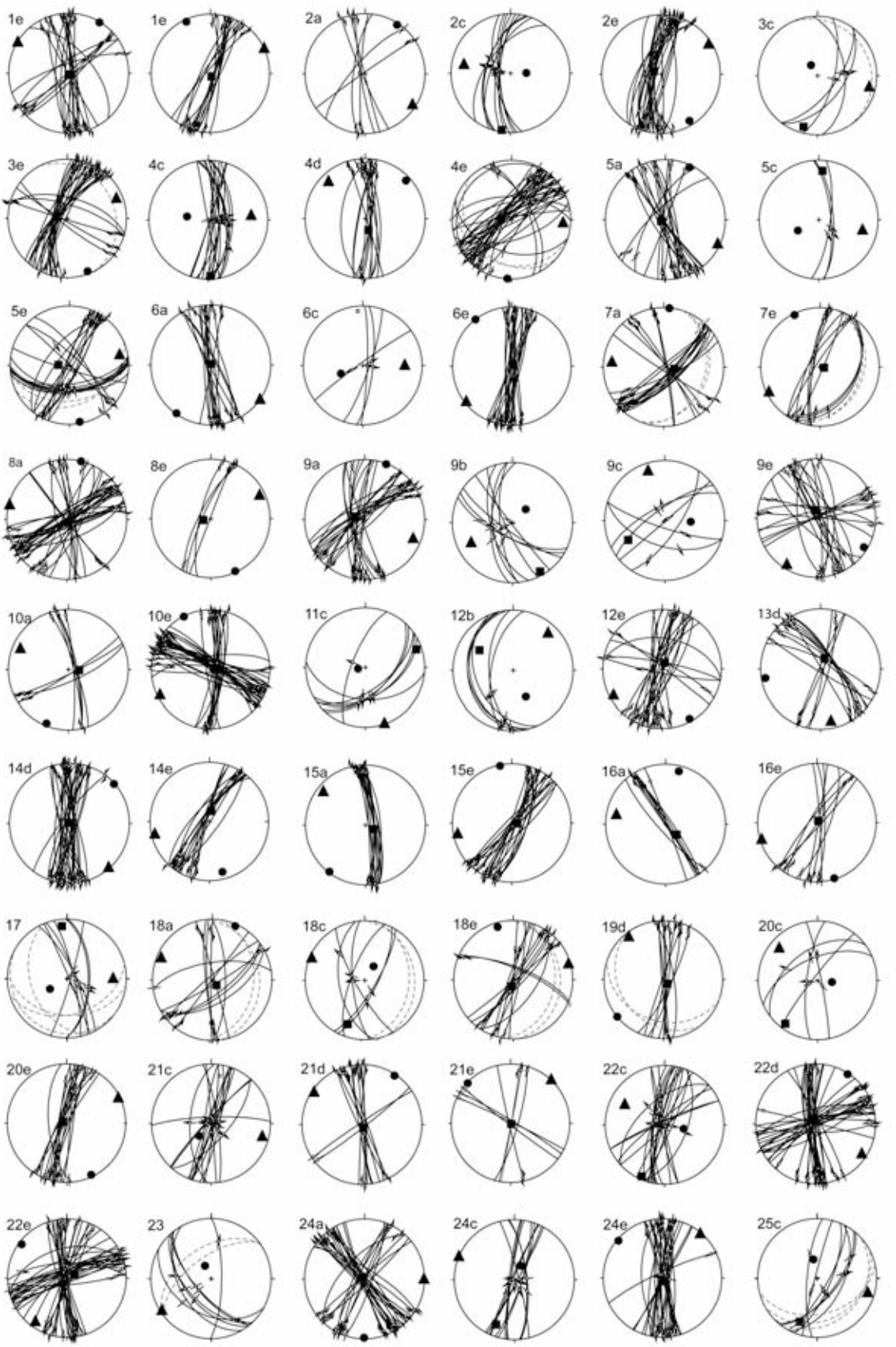
1e
1e
2a
2c
2e
3c
3e
4c
4d
4e
5a
5c
5e
6a
6c
6e
7a
7e
8a
8e
9a
9b
9c
9e
10a
10e
11c
12b
12e
13d
14d
14e
15a
15e
16a
16e
17
18a
18c
18e
19d
20c
20e
21c
21d
21e
22c
22d
22e
23
24a
24c
24e
25c

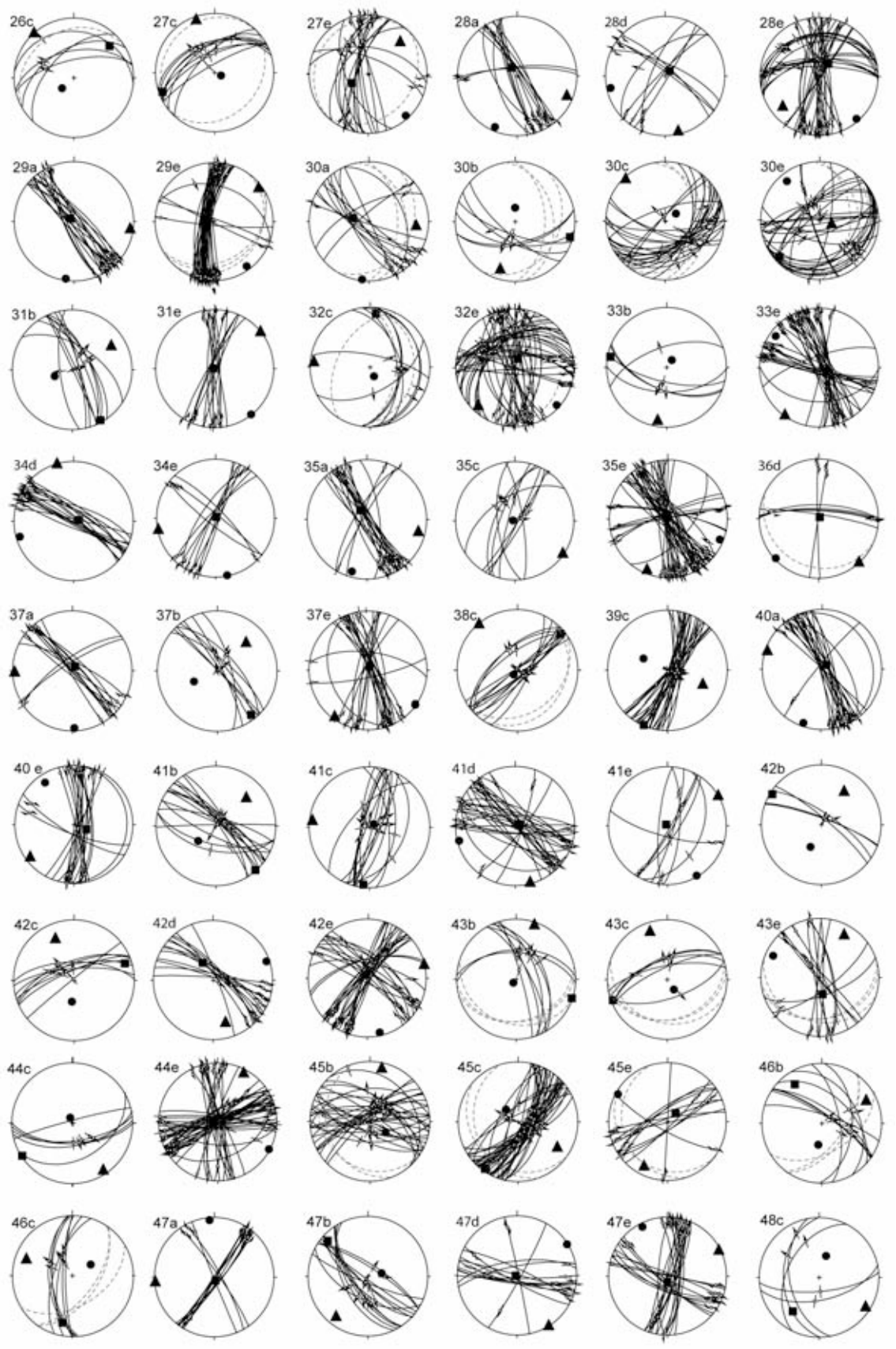
26c
27c
27e
28a
28d
28e
29a
29e
30a
30b
30c
30e
31b
31e
32c
32e
33b
33e
34d
34e
35a
35c
35e
36d
37a
37b
37e
38c
39c
40a
40 e
41b
41c
41d
41e
42b
42c
42d
42e
43b
43c
43e
44c
44e
45b
45c
45e
46b
46c
47a
47b
47d
47e
48c

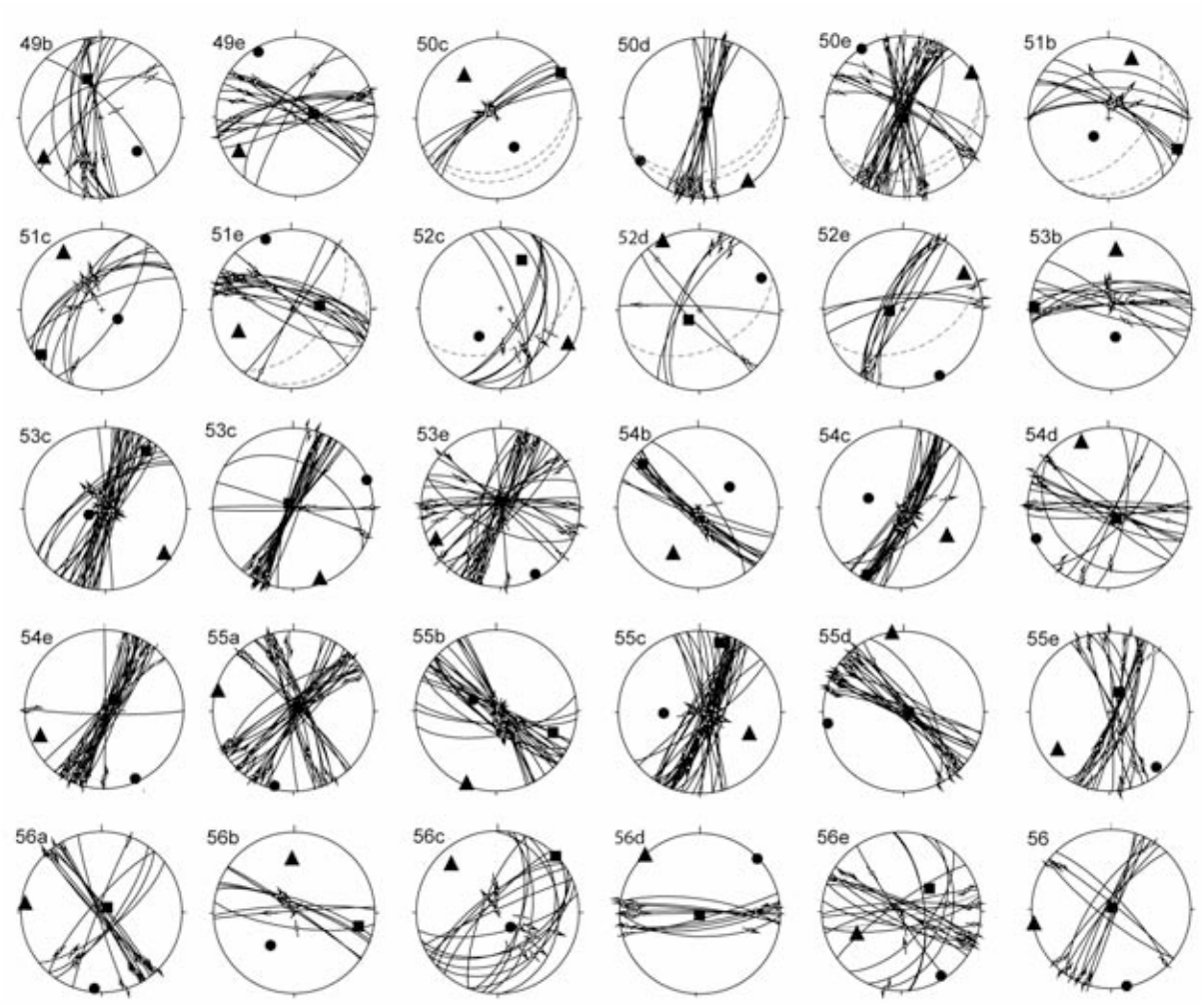
49b
49e
50c
50d
50e
51b
51c
51e
52c
52d
52e
53b
53c
53c
53e
54b
54c
54d
54e
55a
55b
55c
55d
55e
56a
56b
56c
56d
56e
56

Chapter 3

Interactions between thin- and thick-skinned tectonics at the northwestern front of the Jura fold-and-thrust belt (Eastern France)

by

Herfried Madritsch, Stefan M. Schmid and Olivier Fabbri

Accepted for publication in *Tectonics*

Abstract:

This study investigates spatial and temporal interactions of thin- and thick-skinned tectonics in a classical foreland setting located at the front of the Jura fold-and-thrust belt in Eastern France. The working area coincides with the intra-continental Rhine-Bresse Transfer Zone and represents the most external front of the deformed Alpine foreland. The investigation combines analyses of largely unpublished and newly available subsurface information with our own structural data, including an exhaustive paleostress analysis and geomorphologic observations. Results are provided in the form of a new tectonic map and a series of regional cross sections through the study area.

The Besançon Zone, forming the most external part of the thin-skinned fold-and-thrust belt, encroached onto the Eo-Oligocene Rhine-Bresse Transfer Fault System until Early Pliocene times. Thrust propagation was largely controlled by the Late Paleozoic to Paleogene preexisting fault pattern that characterizes the Rhine-Bresse Transfer Zone.

Thick-skinned deformation, dominant throughout the Avant-Monts Zone located further to the west, was associated with compressional to transpressional reactivation of such faults. Overprinting and crosscutting criteria of fault-slip data allow distinguishing between systematically fanning maximum horizontal stress axes that define the front of the thin-skinned Jura fold-and-thrust belt and consistently NW-SE directed maximum horizontal stress axes that characterize deformation of the autochthonous cover of the foreland, which is affected by thick-skinned tectonics.

Tectonic and geomorphic analyses indicate that thick-skinned tectonics started at a very late stage of foreland deformation (post Early Pliocene) and locally overprinted older thin-skinned structures. Geomorphic observations indicate that deformation between Mesozoic cover and basement is locally decoupled. However overprinting relationships and recent seismicity suggest that present-day tectonic activity is thick-skinned, which probably reflects ongoing tectonic underplating in the Alpine foreland.

Keywords: *Jura fold-and-thrust belt, thin-skinned, thick-skinned, paleostress, neotectonics, France*

3.1. Introduction

During the evolution of an orogenic wedge, transmission of collision-related compressional stresses into the foreland can give rise to thin- or thick-skinned foreland deformation. The tectonic style of foreland deformation is controlled by the level at which decoupling (or décollement) at the base of the orogenic wedge occurs: near the basement-cover interface, within the basement of the upper crust, or even deeper within the lithosphere [Ziegler et al., 2002].

According to the definition of Chapple [1978] thin-skinned deformation involves the development of a shallow, gently dipping décollement horizon composed of rheologically weak rocks such as evaporites or shales typically located near or at the base of a sedimentary cover sequence. Rocks immediately beneath the basal detachment level, including the crystalline basement, remain undeformed and become shortened elsewhere, i.e. in the more internal parts of the orogen. The wedge geometry of the deformed sedimentary cover above the detachment and the mechanics of thin-skinned foreland fold-and-thrust belts are described by the critical taper theory [Chapple, 1978; Davis et al., 1983].

Conversely, thick-skinned deformation, as used in this contribution, involves deformation within the crystalline basement that underlies the sedimentary sequence; crystalline basement and sedimentary cover are deformed together. Basement shortening in the foreland of the orogen requires the existence of a crustal-scale décollement that allows for the transmission of compressional orogenic stresses [Coward, 1983]. The crustal décollement may ramp up into shallow upper crustal levels or extend far out into the foreland, causing inversion of sedimentary basins. In both cases thick-skinned deformation mostly involves the compressional to transpressional reactivation and inversion of pre-existing crustal discontinuities [Lacombe and Mouthereau, 2002; Ziegler et al., 2002; Pfiffner, 2006].

The concepts of thin- and thick-skinned tectonics represent extreme cases, and transitions between the two modes of contractional deformation may occur (e.g. “basement involved thin-skinned tectonics” of Pfiffner; 2006). The understanding of the way thin- and thick-skinned tectonics interact in space and time represents a key question for the dynamics of foreland deformation in collisional orogens, particularly regarding the sequence of deformation in foreland fold-and-thrust belts. Accordingly, many studies addressed this topic in recent years and revealed complex interferences of the different tectonic styles, also in fold-and-thrust belts that have long been treated as classical examples of thin-skinned deformation, such as the Apennines [Tozer et al., 2002; Calabrò et al., 2003], the Zagros fold-and-thrust belt [Molinaro et al., 2005; Mouthereau et al., 2007] or the fold-and-thrust belt of NW Taiwan [Lacombe et al., 2003]. The sequence of deformation events in foreland settings that are characterized by different deformational styles is very difficult to establish and is variable within different natural settings [Lacombe and Mouthereau, 2002]. Thick-skinned deformation often sets in during a late stage of deformation and follows initial thin-skinned tectonics; this potentially leads to thick-skinned refolding of shallow thin-skinned thrust nappes [Molinaro et al.,

2005]. On the other hand, there are also natural examples where thick-skinned tectonics occurred during initial stages of foreland deformation far in front of the orogen, controlling the later development of the thin-skinned foreland fold-and-thrust belt [Lacombe et al., 2003].

This study analyzes and discusses temporal and spatial interactions of thin- and thick-skinned tectonics that characterize the northwestern front of the Jura fold-and-thrust belt in Eastern France, that is the most external part of the Alpine orogen. Discussions regarding the formation and tectonic style of the Jura fold-and-thrust belt date back to the beginning of the last century (see review by Sommaruga [1997]). Although some authors considered pure thick-skinned formation of this fold-and-thrust belt [Aubert, 1945; Pavoni, 1961] the large majority of authors agrees that it initially developed along a shallow décollement horizon formed by Mid-to Late Triassic evaporites, and that it hence represents the type example of a thin-skinned foreland fold-and-thrust belt [Buxtorf, 1907; Laubscher, 1961; Burkhard, 1990; Burkhard and Sommaruga, 1998]. However, besides thin-skinned deformation, also a thick-skinned tectonic style, involving compressional to transpressional reactivation of pre-existing basement discontinuities in front, beneath and in the immediate hinterland of the Jura fold-and-thrust belt, was reported [Guellec et al., 1990; Pfiffner et al., 1997; Rotstein and Schaming, 2004; Ustaszewski and Schmid, 2007]. Both tectonic styles apparently occurred during the latest stages of the evolution at the northwestern-most edge of the Alpine collision zone, i.e. during Neogene to recent times. The exact timing and the mutual relations between these two styles of deformation are, however, ill defined and still controversial.

For the first time, this contribution provides evidence for thick-skinned deformation from the northwestern front of the thin-skinned fold-and-thrust belt. The study focuses on the time constraints regarding the two contrasting styles of deformation by analyzing and discussing subsurface, structural, geomorphic and geophysical data. Thereby it also contributes to the ongoing scientific debate as to which style of deformation and associated stress field characterizes the neotectonic activity along the northwestern front of the Jura Mountains [e.g. Becker, 2000]. Ongoing deformation in the area is indicated by low to medium seismicity [Deichmann et al., 2000; Kastrup et al., 2004] and, additionally, by ample evidence for ongoing deformation provided by studies in tectonic geomorphology [Dreyfuss and Glangeaud, 1950; Campy, 1984; Giamboni et al., 2004; Madritsch, 2008]. The question whether thin-skinned, thick-skinned, or a combination of both modes are active at present is of prime importance for any seismic hazard assessment [Meyer et al., 1994; Nivière and Winter, 2000; Ustaszewski and Schmid, 2007].

3.2. Tectonic setting

The area of investigation is part of the northwestern foreland of the European Alps and is located in Eastern France (Figure 1). Furthermore, it coincides with Rhine-Bresse Transfer Zone (RBTZ)

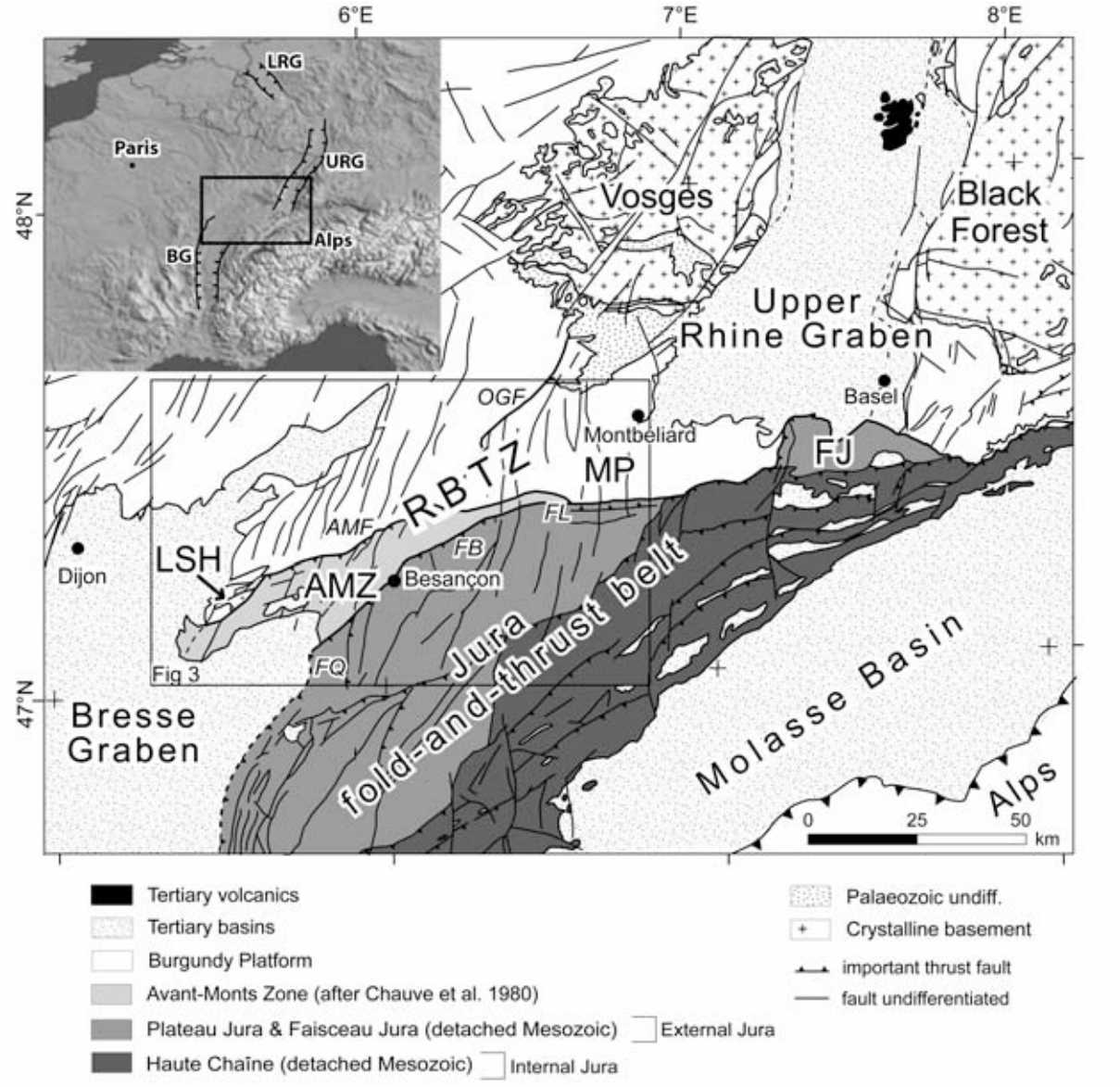

Figure 1: Geological setting of the study area. Subdivisions of the Jura fold-and-thrust belt are taken from Chauve et al. [1980]. Note the difference between this classical subdivision and the new subdivision of the Avant-Monts Zone based on the results of this study, as presented in Figure 3. AMF: Avant-Monts Fault; AMZ: Avant-Monts Zone as defined by Chauve et al. (1980); FB: Faisceau Bisontin; FL: Faisceau du Lomont ; FQ: Faisceau de Quingey; FJ: Ferrette Jura; LSH: La Serre Horst; MP: Montbéliard Plateau; OGF: Ognon Fault; RBTZ: Rhine-Bresse Transfer Zone.

[Laubscher, 1970; Illies and Greiner, 1978; Bergerat and Chorowicz, 1981], a central segment of the European Cenozoic Rift System. The latter extends over a distance of approximately 1100 km from the North Sea coast to the western Mediterranean [Ziegler, 1992]. The formation of this rift system is interpreted to result from the build-up of syn-collisional compressional intra-plate stresses in the forelands of the Pyrenees and the Alps [Dèzes et al., 2004]. Late Eocene to Oligocene extension led to the opening of the NNE-SSW striking Rhine and Bresse grabens (Figure 1). The ENE-WSW striking

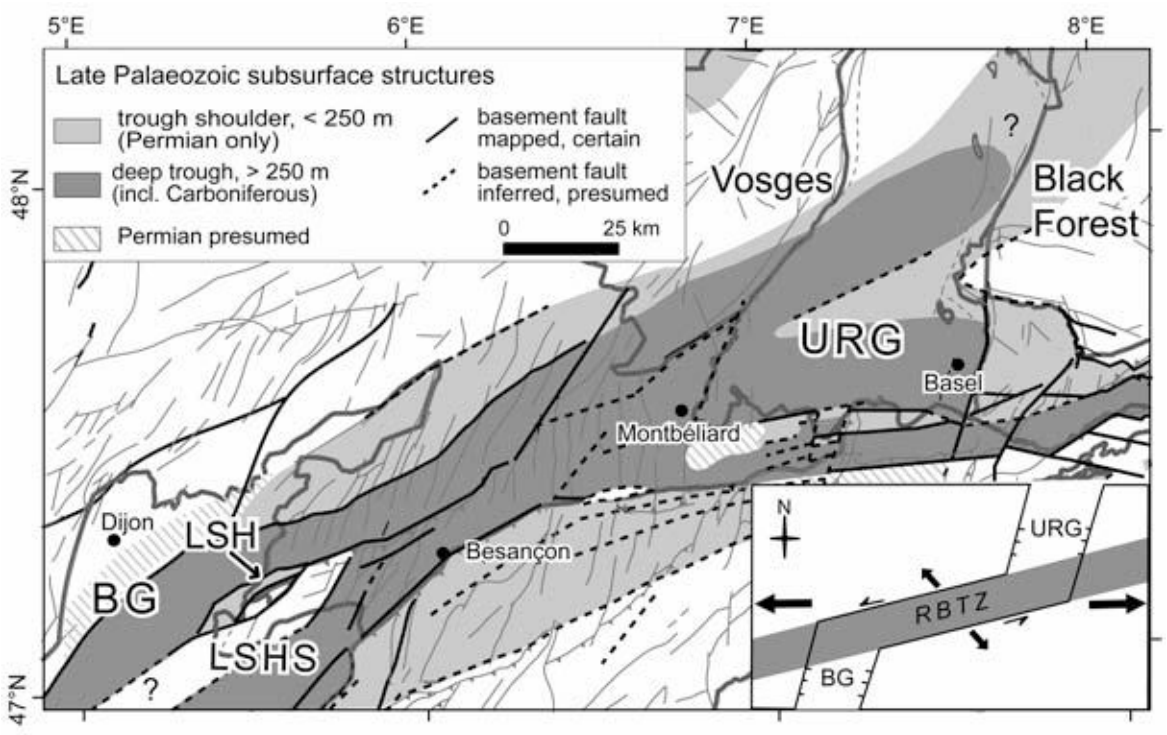

Figure 2: Subsurface map of the Rhine-Bresse Transfer Zone (RBTZ) showing the Late Paleozoic Burgundy Trough (modified after Debrand-Passard and Courbouleix [1984], and Ustaszewski et al. [2005]. Inset in the lower right shows the conceptual model for the Eo-Oligocene formation of the RBTZ proposing sinistral transtensive reactivation of this preexisting fault system (modified from Lacombe et al. 1993). BG: Bresse Graben; BTS: Burgundy Trough system; LSH: La Serre Horst; LSHS La Serre Horst Structure; RBTZ: Rhine-Bresse Transfer Zone; URG: Upper Rhine Graben.

RBTZ cuts trough the autochthonous Mesozoic sediments of the Burgundy Platform and is inferred to have transferred crustal extension between the Rhine and Bresse grabens by sinistral strike-slip motion under ongoing north-south compression [Bergerat, 1977] or, alternatively, by sinistral transtension or oblique extension in an roughly E-W-oriented extensional stress field [e.g. Lacombe et al., 1993; Madritsch 2008] (inset of Figure 2).

The formation and evolution of the European Cenozoic Rift System, and particularly that of the RBTZ, was clearly controlled by structural inheritance of pre-existing Late Paleozoic basement faults that are part of the Burgundy Trough (Figure 2) [Laubscher, 1970; Bergerat and Chorowicz, 1981; Schumacher, 2002; Madritsch, 2008]. This ENE-WSW striking Permo-Carboniferous graben system, which parallels the later formed Cenozoic RBTZ (Figure 2), extends from the northern French Massif Central in the west to the southern end of the Rhine Graben in the east, where it connects with the graben systems of northwestern Switzerland and southern Germany [Boigk and Schönreich, 1970; Debrand-Passard and Courbouleix, 1984; Ziegler, 1992; Diebold and Noack, 1997]. Its formation is probably related to the activity of a Late Variscan, dextrally transtensive, trans-European shear zone [Ziegler, 1986; McCann et al., 2006; Schumacher, 2002]. In the western part of the study area, the

Burgundy Trough includes the La Serre Horst (LSH in Figure 1). This horst exposes pre-Mesozoic strata and is part of a larger Late Paleozoic structural high, the La Serre Horst Structure (LSHS in Figure 2) that extends westward into the Bresse Graben [Rat, 1976; Chauve et al., 1983; Coromina and Fabbri, 2004; Madritsch, 2008]. The reactivation of these Late Paleozoic structures during the Eo-Oligocene formation of the Rhine-Bresse Transfer Zone resulted in a complex pattern of intersecting NNE-SSW and ENE-WSW striking normal faults [Lacombe et al., 1993; Madritsch, 2008].

During the Early Miocene the crustal stress field in the area of investigation changed. This was due to fundamental changes in deformation processes at the lithosphere scale and related to ongoing Alpine collision [Bergerat, 1987; Dèzes et al., 2004]. The Jura fold-and-thrust belt whose northwestern rim parallels the RBTZ (Figure 1) formed in response to this stress field change. The some 400 km long belt is bounded to the SE by the rigidly displaced flexural Molasse Basin and hence represents the northwestern deformation front of the Alpine orogen.

The Jura fold-and-thrust belt is considered as a type example for a thin-skinned foreland fold-and-thrust belt and its initial formation is nowadays widely accepted to be the result of distant push ("Fernschub") [Buxtorf, 1907; Laubscher, 1961; Laubscher, 1978; Burkhard, 1990; Sommaruga, 1997; Sommaruga and Burkhard, 1997]. Crustal shortening and nappe stacking in the external crystalline massifs of the Alps induced a decoupling of deformation between the undeformed crystalline basement that gently dips towards the hinterland and the detached Mesozoic cover along Mid- to Late Triassic evaporites [Burkhard, 1990; Schmid et al., 1996; Burkhard and Sommaruga, 1998]. The Mesozoic cover was displaced far into the northern foreland. Horizontal shortening estimates from balanced cross sections across the arcuate shaped fold-and-thrust belt range from zero at its northeastern termination to an average of about 30km in its central part [Burkhard, 1990; Philippe et al., 1996]. At its northern and western rim the Jura fold-and-thrust belt encroached onto the European Cenozoic Rift System [Laubscher, 1986; Guellec et al., 1990; Ustaszewski and Schmid, 2006]. Pre-existing extensional structures related to the rift system did not only control the geometry and distribution of the most frontal thin-skinned thrusts and folds but also the propagation style of the entire fold-and-thrust belt that typically features divergent stress and strain trajectories towards the deformation front [Laubscher, 1972; Philippe et al., 1996; Hindle and Burkhard, 1999; Homberg et al., 1999; Affolter and Gratier, 2004].

Most authors consider the formation of the thin-skinned Jura fold-and-thrust belt as a rather short-lived event. Near its northern rim a maximum age for the onset of thin-skinned deformation is inferred from the Bois de Raube formation, which reveals a biostratigraphic age between 13.8-10.5 Ma years and whose sedimentation predates thin-skinned Jura folding in that area [Kälin, 1997]. A maximum age of 9 Ma can be inferred from the western front of the Jura where this fold-and-thrust belt thrusted the Bresse Graben [Guellec et al., 1990; Becker, 2000].

Termination of thin-skinned Jura folding is less well constrained. Undeformed karst sediments have been detected in a fold limb located in the central part of the fold-and-thrust belt; their

biostratigraphic age implies that folding terminated before some 4.2-3.2 Ma ago in this area [Bolliger et al., 1993; Steininger et al., 1996]. In the case that propagation of the fold-and-thrust belt toward the foreland was in sequence, which is not always the case as illustrated by the results of recent analogue models [Costa and Vendeville, 2002; Smit et al., 2003], thin-skinned deformation may have operated longer in the more external parts of the fold-and-thrust belt [Ustaszewski and Schmid, 2006]. Evidence for ongoing deformation from the northern and northwestern front of the fold-and-thrust-belt is indeed provided by studies in tectonic geomorphology [Dreyfuss and Glangeaud, 1950; Campy, 1984; Meyer et al., 1994; Nivière and Winter, 2000; Giamboni et al., 2004; Madritsch, 2008].

The style of post Early-Pliocene and recent deformation, however, is a matter of debate. While some authors proposed that thin-skinned deformation is presently still ongoing [Nivière and Winter, 2000; Müller et al., 2002], others, based on the interpretation of seismic reflection data, proposed that thick-skinned present-day activity affects the frontal-most Jura folds [Giamboni et al., 2004; Rotstein and Schaming, 2004; Ustaszewski and Schmid, 2006]. Giamboni et al. [2004] and Ustaszewski and Schmid [2007] hold this type of deformation exclusively responsible for all post-2.9 folding of the Middle-Late Pliocene Sundgau Gravels. According to these authors, ongoing thick-skinned deformation involves the inversion of Paleozoic and/or Paleogene basement faults in dextral transpression. Based on their observations, made east of our area of investigation and at the southern rim of the Rhine Graben, they proposed that thick-skinned deformation post-dated thin-skinned Jura folding and that thin-skinned thrusting came to a halt by the Early Pliocene. However, this remains a hypothesis and furthermore it is a matter of debate as to whether this proposition applies for the area of the Rhine-Bresse Transfer Zone, i.e. over the entire length of the front of the Jura fold-and-thrust belt. Moreover, a temporal coexistence of both styles of deformation, before or after the Early Pliocene, cannot be excluded [Meyer et al., 1994; Niviere and Winter, 2000]. This study will add new field and subsurface data in order to test such hypotheses over a large area located along the northwestern front of the Jura fold-and-thrust belt (Figure 1).

Commonly the Jura fold-and-thrust belt is divided into two major parts [Chauve et al., 1980; Philippe et al., 1996; Sommaruga, 1997] (Figure 1): (1) The internal or "folded" Jura, which features intense shortening along the discrete southeastern border adjacent to the Molasse basin and which is characterized by major folds, thrusts and tear faults, and (2) the more external Plateau Jura further to the north, which comprises largely undeformed tabular areas ("Plateaux"), separated by narrow zones of intense deformation forming discrete map scale linear structures ("Faisceaux") along which shortening is concentrated. The ENE-WSW-striking Faisceau Bisontin is the northwestern-most of these narrow deformation zones. Eastwards it connects with the Faisceau du Lomont; southwest-wards it splays into north-south striking deformation zones, the Faisceau de Quingey being the most prominent and external one (Figure 1). The latter clearly marks the western border of the Jura fold-and-thrust belt with the Eo-Oligocene Bresse Graben.

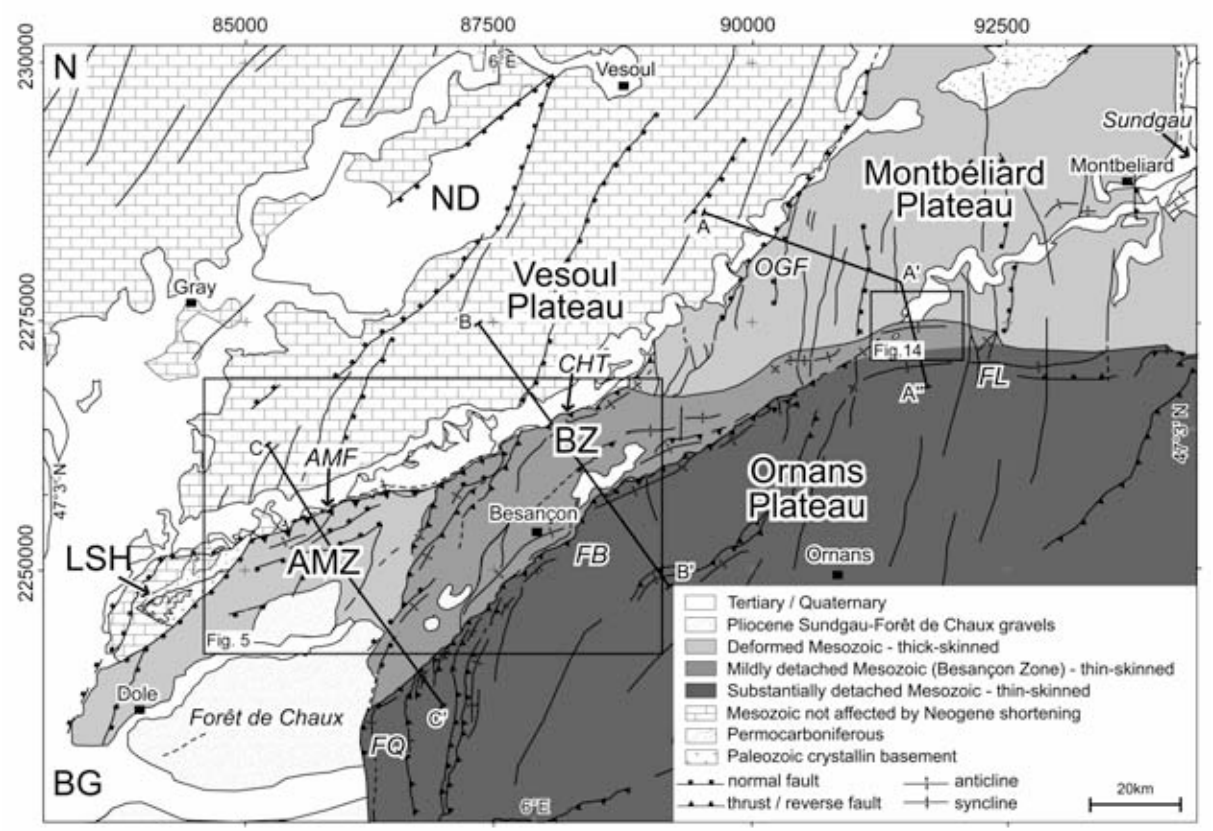

Figure Tectonic map of the study area, showing the new subdivision based on the results of this study (see text for discussion). Note the traces of three cross sections shown in Figure 8. AMF: Avant-Monts Fault; AMZ: Avant-Monts Zone; BZ: Besançon Zone; BG: Bresse Graben ; CHT: Chailluz Thrust; FB: Faisceau Bisontin; FL: Faisceau du Lomont; FQ: Faisceau de Quingey; LSH: La Serre Horst; ND: Noidans Basin; OGF: Ognon Fault.

The exact location of the northwestern front of the thin-skinned Jura fold-and-thrust belt is still ill defined. A large area northwest of the Faisceau Bisontin, often referred to as Avant-Monts Zone, is also weakly deformed (Figure 1) [Chauve et al., 1980; Philippe et al., 1996; Sommaruga, 1997], but it remains unclear whether this area is also part of the thin-skinned taper. The prominent ENE-WSW striking Avant-Monts Fault and the westerly adjacent La Serre Horst define the northern boundary of the Avant-Monts Zone (AMZ Figure 1) towards the Burgundy Platform that shows no signs of contractional deformation (Figure 1). Another zone of weak shortening, the Montbéliard Plateau (MP Figure 1), is located further east and also north of the supposed front of the thin-skinned fold-and-thrust belt (Faisceau du Lomont, FL in Figure 1). Gentle folding is observed well north of the Faisceau du Lomont all the way towards the southwestern rim of the Rhine Graben [Giamboni et al., 2004]; the easternmost folds north of the Faisceau de Lomont and within our study area terminate near the city of Montbéliard [Contini et. al, 1973]. However, previous authors did not consider this area as part of the Avant-Monts Zone nor as belonging to the thin-skinned Jura fold-and-thrust belt [Chauve et al., 1980;

Philippe et al., 1996; Sommaruga, 1997]. It remains unclear whether all the above-mentioned weakly deformed areas were also a part of the thin-skinned fold-and-thrust belt or whether they were deformed in a thick-skinned manner. The locations of the Avant-Monts Zone and the Montbéliard Plateau coincide with the RBTZ that was reported to have been reactivated in a transpressional, thick-skinned manner east to our study area [Giamboni et al., 2004]. Hence, in regard to expected interactions between thin and thick-skinned styles of deformation, the Avant-Monts Zone and similar weakly deformed areas at the front of the Jura Fold-and-thrust belt are of special interest to this study.

For clarity we had to propose a new tectonic subdivision, presented in Figure 3, and discussed below when presenting our data. We subdivide the areas located north of the well defined and substantially detached parts of the thin-skinned Jura fold-and-thrust belt, i.e. the areas which feature weak contractional deformation, as follows, going from west to east: (1) the Avant-Monts Zone that will turn out to be dominated by thick-skinned deformation (2) the Besançon Zone for which we will present evidence for a thin-skinned style of deformation, bordered by the Chailluz Thrust to the north, and (3) the Montbéliard Plateau in the east, only mildly affected by Neogene deformation and largely characterized by thick-skinned deformation.

3.3. Results

3.3.1. Subsurface Analysis

The locations of the subsurface data analyzed are given in Figure 4. Geological logs of boreholes, dating back to the early 20th century, were obtained from the BRGM archive. These reports also include results of reflection seismic campaigns carried out by Safrep in the 1950's yielding additional subsurface information. Total and Gaz de France generously provided more recent seismic reflection data, those of Gaz de France being accessible to an academic institution for the first time. All of the seismic reflection data have been commercially processed and were available to us for interpretation in form of a paper copy.

The analyses and correlations of borehole and seismic reflection data revealed significant differences in the structural style that occur at the northern rim of the Avant-Monts Zone and the Besançon Zone, i.e. along the strike of the prominent ENE-WSW Avant-Monts Fault ("AMF" in Figure 5).

A borehole located at Chailluz (Figures 4, 5 & 6) in the Besançon Zone, and immediately south of the Avant-Monts Fault, provides key information. It reveals a low angle thrust fault at a depth of 113 meters (Figure 6). In the subsurface this thrust places Triassic evaporites over Late Jurassic limestones. The associated anticline was mapped as the "Chailluz anticline" at the surface and is interpreted as a thrust related fault bend fold [Suppe, 1983]. Undoubtedly, this structure is typical for

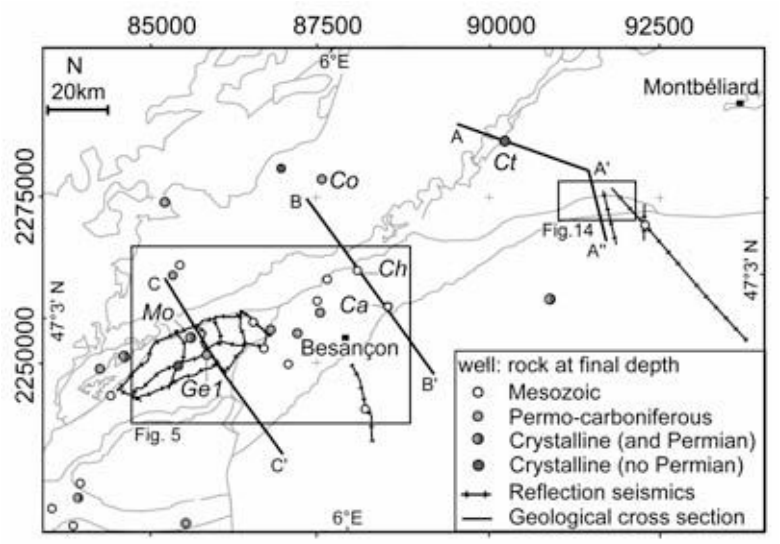

Figure 4: Map depicting the location of subsurface data analyzed in this study and traces of regional cross sections shown in Figure 8. Wells used for the construction of the regional cross sections depicted in Figure 8 are labeled in italics. Grey lines indicate the outlines of the tectonic units shown in Figure 3.

the thin-skinned style of the Jura fold-and-thrust belt [Martin and Mercier, 1996], that is well documented and described by seismic reflection data throughout the more internal parts of the Jura fold-and-thrust belt [Sommaruga, 1997]. Hence, we regard the Besançon Zone as a part of the northwestern most thin-skinned Jura fold-and-thrust belt, which propagated into an area located well north of the Faisceau Bisontin (Figure 5). The segment of the Avant-Monts Fault bordering the Besançon Zone to the north is defined as the Chailluz Thrust and represents the outer most thrust of the thin-skinned Jura. This is the principal reason for separating the Besançon Zone from the Avant-Monts Zone located further to the west (Figure 3) where we found no indications for such shallow decoupling, as will be discussed below.

Further west, along strike of the Avant-Monts Fault, the Moutherot borehole penetrated another anticline (the Moutherot Anticline; Figures 5 & 6). This borehole, however, displays an undisturbed Mesozoic succession. The potential décollement in Middle to Late Triassic evaporites was not tectonically thickened (Figure 6) and remained undeformed. Hence, the previously described low-angle Chailluz Thrust detected in borehole Chailluz cannot be traced along strike further to the west. This indicates that the front of the decoupled Jura fold-and-thrust belt steps back from the Avant-Monts Fault along a series of NNE-SSW-striking transverse structures, which delimit the Besançon Zone from the Avant-Monts Zone located further west. Ultimately these transverse structures link up with the Faisceau de Quingey (see Figure 3).

Furthermore, newly available seismic reflection data across the Avant-Monts Zone provided by Gaz de France (Figure 7) lack evidence for a thin-skinned origin of the Moutherot Anticline. The logs from the Moutherot and Gendrey 1 wells (Figure 6) allowed for the calibration of the reflectors of this seismic section. Both boreholes are located in the immediate vicinity of the seismic line (Figures 4 & 5) and both penetrate the entire Mesozoic succession. The Mesozoic cover sediments are characterized by high amplitude, continuous reflections. By contrast, the underlying Permian strata recorded in both

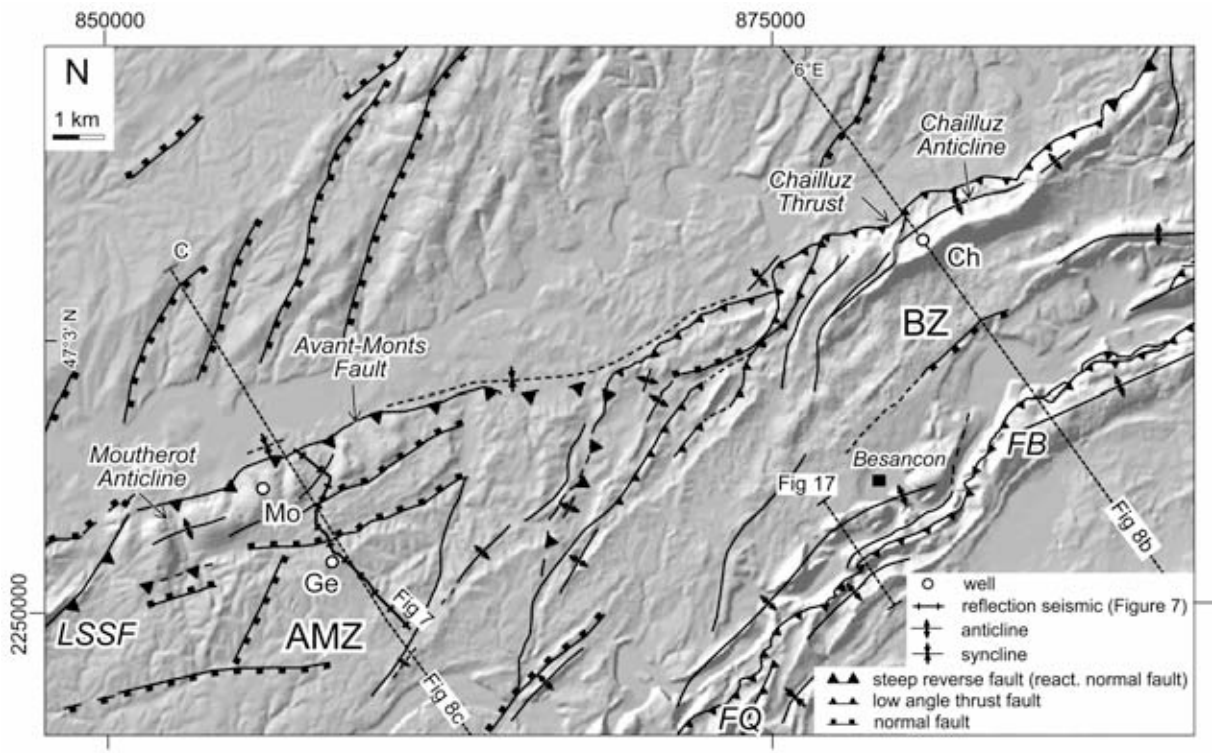

Figure 5: Shaded digital elevation model (horizontal resolution 50m) and structural map of the central part of the Rhine-Bresse Transfer Zone. The anticlines near the Moutherot and Chailluz wells are both aligned along the ENE-WSW striking Avant-Monts Fault. The boundary between the Besançon Zone and the Avant-Monts Zone, as mapped in Figure 3, is marked by an array of minor folds and thrust faults striking NNE-SSW, located in the centre of this figure and west of the city of Besançon. The locations of wells shown in Figure 6, the trace of the seismic reflection line shown in Figure 7 and those of the geological profiles of Figures 8 and 17 are also given. AMZ: Avant-Monts Zone; BZ: Besançon Zone; FB: Faisceau Bisontin; FQ: Faisceau de Quingey; LSSF: La Serre Southern Fault; Mo: Moutherot well; Ch: Chailluz well; Ge: Gendrey1 well.

boreholes feature discontinuous reflections and an occasionally rather chaotic seismic character. In the central part of the seismic section, Permian reflections unconformably toplap against the subhorizontal and continuous Mesozoic reflections; they mark the base Mesozoic angular unconformity.

The top of the Early Triassic Buntsandstein Formation, located at 300 to 350 msec TWT, provides a well-pronounced reflector that is located below the Mid- to Late Triassic evaporites, i.e. the potential décollement horizon. The top of this evaporitic succession, which partly features highly transparent reflections, is again marked by a prominent reflector (50 to 150 msec TWT) that marks the boundary between the top of the Keuper formation and the overlying Liassic marls. This more or less flat-lying sedimentary sequence largely remained undeformed in the southern part of the section. The central part of the seismic section located south of the Avant-Monts Fault, however, displays several E-W striking and steeply north-dipping normal faults. These formed during Paleogene extension in the Rhine-Bresse Transfer Zone and they systematically down-fault the northern compartments. Most

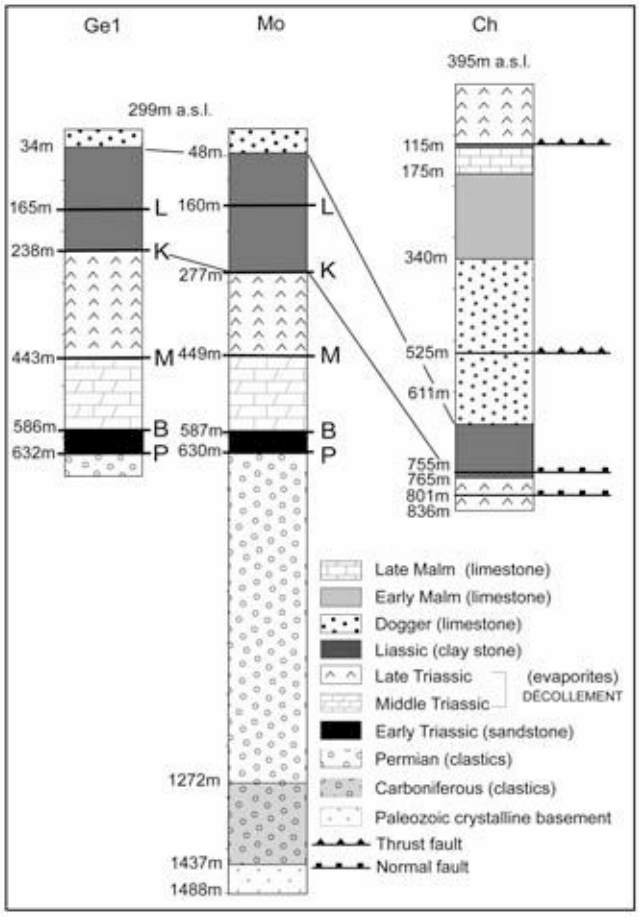

Figure 6: Lithological logs of three deep wells from the Avant-Monts and Besançon zones (see Figures 4 & 5 for locations). Borehole Moutherot (Mo) penetrates the Moutherot Anticline in the Avant-Monts Zone. It displays a continuous sedimentary succession with no indication of low-angle thrust faulting. The correlation with the neighboring Gendrey1 (Ge1) borehole yields no evidence for tectonic thickening of the potential décollement horizon within Middle to Late Triassic evaporites. The borehole Chailluz (Ch) penetrates the Chailluz Anticline located in the frontal part of the Besançon Zone. The low angle thrust fault at a depth of 115m emplaces Triassic evaporites over Upper Jurassic limestones, indicating that the Chailluz Anticline is a fault-related fold, typical for thin-skinned deformation. Note that the correlation of the Top-Liassic horizon between the wells indicates that the Avant-Monts Zone forms a structural high with respect to the Besançon Zone east of it. Also note the stratigraphic position of seismic reflectors L, K, M and B given in Figure 7.

importantly, the westernmost segment of the Avant-Monts Fault, displayed in the northern part of the reflection seismic profile (Figure 7), is clearly seen to represent a steep reverse fault dissecting the entire Mesozoic succession. Hence, this western segment of the Avant-Monts Fault is rooted in the basement and probably represents an inverted former Paleogene normal fault. A contour map of the base Mesozoic in the western Avant-Monts Zone and the area of the La Serre Horst, established on the basis of the entire seismic dataset [Madritsch, 2008], further supports such an interpretation. Interestingly, normal fault inversion occurs only along the south dipping normal faults whereas the north dipping normal faults appear hardly affected by reactivation. Similar observations are reported from other thick-skinned inversion settings e.g. the fold-and-thrust belt of northwestern Taiwan [Lacombe et. al, 2003].

Further west, thick-skinned thrusting along the Avant-Monts Fault is kinematically linked to the La Serre Southern Fault [Coromina and Fabbri, 2004; Madritsch, 2008] which forms the southern boundary of the Late Paleozoic La Serre Horst and which has been reactivated during Paleogene extension and the formation of the Rhine-Bresse Transfer Zone [Madritsch, 2008]. This confirms the

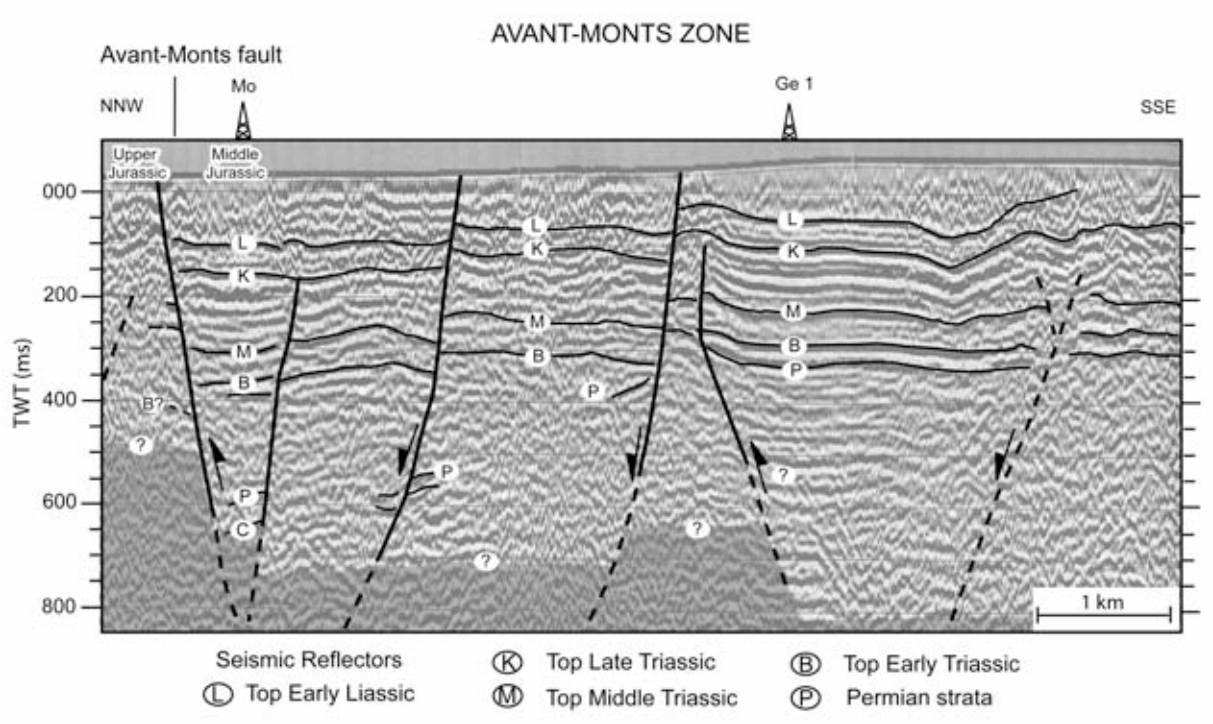

Figure 7: NNW-SSE oriented seismic reflection line across the Avant-Monts Zone (see Figures 4 & 5 for location). Correlations between seismic reflectors and stratigraphy are based on geological logs of boreholes Moutherot and Gendrey 1 (Figure 6). Note that the Avant-Monts Fault in the northern part of the section appears as a steep reverse fault that crosscuts the whole Mesozoic succession, including the supposed detachment horizon within Mid- to Upper Triassic evaporites (reflector M). This clearly indicates thick-skinned tectonics along this segment of the fault, probably associated with inversion of a pre-existing normal fault. (Seismic data: courtesy of GAZ de FRANCE).

interpretation that the Avant-Monts Fault, as seen in Figure 7, formed by the inversion of a pre-existing Paleogene normal fault, that in turn is inferred to have formed along Late Paleozoic structures (see interpretation in the section of Figure 8c). Note that the small amplitude of the Moutherot anticline (Figures 6, 7 & 8c), formed as a result of thick-skinned normal fault reactivation, only features a very gentle surface expression (Figure 5) and is hardly visible in the seismic reflection image (Figure 7). This implies that the amount of shortening of the Mesozoic cover associated with this structure is smaller than that associated with thin-skinned fault-related folding above the low angle Chailuz Thrust further to the east.

In summary, thick-skinned shortening observed throughout the Avant-Monts Zone strongly contrasts with the thin-skinned style of deformation found in the Besançon Zone, where the frontal Chailluz Thrust is soling off as a low angle listric thrust fault within the décollement layer provided by the Late Triassic evaporites (Figure 8b).

3.2. Regional tectonic synthesis

The results of the subsurface data analysis (Figures 4, 5, 6 & 7), together with the study of the available geological maps [Dreyfuss and Kuntz, 1969; Dreyfuss and Kuntz, 1970; Dreyfuss and Théobald, 1972; Contini et al. 1973; Bonte, 1975; Chauve et al., 1983], lead to a new tectonic interpretation, and accordingly, the subdivision of units along the northwestern front of the Jura-fold-and-thrust belt proposed in Figure 3. The following five different tectonic zones are distinguished:

(1) The Vesoul Plateau is part of the autochthonous European foreland, which lacks map-scale contractional deformation features related to Neogene compression. To the west, the Vesoul Plateau borders the Eo-Oligocene Bresse Graben. Its southern and southeastern border follows the Ognon Fault [Ruhland, 1959], a Paleogene-age NE-SW-striking normal fault that formed along a preexisting Paleozoic discontinuity (see profile A-A' in Figure 8)

(2) The Avant-Monts Zone features post-Paleogene thick-skinned reactivation of pre-existing Paleogene to Paleozoic normal faults and is bordered by the crystalline La Serre Horst in the northwest. It is thus not part of the thin-skinned Jura fold-and-thrust belt.

(3) The newly defined Besançon Zone (formerly considered as the eastern part of the Avant-Monts Zone) is affected by thin-skinned Neogene shortening and hence represents the northwestern-most segment of the Jura fold-and-thrust belt.

Figure 8: Interpretive cross sections based on published maps, structural field measurements and subsurface data (see Figures 3 & 4 for location of sections).

8a: Going from SSE to NNW, section A-A'-A" first crosses the Faisceau du Lomont which represents the front of the Plateau Jura, the Clerval anticline further to north, interpreted as the easternmost part of the Besançon Zone, still affected by thin-skinned Jura folding and thrusting, and finally the Montbéliard Plateau, that is primarily affected by normal faulting. Note that the Ognon Fault further to the north represents a normal fault, with only minor presumed thick-skinned Neogene to recent reactivation; it forms the eastern continuation of the Avant-Monts Fault, reactivated by compression later (see Figure 8c).

8b: Section BB' crosses the Besançon Zone near borehole Chailluz (Ch; Figures 5 & 6) where the thin-skinned Jura fold-and-thrust belt propagated a long way north beyond the Faisceau Bisontin, i.e. the eastern continuation of the Faisceau Lomont in section AA'A''. Note the presence of normal faults of Paleozoic and/or Paleogene age underlying the detached Mesozoic sediments, most importantly underneath the Chailluz anticline and the Faisceau Bisontin, where they controlled the location of fault-related folds during thin-skinned tectonics.

8c: Section CC' traverses the Avant-Monts Zone, bordered to north by the western segment of the Avant-Monts Fault representing a steep reverse fault, as imaged by the Moutherot well and seismic reflection data (Figures 5, 6 & 7). The reverse fault formed by inversion of a Paleogene graben, inferred to have formed along the eastern continuation of the La Serre Horst. The fault is thick-skinned since it dissects the evaporitic décollement level of the thin-skinned Jura fold-and-thrust belt located further south. The geometry of the latter is again controlled by NNS-SSE striking Paleozoic and/or Paleogene normal faults that control the location of the front of the Besançon Zone and the Faisceau Bisontin.

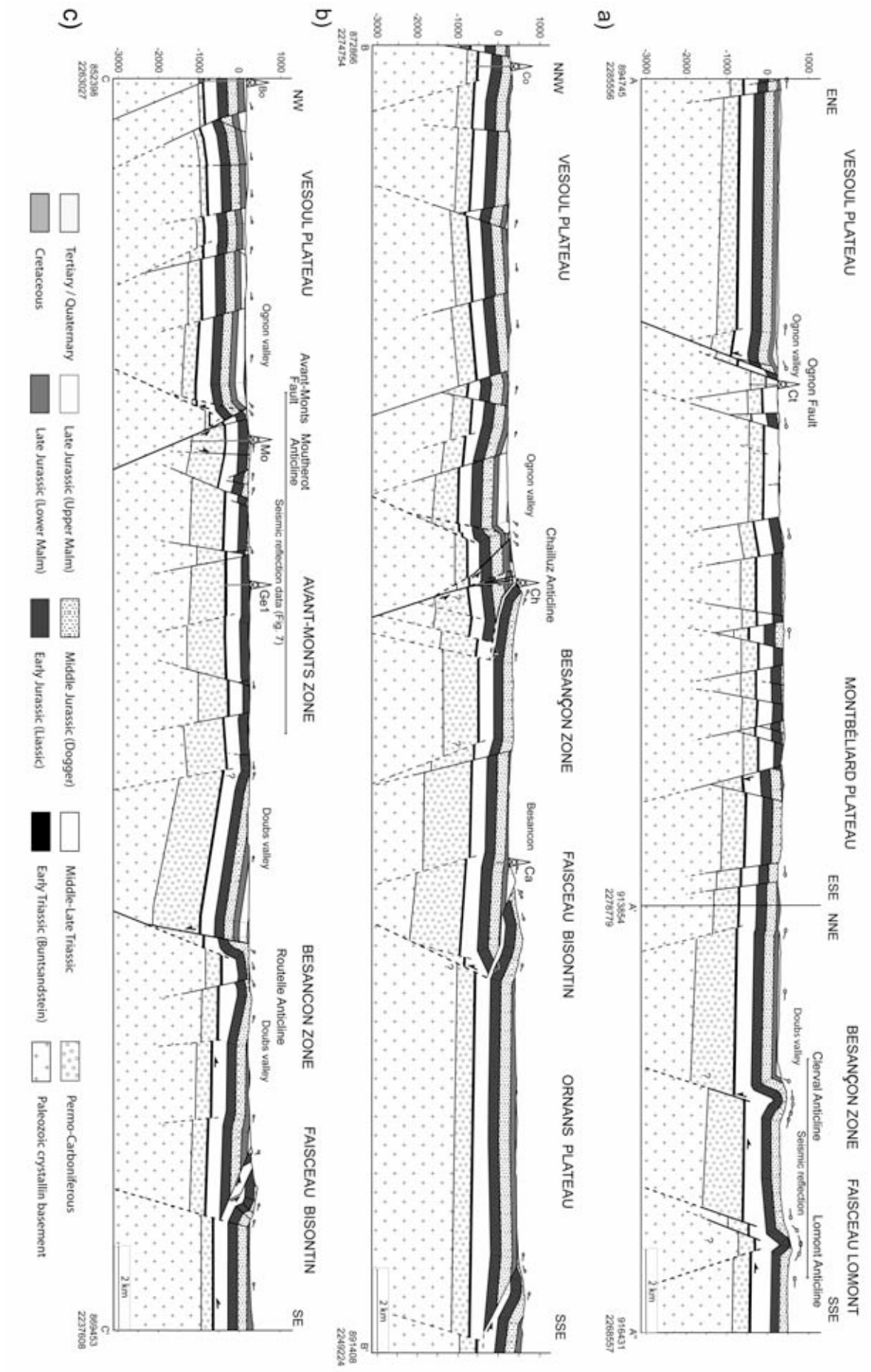
a)
ENE
VESOUL PLATEAU
MONTBÉLIARD PLATEAU
BESANÇON ZONE
FAISCEAU LOMONT
SSE
Ognon Fault
Ognon valley
Ct
Clerval Anticline
Lomont Anticline
Seismic reflection
Doubs valley
2 km
A
894745
2285556
A'
913854
2278779
916431
2268557
b)
NNW
VESOUL PLATEAU
BESANÇON ZONE
FAISCEAU BISONTIN
ORNANS PLATEAU
SSE
Co
Ch
Ca
Chailluz Anticline
Ognon valley
Besancon
2 km
B
872886
2274754
891408
2249224
c)
NW
VESOUL PLATEAU
AVANT-MONTS ZONE
BESANCON ZONE
FAISCEAU BISONTIN
SE
Bo
Mo
Ge1
Avant-Monts Fault
Moutherot Anticline
Seismic reflection data (Fig. 7)
Routelle Anticline
Ognon valley
Doubs valley
2 km
C
853398
2263027
C'
869453
2237608
Tertiary / Quaternary
Cretaceous
Late Jurassic (Upper Malm)
Late Jurassic (Lower Malm)
Middle Jurassic (Dogger)
Early Jurassic (Liassic)
Middle-Late Triassic
Early Triassic (Buntsandstein)
Permo-Carboniferous
Paleozoic crystallin basement

(4) The Montbéliard Plateau further to the east consists of autochthonous Mesozoic strata tilted southwards during Miocene-age uplift of the Vosges Mountains [Ziegler, 1992; Bourgeois et al., 2007]. To the west, the Montbéliard Plateau wedges out between the Ognon Normal Fault in the north and the Besançon Zone in the south. To the east it borders the Rhine Graben. In contrast to the Vesoul Plateau, this area includes isolated anticlines such as those near Montbéliard (Figure 3) [Contini et al., 1973] and was, hence, presumably affected by Late Miocene to recent contraction. The origin of these structures, thick- or thin-skinned, remains controversial [Nivière and Winter, 2000; Ustaszewski and Schmid, 2007].

(5) The Ornans Plateau is part of the Plateau Jura proper and delimited to the northwest by the Lomont, Bisontin and Quingey deformation zones (Faisceaux). While the N-S striking Faisceau de Quingey clearly represents the front of the Jura fold-and-thrust belt towards the Eo-Oligocene Bresse Graben [Guellec et al., 1990], the ENE-WSW striking Faisceau Bisontin is an internal thrust bundle that marks the boundary between Ornans Plateau and Besançon Zone, both these zones being affected by thin-skinned décollement. Eastwards, the Faisceau Bisontin merges into the E-W striking Faisceau du Lomont, connected with the Mont Terri-Landsberg Line [Gürler et al., 1987].

The sections shown in Figure 8 were constructed by integrating existing geological maps [Dreyfuss and Kuntz, 1969; Dreyfuss and Kuntz, 1970; Dreyfuss and Théobald, 1972; Contini et al., 1973; Bonte, 1975; Chauve et al., 1983] and our own field measurements with unpublished well data and seismic sections. Well logs yield rather constant thickness of Mesozoic strata that could be extrapolated throughout the area. While several wells document the existence of the Late Paleozoic Burgundy Trough underneath the Mesozoic cover, the overall geometry and location of border faults of this through system are not precisely known [Debrand-Passard and Courbouleix, 1984] (Figure 2). We assumed that border faults of the Late Paleozoic trough system pre-determined the location of major Paleogene normal faults, generally assumed to have formed by their reactivation [Laubscher, 1970; Illies, 1972; Bergerat and Chorowicz, 1981].

The easternmost section (Figure 8a) crosses the Faisceau du Lomont where the locus of the outermost thin-skinned folds (Clerval Anticline and Lomont Anticline in Figure 8a) appears to be controlled by pre-existing normal faults that formed at the southern margin of the Eo-Oligocene Rhine-Bresse Transfer Zone. The latter caused an offset of the Triassic décollement horizon and flexuring of the overlying sediments, structures also described further east and throughout the southern Upper Rhine Graben area [Ustaszewski et al., 2005a; Ford et al., 2007] as well as throughout the easternmost Jura [Laubscher, 1986]. These flexures triggered the formation of thrust-related anticlines during thin-skinned Neogene contraction [Martin and Mercier, 1996].

Further west (Figure 8b), however, the thin-skinned fold-and-thrust belt propagated further into the foreland, far beyond the Faisceau Bisontin [Martin and Mercier, 1996], i.e. in front of the Besançon Zone that encroached far outwards, all the way to the Chailluz Anticline and onto the pre-existing

normal faults of the Rhine-Bresse Transfer Zone. The Chailluz Anticline is associated with the outer-most thin-skinned Chailluz Thrust, as is well documented by the Chailluz borehole (Figures 5 & 6). The westernmost section (Figure 8c) crosses the Avant-Monts Zone and also integrates a seismic reflection section across the Moutherot anticline and the western segment of the Avant-Monts Fault (Figures 5, 6 & 7). The latter represents a steep reverse fault that dissects the whole Mesozoic succession and particularly the supposed thin-skinned detachment horizon in Middle to Late Triassic evaporites. It is hence clearly related to basement rooted shortening by thick-skinned inversion of pre-existing normal faults; it is not part of classical thin-skinned deformation. In section 8c the front of the Jura fold-and-thrust belt is located further to the south and once more sketched out by a preexisting Paleogene normal fault. The Routelle Anticline is interpreted to have formed along the normal fault flexure. It is located north to the Faisceau de Quingey and is therefore part of the Besançon Zone.

3.3. Brittle tectonics and paleostress analysis

An extensive analysis of outcrop-scale brittle structures was carried out throughout the study area. This analysis attempted to better constrain possible differences in the kinematics and timing of deformation between areas affected either by a thick-, or a thin-skinned, or alternatively, by both styles of deformation.

3.3.1. Methodology

The analysis of fault slip data is based on inferring either incremental strain or stress from a set of fault planes and associated directions of slip. Therefore two different basic hypotheses underlying paleostress methodology can be distinguished.

The kinematic approach assumes that the slip direction on a fault plane is parallel to the maximum resolved shear strain rate governed by a large-scale homogeneous strain rate tensor [Twiss and Unruh, 1998]. This approach is considered to be very robust and basically describes the observed displacements. In fact the results of kinematic "paleostress" analyses yield the approximate orientation of the principal axis of incremental strain based on the graphical or numerical construction of "kinematic axes", or p-t axes, for each fault-slip pair [Marret and Allmendinger, 1990; Twiss and Unruh, 1998]. By contrast, the stress hypothesis, also referred to as dynamic analysis, assumes that the slip direction on a fault plane is parallel to the direction of maximum resolved shear stress induced by a large-scale homogenous stress field [Wallace, 1951; Angelier, 1990]. The results of dynamic analyses yield the orientation of the principal axes of stress ($\sigma1 > \sigma2 > \sigma3$) and in this sense represent a genetic interpretation of the observed structures [Marret and Peacock, 1999].

Besides these principle assumptions, paleostress analysis further assumes that the analyzed rock is physically and mechanical isotropic and behaves as a rheologically linear material [Twiss and Unruh, 1999]. Therefore fault orientation in pre-fractured rocks should be random and different faults should not kinematically interact with each other. Pollard et al. [1993] pointed out that these requirements are often unrealistic. However, in cases where displacements on fault planes are small with respect to fault length, these conditions are likely to be fulfilled [Lacombe et al., 2006].

In this study we applied a combined kinematic-dynamic approach by applying the kinematic p-t axes method [Marret and Allmendinger, 1990] as well as the dynamic Right-Dihedra method [Angelier and Mechler, 1977; Pfiffner and Burkhard, 1987]. The latter method is considered as the simplest but also the most robust dynamic paleostress approach [Angelier, 1989]. While Direct Inversion methods calculate a theoretical "best fit" stress tensor and the stress ratio [Angelier, 1990], the Right-Dihedra method delivers an estimation of the possible orientations of the principal stress axes with the most likely orientation computed at point maxima of superimposed compressional and tensional dihedra, calculated for each fault slip pair [Angelier and Mechler, 1977; Pfiffner and Burkhard, 1987]. Therefore the Right-Dihedra method also considers movements along a non-random set of pre-existing and hence reactivated fault planes that are not necessarily oriented ideally in terms of a theoretical best fit reduced stress tensor. Comparative studies [Meschede and Decker, 1993] have shown that the Right-Dihedra method, in contrast to Direct Inversion methods, is less sensitive to highly asymmetric fault plane associations such as commonly found in tectonic settings of polyphase brittle deformation and also in our study area.

Four consecutive major paleostress fields were proposed to have been active in Cenozoic times [Bergerat, 1987] in the northwestern Alpine foreland. These were reconstructed by numerous studies

Figure 9: Examples of polyphase brittle structures: Faults are shown in stereographic lower hemisphere equal area projections; circles, squares and triangles mark the axes of maximum, intermediate and minimum axis of principal stress, respectively. A) Overprinting criteria testify for fault reactivation and enable to establish a relative chronology between different slip events on the same fault plane. Slickolites formed by NW-SE directed extension (dashed lines) are overprinted by younger sub-horizontal strike-slip-related slickolites (underlined by solid lines). The latter indicate NW-SE-directed compression. B) Crosscutting criteria allow distinguishing between different fault sets; low angle reverse faults are crosscut and dissected by steep strike-slip faults. While the reverse faults record E-W contraction, the strike-slip faults document younger and NW-SE-directed contraction. C) Relative chronology of brittle faulting, as inferred from relations between Neogene faulting and folding. Pre-folding striations L1 became rotated during folding and need to be rotated back to their former position by the amount of bedding dip and around a rotation axis parallel to the strike of bedding before inferring paleostress. A new generation of fault slip striations L2 overprints the rotated striations and shows no signs of rotation by folding. While folding occurred under NS contraction in this area, post-folding striations indicate younger NW-SE contraction.

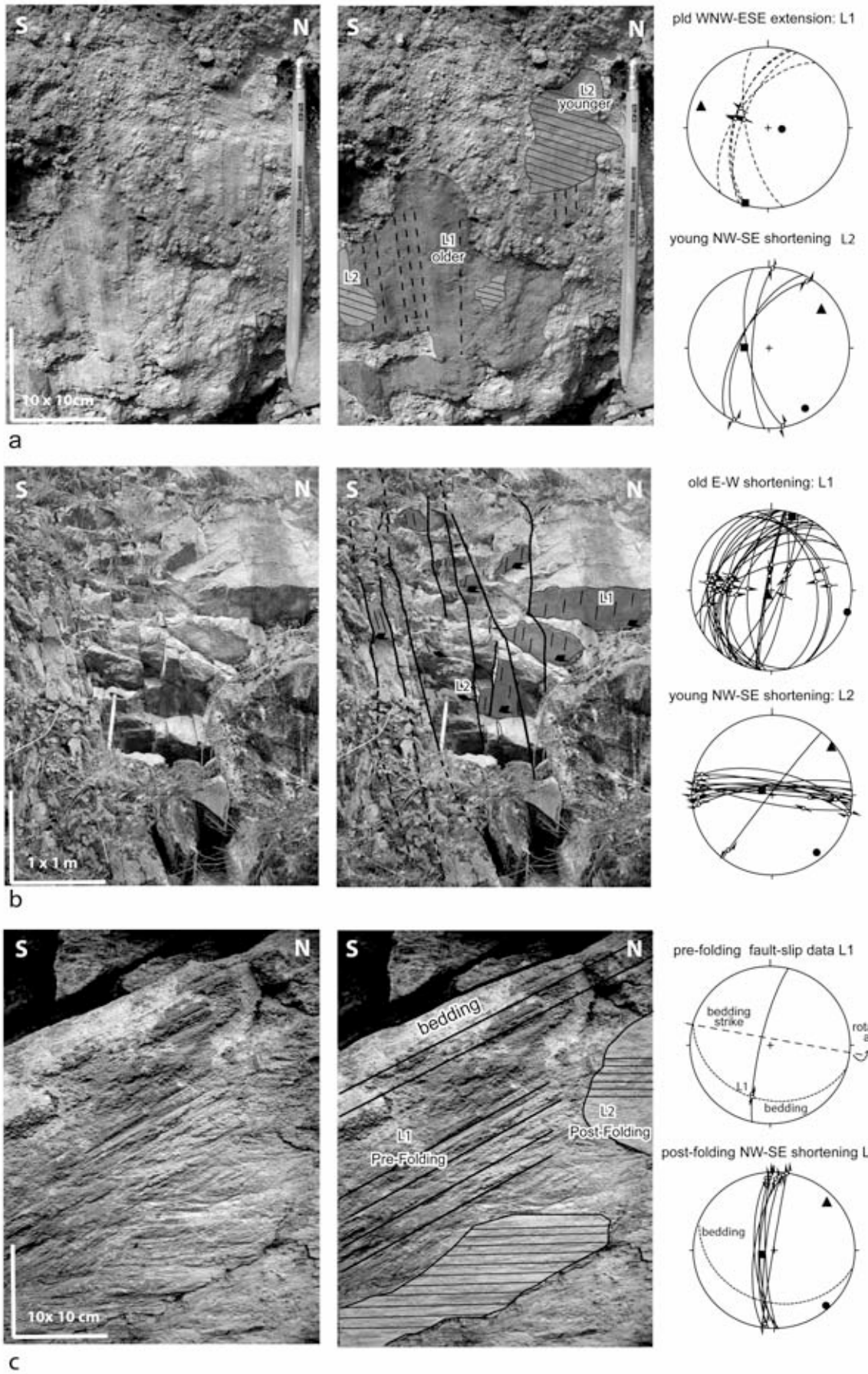
S
N
L2
younger
L1
older
L2
10 x 10cm
a
pld WNW-ESE extension: L1
young NW-SE shortening L2
S
N
L1
L2
1 x 1 m
b
old E-W shortening: L1
young NW-SE shortening: L2
S
N
bedding
L1
Pre-Folding
L2
Post-Folding
10x 10 cm
c
pre-folding fault-slip data L1
bedding
strike
rotation
axis
L1
bedding
post-folding NW-SE shortening L2
bedding

i

n neighboring areas [Lacombe et al., 1993, Homberg et al., 2002; Rocher et al., 2003] and were also encountered in the course of this study [Madritsch, 2008]. These stress fields are: (1) NNE-SSW shortening, attributed an Early Eocene age by most authors, related to the Pyrenean orogeny, (2) E-W to NW-SE directed extension, related to the Eo-Oligocene formation of the European Cenozoic Rift System, including the Rhine-Bresse Transfer Zone, (3) minor NE-SW directed shortening of probably Early Miocene age, and (4) overall NW-SE shortening of Late Miocene to recent age related to the Alpine collision.

A discussion of the entire paleostress dataset and the complete deformation sequence in the study area is beyond the scope of this presentation. The reader is referred to previous investigations mentioned above and to further discussions in Madritsch [2008] regarding our working area. Here we concentrate on the latest, i.e. the Late Miocene to recent deformation event. Attributing fault-slip data sets to a specific event is difficult, especially in the area of investigation where all fault-slip data were collected in Mesozoic rocks and where no stratigraphic age control is available. However, field observations such as overprinting criteria between differently oriented striations on one and the same fault plane (Figure 9a), cross cutting relationships between different and kinematically incompatible fault planes (Figure 9b), and finally, rotation of fault slip pairs in folded areas (Figure 9c) enabled for establishing a relative chronology of the deformation events observed that could be correlated with that established for neighboring areas [Bergerat, 1987; Lacombe et al., 1993; Homberg et al., 1999; Lacombe and Obert, 2000; Homberg et al., 2002; Rocher et al., 2003].

Of particular importance for the purpose of this study is the distinction between strike-slip fault sets that are related to an Early Eocene and so-called “Pyrenean” event [Letouzey, 1986; Bergerat, 1987] on one side from those that are related to Early Miocene to recent structures formed in the context of the Alpine collision and the formation of the Jura fold-and-thrust belt, on the other side. Structures related to the latter, i.e. the Late Miocene to recent deformation events, can be identified as they commonly overprint normal faults related to the prominent Eo-Oligocene extension that led to the formation of the Rhine-Bresse Transfer Zone (Figure 9a) [Bergerat, 1987; Lacombe et al., 1993]. Furthermore, in folded areas the relative age of fracture development and related stress regime with respect to folding may be obtained [Homberg et al., 1999] (Figures 9c & 10). In most cases stresses within the crust fulfill the Andersonian law [Anderson, 1942; Brudy et al., 1997] that predicts two horizontally and one vertically orientated principal stress axes. If this is not the case the fault set has been tilted after its formation, provided it formed near the earth’s surface. In such cases none of the principal stress axes are vertical and two axes lie within the inclined bedding plane [Homberg et al. 1999; Figure 10]. Rotated fault-slip datasets and related paleostress axes fulfill the Andersonian model after back tilting along the strike of the bedding plane by the amount of bedding dip (Figure 10). This criterion has already been successfully applied throughout the internal Jura fold-and-thrust belt in order to distinguish between pre- and post-folding faulting events [Homberg et al., 1999; Homberg et. al., 2002].

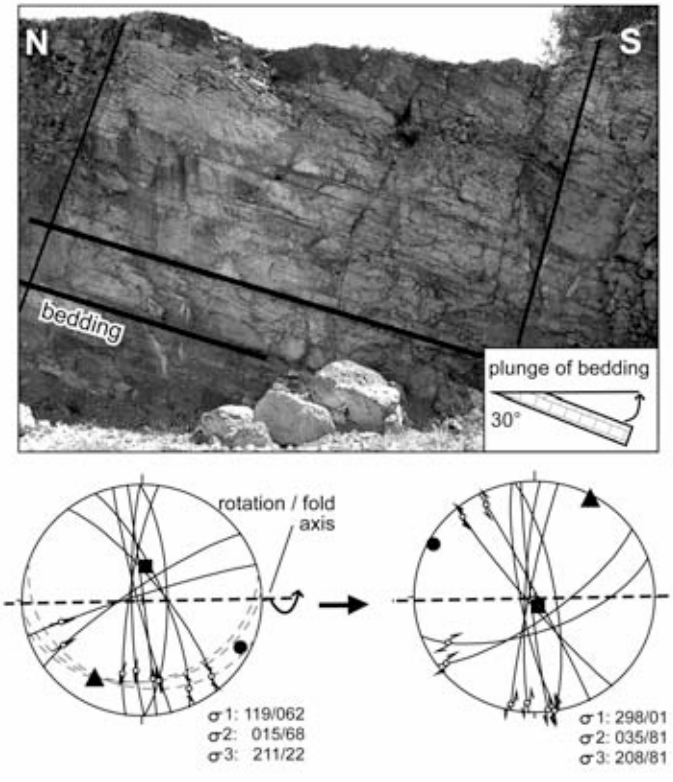

Figure 10: Faulting-folding relationships observed along the thick-skinned Moutherot Anticline. Latest stage folding is recorded by the tilting of the youngest fault set observed throughout the area, defining the widespread NW-SE trending "Alpine" compression. The tilting is evident from the orientation of the paleostress axes prior and after back tilting along a rotation axis parallel to the bedding strike (black dashed line) by the amount of the dip of the bedding. Faults are shown in stereographic lower hemisphere equal area projections; circles, squares and triangles mark the maximum, intermediate and minimum axis of incremental stress, respectively.

In this study more than 1600 fault-slip pairs have been collected from 77 locations. The dataset and the results of the paleostress analysis are given in Table 1 and are displayed in Figures 11 and 12 in the form of a stress tensor map and related stereo plots. All measurements, with a few exceptions only (sites 12, 69, 70, 73), were taken in Mid- (Bathonian to Bajocian) or Late Jurassic (Oxfordian to Kimmeridgian) limestones. Slickolites were the most frequently available sense of slip indicators; calcite slickenfibres and lunate fractures [Petit, 1987] were also used. The kinematic indicators were ranked according to quality from 1 (excellent) to 3 (poor) (see Table 1). Bedding was subhorizontal at most sites investigated during this study. At sites were the inclination of the bedding exceeded 20° its orientation is indicated in Figure 12 (dashed grey lines). Fault sets that were interpreted to have been tilted by folding and were back-rotated prior to paleostress calculations (Figure 10) are noted in Table 1.

The field data were processed with the Windows-based computer program TectonicsFP [Reiter and Acs, 1996-2000]. Data sets from each locality were separated into homogenous subsets, based on overprinting and/or or crosscutting criteria. In addition we applied the pole projection plot [Meschede and Decker, 1993] and the p-t axes method [Marrett and Allmendinger, 1990] in order to graphically test the fault sets for kinematic homogeneity [Madritsch, 2008]. Thereby incompatible fault-striation pairs within a given subset were detected and reconsidered as being part of another subset by additionally taking into account the quality of the slip indicator. The Right-Dihedra-method [Angelier and Mechler, 1977; Pfiffner and Burkhard, 1987] was then used for calculating the orientation of the

principal stress axes (σ1> σ2 > σ3). The comparison of the results of the kinematic p-t axes with those obtained by the dynamic Right-Dihedra method in this study revealed similar results; the orientation of incremental strain and the principal stress axes coincided, which indicates coaxial deformation.

The orientation of these axes yields the tectonic regime at any given location. In this contribution we do not discuss extensional and transtensional stress states that occur widespread throughout the area but which are related to older, i.e. post-Jurassic to Eo-Oligocene deformation events (see [Letouzey, 1986; Bergerat, 1987; Lacombe et al., 1993; Rocher et al., 2003; Madritsch, 2008]). Concentrating on the overall NW-SE shortening of Late Miocene to recent age related to the Alpine collision we only distinguish between reverse faulting (σ1 horizontal, σ3 subvertical, well defined point maxima of p and t axes) and strike-slip faulting (σ1 and σ3 horizontal, well defined point maxima of p and t axes). Furthermore, intermediate cases of transpression (σ1 horizontal, σ2 and σ3 ill defined, p-axes clustered around a point maximum, great circle distribution of t-axes) were observed at sites where kinematically compatible reverse and strike-slip faults coexist in the absence of crosscutting or other overprint criteria (e.g sites 36, 37, 38, Table 1). As the Right-Dihedra method does not yield the stress ratio ($\Phi = (\sigma2-\sigma3)/(\sigma1-\sigma3)$) such intermediate stress states are ill defined. In questionable cases, i.e. when σ3 exhibits a significant plunge (10-80°), we additionally performed a numerical-dynamic paleostress calculation applying the NDA method [Spang, 1972; Sperner et al., 1993] (noted in Table 1). The results of this paleostress calculation were always in good agreement with the Right Dihedra method and yielded the stress ratio (Φ) in order to unambiguously define such intermediate tectonic regimes (transpression: Φ~0.25; reverse and strike-slip faulting: Φ~0.5).

3.3.2 Results

The paleostress analysis indicates that the overall Neogene to recent maximum horizontal stress is oriented NW-SE throughout the area (Figures 11 & 12). This is in agreement with former studies from neighboring areas that applied Direct Inversion methods [Bergerat, 1987; Lacombe et al., 1993; Homberg et al., 2002]. Subtle variations in the orientation of paleostress axes, especially the azimuth of the maximum principal stress axis (σ1), and different types of outcrop-scale brittle structures observed at the various sites, allow for a distinction between an internal and an external paleostress province (Figures 11 & 13). The former comprises the areas governed by thin-skinned deformation, the latter is located north and northwest of the front of the thin-skinned fold-and-thrust belt, comprising the areas of the foreland that are partly affected by thick-skinned deformation.

The internal paleostress province, characterized by a thin-skinned deformation style, extends along the Lomont, Bisontin and Quingey Faisceaux and the Plateau Jura proper and also includes the Besançon Zone. Throughout this province the orientation of the maximum principal stress axes (σ1) undergoes a discernible and systematic change in orientation (Figures 11 & 13): σ1 strikes N-S in the

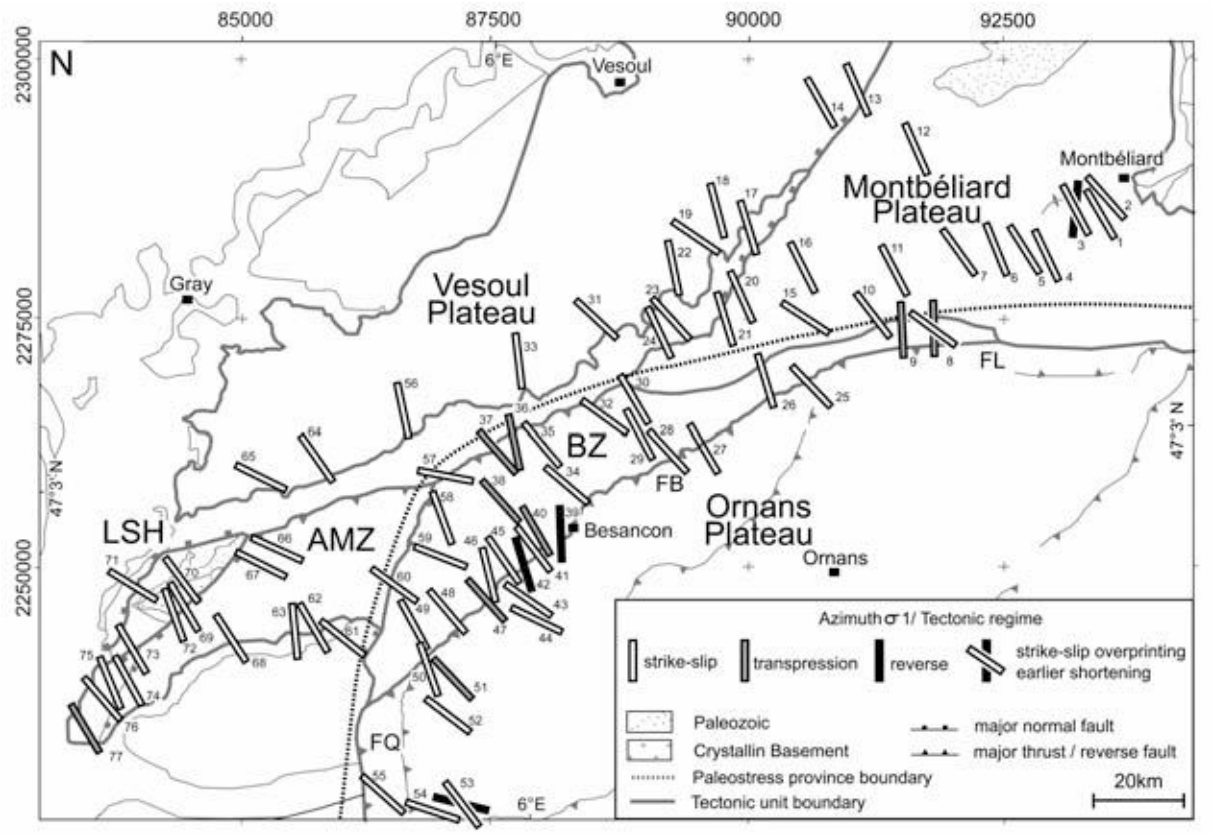

Figure 11: Map showing the azimuth (bars) of the axes of maximum principal stress (σ1), superimposed on a schematic version of the structural map of the study area presented in Figure 3. Numbers next to the bars, given in different gray-tone depending on the tectonic regime, refer to Table 1 and Figure 12. The stippled line marks the boundary between two paleostress provinces (see text for discussion). AMZ: Avant-Monts Zone; BZ: Besançon Zone; FB: Faisceau Bisontin; FL: Faisceau du Lomont; FQ: Faisceau de Quingey; LSH: La Serre Horst.

east, gradually turns over a to a NW-SE orientation further west, and finally into the WNW-ESE direction observed in the southwest. This fanning stress pattern was also noted by previous authors [e.g. Laubscher, 1972; Homberg et al., 1999; Homberg et al., 2002] and represents a typical phenomenon associated with the thin-skinned tectonics of the arcuate Jura fold-and-thrust belt [Philippe et al., 1996; Hindle and Burkhard, 1999; Affolter and Gratier 2004].

The stress trajectories in the internal paleostress province are most often defined by steep conjugate strike-slip faults that define a strike slip tectonic regime (white arrows, σ1 and 3 horizontal σ2 vertical) (Figures 11 & 12). Almost everywhere such strike-slip faults were found to overprint and reactivate older pre-existing normal faults or extension gashes (Figure 9a). The latter are interpreted as having formed during the prominent Eo-Oligocene extension [Lacombe et al., 1993; Madritsch 2008]. In the eastern part of the study area, where strike-slip faults indicate N-S directed stress orientations similar to those related to the "Pyrenean" shortening of presumably Early Eocene age [Bergerat, 1987;

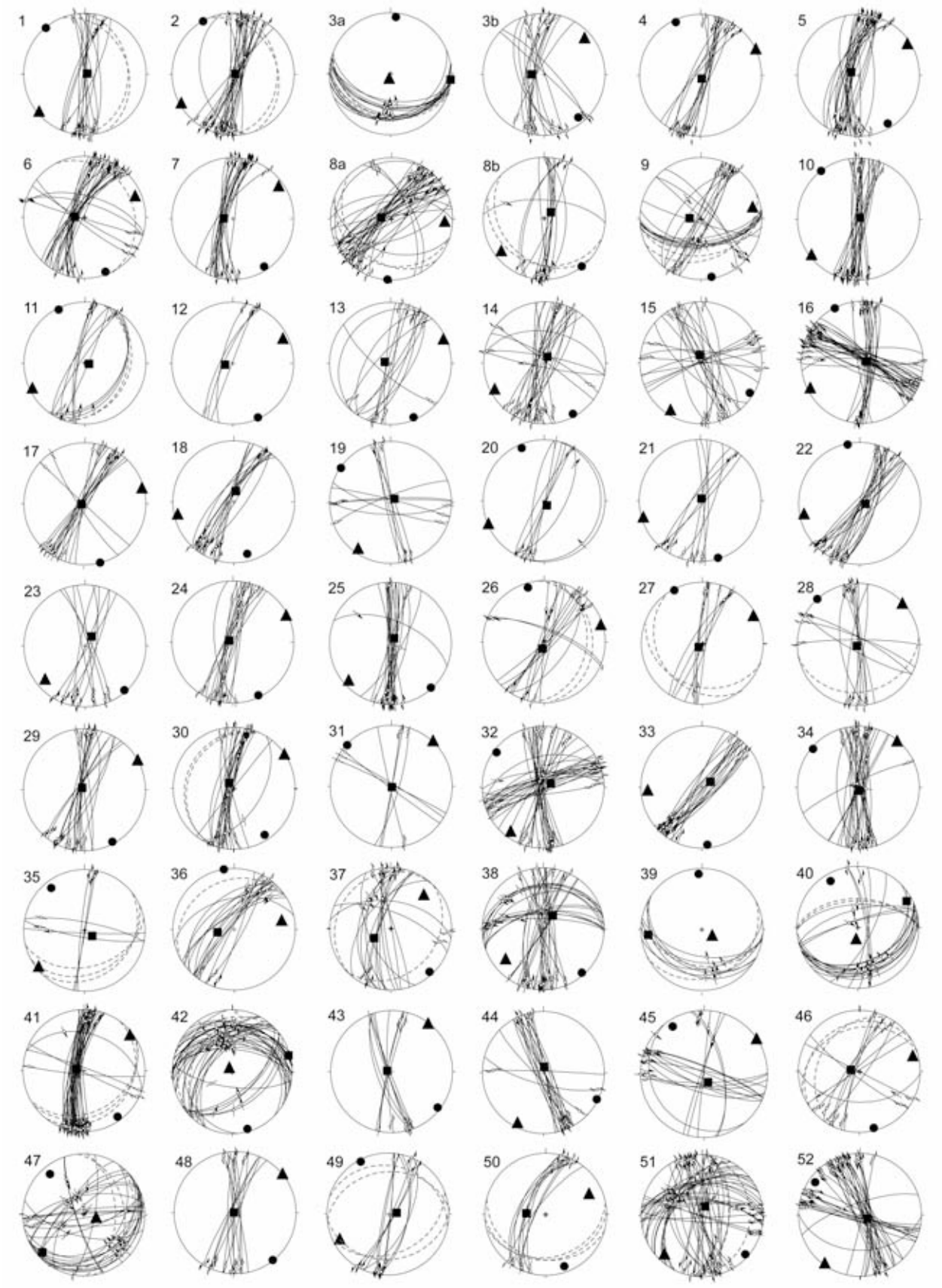
1
2
3a
3b
4
5
6
7
8a
8b
9
10
11
12
13
14
15
16
17
18
19
20
21
22
23
24
25
26
27
28
29
30
31
32
33
34
35
36
37
38
39
40
41
42
43
44
45
46
47
48
49
50
51
52

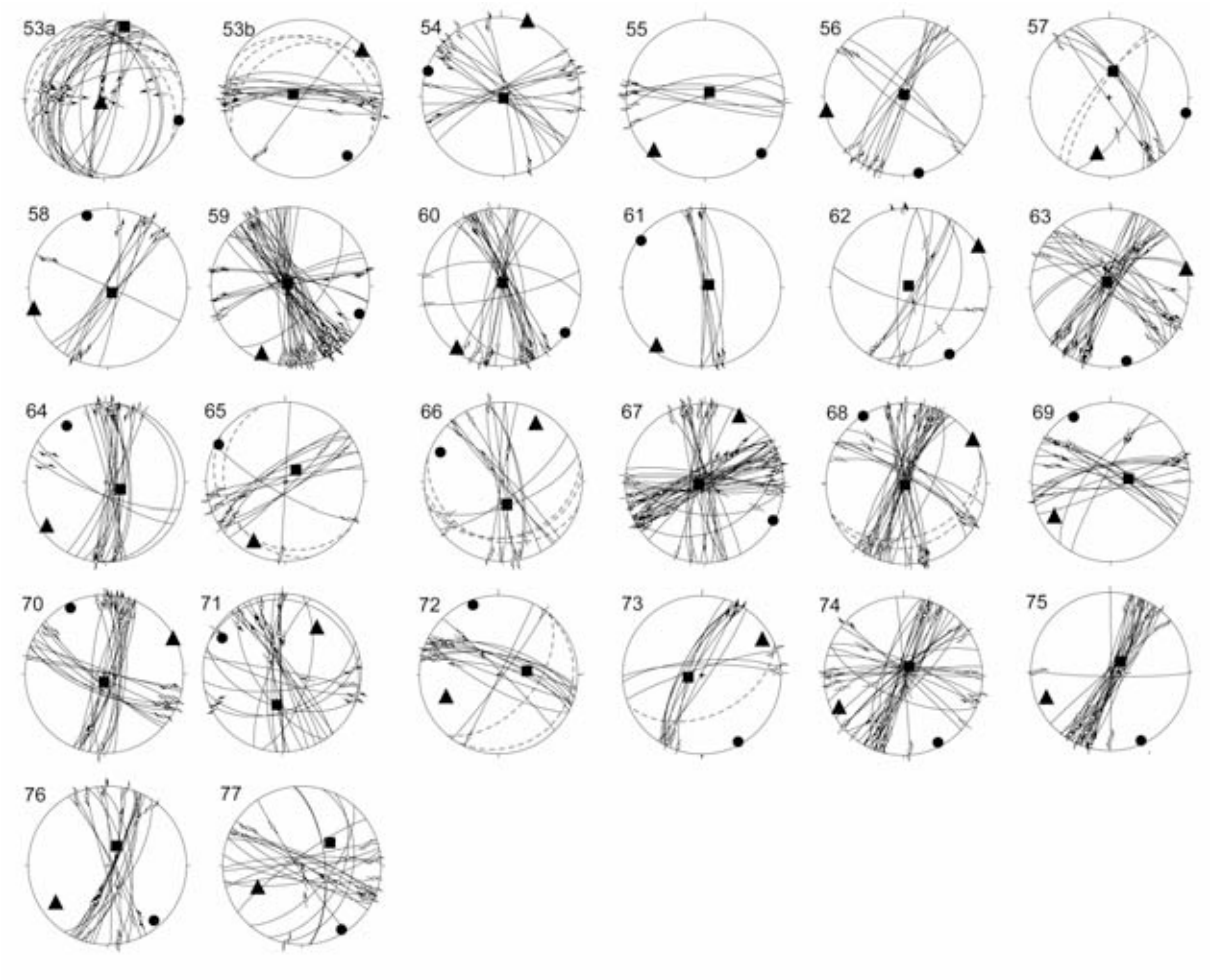

Figure 12: Stereographic lower hemisphere projection of fault-slip data obtained in the study area and results of the Right-Dihedra paleostress determination. Circles, squares and triangles mark the maximum, intermediate and minimum principal stress axes, respectively (see Table 1 and Figure 11 for details and the location of observation points). Dashed grey lines mark the bedding orientation were inclined more than 20°.

Homberg et al., 2002], overprinting criteria in respect to Eo-Oligocene extensional structures provide the main criterion for their attribution to Neogene-age deformation. Moreover, in areas affected by Neogene folding these fault sets are strictly perpendicular to the trend of the Neogene thrust faults and fold axes, which makes their attribution to Neogene deformation even more likely (Figures 11 & 14).
At some localities, near the major deformation fronts of the Faisceau du Lomont, Bisontin and Quingey or, alternatively, at the northern rim of the Besançon Zone, shortening is taken up by low-angle thrust faults that define a tectonic regime of reverse faulting (Figures 11 & 12, e.g. sites 39, 40, 53). These faults consistently developed during a late stage of folding (Figure 14). At other sites, mostly located at the northwestern rim of the Besançon Zone, an intermediate tectonic regime of transpression was inferred (grey arrows in Figure 11, e.g sites 36, 37, 38, 50). Throughout the Jura fold-and-thrust belt, a tectonic regime characterized by permutations of $\sigma 2$ and $\sigma 3$ was found to be

Nr.	Locality	X	Y	Age	Tectonic Unit	σ1		σ2		σ3		Φ	Tectonic regime	N	n	Quality	Rot.
						Azi.	pl.	Azi	pl.	Azi.	pl.						
1	Bart	933869	2285000	Rauracien	Montbéliard Plateau	320	1	76	87	230	2		strike-slip	14	0	2	x
2	Mont Bart	933420	2286010	Sequanien	Montbéliard Plateau	330	1	81	87	240	3		strike-slip	24	0	1	x
3a	Bavans	932186	2285113	Bajocien	Montbéliard Plateau	6	7	96	1	193	82		reverse	13	1	1	
3b	Bavans	932186	2285113	Bajocien	Montbéliard Plateau	141	11	270	73	49	13	0.47	strike-slip	17	1	1	
4	Colombiere Fontaine	928370	2281073	Sequanien	Montbéliard Plateau	335	5	160	85	65	0		strike-slip	14	0	1	
5	Longevelle	926463	2281522	Sequanien	Montbéliard Plateau	149	9	292	79	58	6		strike-slip	26	2	1	
6	Longevelle West	923433	2281634	Sequanien	Montbéliard Plateau	159	5	272	77	68	12	0.48	strike-slip	28	1	1	
7	L'Isle sur le Doubs	920067	2281297	Rauracien	Montbéliard Plateau	147	7	272	78	56	10		strike-slip	19	0	2	
8a	Anteuil	917598	2273891	Bathonien	Besançon Zone	184	1	276	76	94	14	0.37	transpressional	36	3	1	
8b	Anteuil	917598	2273891	Bathonien	Besançon Zone	142	1	48	78	232	12	0.47	strike-slip	14	0	3	
9	Clerval	914680	2273779	Bajocien	Besançon Zone	170	3	272	75	79	15	0.28	transpressional	23	5	1	
10	L'Hopital St. Lieffroy	912212	2275014	Sequanien	Montbéliard Plateau	322	0	53	87	232	3		strike-slip	21	1	1	
11	Soye	913222	2279839	Callovien	Montbéliard Plateau	334	3	100	85	244	4		strike-slip	10	0	1	
12	Vellechevreux	915862	2290580	Middle Triassic	Montbéliard Plateau	155	2	258	80	65	10		strike-slip	5	1	2	
13	Gouhenans	910304	2297344	Bajocien	Vesoul Plateau	157	5	286	82	66	6		strike-slip	13	4	3	
14	Aillevans	906601	2296221	Bajocien	Vesoul Plateau	151	5	25	81	242	7		strike-slip	24	3	2	
15	Vergranne	904581	2280288	Bathonien	Montbéliard Plateau	122	7	349	80	213	7		strike-slip	22	8	1	
16	Romain	904581	2280288	Bathonien	Montbéliard Plateau	333	1	73	85	243	5		strike-slip	41	6	1	
17	Montagney-Servigney	899644	2283654	Sequanien	Vesoul Plateau	165	1	267	86	75	4		strike-slip	16	6	3	
18	Cognieres	896726	2285000	Sequanien	Vesoul Plateau	165	13	11	75	257	6	0.5	strike-slip	14	0	1	
19	Fontenois les Montbozon	894370	2282868	Sequanien	Vesoul Plateau	305	1	47	83	215	7		strike-slip	11	5	2	
20	Tallans	904918	2275125	Bajocien	Montbéliard Plateau	337	7	149	83	247	1		strike-slip	8	1	3	
21	Battenans les Mines	898858	2276809	Bajocien	Vesoul Plateau	163	2	33	87	253	3		strike-slip	9	3	3	
22	Ormenans	897288	2274789	Sequanien	Vesoul Plateau	349	2	94	82	258	8		strike-slip	20	5	1	
23	Germondans la Roche	891340	2274340	Sequanien	Vesoul Plateau	138	3	35	75	229	15	0.52	strike-slip	11	2	1	
24	Rigney la Roche	891000	2273891	Sequanien	Vesoul Plateau	154	4	292	85	64	4		strike-slip	16	9	2	
25	Baume-les-Dames East	905703	2268393	Bajocien	Faisceaux Bisontin	138	2	34	82	228	8		strike-slip	21	4	1	
26	Baume-les-Dames	901103	2268729	Bajocien	Besançon Zone	344	8	193	81	74	4		strike-slip	14	0	1	x
27	Champlive	895267	2262445	Bajocien	Faisceaux Bisontin	332	2	224	83	62	7		strike-slip	8	4	3	x
28	Deluz	891228	2262558	Callovien	Besançon Zone	318	0	226	87	48	3		strike-slip	14	0	2	x
29	Amagney	888759	2662445	Rauracien	Besançon Zone	152	4	314	86	62	1		strike-slip	18	5	2	
30	Chaudefontaine	8888871	2263680	Callovien	Besançon Zone	147	10	316	80	56	2		strike-slip	22	8	2	
31	Tratiefontaine	884495	2275013	Sequanien	Vesoul platform	313	2	138	88	43	0		strike-slip	7	5	2	
32	Marchaux	885618	2265475	Bathonien	Besançon Zone	307	5	64	79	216	10		strike-slip	43	13	2	
33	Boult	877201	2270637	Rauracien	Vesoul Plateau	174	6	58	76	266	12	0.54	strike-slip	18	1	2	
34	Besancon	896165	2259079	Bathonien	Besançon Zone	310	3	172	86	41	3		strike-slip	27	7	1	
35	Tallenay	879221	2262109	Bajocien	Besançon Zone	322	12	125	77	231	4		strike-slip	6	2	3	x
36	Devecey	875967	2262445	Bajocien	Besançon Zone	350	0	260	67	81	23	0.37	transpressional	16	4	3	
37	Auxon-Dessus	875743	2262333	Bajocien	Besançon Zone	138	6	241	65	45	24	0.37	transpressional	17	0	1	
38	Besancon/Temis	876865	2256723	Bajocien	Besançon Zone	139	5	36	68	231	21	0.38	transpressional	36	11	1	
39	Besancon / St.Léonard	881017	2253518	Sequanien	Faisceaux Bisontin	357	10	264	13	124	74	0.49	reverse	7	0	2	
40	Chaudanne	878436	2254142	Bathonien	Besançon Zone	330	13	62	10	188	73	0.32	transpressional	21	2	1	
41	Beure	878099	2252458	Rauracien	Faisceaux Bisontin	144	7	282	80	53	7		strike-slip	39	9	1	
42	Arguel	877987	2251224	Sequanien	Faisceaux Bisontin	165	5	74	3	313	84		reverse	34	7	1	
43	Pugey	877762	2247970	Bajocien	Faisceaux Bisontin	128	5	281	84	38	3		strike-slip	10	3	3	
44	Epeugney	878548	2246062	Bathonien	Faisceaux Bisontin	117	3	7	83	207	7		strike-slip	18	3	2	
45	Planoise	875855	2251336	Bajocien	Besançon Zone	327	11	155	78	57	2		strike-slip	17	1	1	
46	Rancenay	874284	2249653	Bathonien	Besançon Zone	166	5	281	79	75	10		strike-slip	12	2	2	x
47	Busy	874733	2247858	Bajocien/	Faisceaux Bisontin	320	14	228	9	106	73	0.36	transpressional	28	0	1	
48	Bussieres	870356	2246736	Bajocien	Besançon Zone	141	1	288	89	51	1		strike-slip	13	3	2	
49	Routélle	866878	2245389	Bajocien	Besançon Zone	333	4	81	78	242	11	0.49	strike-slip	10	1	1	x
50	Abbans Dessous	868673	2240676	Bajocien	Besançon Zone	160	11	273	64	66	23	0.49	strike-slip	10	3	2	
51	Quingey	870693	2239788	Bathonien	Faisceaux Quingey	132	6	16	77	224	12	0.26	transpressional	47	0	1	
52	Pointvillers	870132	2236637	Portlandien	Faisceaux Quingey	306	11	117	79	216	2		strike-slip	34	2	1	
53a	Ivrey	871478	2227659	Bajocien	Faisceaux Quingey	106	2	16	5	215	84		reverse	25	0	1	
53b	Ivrey	871478	2227659	Bajocien	Faisceaux Quingey	142	10	294	79	51	5		strike-slip	14	1	1	
54	StJospeh	866890	2224486	Portlandien	Faisceaux Quingey	289	1	126	87	19	1		strike-slip	16	3	3	
55	Port Lesney	863736	2229006	Rauracien	Faisceaux Quingey	133	x	24	83	223	8		strike-slip	7	2	3	
56	Pin	865868	2265924	Sequanien	Vesoul Plateau	169	1	30	88	259	1		strike-slip	11	4	2	
57	Chaucenne	869907	2259640	Sequanien	Besançon Zone	101	2	8	63	192	27	0.43	strike-slip	7	0	3	
58	Champagney	869795	2255489	Aalenien	Besançon Zone	344	9	146	81	250	2		strike-slip	9	1	2	
59	Chemaudin	869683	2251673	Bathonien	Besançon Zone	112	7	339	80	203	7		strike-slip	44	7	2	
60	St. Vit	865082	2248531	Bathonien	Besançon Zone	126	2	13	86	216	4		strike-slip	24	11	2	
61	Fraisans	860033	2243930	Rauracien	Avant-Monts Zone	308	4	69	82	217	7		strike-slip	8	2	3	
62	Ranchot	837564	2244604	Bathonien	Avant-Monts Zone	150	2	311	88	60	1		strike-slip	8	4	1	
63	Monteplain	855656	2244379	Callovien	Avant-Monts Zone	167	12	5	76	256	3	0.54	strike-slip	31	4	2	
64	Marnay	857676	2261435	Rauracien	Vesoul Plateau	325	15	115	73	233	8	0.5	strike-slip	20	8	1	
65	Montagney	852290	2258967	Sequanien	Vesoul Plateau	299	5	45	74	208	15	0.44	strike-slip	12	2	3	
66	Taxenne	853637	2252571	Bajocien	Avant-Monts Zone	295	13	171	65	30	19	0.59	strike-slip	14	5	1	x
67	Gendrey	852178	2251000	Bathonien	Avant-Monts Zone	118	2	223	82	28	7		strike-slip	75	28	3	
68	Orchamps	849709	2243594	Bathonien	Avant-Monts Zone	327	1	220	88	57	2		strike-slip	36	20	1	
69	Forêt de la Serre	844772	2247072	Paleozoic Granite	Avant-Monts Zone	330	7	81	71	238	17	0.46	strike-slip	18	8	1	
70	Moissey	843650	2249429	Permian Vulcanite	Avant-Monts Zone	333	7	181	82	64	4		strike-slip	27	7	2	
71	Peintre	839722	2248756	Bathonien	Vesoul Plateau	300	14	189	56	38	30	0.51	strike-slip	23	1	2	
72	Amange	844435	2246175	Bajocien	Avant-Monts Zone	340	7	82	61	246	28	0.53	strike-slip	15	6	3	
73	Jouhe	839834	2242920	Aalenien	Avant-Monts Zone	151	5	260	76	60	13	0.46	strike-slip	12	6	1	
74	Authume	839385	2239778	Bathonien	Avant-Monts Zone	152	6	31	78	243	10		strike-slip	35	18	1	
75	Mont Roland	837702	2239442	Bathonien	Avant-Monts Zone	156	5	45	75	247	14	0.55	strike-slip	26	12	1	
76	Monniere	837702	2238544	Bajocien	Avant-Monts Zone	140	10	25	68	234	20	0.46	strike-slip	18	3	1	
77	Dampiere	834224	2234180	Sequanien	Avant-Monts Zone	148	6	51	52	243	37	0.32	transpressional	20	3	1	

Table 1 Results of the paleostress analysis. Numbers refer to Figures 10 & 11. Coordinates (X/Y) given in France II Lambert Conformal Conic system. σ1, σ2, σ3: maximum, intermediate and minimum principal stress axes; Azi: azimuth; pl: plunge; N: number of fault slip pairs considered for paleostress calculation; n: number fault slip pairs with no indication of slip direction; Φ: stress ration from NDA paleostress calculation indication the tectonic regime (Φ ~ 0.25 transpression; Φ ~ 0.5 reverse / strike-slip faulting compare Figure 12); Quality: 1 excellent, 2 good, 3 poor.; Rot: datasets that were inferred to be tilted and back rotated before paleostress calculation (compare Figure 10).

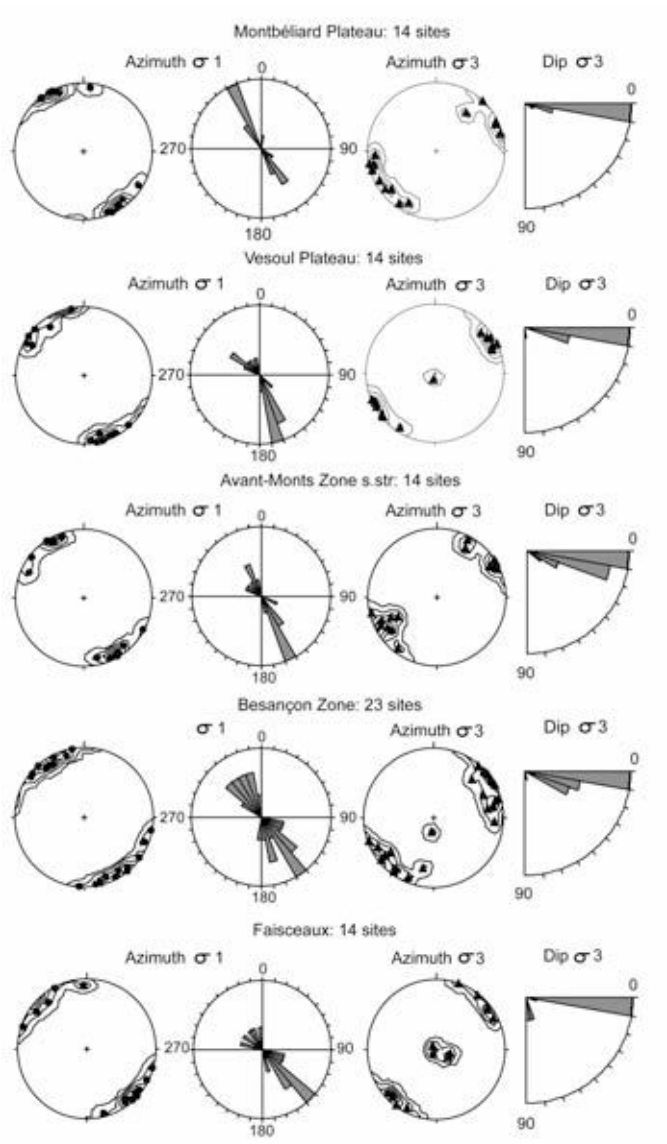

Figure 13: Directional analysis of calculated paleostress axes for the various tectonic units. From left to right: Contoured plot of σ1; rose diagram of the azimuth of σ1; contoured plot of σ3 and inclination diagram of the plunge of σ3 (lower hemisphere stereographic equal area projection). The Montbéliard and Vesoul Plateaux, as well as the Avant-Monts Zone, comprise an external paleostress province (Figure 10) characterized by a uniform direction of σ1 striking NW-SE and by a close to horizontally oriented σ3. By contrast, the orientation of σ1 within in the internal paleostress province, comprising the Besançon Zone and the Lomont, Bisontin and Quingey Faisceaux, has a tendency for fanning, while σ3 is close to vertical at many of the studied sites.

typical for areas characterized by tear faults and lateral ramps [Laubscher, 1972; Homberg et al., 2002; Ustaszewski and Schmid, 2006].

Differing paleostress axis orientations at a given site could, in many places, be explained by strain partitioning controlled by the availability of pre-existing normal faults, and could hence be theoretically related to a unique tectonic event. However, there are some key outcrops where systematic overprinting relationships between two separate Neogene deformation phases of different orientation were observed. At site 53 along the Faisceau de Quingey, top-west low angle thrust faults, which reflect E-W shortening, are overprinted by strike-slip faults that yield NW-SE shortening (Figure 9b). Another evidence is provided at locations 3, 8 and 9 north of the Faisceau du Lomont (Figure 11), where N-S striking strike-slip faults indicating NW-SE directed shortening are seen to post-date N-S directed shortening related to the folding of the Clerval and Montbéliard Anticlines

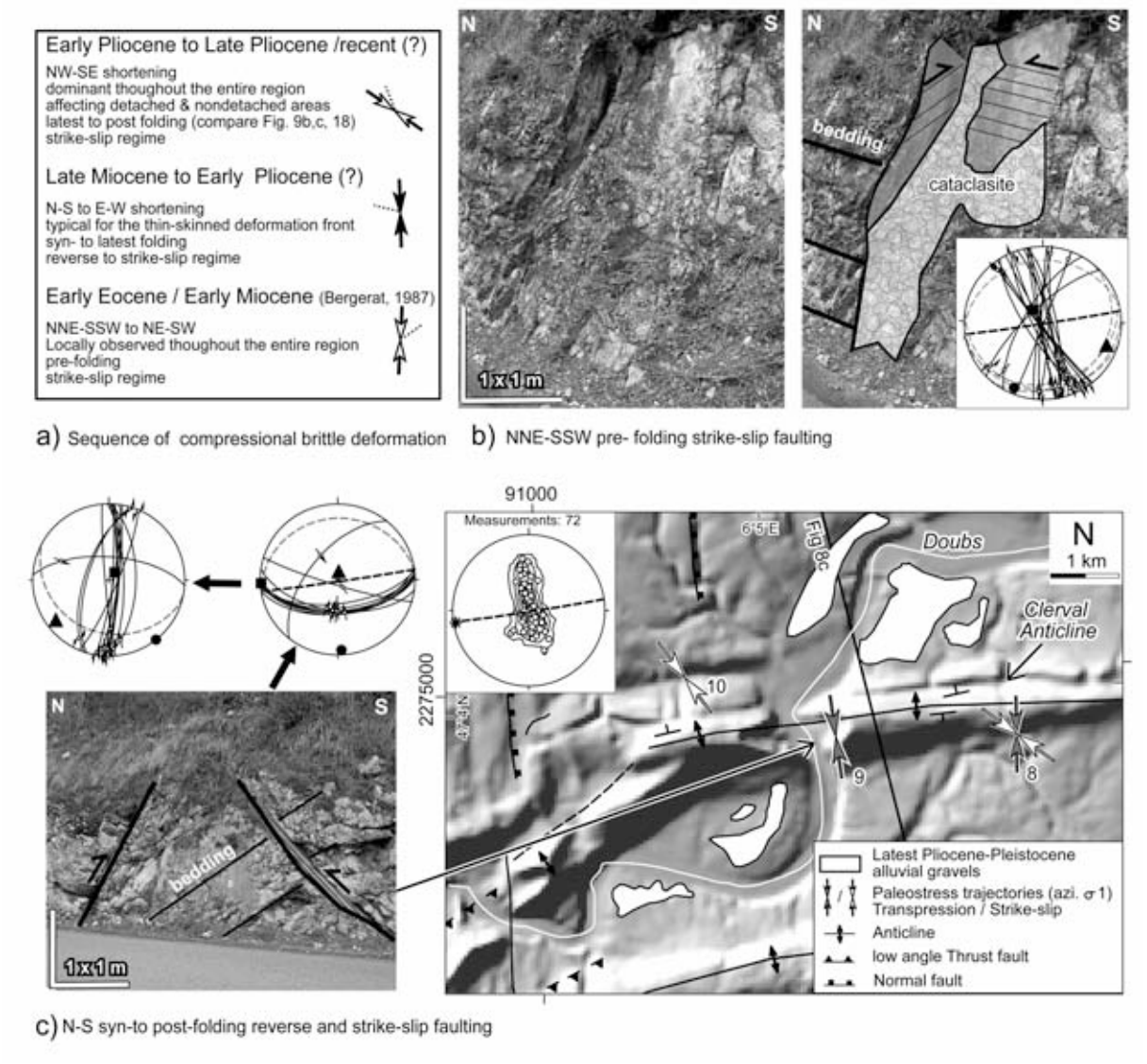

Figure 14: Faulting and folding relationships observed along the thin-skinned Clerval Anticline (see Figure 3 for location). Fault slip data are displayed in form of stereographic lower hemisphere projections; σ1, σ2 and σ3 are shown by circles, squares and triangles, respectively. Grey dashed lines show the orientation of bedding.

a: Succession of brittle deformations with respect to folding. Arrows show the orientation of σ1 as observed at the site, stippled line shows regional variations.

b: Early stage strike-slip faults slightly tilted by folding.

c: Shaded digital elevation model of the Clerval Anticline (horizontal resolution 50m). Syn- to post-folding low angle thrust faults are observed in the core of the anticline, confining N-S shortening perpendicular to the fold axis. The youngest fault sets comprise strike-slip faults, confining NW-SE shortening oblique to the fold axis (compare Figures 9b & c for relative age criteria). Also note the antecedent post-2.9 Ma course of the Doubs River with respect to the fold structure and the distribution of terraces derived from the eroded Sundgau-Forêt de Chaux Gravels.

(Figures 3, 8a, 9c & 14). Hence the fanning stress trajectories observed along the Quingey and Bisontin Faisceaux appear to be overprinted by consistently NW-SE oriented paleostress trajectories.

These combined regional observations result in a sequence of compressional brittle deformations that initiated in the Late Miocene in this part of the Jura fold-and-thrust belt [Becker, 2000; Ustaszewski and Schmid, 2006] (Figure 14a). Figure 14 illustrates the situation along the Clerval Anticline that is located at the eastern margin of the study area and north to the Faisceau du Lomont, and is therefore part of the Besançon Zone (Figures 3 & 8a). Towards the west the fold links up with shallow thrust faults. These observations, together with interpretations of seismic reflection data, strongly suggest a thin-skinned formation of the fold structure, at least during an initial stage, when it probably nucleated along a preexisting normal fault (see interpretation given in Figure 8a).

The earliest compressional structures observed in the Clerval area are strike-slip faults (Figure 14b). The deduced paleostress axes trend oblique to the fold axis. These fault sets are always to some extent affected by folding (Figure 14b), which hints towards a pre- to syn-folding formation. These structures are inferred to have formed in Early Eocene ("Pyrenean compression"; Bergerat; [1987]), or alternatively, in Early Neogene times when found to overprint normal faults [Homberg et al., 2002; Madritsch, 2008], and they will not further discussed here. Reverse faults indicate paleostress axes oriented perpendicular to the fold axis, and they dissect the folded beds (Figure 14c). This suggests a syn- to post folding age. The youngest fault set comprises strike-slip faults that define NW-SE directed shortening oblique to the fold axis (Figure 14c). As outlined above these fault sets frequently overprint reverse faults and are hardly affected by folding (Figures 9b & c). This is in agreement with observations from the internal Jura fold-and-thrust belt [Homberg et al., 2002].

Unfortunately, overprinting criteria allowing for distinguishing distinct events during the Neogene to recent history of faulting are restricted to areas were stress trajectories related to such different shortening events are oriented at a high angle to each other, which is only the case in the far east and west of the study area (Figure 11). Accordingly, no polyphase overprinting Neogene to recent stress trajectories were detectable in the central part of the study area, e.g. the Besançon Zone, where strike-slip and reverse faults commonly yield parallel shortening directions. Notably, the observation that the youngest recorded fault sets defining NW-SE shortening are not, or hardly, affected by folding does not account for the northern rim of the Besançon Zone. Along the Chailluz Anticline these fault sets are frequently tilted and appear to have formed during rather than after folding (Figures 5 & 8b, e.g. site 26, 28, 35).

The external paleostress province comprises the Montbéliard and Vesoul Plateaux as well as the Avant-Monts Zone. The orientation of $\sigma 1$, as defined by the youngest detected fault sets in this province, scatters slightly between NNW-SSE to WNW-ESE. However, and most importantly, the systematic fanning observed along the front of the thin-skinned thrust belt is not detectable throughout this area (Figures 11 & 13). This is best seen at the northern (sites 4-11, Figure 14) and western (51-55 and 61-63) boundary of the fold-and-thrust belt. In both these areas $\sigma 1$ strikes consistently NW-SE in

the external paleostress domain, whereas to the south, and hence within the thin-skinned fold-and-thrust belt, the orientation of σ1 is N-S in the eastern part and WNW-ESE in the western part, respectively. The type of rather consistently NW-SE directed stress trajectories is recorded far into the stable foreland NW of the study area [Bergerat, 1987; Lacombe and Obert, 2000; Rocher et al., 2004]. The stress tensors obtained from the external stress province, similarly to the findings in the internal province, are confined by steep strike-slip faults that reactivated pre-existing Paleogene normal faults (Figure 9a). However, low-angle thrust faults are almost nowhere observed in this area. Notable exceptions are site 3 located along the isolated Montbéliard anticline and sites 71, and 76 from the surroundings of the La Serre Horst (Table 1; Figures 10 & 11). Regarding temporal relationships between faulting and folding a key observation is shown in Figure 10 where the youngest brittle structures confining NW-SE directed shortening are overprinted by thick-skinned folding along the Moutherot anticline (Figure 10). This argues in favor of a very late stage of thick-skinned folding considering the brittle deformation sequence outlined above (Figure 14).

3.3.4. Geomorphic observations

The geomorphology of a region further constrains its tectonic history, provided that sedimentary or morphological deformation markers of known age are available. In intracontinental settings the geometries of fluvial drainage patterns [Twidale, 2004] and incision reconstructions of rivers based on stream terraces [Bull, 1990; Merrits et al., 1994] may yield information on slow and long-term tectonic processes. Many recent studies have successfully applied such geomorphic approaches in order to study the temporal evolution of fold structures in fold-and-thrust belt settings [Oberlander, 1985; Burbank et al., 1996; Alvarez, 1999; Mouthereau et al., 2007].

Along the Avant-Monts Fault, where a clear distinction between pure thick-skinned folding along the Moutherot Anticline in the west and predominately thin-skinned deformation along the Chailluz Anticline in the east can be established (Figures 5, 6, 7, 8b & 8c), geomorphic age constraints are provided by the Plio-Pleistocene evolution and present-day pattern of the drainage system (Figure 15). The area depicted in Figure 15 is characterized by a roughly ENE-WSW trending drainage divide between the drainage areas of the Ognon and the Doubs rivers, both flowing towards the west into the Bresse Graben (BG in Figure 15). While the main Doubs and Ognon rivers have longitudinal courses that parallel the ENE-WSW striking structural trend, their tributary streams are oriented orthogonally, i.e. in a N-S direction. Note the difference to the drainage pattern of the tributary streams. To the east the drainage divide is very close to the topographic barrier formed by the thin-skinned Chailluz Anticline. Tributary streams reveal a consequent pattern around this anticline [Twidal, 2004]. Towards the west, near the transition between Besançon and Avant-Monts Zone, the drainage divide steps back southwards and away from the topographic high which evolved via the formation of the thick-skinned

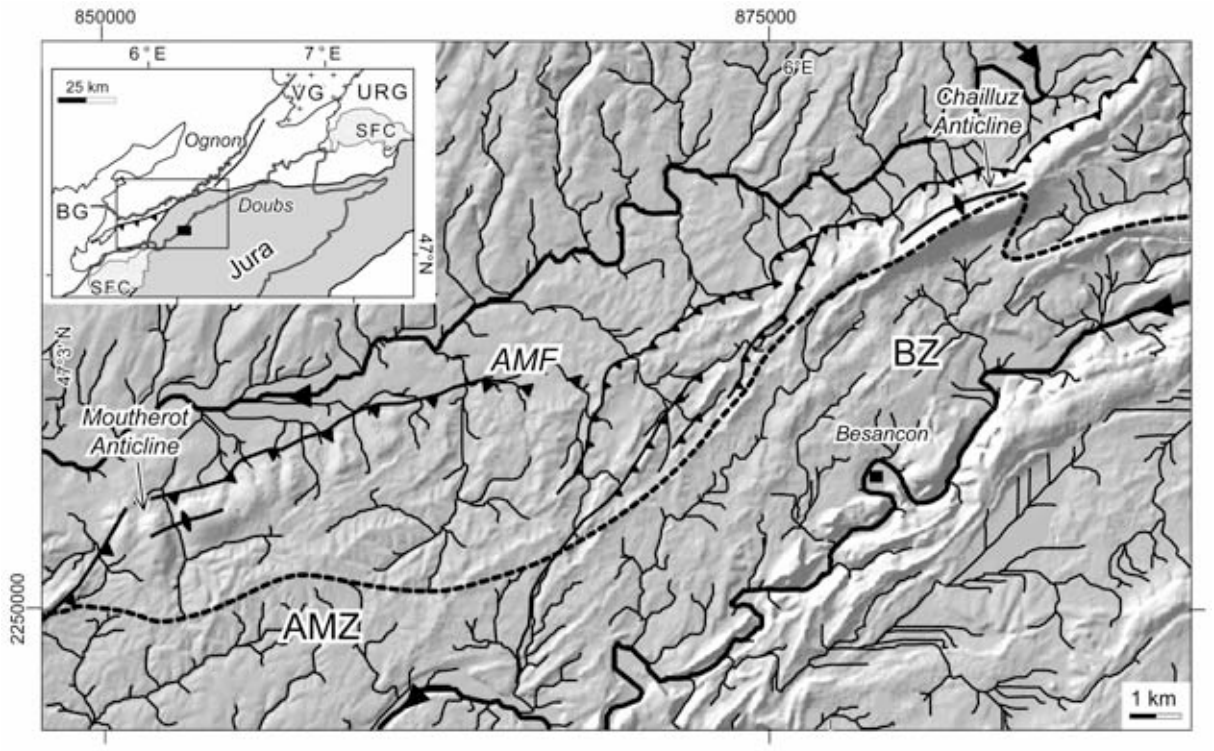

Figure 15: Synthetic drainage pattern calculated with ArcGIS software and drainage divide (dashed line) superimposed on a shaded digital elevation model (horizontal resolution 50m). The inset in the upper left shows the regional drainage pattern and the distribution of the Sundgau and Forêt de Chaux gravels (SFC). The area is characterized by a ENE-WSW striking drainage divide between the drainage areas of the Ognon and Doubs rivers, which both flow towards the SW into the Bresse Graben (BG see inset), and by N-S trending tributary streams. Note the trend of the drainage divide that follows the boundary of the thin-skinned Besançon Zone, as well as the difference in drainage pattern of tributary streams, which reveal a consequent pattern around the thin-skinned Chailluz Anticline, but which are antecedent with respect to the thick-skinned Moutherot Anticline. AMF: Avant-Monts Fault; AMZ: Avant-Monts Zone; BG: Bresse Graben; BZ: Besançon Zone; SFC: Sundgau and Forêt de Chaux Gravels; URG: Upper Rhine Graben; VG: Vosges Mountains.

Moutherot Anticline. The Ognon tributary river system is antecedent [Burbank et al., 1996; Alvarez, 1999] with respect to this fold structure.

The drainage divide between Ognon and Doubs valleys existed from Early Pliocene times onwards when the two drainage basins were already separated [Petit et al., 1996; Sissingh, 2001]. While the Ognon River shed material from the crystalline Vosges mountains (VG see inset Figure 15), the precursor of the Doubs River, namely the Paleo-Aare, shed sediments of Alpine provenance and deposited the Sundgau and Fôret de Chaux Gravels (SFC see inset in Figure 15) in the area south of the Chailluz anticline during the Middle Pliocene (4.2 to 2.9 Ma) [Campy, 1984; Petit et al., 1996; Giamboni et al., 2004; Madritsch, 2008].

Since the thin-skinned Chailluz Anticline controls the location of this drainage divide it indicates a minimum age of 4.2 Ma for structural uplift related this structure. The consequent pattern of tributary streams around the fold structure implies that the rock uplift associated with folding was either too rapid for the streams to maintain their course over the anticline [Burbank et al., 1996], or alternatively, the fold structure evolved prior to the tributary pattern. We favor the latter interpretation, which is constrained by the observation that no significant wind gaps can be observed along the fold crest. Moreover, during the erosion of the Sundgau - Forêt de Chaux Gravels caused by post 2.9 relative rock uplift along the Rhine-Bresse Transfer Zone (see distribution of SFC in the inset of Figure 15) no Alpine derived sediment was apparently shed northward beyond the Chailluz anticline into the Ognon valley [Campy, 1984; Madritsch; 2008].

In contrast, the topographic barrier formed by the thick-skinned Moutherot anticline suggests that the formation of this structure post-dates the Late Pliocene drainage divide. The tributary stream system presently observed is older, as is evident from the antecedent pattern of streams that cut through the topographic barrier. This yields that thick-skinned deformation is characterized by low rates of associated rock uplift and onset during a late stage of the deformation history after the formation of the outermost thin-skinned anticline of Chailluz (post 4.2 Ma).

Nevertheless, subsequent deformation postdating the Middle Pliocene is recorded in the area south of the Chailluz Anticline and throughout the internal parts of the Besançon Zone affected by thin-skinned deformation. This is evidenced by differential erosion of the post-2.9 Ma old deformation marker horizon provided by the Sundgau- and Forêt de Chaux gravels [Campy, 1984; Madritsch, 2008]. Post Mid-Pliocene folding is inferred along the thin-skinned Clerval Anticline (Figure 14). The highly sinuous Doubs river that developed out of the Paleo-Aare braided river system since the Late Pliocene, which incised into the eroded Sundgau and Forêt de Chaux gravel plane (see inset of Figure 15), reveals an antecedent course with respect to the fold structure. Plio-Pleistocene terraces composed of coarse gravels of Alpine provenance are found to the north and south of the anticline [Contini et al., 1973; Madritsch, 2008]. This indicates that fold growth along the Clerval continued after the deposition of the Sundgau and Forêt de Chaux gravels. This interpretation is constrained by the recent detection of Sundgau and Forêt de Chaux gravel remnants on top of other anticlines located north to the Faisceau Bisontin. Within this area folding within the internal parts of thin-skinned fold-and-thrust belt even continued into Late Pleistocene times, as is evident form the differential offsets of paleo-meanders recently dated by optical stimulated luminescence [Madritsch, 2008]. These observations are in contrast to the northern Jura front further to the east, where post-2.9. Ma folding of the Sundgau gravel base only occurs in an area located north of the front of the thin-skinned Jura fold-and-thrust belt [Giamboni et al., 2004; Ustaszewski and Schmid, 2007].

3.4. Discussion

3.4.1. Spatial and temporal interactions of thin and thick-skinned tectonics

The data presented provide evidence for two contrasting styles of Neogene to recent contraction along the northwestern Jura front:

(1) Thin-skinned deformation of the Jura fold-and-thrust belt that also dominates the Besançon zone is characterized by a gently dipping, shallow décollement, penetrated by the borehole of Chailluz (Figures 6 & 8b). Paleostress directions associated with thin-skinned tectonics strike N-S to E-W and reveal a consistently fanning pattern, also detected during previous studies [Laubscher, 1972; Homberg et al., 1999 Ustaszewski and Schmid, 2006].

(2) Thick-skinned deformation, involving both Mesozoic cover and Paleozoic basement, takes place under more or less consistently NW-SE directions of maximum horizontal stress within the area of investigation. This deformation is associated with compressional to transpressional reactivation of pre-existing normal faults of Paleogene to Paleozoic age, which also resembles observations from neighboring areas [Giamboni et al., 2004; Rotstein and Schaming, 2004; Ustaszewski and Schmid, 2007].

The complex structural setting at the northwestern Jura front is schematically illustrated in Figure 16 and results from spatial interferences between the two different styles of deformation. The data clearly indicate that both thin- and thick-skinned shortening post-date Paleogene extension that was associated with the formation of the European Cenozoic Rift System, as is witnessed by the reactivation of meso- to macro-scale Paleogene normal faults. Hence, both styles of deformation are related to contraction that affected the northern Alpine foreland from the Miocene onwards, as a consequence of ongoing Alpine collision [Bergerat, 1987; Dèzes et al., 2004]. Earlier thick-skinned shortening in the area related to the Late Eocene "Pyrenean" compression, as documented for more external parts of the Alpine foreland [Lacombe and Obert, 2000], cannot be entirely excluded. Such earlier deformation would, however, be of minor importance and completely overprinted by later tectonic events, primarily by the Eo-Oligocene extensional reactivation of Late Paleozoic basement structures [Madritsch, 2008].

The propagation of the Jura fold-and-thrust belt appears to be controlled by pre-existing structures, as is its northernmost front in the foreland (Figure 16a). The deformation front of the substantially detached part of the Jura fold-and-thrust belt, as defined by the Lomont, Bisontin and Quingey Faiceaux, coincides with the southern rim of the Paleogene Rhine-Bresse Transfer Zone that is inherited from the Late Paleozoic Burgundy Trough (Figures 2 &16). The Faisceau du Lomont in the eastern part of the study area does not form a clearly defined external front of thin-skinned deformation, and this resembles the situation found along the Jura front further to the east [Laubscher,

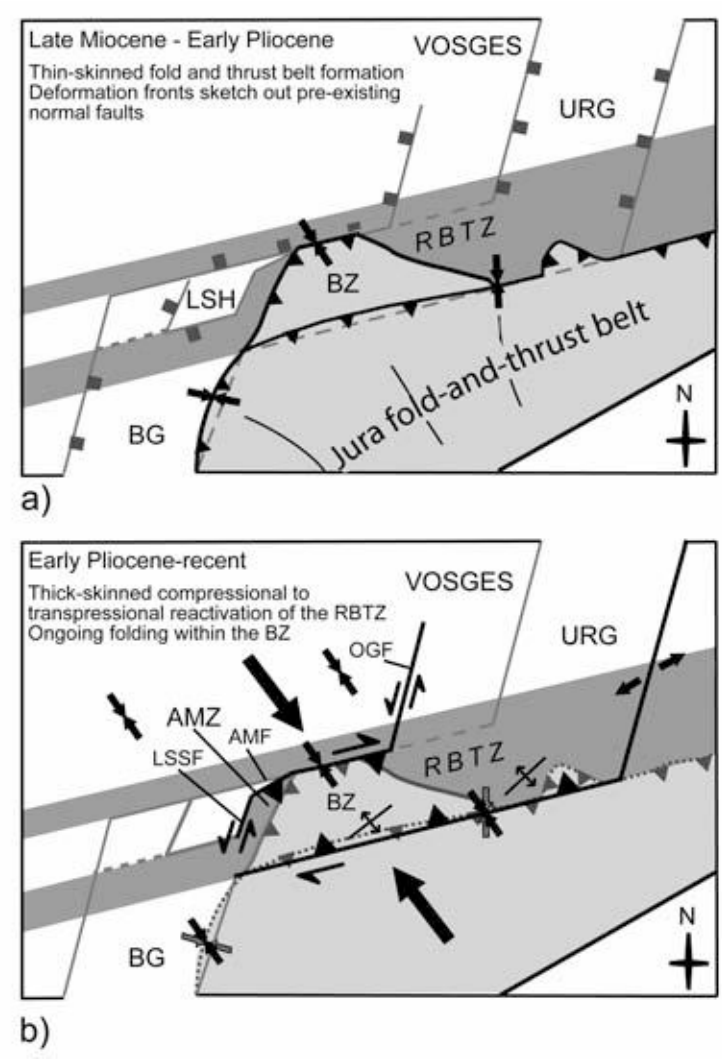

Figure 16 Sketch illustrating Neogene to present interactions between thin- and thick-skinned tectonics at the northwestern front of the Jura Mountains.

a) Late Miocene to Early Pliocene development of the thin-skinned Jura fold-and-thrust belt, involving the formation of the mildly detached Besançon Zone that propagated onto the Rhine-Bresse Transfer Zone and the underlying Late Paleozoic Burgundy Trough. The thin-skinned deformation front is characterized by fanning stress trajectories and sketched out by pre-collisional structures.

b) Thick-skinned tectonics, best documented along the Avant-Monts Fault (AMF), and interpreted in terms of a partial compressive to dextrally transpressive reactivation of the RBTZ. Basement rooted inversion tectonics and further growth of older thin-skinned structures interfere in the Besançon Zone, were deformation continued into Pleistocene times. Note that, in contrast to our working area, the area of the eastern Upper Rhine Graben appears to be rather dominated by a present-day regime of transtension to strike-slip deformation (Kastrup et al. 2004).

Thick black lines mark tectonically active structures. Small arrows mark paleostress trajectories as observed in this study. Large arrows mark the presumed Neogene to recent orientation of maximum principal stress (see text for further discussion). AMF: Avant-Monts Fault; AMZ: Avant-Monts Zone; BG: Bresse Graben; BZ: Besançon Zone; LSH: La Serre Horst; LSSF: La Serre Southern Fault; OGF: Ognon Fault; RBTZ: Rhine-Bresse Transfer Zone; URG: Upper Rhine Graben.

1983]. This is, for example, documented by the Clerval Anticline that is located north of the Faisceau du Lomont (Figures 8a & 14), which we interpret as representing a thin-skinned structure whose location is controlled by a pre-existing normal fault. A thin-skinned style of deformation cannot be excluded for the Montbéliard Anticline either, a structure located within the northeastward adjacent Montbéliard Plateau (Figure 3; compare Laubscher [1983]). However, to the east of the Montbéliard area Giamboni et al. [2004] and Ustaszewski & Schmid [2007] provided evidence from seismic reflection data that suggests a predominance of thick-skinned tectonics in front of the eastern prolongation of the Faisceau du Lomont.

The northward propagation of the only mildly displaced part of the thin-skinned Jura fold-and-thrust belt, the Besançon Zone, beyond the Faisceau du Lomont and the Faisceau Bisontin in the central part of the study area was also largely controlled by the pre-existing Paleogene and Paleozoic fault pattern of the Rhine-Bresse Transfer Zone onto which the thrust sheet encroached, probably during a latest stage of thin-skinned deformation (Figure 16a). The NNE-SSW striking western boundary of the Besançon Zone coincides with a major Paleogene-age normal fault that can be traced from the eastern border fault of the Bresse Graben in the south all the way into the Vesoul Plateau to the north (Figures 3 & 5). It separates the Besançon Zone from the pre-existing structural high, namely the Late Paleozoic La Serre Horst Structure that was reactivated during Eo-Oligocene extension, and it also partly includes the Avant-Monts Zone (Figures 2 & 14) [Madritsch, 2008]. The normal fault is inferred to have acted as a lateral ramp, inducing sinistrally transpressive deformation of the detached cover during its northward propagation. This is expressed by NNE-SSW striking folds and thrust faults mapped west of the city of Besançon, which are markedly oblique to the overall NW-SE orientation of shortening, and by a tectonic regime of transpression such as indicated by the paleostress analysis (Figures 3, 5 & 11). Possibly, the formation of this lateral ramp was related to early stage thick-skinned tectonics that interacted with the thin-skinned thrust sheet; a similar process has been described from the fold-and-thrust belt of northwestern Taiwan [Lacombe et al., 2003].

The existence of a lateral ramp inducing sinistrally transpressive deformation of the detached cover was also invoked for the Ferrette Jura, located east of our study area, which propagated onto the southernmost Upper Rhine Graben (FJ in Figure 1) [Ustaszewski and Schmid, 2006]. There, the propagation of the thin-skinned thrust sheet along a lateral ramp caused transpression and a significant gradient of shortening, the largest amounts of shortening being located close to the ramp. An analogous process is also inferred for the Besançon Zone based on map view and cross sections (Figures 3, 5 & 8). Particularly the Chailluz anticline at the front of the Besançon Zone shows amounts of shortening that continuously decrease from west (near the Chailluz borehole) to east (see topographical expression of the anticline in Figure 5), where the boundary drawn between thin-skinned Besançon Zone and Montbéliard Plateau, largely characterized by thick-skinned deformation, had to be drawn rather artificially in Figure 3.

Occurrence and location of thick-skinned deformation (Figure 16b), as observed in the Avant-Monts Zone, are also closely related to the presence of pre-existing faults. As is evident from the seismic dataset from this area (Figures 7 & 8c) the western segment of the Avant-Monts Faults formed by inversion of a pre-existing Paleogene fault related to graben formation. Since the western prolongation of the Avant-Monts Fault abuts the La Serre Southern Fault that forms the southeastern boundary of the La Serre Massif (Figures 3 & 5) and represents a horst structure, inversion of Paleozoic structures, or combined Paleozoic and Paleogene structures, is likely. Compressive to dextrally transpressive shortening, as observed along the Avant-Monts Fault, is transferred towards the west along the La Serre Southern Fault, as can be implied by the results of the paleostress analysis that yields transpression in that area. In the eastern part of the study area the Avant-Monts Fault connects with the NNE-SSW striking Ognon Normal Fault (Figures 1, 3, 8a, 16b). Similar to the La Serre Southern Fault it represents a major Paleogene normal fault that reactivated a Paleozoic fault traceable into the basement of the Vosges Mountains [Ruhland, 1959]. A mild transpressive inversion is inferred along this fault from geomorphic observations [Theobald et al., 1977; Campy, 1984; Madritsch, 2008].

Thick-skinned deformation is interpreted to result in the partial inversion of the intra-continental Rhine Bresse Transfer Zone and the underlying Late Paleozoic Burgundy Trough due to a change from sinistral transtension, active in the Eo-Oligocene [Lacombe et al., 1993; Madritsch, 2008; Figure 2], to dextral transpression from the Neogene onwards [Laubscher, 1970; Ustaszewski and Schmid, 2007] (Figure 16b). However, as no surface or subsurface continuation of the Avant-Monts Fault can be traced eastwards into the Rhine Graben (Figure 16b) we do not infer a through-going reactivation of the intra-continental Rhine-Bresse Transfer Fault Zone. Instead, we suspect that compressive to dextrally transpressive shortening during the Neogene along the western segment of the Avant-Monts Fault was not transferred all along the northern rim of Rhine-Bresse Transfer Zone towards the Rhine Graben, but was taken up and transferred by transpressive reactivation of the Ognon Normal Fault (Figures 1, 3, 8a & 16b). Thick-skinned partial reactivation of the Rhine-Bresse Transfer Zone spatially interferes with thin-skinned tectonics throughout the Besançon Zone where the Jura fold-and-thrust belt encroached onto the transfer zone (Figures 8b & 16b).

While the coexistence of both types of deformation is well documented in the study area, the question arises as to whether these two Neogene-age modes of deformation also coexisted in time (Meyer et al. 1994; Nivière and Winter 2000), or alternatively, if a younger thick-skinned deformation event followed older thin-skinned deformation, as was proposed by [Ustaszewski and Schmid, 2007].
The brittle tectonic investigations carried out during this study lead to the conclusion that the most recent paleostress trajectories recorded in the area fairly consistently strike NW-SE and are confined by steep strike-slip faults. In the intensively deformed areas along the Faisceau Bisontin, Lomont and Quingey these trajectories frequently overprint fanning stress trajectories related to an early stage of thin-skinned deformation (Figure 11, 16a, b). The late stage persistence of the consistently NW-SE

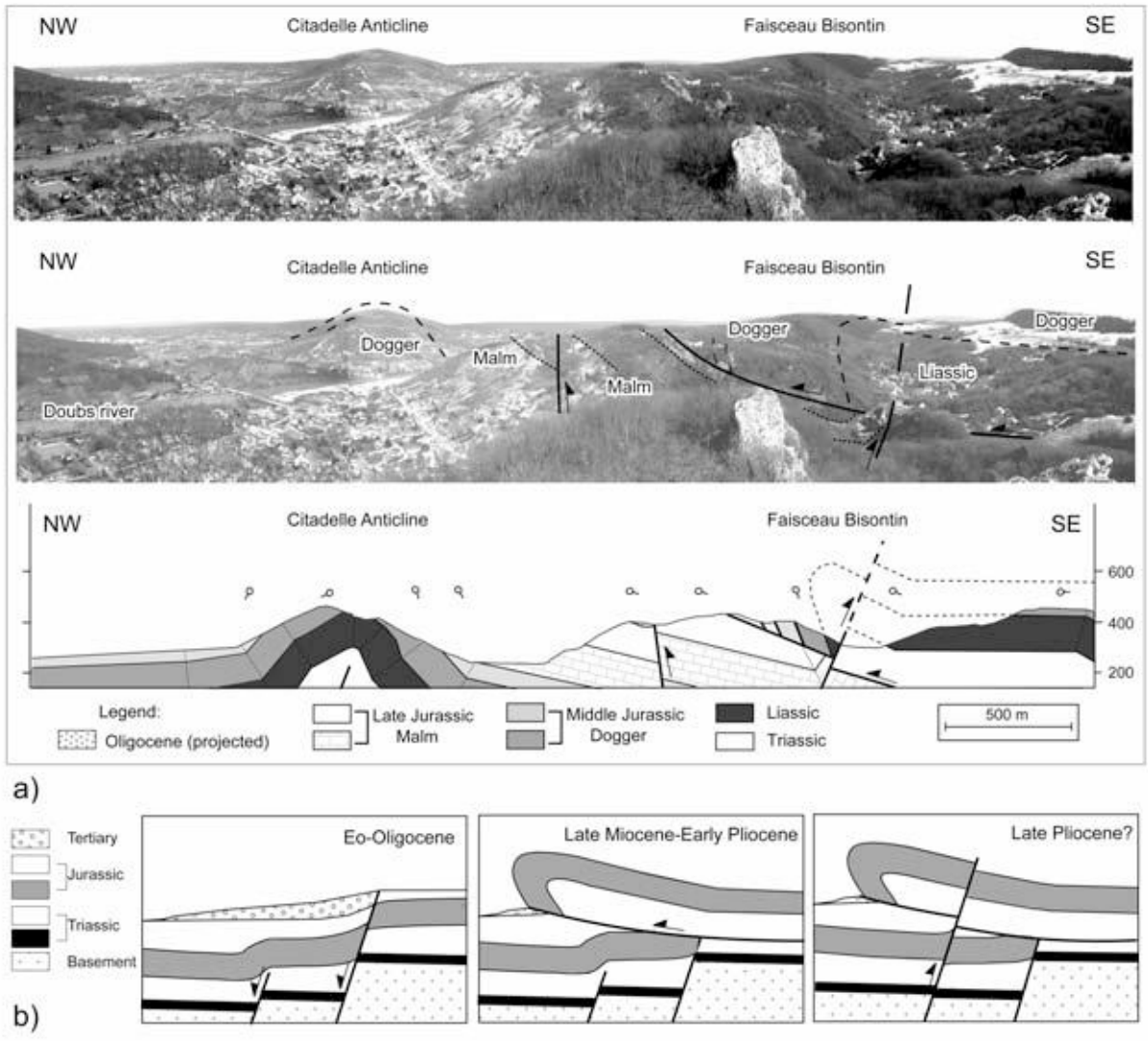

Figure 17: Section across the Faisceau Bisontin near the town of Besançon.

a) Panorama and cross section across the Faisceau Bisontin near the town of Besançon (see Figure 5 for location): Large-scale outcrops provide field evidence for an offset of the northwest facing low angle thrust fault associated with the Faisceau Bisontin by thick-skinned steep reverse faults.

b) Sketch showing the interpretation of the evolution along this profile. Normal faults, formed during the Eo-Oligocene evolution of the Rhine-Bresse Transfer Zone, predetermine the location of the later formed steep reverse faults. Such normal faulting well explains flexuring of the Mesozoic strata in the hanging wall of the normal fault and deposition of syn-rift sediments nearby. During an intermediate stage the main phase of thin-skinned Jura folding the thrust fault associated with the Faisceau Bisontin was localized along the pre-existing Paleogene flexure. In a third stage (Late Pliocene to recent?) the normal fault was inverted, which led to the dissection of the low angle thrust fault and top-SE superposition of its footwall over its hanging wall as observed at the outcrop.

directed stress field beyond the main phase of thin-skinned folding of and thrusting within the Jura fold-and-thrust belt has also been recognized in its internal parts [Homberg et al., 2002]. Folding along the northern rim of the Besançon and Avant-Monts Zone persisted beyond this very latest brittle deformation stage as is evident form several faulting-folding relationships (e.g. site 35, 36, 37, 66). Most notably along the thick-skinned Avant-Monts Fault, a clear rotation of the youngest observed fault slip sets due to folding along the Moutherot Anticline can be observed (Figure 10), suggesting late stage activity of thick-skinned tectonics. Furthermore, geomorphic observations indicate that the thick-skinned Moutherot Anticline formed after the thin-skinned Chailluz Anticline, the latter revealing a minimum age of 4.2 Ma (Figure 15).

Within in the Besançon Zone, where the different tectonic styles potentially interfere (Figures 8b & 16), crosscutting relationships can be inferred from structural data. Large-scale outcrops within the city of Besançon (Figure 17) display the main thrust fault related to the Faisceau Bisontin, a south dipping low angle thrust fault, to be dissected by younger south facing reverse faults. These steep reverse faults are interpreted as basement-rooted former normal faults of Paleogene-age that parallel the Faisceau Bisontin and form the southern rim the Rhine-Bresse Transfer Zone. Hence, they are not regarded as décollement-related back-thrusts. This interpretation is largely based on the observation that the footwall of the low angle thrust fault is characterized by steeply dipping Mesozoic strata; this is typical for extension-related flexures observed along major normal faults throughout the study area (Figures 8a & 8c) and further to the east within the southern Upper Rhine Graben [Ustaszewski et al., 2005a; Ford et al., 2007]. Moreover, the occurrence of Oligocene syn-rift sediments along strike points to the existence of a Paleogene graben structures in the area [Glangeaud, 1949; Dreyfuss and Kuntz, 1969; Chauve et al., 1980]. In the light of the new subsurface data from the Avant-Monts Zone these field observations strongly suggest the interpretation that re-deformation of the shallow thrust fault was caused by basement rooted thick-skinned deformation associated with inversion of preexisting basement faults.

Throughout the internal parts of Besançon Zone tectonic activity related to ongoing shallow décollement along the Triassic evaporites, associated with further growth of folds that initially formed during the thin-skinned stage of deformation (Early Pliocene [Becker, 2000; Ustaszewski and Schmid, 2007]), is strongly suggested given the differential erosion of the Mid Pliocene Sundgau and Forêt de Chaux gravels throughout that area [see Campy, 1984; Madritsch, 2008]. This hypothesis is constrained by the observation that active folding within parts of the Besançon Zone, occurs localized and in response to focused Pleistocene river incision [Dreyfuss and Glangeaud, 1950; Madritsch, 2008]. Enhancement of deformation by this kind of surface process requires that incision and buckling occur simultaneously under regional horizontal compression according to recent numerical models [Simpson, 2004].

3.4.2. Tectonic style of neotectonic deformation

Data on the present-day tectonic activity within the study area are available from seismic and seismotectonic evidence, as well as from in situ borehole measurements of recent stress within the sedimentary cover. Figure 18 shows a compilation of data comprising the instrumentally recorded earthquakes with M_L magnitude larger than 3, extracted from the databases of the Réseau National de Surveillence Sismique [RéNaSS, 2007] and the Swiss Seismological Survey [Swiss Seismological Service, 2007]. Published focal mechanisms were compiled from various sources [Dorel et al., 1983; Bonjer et al., 1984; Pavoni, 1987; Nicolas et al., 1990; Plenefisch and Bonjer, 1997; Lopes Cardozo and Granet, 2003; Kastrup et al., 2004; Baer et al., 2005; Baer et al., 2007; Swiss Seismological Service, 2007]. Orientations of maximum horizontal stress σ1 were obtained from the 2005 world stress map release [Reinecker et al., 2005] and from Becker and Werner [1995], mostly derived from in situ borehole measurements carried out within the Mesozoic cover using the borehole slotter and doorstopper method, that are discussed in detail by Becker [2000].

Seismicity in the northern Alpine foreland is low to moderate. The Rhine-Bresse Transfer Zone shows a significantly lower activity in comparison to the Rhine Graben area [Baer et al., 2007], leading to a rather poorly defined present day stress field [Kastrup et al., 2004]. The direction of σ1 is mostly within a western or northern quadrant and hence most probably approximately strikes NW-SE. The analysis of focal depths of earthquakes clearly shows that ongoing deformation also involves the crystalline basement, all the way down to the Moho (Deichmann et al. 2000). Throughout the central Jura fold-and-thrust belt and the Rhine-Bresse Transfer Zone, earthquakes are mostly found far below the supposed thin-skinned décollement horizon, although there are also apparently shallow events, such as for example recorded around the city of Neuchâtel [Baer et al., 2007]. Focal mechanisms of deep earthquakes underneath the Jura fold-and-thrust belt mostly feature strike-slip regimes. In contrast to the neighboring Rhine Graben area, which is characterized by strike-slip or transtension [Kastrup et al. 2004], the deep earthquakes observed within the Rhine-Bresse Transfer Zone also reveal pure to oblique thrust faulting mechanisms [Lopes Cardozo and Granet, 2003; Baer et al., 2005]. The surface projection of the earthquake of Besançon [Baer et al., 2005] (23rd Feb. 2004; Ml 4.8; depth 15km; marked by white square in Figure 18) that features a focal mechanism indicating oblique thrusting has been interpreted to coincide with the trace of the Avant-Monts Fault (see inset of Figure 18, modified from [Conroux et al., 2004]). Notably, this accounts only for the moment tensor based on first motion polarities but not the one based on full waveform inversion (for details see Baer et al. [2005]).

This evidence strongly supports the suggestion that currently active thick-skinned tectonics involves transpressional to compressional reactivation of structures related to the Paleogene Rhine-Bresse Transfer Zone and the Paleozoic Burgundy trough system (Figure 18). Similar observations suggest basement inversion in the area along the southern boundary of the Jura fold-and-thrust belt

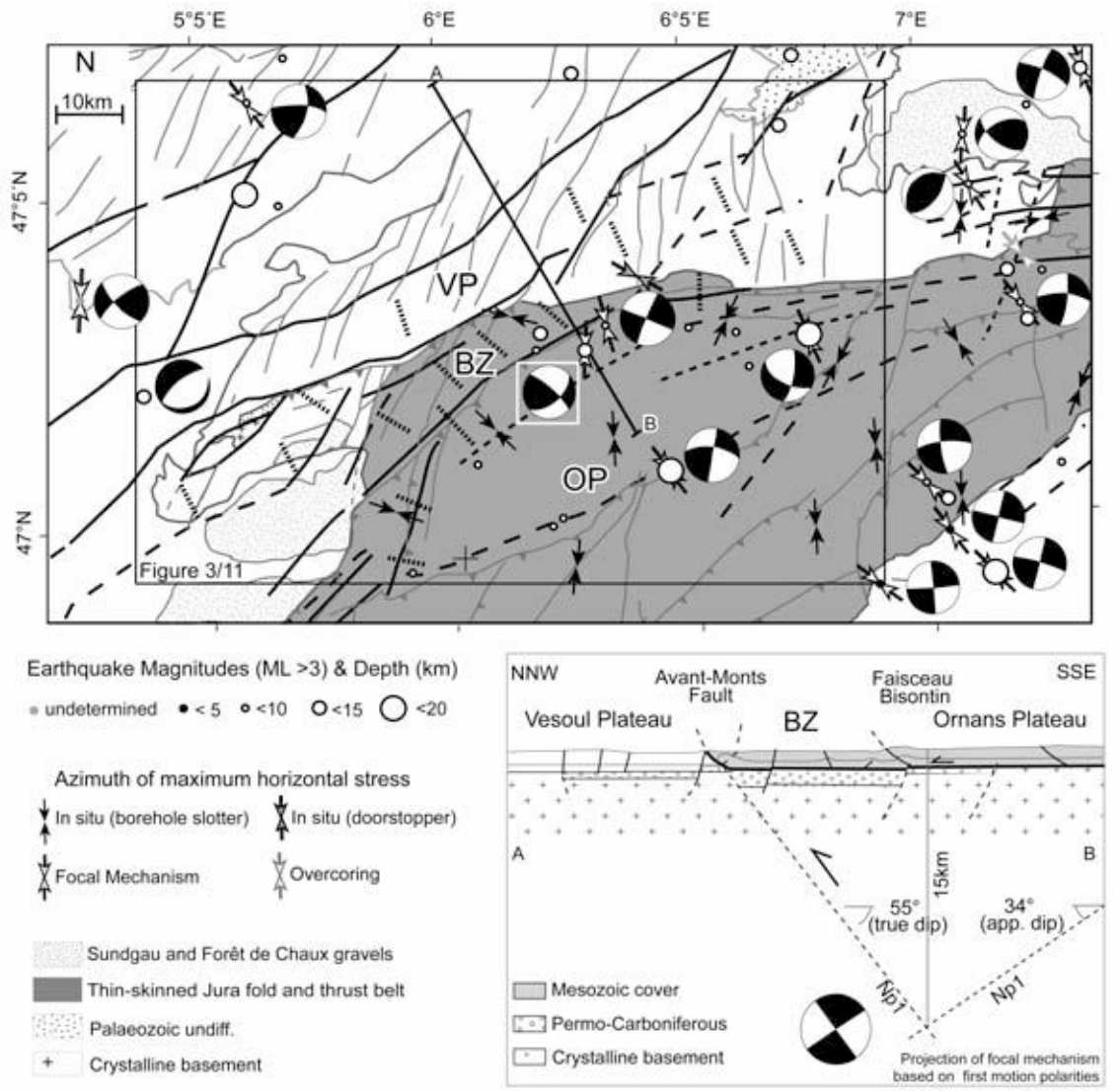

Figure 18: Neotectonic activity within the working area, as documented by focal mechanisms and in situ stress measurements from borehole slotter and doorstopper tests [Becker and Werner, 1995; Becker, 2000]. Further orientations of maximum horizontal stress are taken from the 2005 world stress map release [Reinecker et al., 2005]. Earthquake epicenter locations and depths are taken from the databases of the Réseau National de Surveillence Sismique [RéNaSS, 2007] and the Swiss Seismological Survey [Swiss Seismological Service, 2007]. The focal mechanisms are compiled from various sources (see text). Stippled lines indicate the maximum horizontal shortening directions obtained from paleostress analysis during this study (compare Figure 11). Thick black lines indicate basement-rooted faults related to Late Paleozoic and Eo-Oligocene extension or transtension [modified from Debrand-Passard and Courbouleix, 1984; Philippe et. al., 1996; Ustaszewski et al., 2005b]. Note the extent of the thin-skinned Jura fold-and-thrust belt, which also includes the newly defined Besançon Zone and the Pliocene Sundgau-Forêt de Chaux gravels that are eroded in the latter area (compare Figure 3 & 15). BZ: Besançon Zone; OP: Ornans Plateau; VP: Vesoul Plateau. The inset in the lower right shows a simplified cross section, modified from Conroux et al. [2004] and illustrates the surface projection of the focal mechanism of the earthquake of Besançon (23rd Feb. 2004; Ml: 4.8; depth 15km [Baer et al., 2005] that coincides with the trace of the Avant-Monts Fault.

adjacent to the Molasse basin that have been interpreted as being caused by the accretion of new basement nappes during ongoing tectonic underplating in northern Alpine foreland [Pfiffner et al., 1997; Mosar, 1999; Lacombe and Mouthereau, 2002; Ustaszewski and Schmid, 2007].

While there is ample evidence for ongoing thick-skinned tectonic activity, the question as to whether thin-skinned tectonics is still active today [Nivière and Winter, 2000; Müller et al., 2002], or alternatively, if it ceased by Early Pliocene times [Ustaszewski and Schmid, 2007], is more difficult to answer. Based on in situ stress measurement data, partly shown in Figure 18, Becker [2000] concluded that thin-skinned deformation did cease, based on a series of arguments. He pointed out that recent stress provinces do not coincide with the tectonic zonation of the Jura Mountains and that the orientation of recent stress axes is similar in areas affected by thin-skinned deformation and areas in the foreland not affected by this style of deformation. Becker [2000] raised further arguments against ongoing thin-skinned tectonics such as the deviation between paleo- and recent stresses and the parallelism of the directions of the maximum horizontal stresses derived from surface in situ stress measurements and those obtained from focal mechanisms within the basement, arguing against persisting decoupling between basement and cover.

While the arguments discussed above clearly apply for the southwestern and northern part of the thrust belt, the situation is not as clear in our area of investigation, particularly within the Besançon Zone (Figure 18). As mentioned by Becker [2000] this is about the only area within the entire Jura fold-and-thrust belt where stress provinces defined by in situ stress measurements correlate well with the tectonic units. Unfortunately, there are not enough in situ stress data available for testing if the orientation of the present-day direction of $\sigma 1$ changes north of the Besançon Zone, i.e. outside the area affected by thin-skinned deformation. However from the results of our paleostress analysis (compare Figure 11), one would actually expect them to be parallel in that area. Within the Besançon Zone and along the Faisceaux the recent orientation of $\sigma 1$ obtained by in situ measurements almost perfectly fits the shortening directions obtained by this study (Figure 11) and they show a deviation from the $\sigma 1$ orientation obtained from nearby focal mechanisms by almost 60° in some cases. This implies that the stress field within the sedimentary cover stayed the same throughout this area from at least Early Pliocene times to the present day. Moreover, further growth of folds formed during the thin-skinned stage of deformation (Figure 17) indicates that there still is decoupling between sedimentary cover and crystalline basement. Such decoupling is likely to be rooted within the basement by fault reactivation nearby. Such shallow décollement probably occurs simultaneously with deep-seated thick-skinned inversion that affects the underlying basement nearby and is therefore not thin-skinned in a strict sense and according to original definition by Chapple [1978]. On the other hand, and in the light of insufficient knowledge about the exact geometry of the subsurface in the area, recent tectonic activity related to ongoing décollement of the Jura fold-and-thrust belt throughout the Besançon Zone cannot be excluded.

3.5. Conclusions

This investigation leads to a new structural subdivision of the northwestern front of the Jura fold-and-thrust belt. The area located in front of the substantially detached parts of the Jura fold-and-thrust belt is divided into two parts characterized by different styles of deformation: i) The Besançon Zone that represents the northwestern most and only mildly detached segment of the thin-skinned Jura fold-and-thrust belt that encroached onto the Rhine-Bresse Transfer Zone, and ii) The Avant-Monts Zone proper where seismic reflection data document thick-skinned shortening associated with the reactivation of pre-existing normal faults of the Rhine-Bresse Transfer Zone.

Paleostress analysis yields fanning N- over NW- to W-directed orientations of maximum principal stress ($\sigma 1$) during thin-skinned deformation associated with strike-slip, transpressional and reverse faulting. By contrast, the stable foreland and those areas affected by thick-skinned deformation are characterized by more or less constantly NW-SE directed orientation of $\sigma 1$, predominantly achieved by strike-slip faulting within the Mesozoic cover.

Kinematic and geomorphic observations allow establishing a relative chronology of the different deformation styles. Thick-skinned tectonics initiate during or slightly after the latest stages of the main phase of thin-skinned Jura folding and thrusting, at the earliest at around 4.2 Ma, i.e. during the Early Pliocene.

Within the Besançon Zone, where the thin-skinned fold-and-thrust belt encroached onto the Rhine-Bresse Transfer Zone, deformation continued after the Late Pliocene (post 2.9 Ma), as is evident from the erosion of the Sundgau and Forêt de Chaux gravels throughout that area. There is abundant structural evidence for presently ongoing thick-skinned shortening, as is confirmed by present day seismicity. Ongoing growth of folds within the Besançon Zone that formed during an earlier thin-skinned stage of deformation appears to be positively coupled to erosion and is thus probably related to deformation along the evaporite décollement horizon. Although this deformation is likely to be rooted within the basement by fault reactivation nearby, ongoing thin-skinned deformation cannot be excluded. Hence, at the northwestern Jura front deep-seated seismogenic thick-skinned tectonics and – presumably largely aseismic – shallow décollement tectonics may interact in space and time from Early Pliocene times (4.2 Ma) to the present.

The results of this study highlight the crucial role of pre-existing structures on the evolution of foreland fold-and-thrust belts, also in settings where deformation is governed by classical thin-skinned tectonics. In the case of the northwestern Jura front pre-orogenic extensional faults first controlled the nucleation of shallow thrust faults and folds due to the offset of the detachment horizon and extensional flexuring of the sedimentary sequence. Lateral ramps inherited preexisting horst and graben structures and controlled the propagation of thin-skinned thrust sheets beyond the front of the

thrust belt. Late-stage thick-skinned inversion of deep-seated pre-existing normal faults occasionally led to the thick-skinned re-deformation of older thin-skinned structures.

Acknowledgments:

This project was funded by ELTEM and carried out within the framework of the EUCOR URGENT project. The authors are indebted to Gaz de France for the authorization to analyze and publish seismic reflection data as well as to BRGM and Total for further subsurface data provision. We also would like to thank Patrick Rolin, Kamil Ustaszewski, Pierre Dèzes and the entire past and present Basel EUCOR-URGENT team for helpful discussions. We particularly thank the initiator of this project, Peter Ziegler, for his comments on early versions of the manuscript. Detailed and constructive reviews by Olivier Lacombe and Adrian Pfiffner significantly improved an earlier version of the manuscript.

References:

Affolter, T., and J.P. Gratier (2004), Map view retrodeformation of an arcuate fold-and-thrust belt: The Jura case, *J. Geophys. Res., 109*, doi:10.1029/2002JB002270.

Alvarez, W. (1999), Drainage on evolving fold-thrust belts: A study of transverse canyons in the Apennines, *Basin Research, 11*, 267-284.

Anderson, E. M.(1942), The dynamics of faulting. Oliver and Boyd, pp.206.

Angelier, J. (1989), From orientation to magnitudes in paleostress determinations using fault slip data, *Journal of Structural Geology, 11*, 37-50.

Angelier, J.(1990), Inversion of field data in fault tectonics to obtain the regional stress - III. A new rapid direct inversion method by analytical means, *Geophysical Journal International, 103*, 363-376.

Angelier, J., and P. Mechler (1977), Sur une méthode graphique de recherche des contraintes principales également utilisable en tectonique et en seismologie: la méthode des dièdres droits, *Bull. Soc. géol. France, 19*, 1309-1318.

Aubert, D. (1945) Le Jura e la tectonique d'ecoulement: *Mem. soc. Vaudoise de sci. Nat. 8,* 217-236.

Baer, M., N. Deichmann, J. Braunmiller, J. Clinton, S. Husen, D. Fäh, D. Giardini, P. Kästli, U. Kradolfer, and S. Wiemer (2007), Earthquakes in Switzerland and surrounding regions during 2006, *Swiss Journal of Geosciences, 100*, 517-528.

Baer, M., N. Deichmann, J. Braunmiller, S. Husen, D. Fäh, D. Giardini, P. Kästli, U. Kradolfer, and S. Wiemer (2005), Earthquakes in Switzerland and surrounding regions during 2004, *Eclogae geol. Helv., 98*, 407-418.

Becker, A. (2000), The Jura Mountains - an active foreland fold-and-thrust belt?, *Tectonophysics, 321*, 381-406.

Becker, A., and D. Werner (1995), Neotectonic state of stress in the Jura mountains, *Geodinamica Acta, 8*, 99-111.

Bergerat, F. (1977), La fraturaction de l'avant-pays jurassien entre les fossés de la Saône et du Rhin. Analyse et e ssai d'interpretation dynamique, *Revue de Géographie physique et de Géologie dynamique (2), 14*, 325-338.

Bergerat, F. (1987), Stress Fields in the European Platform at the time of Africa-Eurasia Collision, *Tectonics, 6*, 99-132.

Bergerat, F., and J. Chorowicz (1981), Etude des images Landsat de la zone tranformante Rhin-Saône (France), *Geologische Rundschau, 70*, 354-367,

Boigk, H., and H. Schönreich (1970), Die Tiefenlage der Permbasis im nördlichen Teil des Oberrheingrabens, in *Graben Problems. Proceedings of an International Rift Symposium Karlsruhe 1968, International Upper Mantle Project.*, edited by J.H. Illies and S. Mueller, pp. 45-55, E. Schweitzerbart'sche, Stuttgart.

Bolliger, T., B. Engesser, and M. Weidmann (1993), Première découverte de mammifères pliocènes dans le Jura neuchâtelois, *Eclogae geol. Helv., 86 (3)*, 1031-1068.

Bonjer, K.-P., C. Gelbke, B. Gilg, D. Rouland, D. Mayer-Rosa, and B. Massinion (1984), Seismicity and dynamics of the Upper Rhine Graben, *J. Geophys., 55*, 1-12.

Bonte, A. (1975), Carte géolog. France (1/50000), feuille Quingey, XXXIII-24, BRGM.

Bourgeois, O., M. Ford, C. Diraison, M. Le Carlier de Veslud, R. Gerbault and N. Pik (2007), Separation of rifting and lithospheric folding signatures in the NW-Alpine foreland, *International Journal of Earth Sciences, 2007*, 1003-1031.

Brudy, M., M. D. Zoback, K. Fuchs, F. Rumel, J. Baumgärtner (1997), Estimation of the complete stress tensors to 8km depth in the KTB scientific drilling holes: implications for crustal strength, *J. Geophys. Res. 102,* 18453-18475.

Bull, W. B. (1990), Stream-terrace genesis: implications for soil development, *Geomorphology, 3*, 351-367.

Burbank, D., A. Meigs, and N. Brozovic (1996), Interactions of growing folds and coeval depositional systems, *Basin Research, 8*, 199-223.

Burkhard, M. (1990), Aspects of the large-scale Miocene deformation in the most external part of the Swiss Alps (Subalpine Molasse to Jura fold belt), *Eclogae Geologicae Helvetiae, 83*, 559-583.

Burkhard, M., and A. Sommaruga (1998),Evolution of the western Swiss Molasse basin: structural relations with the Alps and the Jura belt, in *Cenozoic Foreland Basins of Western Europe*, vol. 134, edited by A. Mascle, C. Puidgefàbregas, H.P. Luterbacher and M. Fernàndez, pp. 279-298, Geological Society, London.

Buxtorf, A. (1907), Geologische Beschreibung des Weissenstein Tunnels und seiner Umgebung, *Beiträge der Geologischen Karte der Schweiz.*

Calabrò, R. A., S. Corrado, D. Di Bucci, P. Robustini, and M. Tornaghi (2003), Thin-skinned vs. thick-skinned tectonics in the Matese Massif, Central-Southern Apennines, *Tectonophysics, 337*, 3-4, 269-297.

Campy, M. (1984), Signification dynamique et climatique des formations et terrasses fluviatiles dans un environnement de moyenne montagne, *Bulletin de l'Association française pour l'Etude du Quaternaire, 1*, 87-92.

Chapple, W. M. (1978): Mechanics of thin-skinned fold-and-thrust belts. *Geological Society of American Bulletin, 89,* 1189-1198.

Chauve, P., M. Campy, C. Pernin, and N. Morre-Biot (1983), Carte géolog. France (1/50000), feuille Pesmes, XXXII-23, BRGM.

Chauve, P., R. Enay, P. Fluck, and C. Sittler (1980), L'Est de la France (Vosges, Fossé Rhénan, Bresse, Jura), *Annales scientifiques de l'Université de Besançon, 4*, 3-80.

Conroux, Y., O. Fabbri, T. Lebourg, V. Bichet, and C. Petit (2004), Geological and geophysical investigations along a late Variscan fault exposed near the 23/02/2004 Besancon earthquake epicentral area. Abstract Volume, RST-GV Strasbourg.

Contini, D, G. Kuntz, B. Angély, J. L. Laffly, Y. Kerrien, J. Landry, N. Théobald (1973), Carte géolog. France (1/50000), feuille Montbéliard, XXXV-22, BRGM.

Coromina, G., and O. Fabbri (2004), Late Palaeozoic NE-SW ductile-brittle extension in the La Serre horst, eastern France, *Comptes Rendus Geosciences, 336*, 75-84.

Costa, E., and B.C. Vendeville (2002), Experimental insights on the geometry and kinematics of fold-and-thrust belts above weak, viscous evaporitic décollement, *Journal of Structural Geology, 24*, 1729- 1739.

Coward, M.P. (1983), Thrust tectonics, thin skinned or thick skinned, and the continuation of thrusts to deep in the crust, *Journal of Structural Geology, 5*, 113-123.

Davis, D., J. Suppe, and F.A. Dahlen (1983), Mechanics of fold-and-thrust-belts and accretionary wedges, *Journal of Structural Geology, 88*, 1153-1172.

Deichmann, N., D. Ballarin Dolfin, and U. Kastrup (2000), *Seismizität der Nord- und Zentralschweiz*, 94 pp., NAGRA, Wettingen.

Dèzes, P., S.M. Schmid, and P.A. Ziegler (2004), Evolution of the European Cenozoic Rift System: interaction of the Alpine and Pyrenean orogens with their foreland lithosphere, *Tectonophysics, 389*, 1-33.

Diebold, P., and T. Noack (1997),Late Palaeozoic troughs and Tertiary Structures in the eastern Folded Jura, in *Deep structure of the Swiss Alps. Results of NRP 20*, edited by O.A. Pfiffner, P. Lehner, P. Heitzmann, S. Mueller and A. Steck, pp. 59-63, Birkhäuser,

Dorel, J., J. Frechet, J. Gagnepain-Beyneix, H. Haessler, M. Lachaize, R. Madariaga, T. Modiano, G. Pascal, G. Perrier, H. Philip, D. Rouland, and G.G. Wittlinger (1983), Focal mechanism in metropolitan France and the lesser Antilles, *Annales Geophysicae, 1*, 299-306.

Dreyfuss, M., and L. Glangeaud (1950), La valée de Doubs et l'évolution morphotectonique de la région bisontine, *Annales scientifiques de l'Université de Besançon, 5*, 2.

Dreyfuss, M., and G. Kuntz (1969), Carte géolog. France (1/50000), feuille Besancon, XXXII-23, BRGM.

Dreyfuss, M., and G. Kuntz (1970), Carte géolog. France (1/50000), feuille Gy, XXXIII-22, BRGM,

Dreyfuss, M., and N. Théobald (1972), Carte géolog. France (1/50000), feuille Baume-les-Dames, XXXIV-22, BRGM.

Ford, M., C. Le Carlier de Veslud, and O. Bourgeois (2007), Kinematic and geometric analysis of fault related folds in a rift setting: The Dannemarie basin, Upper Rhine Graben, France, *Journal of Structural Geology, 29*, 1811-1830.

Giamboni, M., K. Ustaszewski, S.M. Schmid, M.E. Schumacher, and A. Wetzel (2004), Plio-Pleistocene Transpressional Reactivation of Paleozoic and Paleogene Structures in the Rhine-Bresse transform Zone (northern Switzerland and eastern France). *International Journal of Earth Sciences, 93*, 207–223, DOI: 10.1007/s00531-003-0375-2.

Glangeaud, L. (1949), Les caractères structuraux du Jura, *Bull. Soc. géol. France,19,* 669-688.

Guellec, S., J.L. Mugnier, M. Tardy, and F. Roure (1990), Neogene evolution of the western Alpine foreland in the light of ECORS data and balanced cross-sections, in *Deep Structure of the Alps*, vol. 1, Vol. spec. Soc. Geol. It., edited by F. Roure, P. Heitzmann and R. Polino, pp. 165-184.

Hindle, D., and M. Burkhard (1999), Strain, displacement and rotation associated with the formation of curvature in fold belts; the example of the Jura arc, *Journal of Structural Geology, 21*, 1089-1101.

Homberg, C., O. Lacombe, J. Angelier, F. Bergerat (1999), New constraints for indentation mechanisms in arcuate belts from the Jura Mountains, France, *Geology, 27,* 9, 827-830.

Homberg, C., F. Bergerat, Y. Philippe, O. Lacombe, and J. Angelier (2002), Structural inheritance and cenozoic stress fields in the Jura fold-and-thrust belt (France), *Tectonophysics, 357*, 137– 158.

Illies, J.H. (1972), The Rhinegraben rift system - plate tectonics and transform faulting. *Geophysical Surv., 1*, 27-60.

Illies, J.H., and G. Greiner (1978), Rhine Graben and Alpine System, *Geological Society of America Bulletin, 89*, 770-782.

Kälin, D. (1997), Litho- und Biostratigraphie der mittel- bis obermiozänen Bois de Raube-Formation (Nordwestschweiz), *Eclogae Geologicae Helvetiae, 90*, 97-114.

Kastrup, U., M.L. Zoback, N. Deichmann, K.F. Evans, D. Giardini, and A.J. Michael (2004), Stress field variations in the Swiss Alps and the northern Alpine foreland derived from inversion of fault plane solutions, *J. Geophys. Res., 109*, doi:10.1029/2003JB002550.

Lacombe, O., J. Angelier, D. Byrne, and J. Dupin (1993), Eocene-Oligocene tectonics and kinematics of the Rhine-Saone continental transform zone (Eastern France), *Tectonics, 12*, 874-888.

Lacombe, O., and D. Obert (2000), Héritage structural et déformation de couverture: plissement et fracturation tertiares dans l'Ouest du Bassin de Paris, *C. R. Acad. Sc. Paris, 330, II*, 793-79.

Lacombe, O., and F. Mouthereau (2002), Basement-involved shortening and deep detachment tectonics in forelands of orogens: Insights from recent collision belts (Taiwan, Western Alps, Pyrenees), *Tectonics, 21(4)*, 1029/2001TC901018.

Lacombe, O., F. Mouthereau, J. Angelier, H-T. Chu, and J.-C. Lee, (2003), Frontal curvature and oblique ramp development at an oblique ramp development at an obliquely collided irregular margin: Geometry and kinematics of the NW Taiwan fold-thrust belt, *Tectonics* 22 (3), 1025, doi:10.1029/2002TC001436.

Lacombe, O., F. Mouthereau, S. Kargar, and B. Meyer, (2006), Late Cenozoic and modern stress fields in the western Fars (Iran): implications for the tectonic and kinematic evolution of Central Zagros, *Tectonics, 25*, TC1003, doi:10.1029/2005TC001831,

Laubscher, H. (1961), Die Fernschubhypothese der Jurafaltung, *Eclogae Geologicae Helvetiae, 54*, 222-282.

Laubscher, H. (1970), Grundsätzliches zur Tektonik des Rheingrabens, in *Graben Problems. Proceedings of an International Rift Symposium held in Karlsruhe 1968, International Upper Mantle Project.*, edited by J.H. Illies and S. Mueller, pp. 79-86, E. Schweitzerbart'sche, Stuttgart.

Laubscher, H. (1972), Some overall aspects of Jura dynamics, *American Journal of Science, 272*, 293-304.

Laubscher, H. (1978), Foreland folding, *Tectonophysics, 47*, 325-337.

Laubscher, H. (1983), Ueberschiebungen im Jura, *Jber. Mitt. Oberrhein. Geol. Ver. N. F. 65*, 181-189.

Laubscher, H. (1986), The eastern Jura: Relations between thin-skinned and basement tectonics, local and regional, *Geologische Rundschau, 75*, 535-553.

Letouzey, J. (1986), Cenozoic paleo-stress pattern in the Alpine Foreland and structural interpretation in a platform basin, *Tectonophysics, 132,* 215-231.

Lopes Cardozo, G.G.O., and M. Granet (2003), New insight in the tectonics of the southern Rhine Graben-Jura region using local earthquake seismology, *Tectonics, 22*, 1078, doi:10.1029/ 2002TC001442.

Madritsch, H. (2008), Structural evolution and neotectonics of the Rhine-Bresse Transfer Zone, unpubl. PhD Thesis, University of Basel.

Marrett, R., and R.W. Allmendinger (1990), Kinematic analysis of fault-slip data, *Journal of Structural Geology, 12*, 973-986.

Marrett, R., and D.C.P. Peacock (1999), Strain and stress, *Journal of Structural Geology, 21*.

Martin J. and E. Mercier (1996), Héritage distensif et structuration chevauchante dans une chaîne de couverture : apport de l`équilibrage par modélisation géométrique dans le Jura nord-occidental. *Bull. Soc. Géol. France, 167, 1* 101-110.

McCann, T., C. Pascal, M.J. Timmerman, P. Krzywiec, J. López-Gómez, A. Wetzel, C.M. Krawczyk, H. Rieke, and J. Lamarche, J. (2006), Post-Variscan (end Carboniferous-Early Permian) basin evolution in Western and Central Europe, *in* European Lithosphere Dynamics, Geological Society of London Memoirs, 32, edited by Gee, D.G., and Stephenson, R.A., pp. 355-388, London.

Merrits, D.J., K.R. Vincent, and E.E. Wohl (1994), Long river profiles, tectonism and eustasy: a guide to interpreting fluvial terraces, *Journal of Geophysical Research, 99 (B7)*, 14301-14050.

Meschede, M., and K. Decker (1993), Störungsflächenanalyse entlang des Nordrandes der Ostalpen - ein methodischer Vergleich, *Z. dt. Geol. Ges., 144*, 419-433.

Meyer, B., R. Lacassin, J. Brulhet, B. Mouroux (1994), The Basel 156 earthquake which fault produced it? *Terra Nova, 6*, 54-63.

Molinaro, M., J.-C. Leturmy, D. Guezou, D. Frizon De Lamotte, and S.A. Eshraghi (2005), The structure and kinematics of the southeastern Zagros fold-thrust belt Iran: From thin-skinned to thick-skinned tectonics, *Tectonics, 24*, TC3007, doi:10.1029/2004TC001633.

Mosar, J. (1999), Present-day and future tectonic underplating in the western Swiss Alps: reconciliation of basement/wrench-faulting and décollement folding of the Jura and Molasse basin in the Alpine foreland, *Earth and Planetary Science Letters, 173*, 143-155,

Mouthereau, F., J. Tensi, N. Bellahsen, O. Lacombe, T. De Boisgrollier, and S. Kargar (2007), Tertiary sequence of deformation in a thin-skinned / thick-skinned collision belt: The Zagros Folded Belt (Fars, Iran), *Tectonics, 26* TC5006, doi:10.1029/2007TC002098.

Nicolas, M., M. Santoire, and P.Y. Delpech (1990), Intraplate seismicity: new seimotectonic data in Western Europe, *Tectonophysics, 179*, 27-54.

Nivière, B., and T. Winter (2000), Pleistocene northwards fold propagation of the Jura within the southern Upper Rhine Graben: seismotectonic implications, *Global and Planetary Change,* 263-288.

Oberlander, T.M. (1985), Origin of drainage transverse to structures in orogens, in *Tectonic Geomorphology*, edited by M. Morisawa and J.T. Hack, pp. 155-182, Allen and Unwin, Boston.

Pavoni, N. (1961), Faltung durch Horizontalverschiebung, *Eclogae. geol. Helv. 54*, 515-534.

Pavoni, N. (1987), Zur Seismotektonik der Nordschweiz, *Eclogae Geol Helv, 80*, 461-472,

Petit, C., M. Campy, J. Chaline, and J. Bonvalot (1996), Major palaeohydrographic changes in Alpine foreland during the Pliocene-Pleistocene, *Boreas, 25*, 131-143.

Petit, J.P. (1987), Criteria for the sense of movement on fault surfaces in brittle rocks, *Journal of Structural Geology, 9*, 597-608.

Pfiffner, O.A., and M. Burkhard (1987), Determination of paleo-stress axes orientations from fault, twin and earthquake data, *Annales Tectonicae, 1*, 48-57,

Pfiffner, O.A., P. Erard, and M. Stäuble (1997),Two cross sections through the Swiss Molasse Basin (lines E4-E6, W1, W7-W10), in *Deep structure of the Swiss Alps. Results of NRP 20*, edited by O.A. Pfiffner, P. Lehner, P. Heitzmann, S. Mueller and A. Steck, pp. 64-72, Birkhäuser.

Pfiffner, O.A. (2006), Thick-skinned and thin-skinned styles of continental contraction, in *Styles of Continental Contraction: Geological Society of America Special Papers*, vol. 414, edited by S. Mazzoli and R.W.H. Butler, pp. 153-177.

Philippe, Y., B. Colletta, E. Deville, and A. Mascle (1996),The Jura fold-and-thrust belt: a kinematic model based on map-balancing, in *Peri-Tethys Memoir 2: Structure and prospects of Alpine Basins and Forelands.*, vol. 170, edited by P. Ziegler and F. Horvath, pp. 235-261, Mem. Mus. natn. Hist. nat., Paris.

Plenefisch, T., and K. Bonjer (1997), The stress field in the Rhine Graben area inferred from earthquake focal mechanisms and estimation of frictional parameters, *Tectonophysics, 275*, 71-97.

Pollard, D.D., S.D. Saltzer, and A.M. Rubin (1993), Stress inversion methods : are they based on faulty assumption? *Journal of Structural Geology, 15*, 1045-1054.

Rat, P.(1976), Structures et phases de structuration dans les plateaux bourguignons et le Nord Ouest du fossé bressan (France), *Geologische Rundschau, 65,* 101-126.

Reinecker, J., O. Heidbach, M. Tingay, B. Sperner, and B. Mueller (2005), The 2005 release of the World Stress Map (available online at www.world-stress-map.org).

Reiter, F. and Acs, P. (1996-2000), TectonicsFP, Innsbruck, Computer Software for Structural Geology, version 2.0 PR. http://www.tectonicsfp.com/.

Rocher, M., F. Chevalier, C. Petit, and M. Guiraud (2003), Tectonics of the Northern Bresse region (France) during the Alpine cycle, *Geodinamica Acta, 16*, 131-147.

Rocher, M., M. Cushing, F. Lemeille, Y. Lozac'h, J. Angelier (2004), Intraplate paleostresses reconstructed with calcite twinning and faulting: improved method and application to the eastern Paris Basin (Lorraine, France), *Tectonophysics, 387*, 1-21.

Rotstein, Y., and M. Schaming (2004.), Seismic Reflection evidence for thick-skinned tectonics in the northern Jura., *Terra Nova, 16*, 250-256.

Ruhland, M. (1959), Une dislocation majeure du socle Vosgien dans la haute Vallée de l' Ognon, *Bull. Serv. Carte Géol. Als. Lorr., 12*, 61-64.

Schmid, S.M., O.A. Pfiffner, N. Froitzheim, G. Schönborn, and E. Kissling (1996), Geophysical-geological transect and tectonic evolution of the Swiss-Italian Alps, *Tectonics, 15*, 1036-1064.

Schumacher, M.E. (2002), Upper Rhine Graben: Role of preexisting structures during rift evolution, *Tectonics, 21(1)*, 6-1-6-17.

Simpson, G.(2004), Role of river incison in enhancing deformation, *Geology, 32*, 341-344.

Sissingh, W. (2001), Tectonostratigraphy of the West Alpine Foreland: correlation of Tertiary sedimentary sequences, changes in eustatic sea-level and stress regimes, *Tectonophysics, 333*, 361-400.

Smit, J.H.W., J.P. Brun, and D. Sokoutis (2002), Deformation of brittle-ductile thrust wedges in experiments and nature, *Journal of Geophysical Research, 108,* NO. B10, 2480, doi:10.1029/2002JB002190.

Sommaruga, A. (1997), Geology of the Central Jura and the Molasse Basin: New insights into an evaporite-based foreland fold and thrust belt, PhD thesis, 176 pp., Schweizerische Akademie der Naturwissenschaften, Neuchatel.

Sommaruga, A., and M. Burkhard (1997),Jura Mountains, in *Deep structure of the Swiss Alps. Results of NRP 20*, edited by O.A. Pfiffner, P. Lehner, P. Heitzmann, S. Mueller and A. Steck, pp. 45-53, Birkhäuser.

Spang, J. H. (1972), Numerical method for dynamic analysis of calcite twin lamellae. *Geol. Soc. Am. Bull. 83,* 1, 467-472.

Sperner, B., R., Ott, L. Ratschbacher (1993), Fault-striae analysis: a turbo pascal program package for graphical presentation and reduced stress-tensor calculation, *Computers & Geosciences 19*, 9, 1361-1388.

Steininger, F.F., W.A. Berggren, D.V. Kent, R.L. Bernor, S. Sen, and J. Agusti (1996),Circum-Mediterranean Neogene (Miocene and Pliocene) marine-continental chronologic correlations of European Mammal Units, in *The Evolution of Western Eurasian Neogene Mammal Faunas*, edited by R.L. Bernor, V. Fahlbusch and H.-W. Mittmann, pp. 7-46, Columbia University Press, New York.

Suppe, J. (1983), Geometry and kinematics of fault-bend folding, *American Journal of Science, 283*, 684-721.

Swiss Seismological Service, E.T.H.Z. (2007), Regional Moment Tensor catalogue, http://www.seismo.ethz.ch/mt/.

Theobald, N., H. Vogt, O. Wittmann (1977), Néotectonique de la partie méridionale du bloc rhénan, *Bull. B.R.G.M., 2*, 4, 121-140.

Tozer, R.S.J., R.W.H. Butler, and S. Corrado (2001), Comparing thin- and thick-skinned thrust tectonic models of the Central Apennines, Italy, in *Continental collision and the tectono-sedimentary evolution offorelands, vol. 1,* edited by B. Bertotti, K. Schulmann and S.A.P.L. Cloetingh, *pp. 181-194,* EUG Stephan Mueller Publication Series.

Twidal, C.R. (2004), River patterns and their meaning, *Earth Science Reviews, 67/3-4*, 159-219.

Twiss, R., J., and J. Unruh, R. (1998), Analysis of fault slip inversions: Do they constrain stress or strain rate?, *Journal of Geophysical Research, 103*, NO. B6, 12205-12222.

Ustaszewski, K., and S.M. Schmid (2006), Control of preexisting faults on geometry and kinematics in the northernmost part of the Jura fold-and-thrust belt, *Tectonics, 25*.

Ustaszewski, K., and S.M. Schmid (2007), Latest Pliocene to recent thick-skinned tectonics at the Upper Rhine Graben - Jura Mountains junction, *Swiss Journal of Geosciences, 100*, 293-312.

Ustaszewski, K., M.E. Schumacher, and S.M. Schmid (2005a), Simultaneous normal faulting and extensional flexuring during rifting - an example from the southernmost Upper Rhine Graben, *International Journal of Earth Sciences, 94*.

Ustaszewski, K., M.E. Schumacher, S.M. Schmid, and D. Nieuwland (2005b), Fault reactivation in brittle-viscous wrench systems - dynamically scaled analogue models and application to the Rhine-Bresse Transfer Zone, *Quaternary Science Reviews, 24*, 363- 380.

Wallace, R.E. (1951), Geometry of shearing stress and relation to faulting, *J. Geol., 59*, 118-130,

Ziegler, P. (1986), Geodynamic model for the Paleozoic crustal consolidation of Western and Central Europe: *Tectonophysics, 126*, 303-328.

Ziegler, P.A. (1992), European Cenozoic rift system, *Tectonophysics, 208*, 91-111.

Ziegler, P.A., G. Bertotti, and S.A.P.L. Cloetingh (2002), Dynamic processes controlling foreland development - role of mechanical (de)coupling of orogenic wedges and forelands., in *Continental collision and the tectono-sedimentary evolution of forelands.*, vol. 1, edited by B. Bertotti, K. Schulmann and S.A.P.L. Cloetingh, pp. 17-56, EUG Stephan Mueller Publication Series.

Chapter 4

Incision boosted buckling: Field evidence from an active fold at the front of the Jura Mountains (France)

by

Herfried Madritsch, Frank Preusser, Olivier Fabbri,

Fritz, Schlunegger, Vincent Bichet, Stefan M. Schmid

submitted to *Geology*

Abstract:

Positive coupling between erosion and deformation has been intensively investigated at the scale of orogens but has not yet been adequately documented for individual faults or folds. Herein, we present a field example of active deformation along a single fold structure that occurs in response to river incision. At the northwestern front of the Jura fold-and-thrust belt in eastern France, differentially uplifted paleo-meanders of the Doubs River record Pleistocene to recent growth of the Citadelle Anticline associated with a minimum rock uplift of 10 ± 2 meters. This observation marks the first evidence for active fold growth within the internal parts of the Late Miocene to Early Pliocene Jura fold-and-thrust belt. Reconstruction of the river incision and deformation history based on paleo-topographic markers and OSL-dating of oxbow lake deposits reveal that buckling took place simultaneously to focused Pleistocene river incision. The structural, geomorphic and temporal setting implies that incision enhanced deformation and localized strain at a fixed position. Initiation of Pleistocene erosion led to a back stepping of the fold-and-thrust belt front and induced presently active out-of-sequence deformation.

Keywords*: active folding, river incision, erosion-deformation coupling, Jura fold-and-thrust belt*

4.1. Introduction

The recognition that mass redistribution by surface processes potentially results in a modulation of the geodynamic evolution of mountain ranges (Pinter and Brandon, 1997) has been one of the most exciting recent developments in geosciences. Our present understanding of this coupled system is mainly based on numerical models of lithospheric deformation, quantitative description of surface processes, and application of new geochronological techniques to landscape shaping processes (Beaumont et al., 1992; Burbank et. al, 1996; Koons et al., 2002; Simpson and Schlunegger, 2003). Despite significant progress in exploring the feedbacks between climate, erosion and tectonics

(Simpson, 2004; Zeilinger et al., 2005; Montgomery and Stolar, 2006), the detection of positive coupling mechanisms between erosion and crustal deformation of simple systems, down to the scale of landscapes associated with individual folds in the upper crust, has remained a major challenge (Buck et al., 2007).

Here we present an example of active fold growth boosted by river incision that localized deformation at a fixed position. Our observations shed new light on the most recent deformation dynamics of the Jura Mountains, a text book example of a thin-skinned foreland fold-and-thrust belt, whose present day tectonic activity is a matter of ongoing scientific debate (Becker, 2000).

4.2. Geological setting

The study area is located at the northwestern fringe of the arcuate Jura fold-and-thrust belt that represents the most external deformation front of the European Alps (Fig. 1a, inset). Its formation is widely accepted to have resulted from "distant push" (Laubscher, 1961; Laubscher, 1972) induced by Late Miocene crustal shortening and nappe stacking in the external crystalline massif of the Central Alps. Large-scale decoupling of the Mesozoic sedimentary cover along a sole thrust in Middle to Late Triassic evaporites ("décollement") enabled the propagation of the thrust front towards the distal foreland in the northwest (Burkhard, 1990; Burkhard and Sommaruga, 1998). The formation of the thin-skinned Jura belt was a short lived event. In its outermost northern parts the main deformation stage is known to have lasted from Late Miocene to Early Pliocene times (10.5 - 4.2 Ma) (Kälin, 1997; Ustaszweski and Schmid, 2006). Late Pliocene to recent shortening in the frontal most parts of the Jura Mountains is characterized by low rates of deformation; whether this deformation is still thin-skinned or whether it involves fault reactivation within the basement, is a matter of controversies (e.g. Nivière and Winter, 2000; Ustaszewski and Schmid, 2006).

The Besançon Zone (BZ in Fig. 1a) represents the most external segment of the thin-skinned fold-and-thrust belt that encroached onto the Eo-Oligocene intra-continental Rhine-Bresse Transfer Zone (RBTZ in Fig 1a) (Madritsch et al., 2008). The northern boundary of the BZ is the Chailluz Thrust (CHT in Fig. 1a). The southern boundary is known as the Faisceau Bisontin (FB in Fig. 1a) (Chauve et al., 1980), an approximately 100 km long ENE-WSW striking thrust zone.

After the main deformation phase of the Jura fold-and-thrust belt, the Middle Pliocene Sundgau-Forêt de Chaux Gravels (SFC in Fig. 1a) were deposited by a low-gradient braided river that flowed along the northern tip of the Faisceau Bisontin and discharged to the Bresse Graben farther west (BG in Fig.1a) (Giamboni et al., 2004). The gravels have a biostratigraphic deposition age of 4.2-2.9 Ma (Petit et al., 1996; Fejfar et al., 1998) and feature pebble and heavy mineral spectra indicating an Alpine provenance (Liniger and Hofmann, 1965; Bonvalot, 1974).

In Late Pliocene times (2.9 Ma) this braided river system was deflected towards the Upper Rhine Graben (URG in Fig. 1a) and the valley north of the Faisceau Bisontin became occupied by the Doubs River that has been the major drainage system in the Jura fold-and-thrust belt ever since (Fig. 1a inset) (Liniger and Hofmann, 1965; Giamboni et al., 2004). West of the city of Montbéliard (M in Fig. 1a) the high-sinuosity lower reach of the Doubs parallels the course of the former SFC braided river system.

From 2.9 Ma onwards the combined effects of base level fall due to subsidence of the Upper Rhine and Bresse Graben and lithospheric to intracrustal rooted compressional foreland deformation in the RBTZ (Dèzes et. al., 2004) caused differential erosion of the SFC Gravels (Fig. 1a) (Campy, 1984). The Doubs incised into the Middle Pliocene gravel plain and the underlying Jurassic limestones and marls and carved out a narrow canyon of up to 350 meters depth parallel to the FB thrust zone (Fig. 1a). Spectacular paleo-meanders that were formed during this incision are found all along the lower reach of the Doubs.

4.3. Structure and topography

The Citadelle Anticline (Fig. 1b) is located within the town of Besançon (B in Fig. 1a). It formed within the BZ, immediately in front of the Faisceau Bisontin thrust zone (Fig. 2a) (Dreyfuss and Kuntz, 1969; Chauve et al., 1980). The Citadelle Anticline has a clear topographic expression and is built up by Middle Jurassic limestones. The gently double plunging fold axis strikes ENE-WSW. The total length of the anticline, as observed at the surface, is about 15 km.

Abundant evidence of bedding parallel slip indicates that the Citadelle Anticline formed by flexural slip, a typical deformation mechanism associated with décollement and fault-related folding in the Jura fold-and-thrust belt (Burkhard and Sommaruga, 1998). Paleostress analysis of fault-slip pairs indicate that folding occurred by buckling under NW-SE directed compression (Madritsch et al., 2008), which is roughly parallel to the present day orientation of maximum horizontal stress as determined from in-situ measurements of borehole breakouts within the Mesozoic cover sediments (Becker, 2000). Buckling of the competent Middle to Late Jurassic limestones forming the fold limbs is compensated by ductile deformation of Triassic evaporites and Early Jurassic marls in the core of the anticline (Fig. 2a). The horizontal shortening taken up by the anticline, as inferred from line balancing of a cross section perpendicular to the fold axis is 150 m.

Strath-terraces, wind gaps and three distinctive paleo-meanders of the Doubs River were cut into the Citadelle Anticline (Fig. 1b). Furthermore, the highly sinuous active channel of the Doubs River repeatedly traverses the anticline perpendicular to its axis. The culmination of the fold crest line (Fig. 2b), where the anticline forms a 260 m high hill, coincides with the area of most intense river incision. At this location, incision was structurally guided once the river became locked between the Citadelle

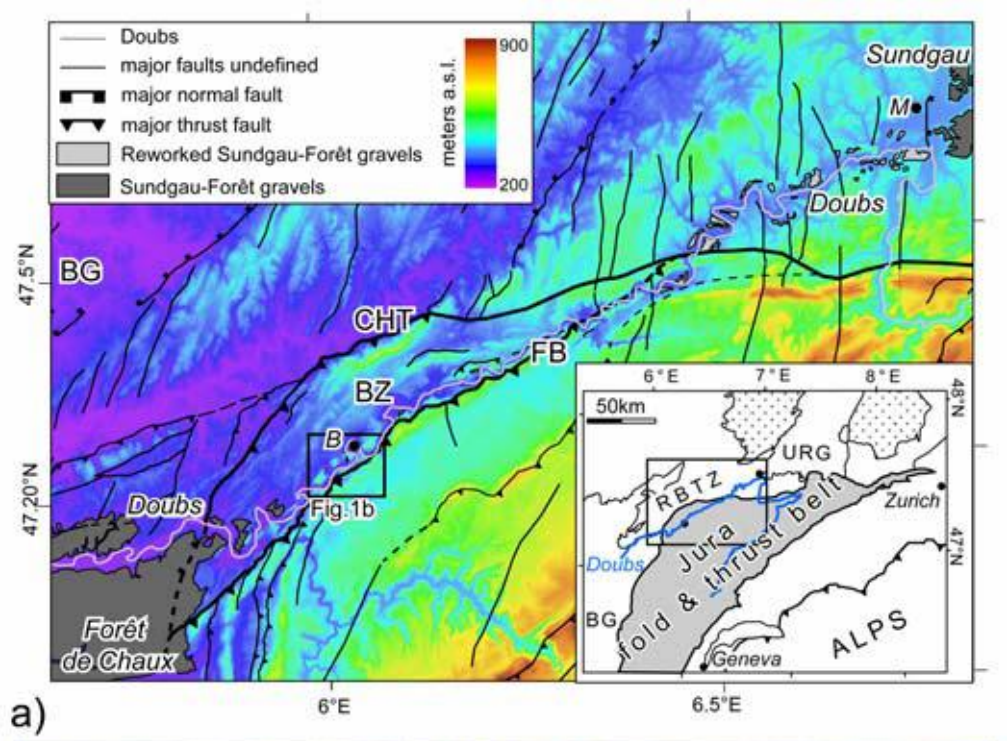
Doubs
major faults undefined
major normal fault
major thrust fault
Reworked Sundgau-Forêt gravels
Sundgau-Forêt gravels
meters a.s.l.
900
200
Sundgau
M
Doubs
BG
CHT
FB
BZ
B
Fig.1b
Doubs
Forêt de Chaux
47.5°N
47.20°N
6°E
6.5°E
6°E
7°E
8°E
48°N
47°N
50km
URG
RBTZ
Zurich
Doubs
Jura fold & thrust belt
BG
ALPS
Geneva
a)


NW
Citadelle Anticline
SE
Doubs
MAC
RDO

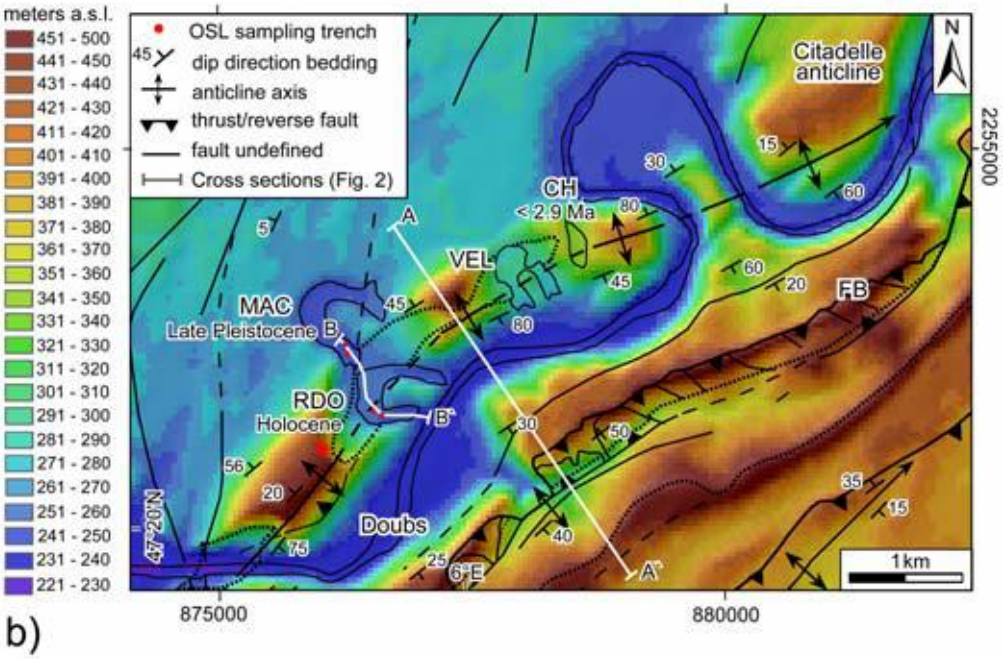
meters a.s.l.
451 - 500
441 - 450
431 - 440
421 - 430
411 - 420
401 - 410
391 - 400
381 - 390
371 - 380
361 - 370
351 - 360
341 - 350
331 - 340
321 - 330
311 - 320
301 - 310
291 - 300
281 - 290
271 - 280
261 - 270
251 - 260
241 - 250
231 - 240
221 - 230
OSL sampling trench
dip direction bedding
anticline axis
thrust/reverse fault
fault undefined
Cross sections (Fig. 2)
N
Citadelle anticline
CH
< 2.9 Ma
VEL
MAC
Late Pleistocene
RDO
Holocene
FB
Doubs
A
A'
B
B'
2255000
47°20'N
6°E
875000
880000
1km
b)

Anticline and the Faisceau Bisontin thrust zone (Figs. 1b and 2a). Moreover, incision was lithologically facilitated after the river had reached the marls within the core of the anticline (stippled line in Fig. 1b).

The highest remnants of fluvial deposits detected along the anticline are located 110 m above the active channel in the Chaudanne (CH) wind gap (Figs. 1b and 2b). Pebble petrography and heavy mineral spectra of these deposits reveal an Alpine provenance, indicating that they represent reworked SFC Gravels (see appendix). Thus, the 2.9 Ma minimum deposition age of the SFC Gravels (Fejfar et al., 1998; Petit et al., 1996) gives the maximum age of the Chaudanne wind gap. The paleo-meander of Velotte (VEL) is located 60 meters below the Chaudanne wind gap, and hence, is presumably younger.

The Malcombe (MAC) and Roche d'Or (RDO) paleo-meanders, both about 700 m wide, are located further to the west and at lower elevations. Most intriguingly the elevation of the more distal Malcombe paleo-meander is lower (about 10 m above the active channel) relative to that of the more proximal Roche d' Or paleo-meander (17 m above the active channel), located on the crest of the anticline (Fig. 1b). This indicates that the Roche d'Or paleo-meander was uplifted along the fold axis with respect to the distal Malcombe paleo-meander, as was proposed in the pioneering work by Dreyfuss and Glangeaud (1950).

In an effort to constrain the surface observations we performed high precision geodetic leveling and geoelectric subsurface imaging to determine the bedrock elevation of the abandoned meander channels (see appendix). The top bedrock elevation difference between the Malcombe and the Roche d'Or paleo-meander was found to be 10 ± 2 meters (Fig. 2c). It reflects the minimum relative rock uplift between the abandoned meanders and is larger than the 7 meters inferred from the topography.

Figure 1a: Digital elevation model of the northwestern Jura fold-and-thrust belt (50 m horizontal resolution). Note the course of the Doubs River that incises parallel to the deformation front of the Faisceau Bisontin (FB). Post-Pliocene relative rock uplift of the area is attested by the differential erosion of the Sundgau-Forêt de Chaux-gravels (SFC). CHT: Chailluz Thrust; B: Besançon; BG: Bresse Graben; M: Montbéliard; FB: Faisceau Bisontin; URG: Upper Rhine Graben; RBTZ: Rhine-Bresse Transfer Zone

1b: Shaded digital elevation model of the study area showing the Citadelle Anticline and the paleo-meanders. Pleistocene growth of the Citadelle Anticline led to a cutoff of the Malcombe (MAC) and subsequent relative rock uplift of the Roche d'Or (RDO) and the Velotte (VEL) paleo-meanders. A further important paleo-topographic marker is given by the Chaudanne wind gap (CH). The stippled line marks the boundary between outcrops of Middle Jurassic limestones that form the limbs of the anticline and Early Jurassic marls that outcrop in its core. Note the positions of cross sections shown in Fig. 2a and 2c. The red star marks the position from which the photograph was taken (view onto the Citadelle Anticline, Malcombe and Roche d'Or meander towards NE).

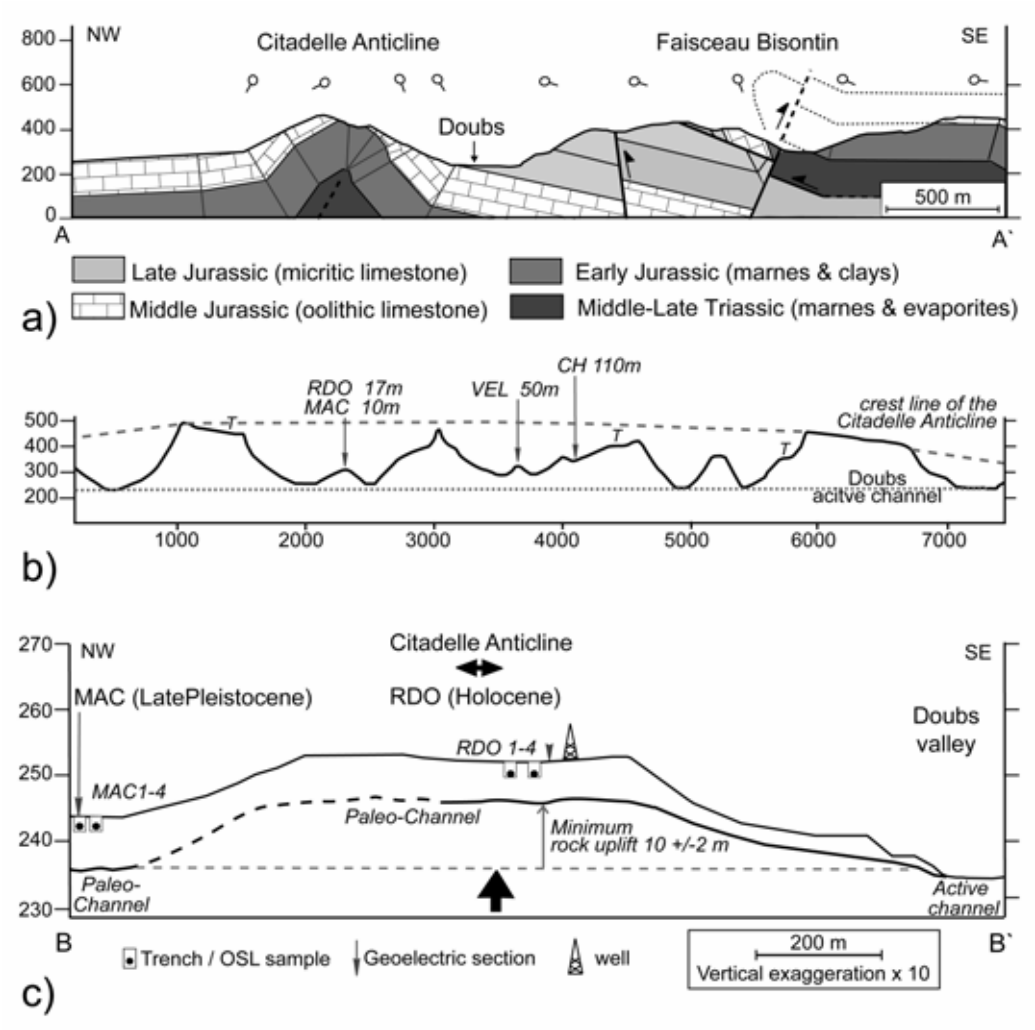

Figure 2a: Geological section across the Citadelle Anticline and the Faisceau Bisontin thrust zone. **2b:** Topographic cross section along the crest of the Citadelle Anticline, parallel to the fold axis (see Fig. 1B) illustrating strath terraces, wind gaps, and paleo-meanders that were cut into the fold during Pleistocene incision of the Doubs River. The dashed grey line marks the trend of the double plunging fold crest line that is parallel to the fold axis and culminates in the area of deepest incision. **2c:** Vertically exaggerated topographic profile across the Roche d'Or (RDO) and Malcombe (MAC) paleo-meanders, as constrained by high precision geodetic leveling and geoelectric subsurface imaging correlated with well information. Note the relative rock uplift of the younger Roche d'Or with respect to the older and more distal Malcombe paleo-meander. Also indicated are the locations of geoelectric sections and trenches for OSL sampling. CH: Chaudanne wind gap; MAC: Malcombe paleo-meander; RDO: Roche d'Or paleomeander; T: Strath terrace, interpreted; VEL: Velotte paleo-meander.

We also carried out Optical Stimulated Luminescence (OSL) dating on the oxbow deposits of the Malcombe and Roche d'Or paleo-meanders. 8 samples from 4 trenches were dated (Figs. 1b and 2c, see appendix). Burial ages from the samples of the lower lying, distal Malcombe paleo-meander are significantly older (Middle Late Pleistocene) compared to those obtained from the higher and more proximal sites within the Roche d'Or paleo-meander (Holocene).

4.4. Discussion and Conclusion

This study points out an inversion of the paleo-meander sequence preserved along the Citadelle Anticline (Figs. 1b and 2c). The younger Roche d'Or paleo-meander, located on the crest of the anticline has been uplifted with respect to the older Malcombe paleo-meander located on the fold limb. These observations indicate that deformation along the Citadelle Anticline that most likely initiated during the Late Miocene to Early Pliocene main phase of Jura folding is still active and moreover, occurs in relation to erosion.

Recent mathematical coupled deformation - surface process models demonstrate that river incision is theoretically able to modulate and enhance tectonic deformation (Simpson, 2004). The numerical experiments indicate that erosional unloading of a rigid crust by river incision exerts a significant control on small-scale structures if incision occurs contemporaneously with buckling under regional horizontal compression. These mechanical and temporal conditions apply to the Citadelle Anticline, as is indicated by the following field observations:

1) The Citadelle Anticline formed by buckling as is evident from flexural slip observed along the bedding surfaces of the fold limbs
2) Paleo- and recent maximum horizontal stress measurements within the Mesozoic cover are consistently oriented perpendicular to the fold axis of the Citadelle Anticline (Becker, 2000; Madritsch et al., 2008). Hence, the direction of compression did not significantly change since the onset of buckling.
3) River incision and buckling occurred simultaneously since 2.9 Ma. This is evident from the presence of reworked Middle Pliocene Sundgau-Forêt de Chaux Gravels in the Chaudanne wind gap and the inversion of the Late Pleistocene paleo-meander sequence.
4) Presently active deformation by buckling occurs in a fixed position that coincides with the area of deepest incision where the ancient and recent high sinuosity course of the Doubs River repeatedly crosses the anticline perpendicular to its fold axis.

Thus, we conclude that active deformation along the Citadelle Anticline has been localized and been enhanced by river incision. While previous numerical models and field observations suggest positive coupling between buckle folding and transverse river incision (Simpson, 2004; Zeilinger et. al, 2005) the Citadelle Anticline represents the first reported example where buckling is apparently boosted by overall along-strike incision. The observed active deformation occurs within the internal parts of the Jura fold-and-thrust belt some 20 km southwest of the outermost Chailluz Thrust (CHT Fig. 1a). Hence, it is likely that the down-cutting of the Doubs River, probably driven by Pleistocene base level drop due to large scale foreland deformation processes, caused a back-stepping of the Pliocene fold-and-thrust belt front and localized active out-of-sequence deformation.

Acknowledgements:

The first author received funding by ELTEM and would like to thank the entire past and present EUCOR URGENT team at the University of Basel, led by P. Ziegler. B. Regent and F. Souquière lent a strong helping hand during field work. E.M. Hagedorn is kindly thanked for heavy mineral analyses. Field discussions with M. Schnellmann and T. Vietor helped to shape the ideas for the manuscript.

Appendix

A.1. Heavy Mineral Analysis

A.1.1. Methodology

A regional comparative heavy mineral analysis comprising samples from 19 sites was carried out in order to determine the provenance of fluviatile deposits including those from the Chaudanne wind gap (Fig. A1). The sample set includes reference samples from the Sundgau and Forêt de Chaux (SFC) gravel plains that contain Alpine derived material (samples 1, 7-9), Pleistocene Doubs terraces (samples 2, 6) and fluvial sediments of the Ognon River that drains the Vosges Mountains (samples 10-19) were taken (Fig. A1). Additional correlations were carried out with the results of regional analyses from neighboring areas by Boenigk (1987) and Hagedorn (2004)

Heavy mineral analyses followed the guidelines by Boenigk (1983). The grain size fraction between 64-500 μm was obtained from the dissolved samples by wet sieving. Density separation was carried out using separatory funnels and Bromoform (density 2.83 g/cm3) as separation liquid. Quantitative heavy mineral determination and counting using a polarization microscope was performed according to the line count method (analyst: E. M. Hagedorn). A minimum of 100 grains per sample were counted.

A.1.2. Results and interpretation

The samples taken from remnants of fluvial sediments along the Doubs Valley including those from the Chaudanne wind gap (Sample 5) show a clear similarity with those from the Sundgau and Forêt de Chaux areas (Sample 1, 7-9) (Fig. A1). These samples are characterized by relatively high amounts of unstable minerals, especially epidote, but also contain significant amounts of hornblende and garnet. Most notably, staurolite occurs in all these samples. In contrast to the samples from the Sundgau area the samples from the Doubs Valley are also rich in zircon and tourmaline. These differences in the heavy mineral spectra are most likely due to a general downstream increasing influence of tributaries to the SFC braided river that drained the foothills of the Vosges

Mountains that are built up by Late Paleozoic and Triassic sediments (Théobald et al., 1976). Weathering may also play a minor effect.

Most importantly the heavy mineral analysis permits to exclude the other possible source area for the Chaudanne wind gap deposits namely the Late Miocene so called Bois de Raube Formation that exclusively carries material derived from the Vosges Mountains and which pre-dates the formation of the Jura fold-and-thrust belt (Kälin, 1997). Reference samples from this source area (samples 10-19) do not contain any high grade metamorphic minerals such as staurolite and are characterized by far smaller amounts of epidote and garnet. Thus the deposits of the Chaudanne wind gap are clearly derived from SFC Gravels.

Note that these remnants are elevated with respect to the Sundgau and Forêt de Chaux areas, as is visible from the inset in Figure A1. This hints towards a large-scale relative rock uplift along the Rhine-Bresse Transfer Zone (RBTZ see inset Figure 1a; (Campy, 1984)). Also note that the eroded base of the Middle Pliocene SFC gravel sheet must have been located at an even higher elevation above the Chaudanne wind gap. This is constrained by other SFC remnants detected further upstream at elevations of up to 240 m above the active channel of the Doubs (site of Deluz, sample 3). This suggests that the remnants found in the Chaudanne windgap represent reworked SFC gravels and the minimum SFC gravel deposition age of 2.9 Ma (Petit et al., 1996; Fejfar et al., 1998) must be regarded as maximum age of the Chaudanne wind gap.

A.2. Geodetic and geophysical prospection of paleo-meanders

The profile across the Roche d'Or and Malcombe paleo-meanders presented in Figure 2c is based on geodetic and geophysical prospection methods.

A.2.1. Methodology

Geodetic leveling for the determination of the surface altitude of the abandoned meanders was done using a PRO XRS Trimble GPS for field measurements and Trimble GPS Pathfinder software for data treatment**.** Field measurements were carried out in phase of the GPS signal and during an optimal period of the GPS satellite network position. The acquisition time for each measurement point was about 15 min. The field data were then post-treated with reference to the DGPS station of the Besançon Observatory (BSCN, weblink: (*http://rgp.ign.fr/STATIONS/station.php?acro=BSCN)* located approximately 6 km north of the study area. This procedure allowed the determination of the surface elevation at a precision of ± 10 cm or even better in most cases. Measurements were taken at 52 sites along a profile from the active channel of the Doubs River across the Roche d'Or and

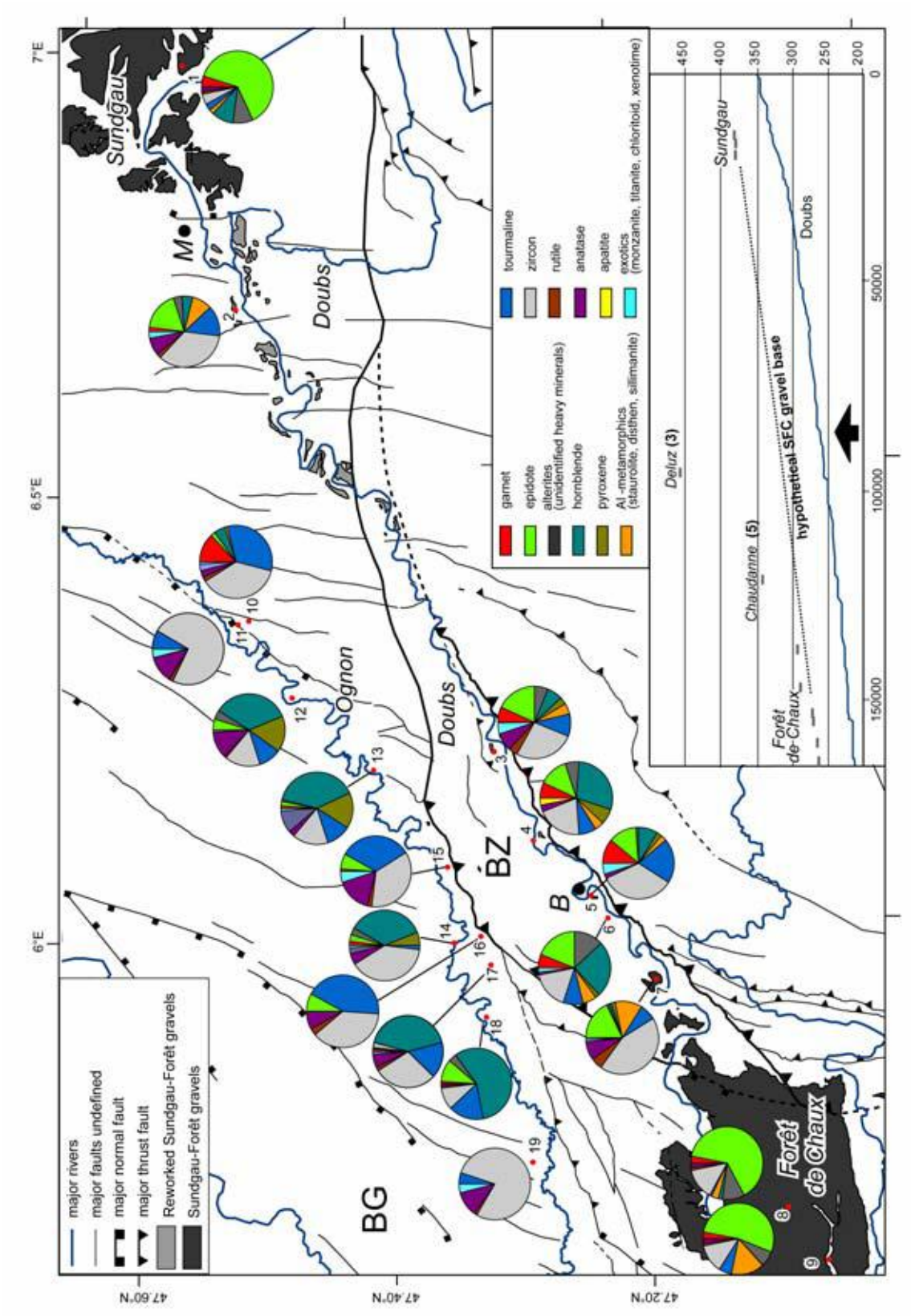

Figure A1: Results of regional heavy mineral analysis. Note the occurrence of unstable heavy minerals such as staurolite and epidote in all samples from the Doubs Valley including the Chaudanne wind gap (sample 4). B: Besançon; BG: Bresse Graben; BZ: Besançon Zone; FB: Faisceau Bisontin; M: Montbéliard.

Data point signature	Altitude [meters a.s.l.]	Vertical precision [cm]	X [meters]	Y [meters]	Horizontal precision [cm]
1	236	10	877200	2252243	7
2	238	7	877165	2252248	5
3	238	5	877137	2252248	5
4	241	6	877103	2252250	6
5	241	6	877057	2252267	6
6	241	4	877013	2252264	5
7	242	4	876960	2252263	5
8	243	5	876900	2252254	6
9	245	6	876866	2252210	7
10	246	4	876811	2252203	5
11	246	5	876765	2252214	6
12	250	7	876711	2252221	7
13	252	3	876656	2252250	5
14	252	4	876594	2252298	6
15	253	4	876551	2252330	6
16	252	4	876500	2252382	5
17	253	3	876459	2252435	4
18	253	6	876428	2252503	6
19	253	3	876737	2252269	4
20	252	3	876635	2252320	4
21	254	3	876659	2252358	4
22	252	3	876618	2252345	4
23	252	3	876602	2252380	4
24	252	3	876612	2252463	4
25	253	4	876498	2252493	4
26	253	2	876457	2252559	3
27	253	3	876449	2252620	3
28	252	4	876438	2252651	4
29	251	7	876434	2252684	5
30	250	5	876431	2252712	5
31	248	6	876415	2252754	5
32	247	5	876408	2252789	5
33	246	4	876396	2252826	4
34	245	3	876379	2252861	4
35	245	3	876310	2252872	4
36	244	3	876328	2252911	4
37	245	4	876365	2252990	4
38	244	5	876348	2252943	5
40	246	5	876416	2252867	5
41	247	4	876442	2252814	5
42	249	3	876465	2252774	4
43	250	4	876480	2252730	5
44	252	4	876510	2252704	4
45	253	5	876534	2252657	4
46	252	6	876574	2252703	4
47	253	6	876659	2252708	4
48	253	6	876689	2252587	5
49	252	4	876763	2252638	4
49	244	3	876364	2252902	4
50	252	5	876778	2252663	4
51	250	4	876875	2252654	4
52	250	5	876888	2252632	5

Table A1: Results of GPS leveling. X/Y coordinates are given in meters (French II Lambert Conformal Conic projection).

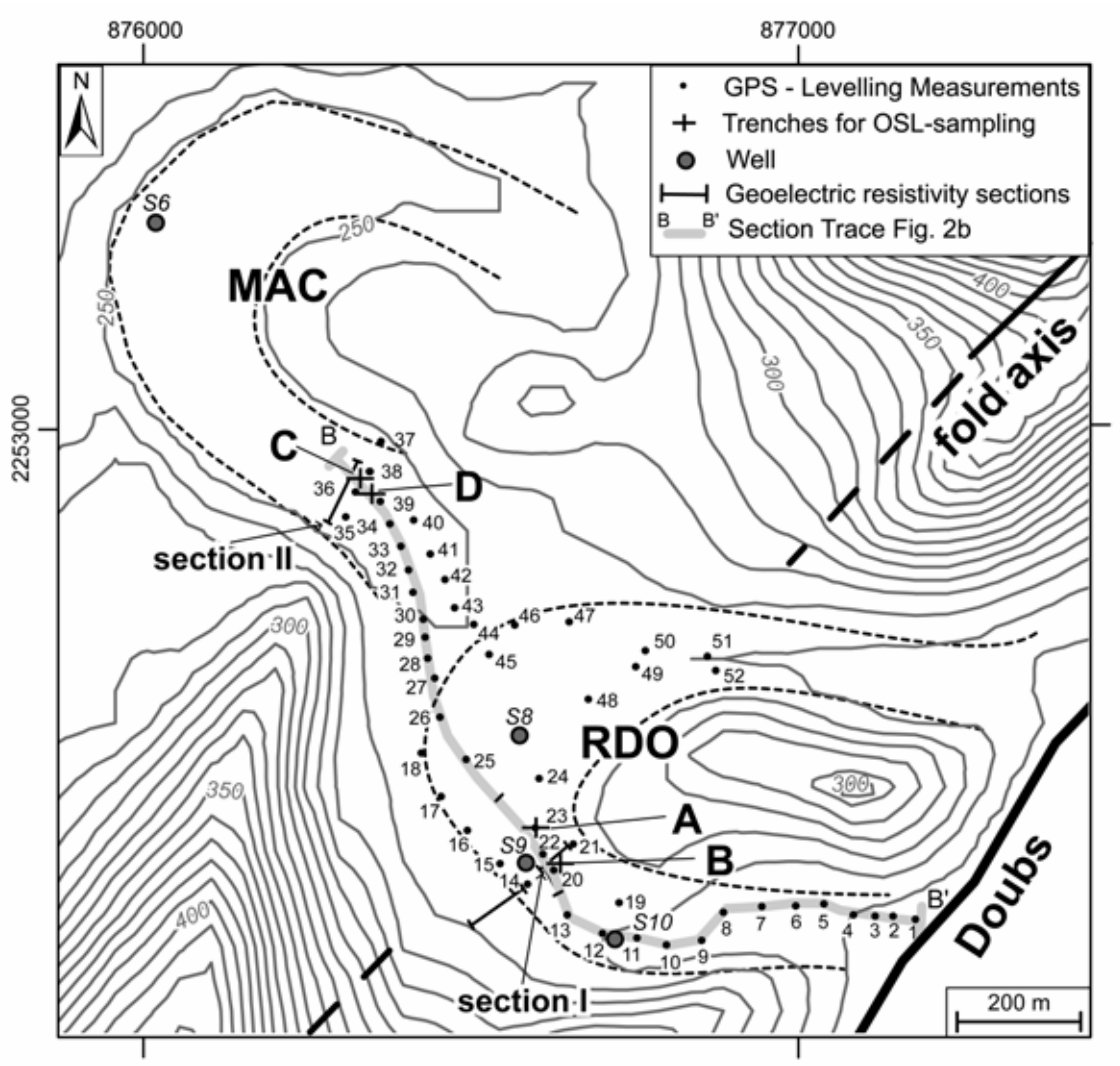

Figure A2: Topographic map of the Roche d'Or (RDO) and Malcombe (MAC) paleo-meanders showing the position of geodetic leveling points, wells (Fig. A3), geoelectrical profiles (Fig. A4) and trenches for OSL sampling (Fig. A5). The thick grey line marks the trace of the topographic section shown in the paper (Fig. 2c). Numbers of leveling points refer to Table A2. MAC: Malcombe paleo-meander; RDO: Roche d'Or paleo-meander.

Malcombe paleo-meanders. The location and index numbers of the measurement points are shown in Figure A2 and the results given in Table A1.

Geoelectric resistivity profiling was used to determine the bedrock elevation below the alluvial sediment fill of the paleo-meanders. We used an IRIS Instruments SYSCAL R1 device. A multi-electrode dipole-dipole array (36 electrodes, electrode distance 1.5 to 5 meters depending on the needed profile length) was used for data acquisition. Field data were treated with Res2Dinv software to perform numerical least square inversion of resistivity pseudo-sections (Locke and Barker, 1995). The geological interpretation of the geolelectric images was backed by correlation with geological logs from nearby wells (position Figure A2) that were obtained from the InfoTerre archive of the French

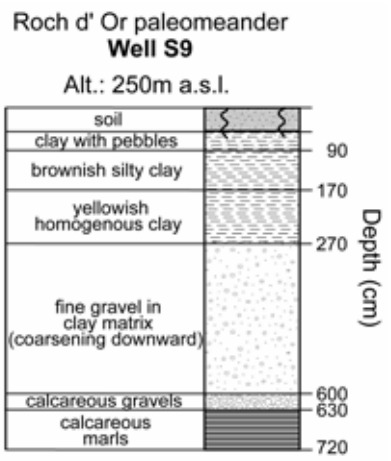

Figure A3: Geological log of the well S9 which was used for correlation with geoelectric resistivity sections (see Figure A2 for location)

Bureau de Recherches Géologiques et Minières (BRGM, weblink: *http://infoterre.brgm.fr/*). The geological log of the well S9, located near section I across the Roche d'Or meander is shown in Figure A3.

A.2.2 Results and interpretation

The results of the geodetic leveling constrain the difference in surface elevation between the two abandoned meanders (Fig. 2b) and furthermore allow to better characterize the slope morphology. The slope between the lower lying but more distal Malcombe paleo-meander and the proximal Roche d'Or paleo-meander is gentle. No distinctive scarp between the two paleo-meanders is visible. The surface morphology of the central segment of the Roche d'Or paleo-meander is horizontal, resembling a rather juvenile alluvial plain that appears to have been hardly affected by long term soil creep which would result in a more undulating surface morphology. This observation is in agreement with the results of OSL dating that revealed a Holocene age of the Roche d'Or paleo-meander (see below). Towards the active river channel of the Doubs River, the abandoned arm of the Roche d'Or meander becomes significantly steeper. We interpret this as head-ward erosion of the channel in response the incising Doubs River before the meander was finally abandoned.

Geolelectrical profiling, combined with geological well information (Fig. A3), allow determining the bedrock elevation of the paleo-meanders. The alluvial sediments consist of a lower sequence of coarse gravels embedded in a clay rich matrix and an upper sequence of clay to silty clay, interpreted as oxbow lake deposits. The bedrock below the alluvial sediments is composed of Early Jurassic marls or Middle Jurassic limestone. The alluvial sediments are characterized by low electrical resistivity values, especially those lying below the ground water table. By contrast, the bedrock, especially where formed by limestone shows high electrical resistivity values.

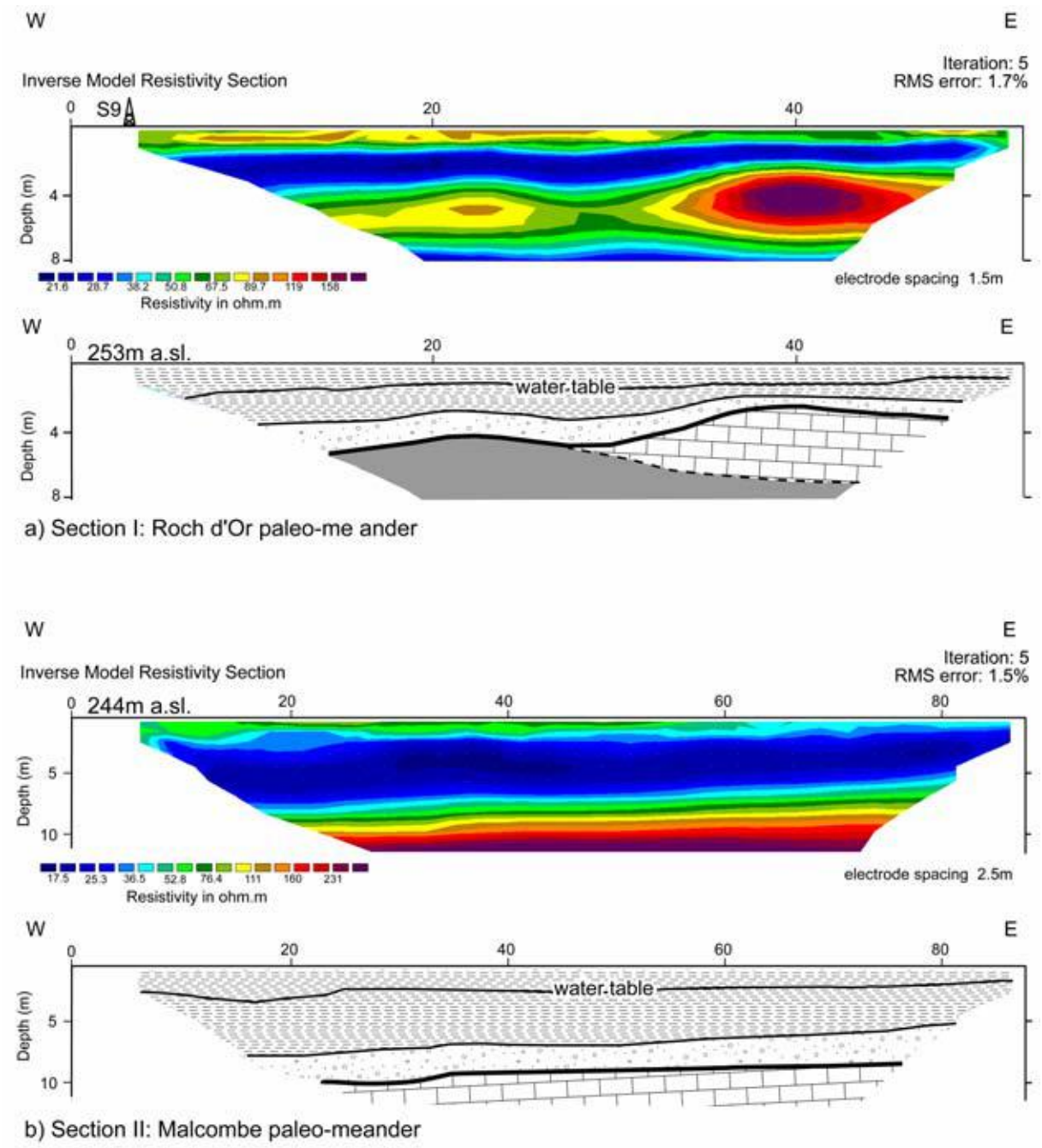

Figure A4: Interpretation of two geoelectrical resistivity profiles across the abandoned Roche d'Or and Malcombe meander. Note the differential vertical scale between the two sections. The bedrock elevation of the distal and older Malcombe meander is lower than that of the more proximal and younger Roche d'Or meander.

A total of four geoelectrical profiles were obtained (Fig. A2). The results of two campaigns and their geological interpretation are shown in Figure A4. Section I and II are perpendicular to the channel axes of the Roche d'Or and Malcombe paleo-meanders respectively. Section I across the Roche d'Or paleo-meander was correlated with the well S9 shown in Figure A3 (location see Fig. A2). The alluvial fill unconformably overlies the bedrock composed of Early Jurassic marls and Middle

Jurassic limestones. Along this section the maximum bedrock depth reaches 244 m a.s.l.. Section II crosses the Malcombe paleo-meander. The bedrock is composed of limestone as suggested by nearby exposures. The clear and continuous resistivity contrast between the high-resistivity bedrock and the above-lying low resistivity alluvial deposits shows that the elevation of the bedrock-alluvial deposit interface is at maximum at 236 a.s.l. in this section. That is 10+/- 2 m below the bedrock-alluvial deposit interface of the Roch d'Or paleo-meander (244 m a.sl. see above).

A.3. Optically Stimulated Luminescence dating

A.3.1. Methodology

Samples for Optically stimulated luminescence dating (OSL) were obtained from four trenches dug into the Malcombe (MAC) and Roche d'Or (RDO) paleo-meanders (Figure A5). Two samples were taken out of each. At all sites homogenous silty clays were excavated underneath a disturbed soil and sediment cover of 80 to 100 cm thickness. Samples were taken at a depth of 135-150 cm. The sampled sediments mimic other fluvial terrace deposits found along the Doubs valley in terms of grain size and heavy mineral composition and are interpreted as oxbow lake deposits. All samples revealed very little to no carbonate content which excludes a colluvial sediment source from the slopes of the meander arms that are composed of Middle Jurassic limestones and Early Jurassic calcareous marls.

Determination of the paleo-dose (D_e) was carried out on fine-grained quartz separates. We first applied usual chemical pre-treatments (HCl, H_2O_2, Na-oxalate), isolated the grain fraction 4-11 µm by settling, and then treated the samples for one week with H_2SiO4. The purity of the samples was confirmed by IR shine tests. Paleo-dose was determined using the Single-Aliquot Regenerative Dose (SAR) protocol, after applying a series of standard tests to identify appropriate measurement conditions (dose recovery, preheat, thermal transfer tests, cf. Wintle and Murray, 2006). A preheat of 230°C for 10 s has been applied prior to all OSL measurements (60 s at 125°C). Altogether, the samples revealed very good luminescence properties in the standard tests, <1 % recuperation even for the youngest samples, and recycling ratios of all measured aliquots are within 5 % of unity. Mean and standard deviation of at least five measurements have been used for age calculation (Table A3). Measurement of dose rate relevant elements (K, Th, U) was carried out by high-resolution low-level gamma-spectrometry by D. Degering (VKTA Rossendorf e.V., Dresden, Germany) (Table A2). Present day moisture of all samples has been measured (Table A2) and, based on this, an average water content of the sediment of 15-25 % has been assumed, which accounts for possible changes in past hydrological conditions. Age calculation was carried out using ADELE software (Kulig, 2005) considering geographical position and sediment overburden for estimating the contribution by cosmic rays to the total dose rate.

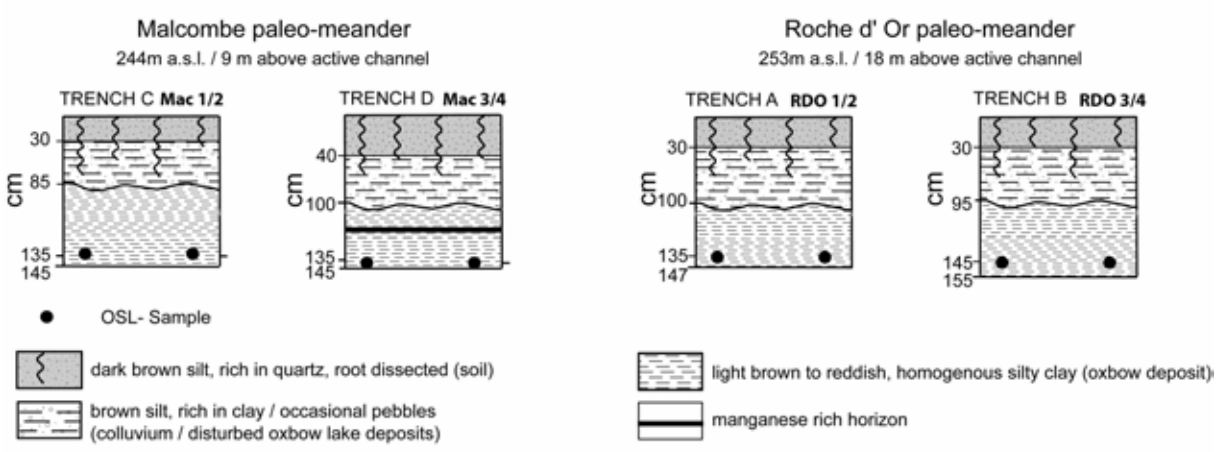

Figure A5: Geological logs of trenches from which the OSL-samples were taken (compare Figure A2 for location)

Sample	Moisture (%)	Water (%)	Grain size (µm)	n	Depth (m)	K (%)	Th (ppm)	U (ppm)	D (Gy ka^{-1})	De (Gy)	Age (ka)
MAC1	19.1	20 ± 5	4-11	5	1.35	1.32 ± 0.07	15.60 ± 0.40	4.66 ± 0.16	3.80 ± 0.23	125.5 ± 1.0	33.0 ± 2.0
MAC2	19.0	20 ± 5	4-11	5	1.35	1.38 ± 0.07	15.90 ± 0.40	5.08 ± 0.18	3.99 ± 0.25	107.8 ± 0.8	27.0 ± 1.7
MAC3	21.0	20 ± 5	4-11	5	1.40	1.30 ± 0.07	18.20 ± 0.40	4.42 ± 0.16	3.93 ± 0.25	247.4 ± 2.7	63.0 ± 4.1
MAC4	20.0	20 ± 5	4-11	5	1.40	1.25 ± 0.06	17.60 ± 0.40	4.72 ± 0.17	3.92 ± 0.25	375.9 ± 9.9	95.8 ± 6.5
RDO1	17.2	20 ± 5	4-11	5	1.35	1.45 ± 0.04	14.70 ± 0.30	4.66 ± 0.22	3.69 ± 0.23	30.1 ± 0.5	8.16 ± 0.52
RDO2	19.8	20 ± 5	4-11	12	1.35	1.47 ± 0.07	14.70 ± 0.50	5.02 ± 0.17	3.80 ± 0.25	25.1 ± 0.1	6.61 ± 0.43
RDO3	17.1	20 ± 5	4-11	5	1.45	1.34 ± 0.07	14.30 ± 0.30	4.81 ± 0.18	3.61 ± 0.21	17.2 ± 0.1	4.77 ± 0.28
RDO4	16.7	20 ± 5	4-11	7	1.45	1.30 ± 0.07	13.80 ± 0.50	4.66 ± 0.15	3.49 ± 0.23	16.9 ± 0.2	4.84 ± 0.32

Table A2. Result of OSL dating

A.3.1 Results and interpretation

For the Malcombe paleo-meander, OSL ages of 33.0 ± 2.0 ka and 27.0 ± 1.7 ka have been determined for Trench C, and 63.0 ± 4.1 ka and 95.8 ± 6.5 for Trench D. The parallel samples from Trench D have ages that are neither internally consistent nor do they agree with the ages determined for Trench C. The problem may be that in this trench samples have been taken from the very bottom of the exposed profile with poor stratigraphic control in this part of the profile. Most likely, older sediment from the bottom of the former channel was included during sampling and we consequently assume that the samples from Trench C are more likely to represent the filling of the oxbow lake. The

OSL ages (ca. 30 ka) correlate with the end of the middle Late Pleistocene, a period with relatively temperate climatic conditions in central Europe (cf. Preusser, 2004). The OSL ages for the Roche d'Or paleo-meander are 8.16 ± 0.52 ka and 6.61 ± 0.43 ka for Trench A, and 4.77 ± 0.28 ka and 4.84 ± 0.32 ka for Trench B. All ages indicate deposition during the Middle Holocene.

References:

Beaumont, C., Fullsack, P., and Hamilton J., 1992, Erosional control of active compressional orogens, *in* McClay, K.R. ed., Thrust Tectonics: London, Chapman & Hall, p. 1-18.

Becker, A., 2000, The Jura Mountains - an active foreland fold-and-thrust belt?: Tectonophysics, v. 321, p. 381-406.

Boenigk, W., 1983, Schwermineralanalyse: Stuttgart, Enke, p.158

Boenigk, W., 1987, Petrographische Untersuchungen juntertiärer und quartärer Sediments am linken Oberrhein, Jahresberichte und Mitteillungen des oberrheinischen geologischen Vereins, v. 69, p. 357-394.

Bonvalot, J., 1974, Les cailloutis de la Forêt de Chaux (Jura): leurs rapports avec les matériaux détritiques de Sundgau et du Nord de la Bresse [thesis], Université de Dijon, Dijon, p. 89.

Buck, W.R., Densmore, A.L., Friedrich, A.M., Hovius, N., Kirby, E., Koons, P.O., Nagel, T.J., Schlunegger, F., Strecker, M., and von Blanckenburg, F., 2007, Group Report : Surface environmental effects on and of faulting, *in* Handy, M., Hirth, G. and Hovius, N., eds., Tectonic faults, agents of change on a dynamic earth: Dahlem workshop reports: Massachusetts, MIT press, p. 273-294.

Burbank, D.W., Leland J., Fielding E., Anderson R.S., Brozovic, N., Reid M.R., and Duncan C., 1996, Bedrock incision, rock uplift and threshold hillslopes in the western Himalaya: Nature, v. 379, p. 505-510.

Burkhard, M., 1990, Aspects of the large-scale Miocene deformation in the most external part of the Swiss Alps (Subalpine Molasse to Jura fold belt): Eclogae Geologicae Helvetiae, v. 83, p. 559-583.

Burkhard, M., and Sommaruga, A., 1998, Evolution of the western Swiss Molasse basin: Structural relations with the Alps and the Jura belt, *in* Mascle, A., Puigdefàbregas, C., Luterbacher, H. P., Fernàndez, M., eds., Cenozoic Foreland Basins of Western Europe: London, Geological Society Special Publications 134, p. 279-298.

Campy, M., 1984, Signification dynamique et climatique des formations et terrasses fluviatiles dans un environnement de moyenne montagne: Bulletin de l'Association française pour l'Etude du Quaternaire, v. 1, p. 87- 92.

Chauve, P., Enay, R., Fluck, P., and Sittler, C., 1980, L'Est de la France (Vosges, Fossé Rhénan, Bresse, Jura): Annales scientifiques de l'Université de Besançon, v. 4, p. 3-80.

Dèzes, P., Schmid, S.M., and Ziegler, P.A., 2004, Evolution of the European Cenozoic Rift System: interaction of the Alpine and Pyrenean orogens with their foreland lithosphere: Tectonophysics, v. 389, p. 1-33.

Dreyfuss, M., and Glangeaud, L., 1950, La vallée du Doubs et l'évolution morphotectonique de la région bisontine: Annales scientifiques de l'Université de Besançon, v. 5, p. 2-16.

Dreyfuss, M., and Kuntz, G., 1969, Carte géologique France, feuille Besancon, XXXII-23, Bureau de Recherches Géologiques et Minières (BRGM), scale 1 :50000, 1 sheet, 12 p. text.

Fejfar, O., Heinrich, W.-D., and Lindsay, E.H., 1998, Updating the Neogene rodent biochronology in Europe: Mededelingen Nederlands Instituut voor Toegepaste Geowetenschappen, v. 60, p. 533-554.

Giamboni, M., Ustaszewski, K., Schmid, S.M., Schumacher, M.E., and Wetzel, A., 2004, Plio-Pleistocene transpressional reactivation of Paleozoic and Paleogene structures in the Rhine-Bresse Transform Zone (northern Switzerland and eastern France): International Journal of Earth Sciences, v. 93, p. 207–223.

Hagedorn, E.M., 2005, Sedimentpetrographie und Lithofazies der jungtertiären und quartären Sedimente im Oberrheingebiet: unpublished PhD thesis, University of Cologne, p. 310

Kälin, D., 1997, Litho- und Biostratigraphie der mittel- bis obermiozänen Bois de Raube-Formation (Nordwest-schweiz): Eclogae Geologicae Helvetiae, v. 90, p. 97-114,

Koons, P.O., Zeitler, P.K., Chamberlain, C.P., Craw, D. and Melzer, A.S., 2002, Mechanical links between river erosion and metamorphism in Nanga Parbat, Pakistan Himalaya: American Journal of Science, v. 302, p.749-773.

Kulig, G. 2005, Erstellung einer Auswertesoftware zur Altersbestimmung mittels Lumineszenzverfahren unter spezieller Berücksichtigung des Einflusses radioaktiver Ungleichgewichte in der 238U-Zerfallsreihe, unpublished BSc thesis, Freiberg.

Laubscher, H., 1961, Die Fernschubhypothese der Jurafaltung: Eclogae Geologicae Helvetiae, v. 54, p. 222-282.
Laubscher, 1972, Some overall aspects of Jura dynamics: American Journal of Science, v. 272, p. 293-304.
Liniger, H., and Hofmann, P., 1965, Das Alter der Sundgauschotter westlich von Basel: Eclogae Geologicae Helvetiae, v. 58, p. 215-230.
Locke, M.H. and Barker, R.D., 1995, Least-Squares Deconvolution of Apparent Resistivity Pseudosections: Geophysics, v. 60, N. 6, p. 1682-1690.
Madritsch, H., Schmid, S.M., and Fabbri, O., 2008, Interactions between thin- and thick-skinned tectonics at the northwestern front of the Jura fold-and-thrust-belt (Eastern France): Tectonics (in press).
Montgomery, D.R., and Stolar, D.B., 2006, Reconsidering Himalayan river anticlines: Geomorphology, v. 82, p. 4-15.
Niviere, B., and Winter, T., 2000, Pleistocene northwards fold propagation of the Jura within the southern Upper Rhine Graben: seismotectonic implications: Global and Planetary Change, v. 27, p. 263-288.
Pinter, N., and Brandon M.T., 1997, How erosion builds mountains: Scientific American, v. 276, p. 74-79.
Petit, C., Campy, M., Chaline, J., and Bonvalot, J., 1996, Major palaeohydrographic changes in Alpine foreland during the Pliocene-Pleistocene: Boreas, v. 25, p. 131-143.
Preusser, F. 2004, Towards a chronology of the Late Pleistocene in the northern Alpine Foreland. Boreas v. 33, p. 195-210.
Simpson, G., 2004, Role of river incision in enhancing deformation: Geology, v. 32, p. 341-344.
Simpson, G., and Schlunegger, F., 2003, Topographic evolution and morphology of surfaces evolving in response to coupled fluvial and hillslope sediment transport: Journal of Geophysical Research, v. 108, ETG 7-1 - 7-16.
Théobald, N., Schweitzer, M., and Hudeley, H., 1976, Carte Géologique de la France à 1/50 000 Mulhouse, feuille XXXVII-XXXVIII-20: Orléans, Ministère de l'industrie et de la recherche, Service Géologique National.
Ustaszewski, K., and Schmid, S.M., 2006, Control of preexisting faults on geometry and kinematics in the northernmost part of the Jura fold-and-thrust belt: Tectonics 25/5, TC5003doi:10.1029/ 2005TC001915.
Wintle, A.G. and Murray, A.S. 2006, A review of quartz optically stimulated luminescence characteristics and their relevance in single-aliquot regeneration dating protocols. Radiation Measurements v. 41, p. 369-391.
Zeilinger, G., Schlunegger, F., and Simpson, G., 2005, The Oxaya anticline (northern Chile): a buckle enhanced by river incision?: Terra Nova, v. 17, p. 368-375.

Chapter 5

Feedbacks between uplift, erosion and active deformation: Geomorphic constraints from the frontal Jura fold-and-thrust belt (Eastern France)

by

Herfried Madritsch, Olivier Fabbri, Eva-Maria Hagedorn,

Frank Preusser, Stefan M. Schmid and Peter A. Ziegler

In preparation

Abstract:

A regional tectono-geomorphic analysis indicates Pliocene to recent relative rock uplift of the outer most segment of the Jura fold-and-thrust belt in Eastern France. The uplifted area coincides with the Eocene-Oligocene intra-continental Rhine-Bresse Transfer Zone (RBTZ). Results of regional comparative heavy mineral analyses allow reconstructing the paleo-topography of the partly eroded Middle Pliocene Sundgau-Forêt de Chaux (SFC) gravels. Elevated erosional remnants of this gravel sheet yield minimum regional Pliocene-Pleistocene uplift rates of 0.05 +/- 0.02 mm/yr.

The effects of this uplift are of tectonic nature as is inferred from the Latest Pliocene to Pleistocene evolution of the Ognon and Doubs drainage basins, which parallel the axis of the uplifting area to the north and south, respectively. Subsidence and sediment aggradation characterize the Ognon Valley to the north. The Ognon River shifted laterally N-ward in response to uplift of the southward adjacent area. The Doubs River in the south degraded the Sundgau-Forêt de Chaux gravel sheet and deeply incised into the bedrock at the same time. Enhanced incision of the Doubs into the uplifted region also triggered localized deformation along fold structures that previously initiated during the formation of the thin-skinned Jura fold-and-thrust belt. At present this erosion-driven deformation takes place synchronously with thick-skinned tectonics associated with the inversion of the Rhine-Bresse Transfer Zone. This suggests local decoupling between seismogenic faulting in the basement and erosion-triggered deformation of the Mesozoic cover.

Keywords: *neotectonics, rock uplift, incision, alluvial terraces, Jura fold-and-thrust belt*

5.1. Introduction and objectives of this study

The region of the Franche-Comté in Eastern France is located at the boundary of the northwestern deformation front of the Alpine orogen and its foreland. Here the Neogene Jura fold-and-thrust belt encroached onto the Eo-Oligocene fault system of the Rhine-Bresse Transfer Zone, a segment of the

1970; Contini and Theobald, 1974; Bergerat and Chorowicz, 1981; Lacombe et al., 1993; Martin and Mercier, 1996; Madritsch et al., 2008 in press).

At present this area is characterized by low to intermediate seismicity, being significantly lower as compared to that of the adjacent Southern Upper Rhine Graben (Figure 2) (Baer et al., 2007; RéNaSS, 2007). Consequently, the present day stress field of the area is poorly defined (Kastrup et al., 2004). Nevertheless, the region is prone to seismic hazard as evidenced by the M_L 4.8 Rigney earthquake of 23rd February 2004 (Baer et al., 2005), one of the strongest recent seismic events in the wider area. Moreover, the famous 1356 Basel earthquake, which represents one of the strongest historically recorded seismic events throughout central Western Europe (Mayer-Rosa and Cadiot, 1979), was possibly triggered by an ENE-WSW striking basement fault that reactivated the Late Paleozoic Burgundy Trough System that underlies the Cenozoic Rhine-Bresse Transfer Zone (Meyer et al., 1994; Ustaszewski and Schmid, 2007).

Middle to short term geodetic surveying indicates very slow vertical and horizontal recent displacement rates throughout the northwestern Alpine foreland, close to the margin of error inherent to current GPS technology (Tesauro et al., 2005). Despite this, there are indications for ongoing deformation within the area provided by pioneering studies in tectonic geomorphology (Dreyfuss and Glangeaud, 1950; Liniger, 1967; Theobald et al., 1977; Campy, 1984). More ecent studies applying modern techniques based on high resolution digital elevation models are so far restricted to areas in the southern and northern parts of the Upper Rhine Graben area (Nivière and Marquis, 2000; Giamboni et al., 2004b; Peters and van Balen, 2007) but are yet lacking the Rhine-Bresse Transfer Zone proper.

This study aims at a better understanding of the Pliocene to recent tectonic evolution of the region of the central Rhine-Bresse Transfer Zone. We consider two different geomorphic markers that both record slow and possibly partly aseismic deformation that occurred over long timescales. A first marker is provided by the paleo-topographic reconstruction of the Middle Pliocene Sundgau - Forêt de Chaux gravel surface. These gravels were shed by a braided river system that was part of the Aare-Doubs drainage system (Liniger, 1967; Bonvalot, 1974; Petit et al., 1996; Ziegler and Fraefel, 2008 submitted) and presumably post-date the formation of the thin-skinned Jura fold-and-thrust belt (Becker, 2000; Ustaszewski and Schmid, 2007). Comparing the Plio-Pleistocene valley evolution related to the Ognon and Doubs drainage areas, based on the sedimentological and geomorphic record, provides a second geomorphic marker. Our investigations build upon a new tectonic map of the area (Figure 1) (Madritsch et al., 2008 in press), combined with a revised map of alluvial sediments based on published geological maps, our own field observations and analyses of digital elevation models. Furthermore, we implemented a comparative heavy mineral analysis on a regional scale in order to constrain the provenance of river deposits at key locations.

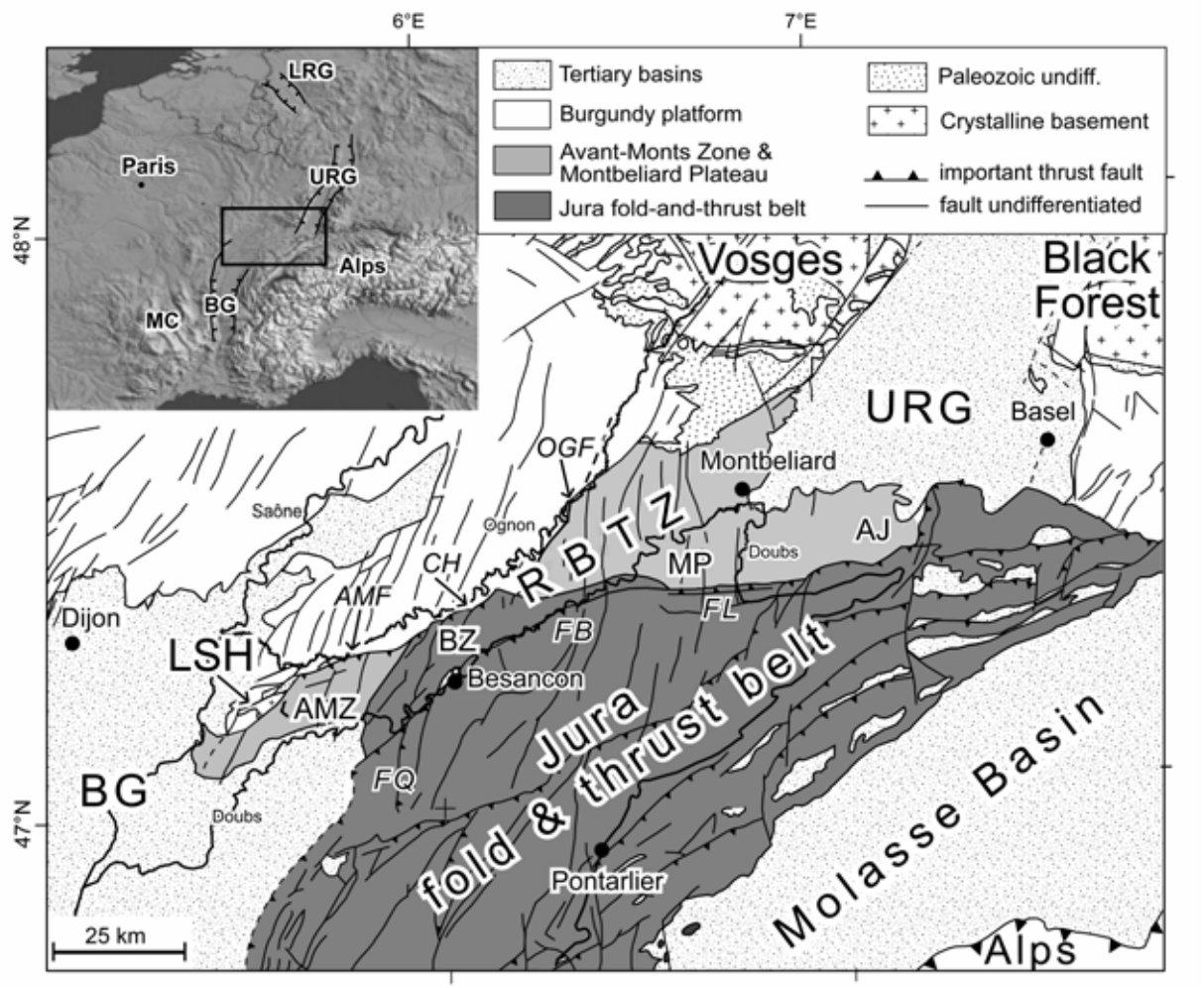

Figure 1: Tectonic setting of the study area located at the northwestern front of the Jura fold-and-thrust belt that coincides with intracontinental Rhine-Bresse Transfer Zone. Tectonic units according to Madritsch et al. (2008 in press). AMF: Avant-Monts Zone; AMZ: Avant-Monts Zone; BG: Bresse Graben; BZ: Besançon Zone; CH: Chailluz Thrust; FB: Faisceau Bisontin; FL: Faisceau du Lomont; FQ: Faisceau de Quingey; LRG: Lower Rhine Graben; LSH: La Serre Horst; MC: Massif Central; MP: Montbéliard Plateau; RBTZ: Rhine-Bresse Transfer Zone; URG: Upper Rhine Graben.

5.2. Tectonic Setting

The area of investigation is characterized by three major tectonic elements: i) the Permo-Carboniferous Burgundy Trough, ii) the Eo-Oligocene Rhine-Bresse Transfer Zone (RBTZ), which is superimposed on the Burgundy Trough and forms part of the European Cenozoic Rift System (ECRIS), and iii) the Neogene Jura fold-and-thrust belt (Figure 1).

The roughly ENE-WSW striking Permo-Carboniferous Burgundy Trough System is oriented parallel to the RBTZ. It extends over a distance of about 300 km from the northern parts of the Massif Central, through the Bresse Graben into the area of the RBTZ, and further to Basel where it links with

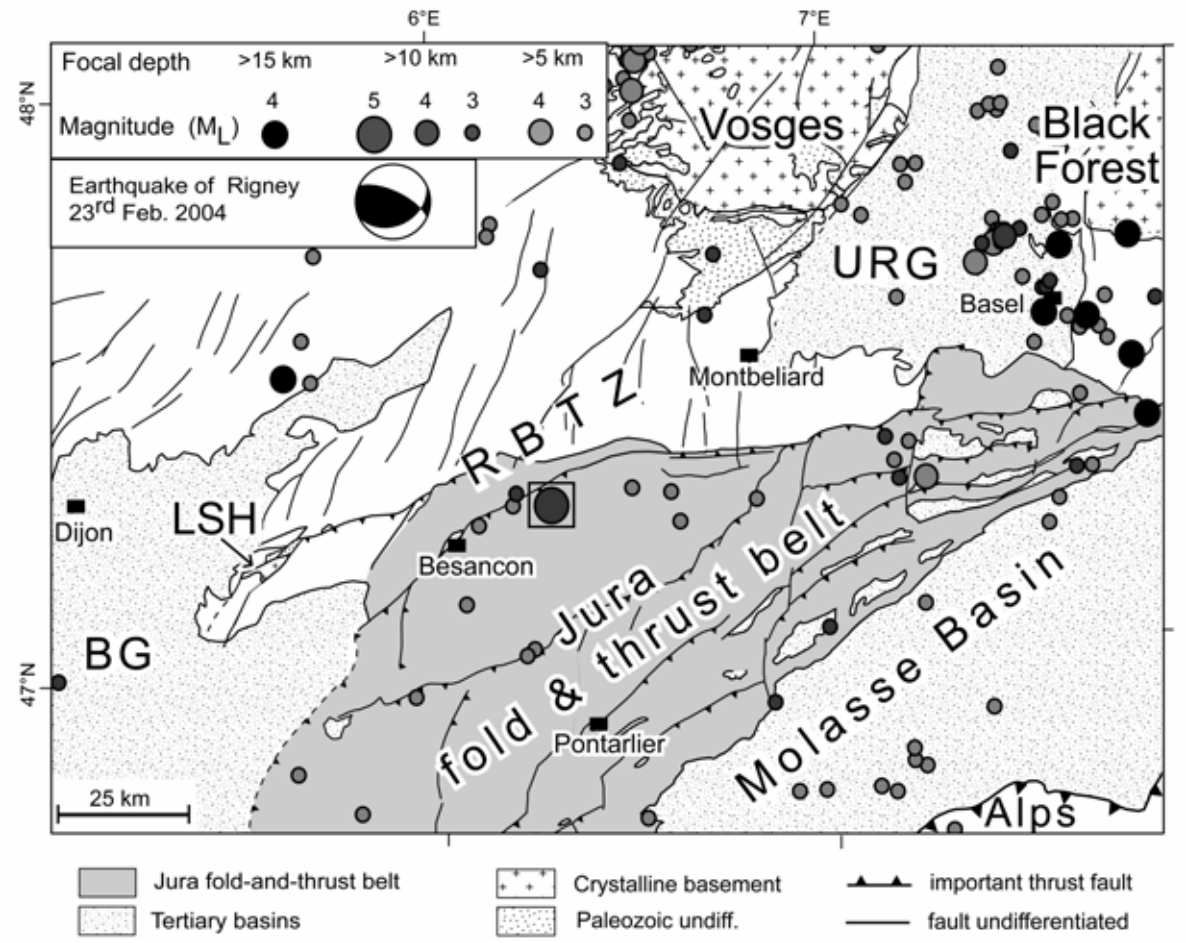

Figure 2: Epicenters and intensity of instrumentally recorded earthquakes (M_L >3) in the vicinity of the study area. (Source: (RéNaSS, 2007). Focal mechanism based on full waveform moment tensor inversion of the earthquake of Rigney northeast of Besançon from Baer et al. (2005). BG: Bresse Graben; LSH: La Serre Horst; URG: Upper Rhine Graben.

the Permo-Carboniferous graben system of Northern Switzerland and Southern Germany (Boigk and Schöneich, 1970; Debrand-Passard and Courbouleix, 1984; Schumacher, 2002; Ziegler et al., 2004).

In the area of the RBTZ the Burgundy Trough is buried beneath Mesozoic sediments except for the narrow La Serre Horst, located at the intersection of the RBTZ and the Bresse Graben, exposing Palaeozoic sediments (Coromina and Fabbri, 2004; Madritsch et al., 2008, submitted) (LSH in Figure 1). Deep wells drilled in the area of the RBTZ penetrated up to 800 m of Permo-Carboniferous sediments beneath Mesozoic series (Chauve et al., 1983). The Burgundy Trough System forms part of the complex dextral-transtensional trans-European shear system that was active during latest Carboniferous and Early Permian times and controlled the demise of the Variscan Orogen (Matte, 1986; Ziegler, 1990).

The ECRIS developed in Eo-Oligocene times and dissects the European continent over a distance of approximately 1100 km from the Dutch North Sea coast to the western Mediterranean (Ziegler,

1992). The RBTZ forms an important element of this rift system and connects the Upper Rhine Graben with the Bresse Graben (Laubscher, 1970; Illies, 1972; Contini and Theobald, 1974; Bergerat and Chorowicz, 1981). During the main phase of rifting that started in Middle to Late Eocene times (Berger et al., 2005; Hinsken et al., 2007) the RBTZ formed by extensional to sinistrally transtensive reactivation of the Late Permo-Carboniferous Burgundy Trough System (Lacombe et al., 1993; Schumacher, 2002; Madritsch et al., 2008 in press). This reactivation also contributed to the exhumation of the La Serre Horst.

During the Middle Miocene (Burdigalian) the Vosges-Black Forest Arch was uplifted, together with the southern parts of the Upper Rhine Graben. Very likely this uplift occurred in response to lithospheric folding, reflecting the build-up of collision related compressional stresses in the Alpine foreland (Ziegler et al., 2002; Dèzes et al., 2004). This hypothesis is supported by the configuration of the Moho discontinuity that forms a large anticlinal structure, which extends from the northern parts of the Massif Central towards the Bohemian Massif and which culminates beneath the Southern Upper Rhine Graben (Dèzes et al., 2004; Bourgeois et al., 2007). The RBTZ, located on the SE flank of this structure, was also uplifted during the Middle Miocene.

To the south the RBTZ is bordered, and partially overridden, by the thin-skinned Neogene Jura fold-and-thrust belt, which is considered as a text book example for a thin-skinned foreland fold-and-thrust belt (see review in Sommaruga, 1997). Its development is widely accepted as resulting from "distant push" (Laubscher, 1961), induced by Late Miocene crustal shortening and nappe stacking in the external crystalline massif of the Central Alps. Large scale thin-skinned decoupling (décollement) of the Mesozoic sedimentary cover along a sole thrust in Middle to Late Triassic evaporites enabled the propagation of the thrust front towards the distal foreland in the northwest (Laubscher, 1972; Burkhard, 1990; Schmid et al., 1996; Burkhard and Sommaruga, 1998). The Besançon Zone (Figure 1) represents the most external segment of this fold-and-thrust belt that encroached onto the preexisting fault systems of the RBTZ and the underlying Burgundy Trough (Madritsch et al., 2008 in press), the outermost Chailluz Thrust (CH in Figure 1, 3) forming the northern boundary of this thin-skinned Neogene fold-and-thrust belt. Toward the SE the weakly deformed Besançon Zone is delimited by the Faisceau Bisontin, an approximately 100km long closely spaced bundle of ENE-WSW striking folds and thrust delimiting the front of the more strongly deformed part of the Neogene Jura fold-and-thrust belt (Chauve et al., 1980; Dreyfuss and Glangeaud, 1950).

Development of the thin-skinned Jura fold-and-thrust belt is generally considered as a relatively short-lived event, spanning Late Miocene to Early Pliocene times (10.5 - 4.2 Ma according to Ustaszewski and Schmid, 2006). The occurrence of deformation post dating 4.2 Ma, i.e. the onset of deposition of the Middle Pliocene Sundgau - Forêt de Chaux gravels, is interpreted in controversial ways. While some authors proposed that the thin-skinned propagation of the Jura fold-and-thrust belt, rooted in the Alps, continued into Pleistocene times (Nivière and Winter, 2000), others infer a switch towards thick-skinned tectonics involving shortening of the crystalline basement underneath the

detached Mesozoic cover sediments in the foreland of the orogen (Meyer et al., 1994; Giamboni et al., 2004a; Rotstein and Schaming, 2004; Ustaszewski and Schmid, 2007). In the Avant-Monts Zone, located to the west of the Besançon Zone, thick-skinned deformation is documented by reflection-seismic data (Madritsch et al., 2008 in press). The northern boundary of this tectonic unit is formed by the Avant-Mont Fault, a steeply south dipping reverse fault that is rooted in the basement and most likely formed by inversion of former normal fault of Paleogene to Paleozoic age. Thick-skinned tectonics have been interpreted to result in a partial compressive to dextral transpressive reactivation of the RBTZ (Giamboni et al., 2004a; Ustaszewski and Schmid, 2007; Madritsch et al., 2008 in press). Most likely this type of deformation post-dates the main stage of thin-skinned deformation and the development of the Jura fold-and-thrust belt proper and thus continued beyond 4.2. Ma.

5.3. Geomorphic setting and drainage system evolution

The digital elevation model of Franche Comtè (horizontal resolution 50m) (Figure 3) shows that the topographic relief is closely related to tectonic structures. The main structural and morphological features of the region strike ENE-WSW. The fault-related folds along the Avant-Monts Fault and of the Faisceaux Lomont, Bisontin and Quingey form distinct ridges. The modern drainage pattern of the region roughly parallels the ENE-WSW striking structural trend and has undergone a complex Neogene evolution that was controlled by tectonic and climatic events (Liniger, 1966; Petit et al., 1996; Giamboni et al., 2004b; Berger et al., 2005; Ziegler and Fraefel, 2008 submitted).

In the Late Miocene, i.e. prior to the formation of Jura fold-and-thrust belt, the RBTZ was characterized by a south directed drainage system that developed in response to the Burdigalian uplift and exhumation of the Vosges Mountains (Ziegler and Dèzes, 2007; Ziegler and Fraefel, 2008 submitted) (Figure 4a). This drainage system controlled the deposition of Bois de Raube formation of the Ajoie area (Figure 1) and the central Jura Mountains derived from the Vosges (Kälin, 1997). Remnants of fluviatile deposits possibly related to this early drainage system occur only very locally in the area of the RBTZ.

The Aare-Doubs drainage system developed only after the main deformation phase of the thin-skinned Jura fold-and-thrust belt (Figure 4b) (Liniger, 1967; Bonvalot, 1974; Petit et al., 1996; Giamboni et al., 2004a; Ziegler and Fraefel, 2008 submitted). During this stage the Paleo-Aare River, draining the Molasse basin, flowed along the deformation front of the Jura fold-and-thrust belt westward and drained into the Bresse Graben and ultimately the Mediterranean (Figure 4b). As such the course of the Paleo-Aare paralleled the lower reach of the present day Doubs River. It is this Middle Pliocene Aare-Doubs drainage system that controlled the deposition of the Sundgau- Forêt de

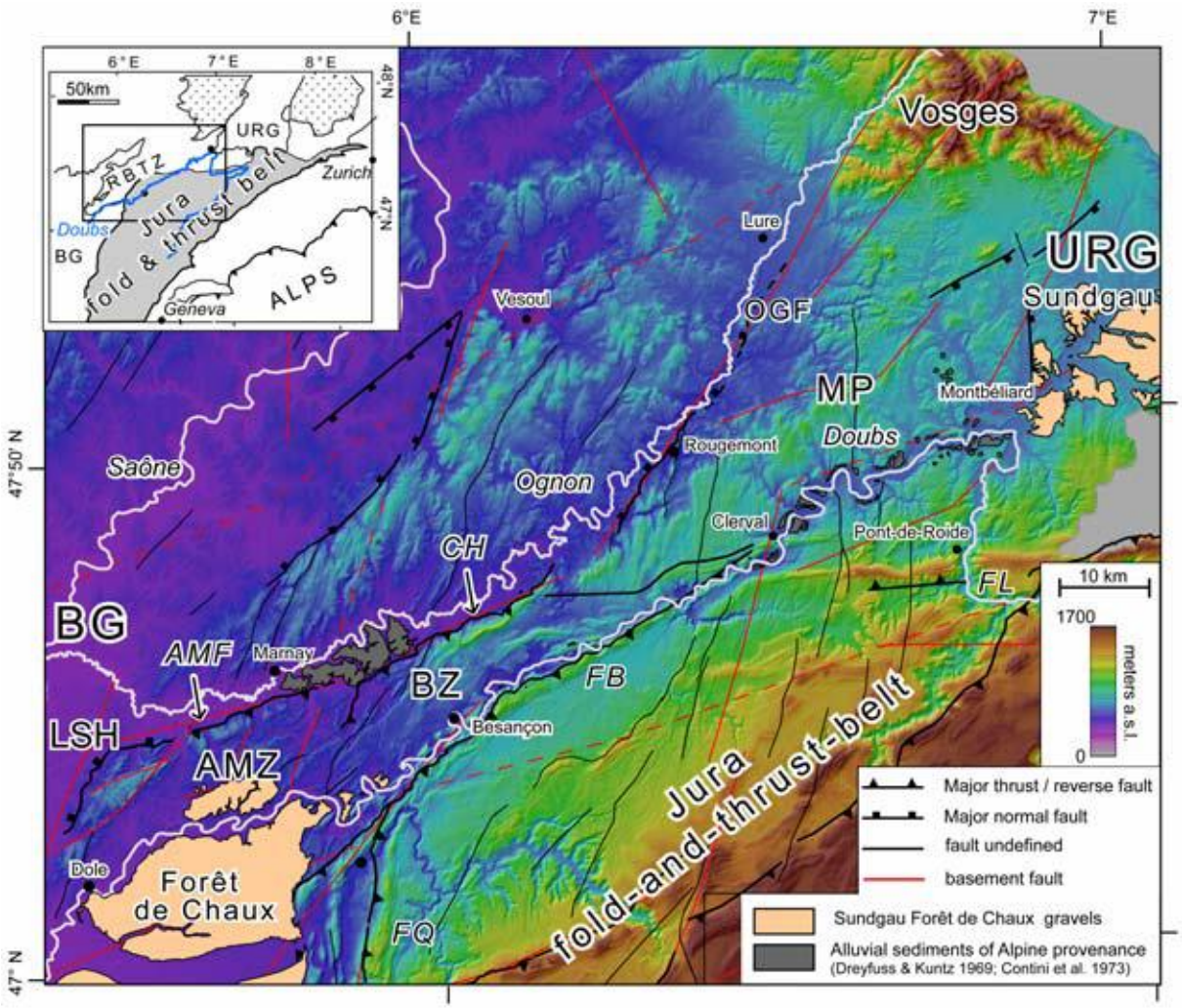

Figure 3: Shaded digital elevation model (50m horizontal resolution) of the study area showing major faults and the two drainage basins of the Doubs and Ognon River that parallel the ENE-WSW striking structural trend of the study area. Note that the Middle Pliocene Sundgau – Forêt de Chaux gravels are extensively eroded in the study area. AMF: Avant-Monts Fault; AMZ: Avant-Monts Zone; BG: Bresse Graben; BZ: Bresse Graben; CH: Chailluz Thrust; FB: Faisceau Bisontin; FL: Faisceau du Lomont; FQ: Faisceau de Quingey; LSH: La Serre Horst; MP: Montbéliard Plateau; URG: Upper Rhine Graben.

Chaux (SFC) Gravels (Figure 5a). These deposits feature characteristic pebble and heavy mineral spectra of Alpine provenance (Liniger and Hofmann, 1965; Bonvalot, 1974; Hagedorn, 2004) and have a bio-stratigraphically constrained Middle Pliocene deposition age of 4.2-2.9 Ma. (Petit et al., 1996; Fejfar et al., 1998).

The course of the Paleo-Aare River only persisted until the early Pliocene (2.9 Ma) (Petit et al., 1996; Fejfar et al., 1998). Due to Pleistocene subsidence in the Rhine and Bresse Graben and/or due to shortening induced relative uplift of the RBTZ area the Paleo- Aare was affected by head ward erosion

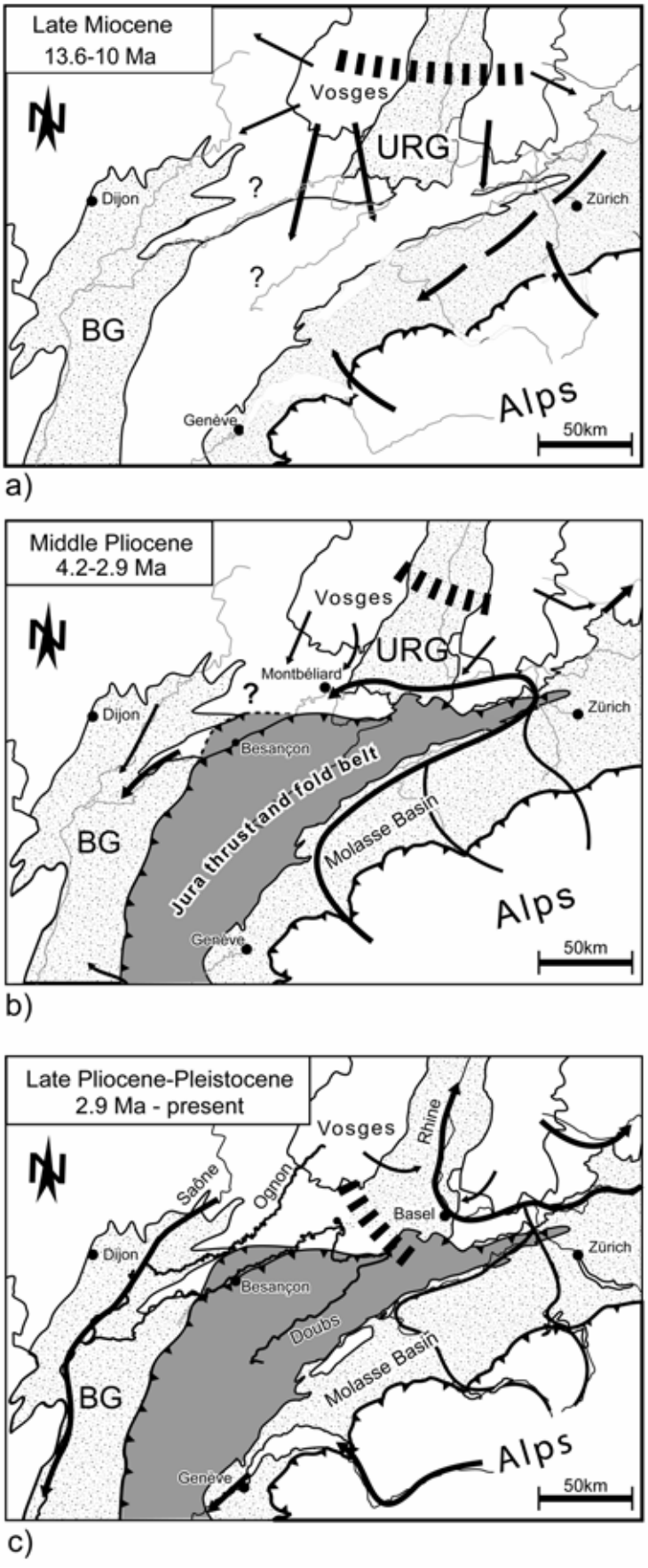

Figure 4: Major drainage system changes in the northwestern Alpine foreland (modified from Giamboni et al. 2004).

4a) The Late Miocene drainage system is north-south orientated. Presumably alluvial sediments from the Vosges Mountains were shed into the area of the future Jura Mountains.

4b) The Middle Pliocene Aare-Doubs drainage system is characterized by the Paleo-Aare that flowed from the Molasse basin along the northern and northwestern rim of the Jura fold-and-thrust belt (course marked by the thick black line) and it controlled the deposition of the Sundgau - Forêt de Chaux Gravels (Figure 3, 5).

4c) Late Pliocene to recent drainage system. The Paleo-Aare was rerouted towards the Upper Rhine Graben, its former course being occupied the lower reach of the Doubs River. The thick dashed line marks the major drainage divide between North Sea and the Mediterranean Sea. BG: Bresse Graben; URG: Upper Rhine Graben.

a)

b)

Figure 5 a) The Sundgau-Forêt de Chaux Gravels that were deposited by the Paleo-Aare in Middle Pliocene times and are preserved at the fringes of southern Upper Rhine Graben and northern Bresse Graben (locality 8 in Figure 10, Table 1).

b) Remnants of Miocene and / or Pliocene fluvial gravels that are found in karst fissures or reworked within colluvial and alluvial deposits throughout the Rhine-Bresse Transfer Zone (locality 3 in Figure 10, Table 1).

towards the east and was eventually captured by the Proto-Rhine river that flowed northward through the Rhine Graben into the North Sea (Liniger, 1966; Petit et al., 1996; Giamboni et al., 2004a; Ustaszewski & Schmid 2007; Ziegler and Fraefel, 2008 submitted). Due to this Late Pliocene drainage system reorganization the area of the RBTZ was permanently isolated from Alpine sediment supply.

The deposits of the Middle Pliocene Paleo-Aare (4.2-2.9 Ma) are only well preserved in the Sundgau region at the southern end of the Upper Rhine Graben and again over 100km further to the west in the Forêt de Chaux area adjacent to the Bresse Graben (Figure 1, 3). The SFC gravels form a more or less continuous depositional surface only in those two areas. These gravels rest with an erosional unconformity on Mesozoic or Tertiary strata (Liniger, 1967). In the Sundgau area the gravel sheet reaches a thickness of 30 meters (Giamboni et al., 2004b) while in the Forêt de Chaux thicknesses of up to 65 meters are reported (Chauve et al., 1979). Sedimentological features of the Sundgau Gravels imply that they have been deposited by a low gradient braided river system characterized by low sinuosity shifting channels (Giamboni et al., 2004b). These observations indicate that the SFC Gravels were deposited on a broad and gentle inclined peneplane and were unable to bury

a paleorelief exceeding some 30-65 meters. The fact that the SFC Gravels were deposited during a closely constrained time span (4.2 - 2.9 Ma) and on a more or less flat surface (+/- 65 meters) makes them an excellent marker horizon that permits to reconstruct the Middle Pliocene paleo-topography and that records possible late-stage deformations (Giamboni et al., 2004a).

In the study area, however, located between the Sundgau and Forêt de Chaux areas, no intact SFC gravel deposits are preserved (Figure 3). Only isolated remnants of fluvial deposits are reported throughout the area, particularly along the present day valley of the Doubs River (Dreyfuss and Glangeaud, 1950; Goguel and Dreyfuss, 1965; Dreyfuss and Kuntz, 1969; Dreyfuss and Théobald, 1972; Contini et al., 1973; Campy, 1984). These remnants consist of well-rounded crystalline pebbles, which are commonly found in karst fissures and caves, as colluvial slope deposits, and, within terraces of the Doubs River (Figure 5b). The paleo-hydrographic considerations outlined above (Figure 4) suggest two possible sources for these remnants: the Middle Pliocene SFC Gravels or the Late Miocene Bois de Raube formation.

The present day drainage system of the Rhine-Bresse Transfer Zone (Figure 3, 4c) evolved after the Paleo-Aare was rerouted towards the Rhine-Graben from Late Pliocene times onwards and is characterized by two major drainage basins. The Ognon River drains the southwestern Vosges Mountains (Figure 3). Its course is divided into and upper and lower reach that are separated by the prominent NE-SW striking Ognon Normal Fault (Ruhland, 1959; Theobald et al., 1977) (OGF in Figure 1, 3). The lower reach of the Ognon Valley can further be subdivided into two segments. A high sinuosity river and a distinctive succession of alluvial terraces characterize an upper valley segment that parallels the Ognon Normal Fault. In the second and lower segment the valley widens and the river takes a more westerly course, paralleling the front of the thin-skinned Besançon Zone formed by the Chailluz Thrust and the basement-rooted Avant-Monts Fault (Madritsch et al., 2008 in press). Northwest of the La Serre Horst the Ognon flows into the Saône River (Figure 3).

The Doubs River drains large parts of the Jura Mountains (Figs. inset 3, 4c). Its lower reach leaves the fold-and-thrust belt 20km south of the city of Monbéliard via the distinct Pont-de-Roide water gap (Figure 3). Near Montbéliard the Doubs bends sharply W-ward and cuts through the autochthonous Mesozoic succession of the Montbéliard Plateau. At the Clerval water gap the river re-enters the fold-and-thrust belt (Figure 3). From this point onward the river flows through the Besançon Zone parallel to the deformation front of the Faisceau Bisontin. Along this segment the river maintains a fairly high sinuosity, is deeply incised into bedrock and has carved out a narrow up to 350 m deep canyon. Strath terraces in the form of spectacular paleo-meanders result from this incision (Dreyfuss and Glangeaud, 1950; Chauve et al., 1980; Madritsch et al., 2008 submitted). After leaving the thin-skinned fold-and-thrust belt downstream from Besançon the valley of the river Doubs widens. The Doubs finally flows into the Saône 30km southwest of the city of Dole (Figure 3). As these drainage basins developed in different tectonic settings, reconstruction of their Plio-Pleistocene morphologic evolution may reveal potential controlling tectonic processes.

5.4. Methodology

5.4.1 Terrace mapping and digital elevation model analysis

In order to develop a robust and consistent database of Plio-Pleistocene deposits covering the entire study area the terraces along the lower reaches of the Rivers Ognon and Doubs were remapped. This remapping is based on compilation and correlation of published geological maps and subsurface information (Goguel and Dreyfuss, 1965; Dreyfuss and Kuntz, 1969; Dreyfuss and Kuntz, 1970; Dreyfuss and Théobald, 1972; Contini et al., 1973; Chauve et al., 1979; Chauve et al., 1983), own field observations and an analysis of the digital elevation model of the Franche Comté (horizontal resolution 50m) using ArcGIS software. Terraces were mapped in the field on the basis of 1:25000 topographic maps.

Sedimentological investigations were mostly restricted to surface observations (size and lithology of fluvial pebbles). However, railroad construction opened new large-scale outcrops especially along the lower Ognon Valley. This permitted to study the lithofacies architecture of the alluvial deposits.

Slope gradient analyses of the digital elevation data were carried out to further enhance the results of field mapping. A slope of 0-2° was attributed to unaltered terrace surfaces. Alluvial surfaces with higher inclinations were regarded as terrace bodies that were degraded by surface processes and soil creep. Such degraded alluvial surfaces were not further considered as geomorphic markers of former riverbed elevations. Terraces considered juvenile were projected orthogonally onto the course of the river and displayed as longitudinal river profiles extracted from topographic maps.

In an attempt to better characterize the observed valley morphology we applied calculation of geomorphic indices from the digital elevation model. The Valley-Width vs. Valley-Height ratio (Vf) (Bull and McFadden, 1977) was used to quantify the incision intensity. It is expressed as:

$$V_f = 2V_{fw} / ((E_{ld}-E_{sc}) + (E_{rd}-E_{sc}))$$

where V_{fw} is the width of the valley floor, E_{sc} is the elevation of the valley floor and E_{ld} and E_{rd} are the elevations of the left and right valley divides respectively. Low V_f values indicate strong incision, while high values yield broad valleys.

5.4.2. Heavy mineral analysis

Samples for heavy mineral analyses were collected at 19 key locations. These include the Sundgau and Forêt de Chaux gravel surfaces as such, the remnants of fluvial deposits preserved along theDoubs Valley of yet unknown origin and alluvial sediments of the Ognon River (Table 1). The latter presently drains the crystalline Vosges Mountains and its foothills, consisting of Devonian to Late

Triassic sediments. Its deposits are therefore representative for a provenance similar to that of the Late Miocene Bois de Raube Formation (see Figure 4a and 4c).

Heavy mineral analyses were carried out following the guidelines by Boenigk (1983) and Hagedorn (2004). The grain size fraction between 64-500 µm was obtained from the dissolved samples by wet sieving. Density separation was carried out manually using separatory funnels and Bromoform (density 2.83 g/cm3) as separation liquid. Meltmount (refraction index: 1.662) was used to embed the heavy minerals onto thin sections. Quantitative heavy mineral counting using a polarization microscope was performed according to the line count method (analyst: Dr. E.-M. Hagedorn). A minimum of 100 grains per sample were counted.

Due to high content in organic matter and carbonate minerals, as well as the occurrence of Fe-hydroxide crusts, some samples were treated hydro-chemically before heavy mineral separation (Table 1). Hydrogen peroxide (H_2O_2) was used to destroy organic matter and clay minerals and to disintegrate the samples prior to sieving. In addition, some samples were cooked with HCl acid (conc.: 25%) to dissolve carbonate minerals and Fe-hydroxide crust. Samples showing very high amounts of opaque minerals were separated using an automatic magnetic separation device. Possible effects of hydro-chemical treatment and magnetic separation on the counting results were crosschecked with non treated aliquots of the same sample.

5.5. Results

5.5.1. Terrace systems and morphology of the lower Ognon and Doubs Valley

5.5.1.2 The Ognon Valley

The results of the revised terrace mapping from the Ognon Valley are shown in Figure 6. Up to 5 different terrace levels, excluding the one that forms the present-day flood plain, are distinguished on the basis of their elevation above the active channel. Due to the lack of sufficiently dense age information no temporal correlation of these terrace levels along the river could be attempted during this study (Figure 7). Hence, we only examine the spatial distribution of terraces along the longitudinal river profile, which yields information on its incision history. These observations are complemented by Valley-Height vs. Valley-Width ratios (Vf) that were calculated at roughly 10 km intervals along the valley (Figure 7).

Figure 6: Map of alluvial terraces in the Rhine-Bresse Transfer Zone. AMF: Avant-Monts Fault; AMZ: Avant-Monts Zone; BZ: Besançon Zone; FB: Faisceau Bisontin; FL: Faisceau Lomont; LSH: La Serre Horst; MP: Montbéliard Plateau.

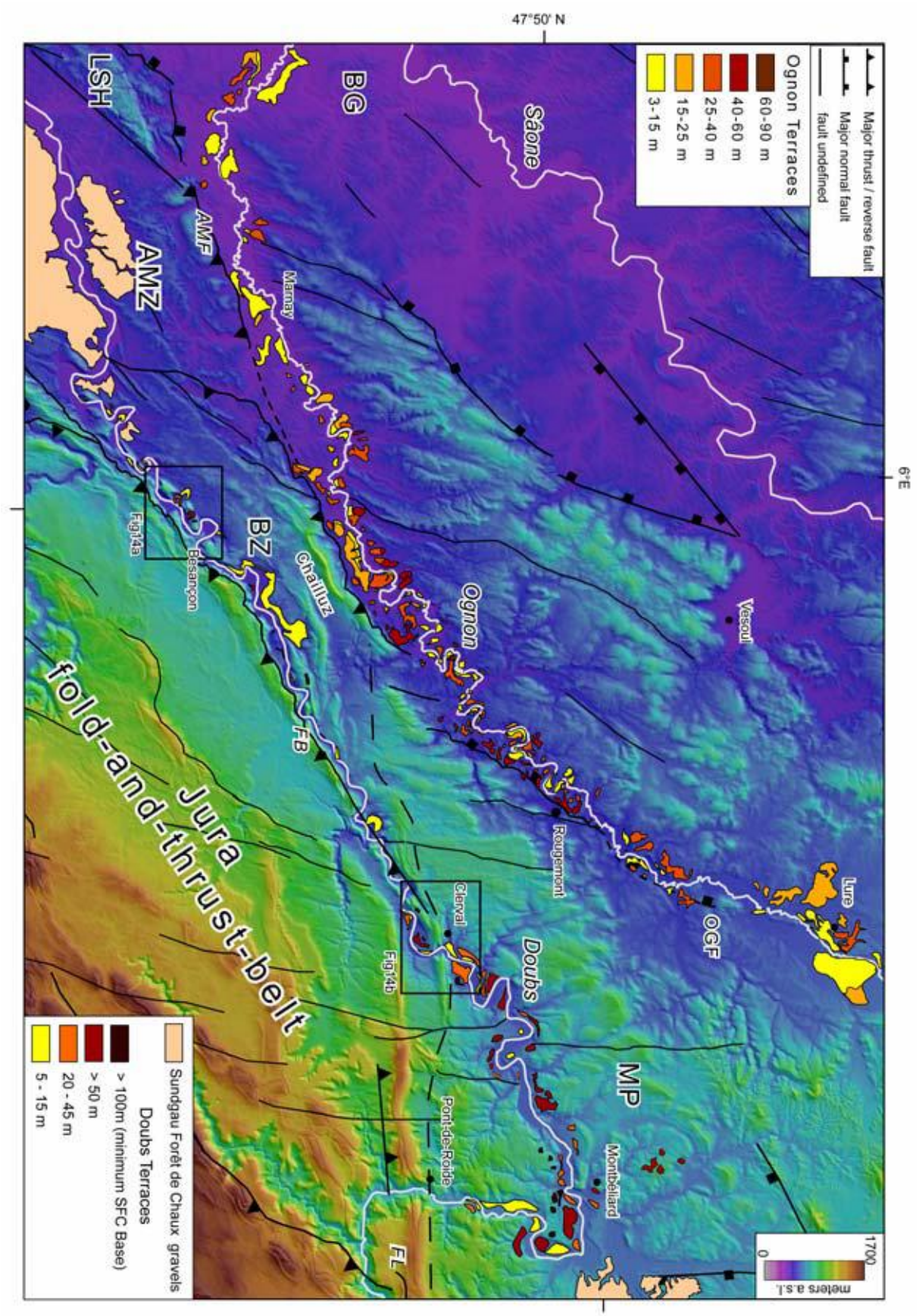
47°50' N
6°E
Major thrust / reverse fault
Major normal fault
fault undefined
Ognon Terraces
60-90 m
40-60 m
25-40 m
15-25 m
3-15 m
Sundgau Forêt de Chaux gravels
Doubs Terraces
> 100m (minimum SFC Base)
> 50 m
20 - 45 m
5 - 15 m
meters a.s.l.
1700
0
Jura fold-and-thrust-belt
LSH
AMZ
BG
BZ
AMF
FB
FL
OGF
MP
Saône
Ognon
Doubs
Mamay
Chailluz
Vesoul
Rougemont
Clerval
Pont-de-Roide
Montbéliard
Besançon
Lure
Fig14a
Fig14b

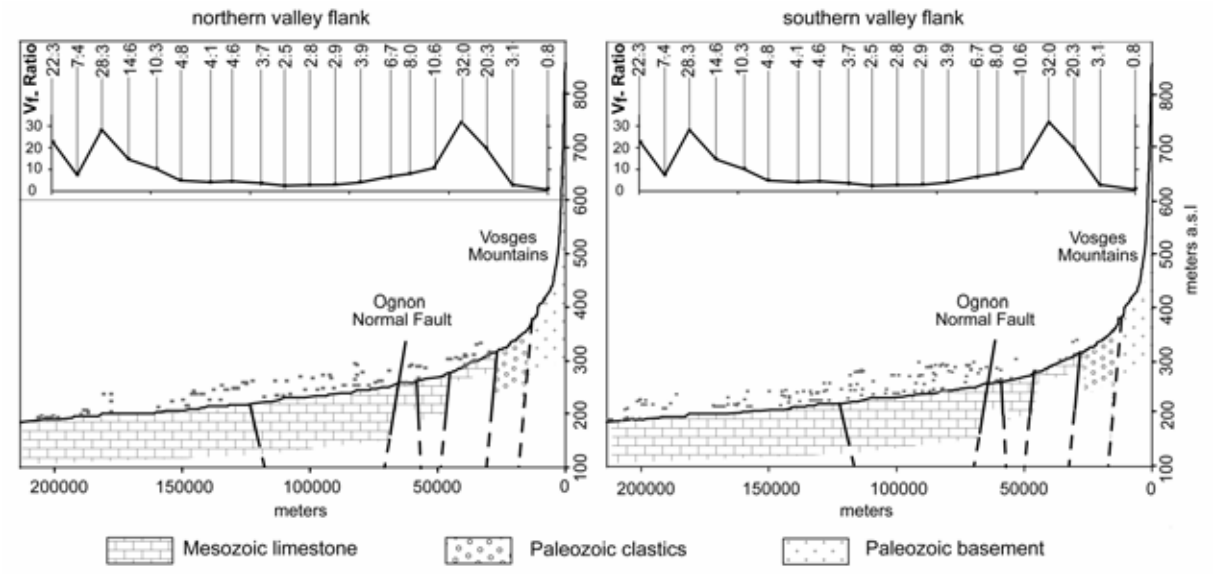

Figur. **7**: Longitudinal profile of the Ognon River (vertical exaggeration: 200). Terraces from both the northern and southern side of the valley (Figure 6) were projected orthogonally onto the profile. Also shown are the V_f ratios that were calculated at roughly 10 km intervals along the valley.

As outlined above, the Ognon Valley is divided into an upper and lower reach, which occupy the foot- and hanging-wall of the Ognon Normal Fault, respectively (Figure 1, 3, 6). The upper reach of the Ognon is characterized by a low sinuosity to straight channel pattern. The uppermost section of this stream segment is deeply entrenched into the Paleozoic rocks that build up the Vosges Mountains. Further downstream the river occupies a broad plain characterized by fluvio-glacial sediments (Thiebaut et al., 1974; Mercier and Jeser, 2004). Once the river traverses the Ognon Normal Fault and enters its lower reach it develops a high sinuosity course that increasingly incised and formed up to 5 terraces levels (Figure 6, 7). The depth of the valley is about 60 meters along this segment. Further downstream, were the river bends to the West and parallels the Avant-Monts fault, incision was slightly less intense as evidenced by the terrace distribution and the Vf indices (Figure 6, 7). A comparison of the longitudinal river profiles between the northern and southern valley sides (Figure 7) shows that the distribution of terraces along the Ognon Valley is asymmetric. The southern valley side systematically shows more preserved terrace levels than the northern valley side.

The terraces of the Ognon Valley are mostly of the fill-cut type (Bull, 1990) and are built up by a diverse alluvial succession that reaches a thickness of up to 50 meters in the lowermost Ognon Valley (Dreyfuss and Kuntz, 1969; Chauve et al., 1983). Aggradational phases are characterized by a variety of depositional environments and channel types as can be inferred from outcrop investigations (Figure 8). Deposits building up the Upper Ognon terraces comprise yellowish fine grained gravels, bedded sands and silts (Figure 8a) that overly a thick succession of greenish clays of probable Pliocene age (Dreyfuss and Kuntz, 1969). While the latter sediments point towards a low energy depositional environment, the sedimentological properties of the overlying coarser series indicate a very dynamic

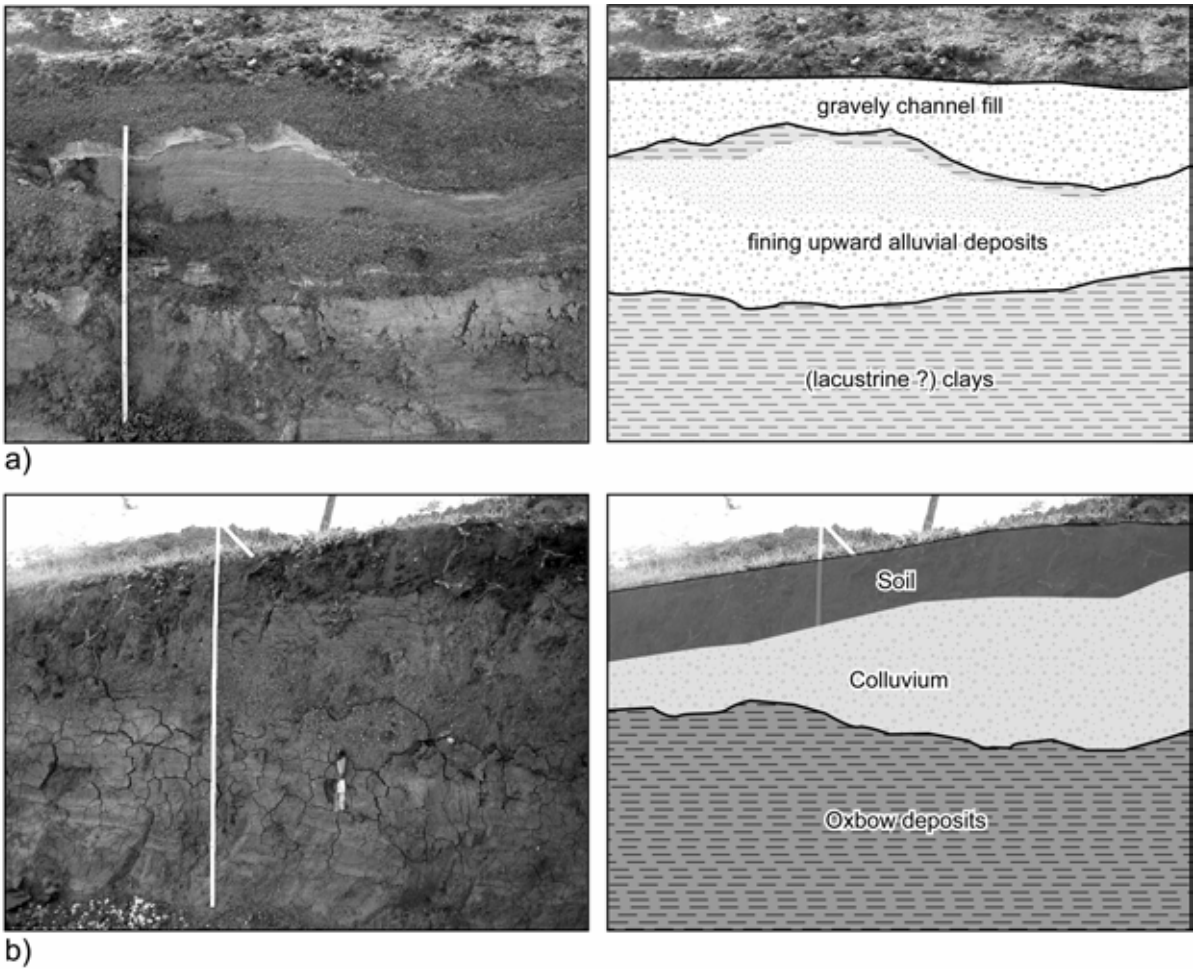

Figure 8: Alluvial sediments of the Ognon Valley. a) Typical lithofacies architecture of the Upper Ognon terraces. Fining upward sequence of fine gravels sands and silts that is unconformably overlain by another gravely channel deposit (locality 15 in Figure 10, Table 1). b) Typical Lower Ognon terrace deposits. Reddish clays interpreted as oxbow lake sediments that are unconformably overlain by some 50 cm of coarse colluvial deposits. Vertical scale on both pictures is 1 meter (locality 18 in Figure 10, Table 1).

depositional environment characterized by small and rapidly shifting channels.

The lower Ognon terraces consist of coarse gravel sheets in the upper reach of the valley. In the lower reach, however, they consist of homogenous reddish sands or clays. The latter resemble the overbank and oxbow lake deposits that form the present day floodplain of the high sinuosity Ognon River.

5.1.2. The lower Doubs Valley

The results of morphological analysis from the lower Doubs Valley are illustrated in Figure 6 and 9. A well pronounced aggradational terrace succession is only preserved along the uppermost segment of the reach upstream from the water gap at Clerval (Figure 6), where the meandering river

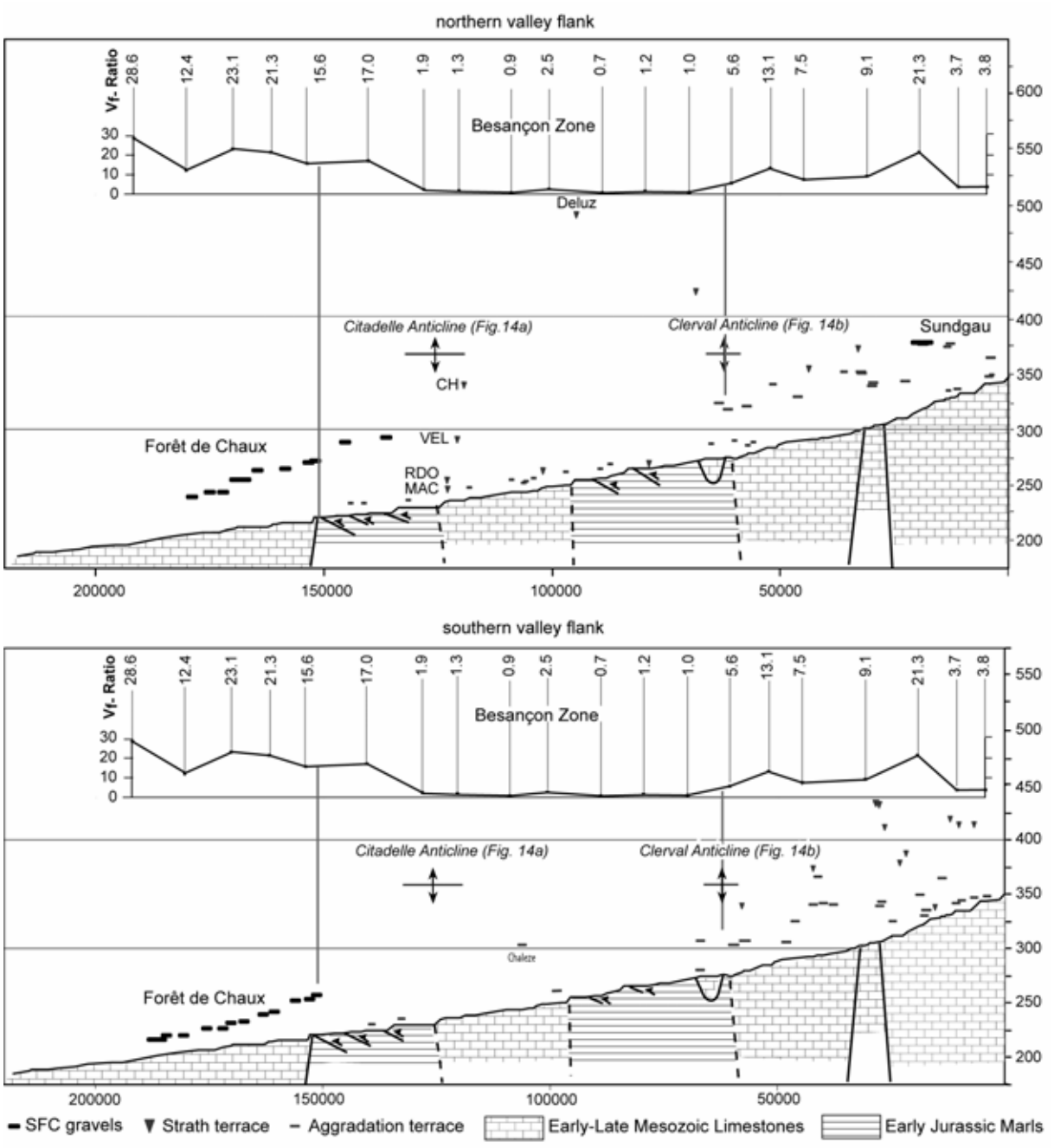

Figure 9: Longitudinal profile of the lower Doubs River starting from the water gap of Pont de Roide (Figure 3) (vertical exaggeration: 200). Terraces of the northern and southern valley side (Figure 6) were projected orthogonally onto the profile. Also shown are the results of V_f ratios calculated at roughly 10 km intervals along the valley. SFC: Sundgau-Forêt de Chaux gravels.

cuts through the autochthonous Mesozoic sediments of the Montbéliard Plateau. The incision intensity along this river segment is moderate as inferred from V_f ratios (Figure 9). The uppermost terraces are most often bedrock strath surfaces on which remnants of fluviatile deposits are preserved. A comparison of the elevation of these surfaces with that of the nearby Sundgau-gravel plain further to the east (Figures 6, 9), suggests that they represent the minimum elevation of the former base of the

SFC gravel plain. Below this erosional surface, up to three aggradational terrace levels can be distinguished. The two upper levels at about 20-45 and 50-75 meters above the active channel (Figures 6, 9) often consist of coarse gravels. Contini et al. (1973) concluded from the pebble spectra of these terrace deposits that they either represent or were derived from the Middle Pliocene SFC Gravels. The lowermost terraces along this segment of the Doubs are located between 5 to 10 meters above the active channel and are characterized by a larger percentage of calcareous clasts (Goguel and Dreyfuss, 1965; Contini et al., 1973).

Downstream from the Clerval water gap (Figure 6, 9) the incision intensity changes drastically as illustrated by the V_f ratio. Strath terraces that were cut into the limestone bedrock are commonly preserved along this valley segment whereas aggradational terraces that are composed of coarse gravels occur only rarely. Reports of fluvial deposits located more than 250 m above the active river channel (Dreyfuss and Glangeaud, 1950; Goguel and Dreyfuss, 1965) could be confirmed during this study (Figure 4, 9, 10). At several locations spectacular paleo-meanders were formed during river incision that are best preserved near the city of Besançon (Dreyfuss and Glangeaud, 1950; Chauve et al., 1983; Madritsch et al., 2008 submitted). All preserved paleo-meanders systematically face towards the south, which indicates that they have formed by combing during a continuous southward shift of the river course (Leeder and Alexander, 1987; Holbrook and Schumm, 1999). Differential incision of the Doubs River along its course is also evident from the elevation of terraces above the active channel. Terrace elevations are significantly higher along the section where the Doubs flows through the Besançon Zone and where incision has been strongest (Figure 9).

About 15 km downstream from the city of Besançon, the Doubs leaves the thin-skinned Jura-fold-and-thrust belt. From that point downwards it incises into the Middle Pliocene Forêt de Chaux gravels and the underlying Jurassic limestones. Along this sector the V_f ratios indicate moderate incision intensity.

5.2. Provenance analysis

The regional comparative heavy mineral analyses carried out during this study allow determining the provenance of fluvial sediments preserved in the Doubs and Ognon Valleys. Results are summarized in Figure 10 and Table 1. The most common heavy minerals detected in the samples are garnet, epidote, hornblende tourmaline and zircon. Also common in some samples are anatase, augite and aluminum rich silicates typical for medium to high metamorphic terrains that are given as Al-metamorphics in Figure 10 (mostly staurolite and subordinately kyanite and sillimanite, compare Table 1). Apatite, rutile and other rare minerals occur only in minor percentages. Unidentified heavy mineral fragments (fine grained aggregates or altered heavy minerals) were also counted and summed up as alterite in Table 1 and Figure 10.

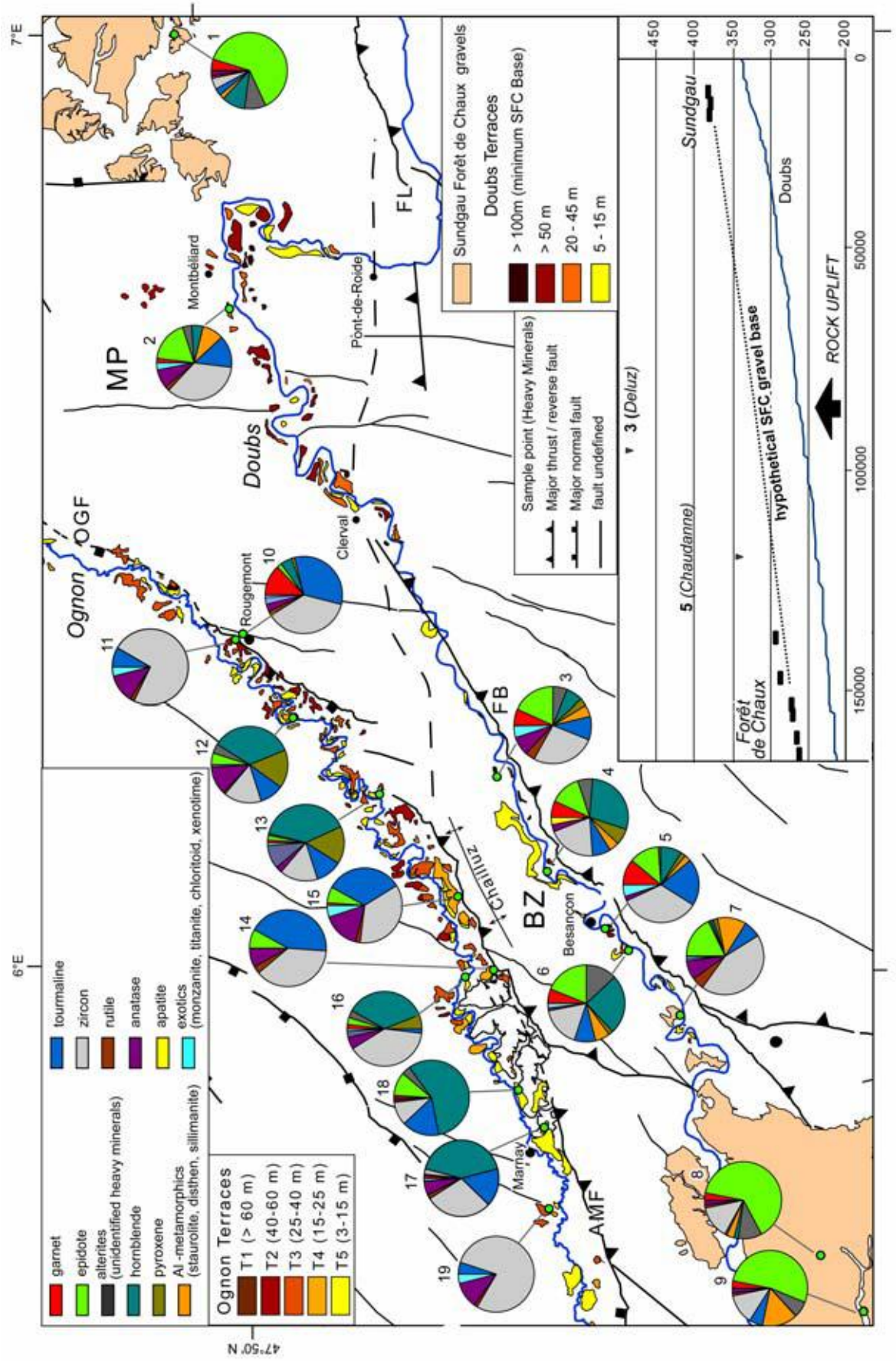
7°E
6°E
47°50' N
garnet
epidote
alterites
(unidentified heavy minerals)
hornblende
pyroxene
Al -metamorphics
(staurolite, disthen, sillimanite)
tourmaline
zircon
rutile
anatase
apatite
exotics
(monzanite, titanite, chloritoid, xenotime)
Ognon Terraces
T1 (> 60 m)
T2 (40-60 m)
T3 (25-40 m)
T4 (15-25 m)
T5 (3-15 m)
Sundgau Forêt de Chaux gravels
Doubs Terraces
> 100m (minimum SFC Base)
> 50 m
20 - 45 m
5 - 15 m
Sample point (Heavy Minerals)
Major thrust / reverse fault
Major normal fault
fault undefined
MP
OGF
FL
FB
BZ
AMF
Ognon
Doubs
Montbéliard
Pont-de-Roide
Clerval
Rougemont
Besançon
Marnay
Chaillexon
3 (Deluz)
5 (Chaudanne)
Sundgau
Forêt de Chaux
hypothetical SFC gravel base
Doubs
ROCK UPLIFT
450
400
350
300
250
200
0
50000
100000
150000

The samples from the Plio-Pleistocene terraces of the Ognon River draining the Vosges Mountains reveal two distinctively different heavy mineral assemblages. Samples of the Upper Ognon terraces (samples, 11, 15, 16, 19) are characterized by a very high percentage of stable heavy minerals (minimum of 50%, sometimes more than 75%), namely zircon and tourmaline, as well as anatase and rutile. Unstable heavy minerals such as epidote make up a subordinate fraction only. Minerals such as garnet or hornblende have not been observed except for the Fouchères area located southeast of Marnay (sample 17, see Figure 3, 10, Table 1) where a significant amount of hornblende was found. Sediments from the Lower Ognon terraces (sample 3-5, 10) show clearly different and highly diversified heavy mineral spectra. These samples are rich in unstable heavy minerals (about 50%). Characteristic are the high amounts of hornblende (more than 25%). Most samples also contain pyroxene (sample 12-14).

Systematic heavy mineral analyses from sediments of different catchments of the Southern Upper Rhine Graben showed that such heavy mineral assemblages are typical for sediments derived from crystalline basement and Mesozoic cover of the Vosges Mountains (Andel van, 1950; Hagedorn, 2004; Hagedorn and Boenigk, 2008). A so called "Alpine" heavy mineral assemblage, which is defined by a dominance of garnet, epidote, hornblende and the occurrence of medium-grade to high-grade metamorphic minerals (staurolite, kyanite) (Boenigk, 1987; Bonvalot, 1974; Liniger and Hofmann, 1965), has not been detected in any of the samples from the Lower Ognon Valley.

The samples from the Sundgau and Forêt de Chaux areas (sample 1, 7-9) show strikingly similar heavy mineral spectra, thus testifying their genetic relation (Liniger and Hofmann, 1965; Bonvalot, 1974; Petit et al., 1996). In both areas high amounts of epidote, as well as the occurrence of hornblende, garnet and staurolite, are typical. This characteristic "Alpine" heavy mineral assemblage was also found indicative for samples of the Sundgau-Forêt de Chaux Gravels further upstream of the former Paleo-Aare braided river system and to the east of our study area (Liniger and Hofmann, 1965; Hagedorn, 2004).

The samples taken from remnants of fluvial sediments and alluvial terraces along the Doubs Valley (samples 2-6) are similar to those from the Sundgau and Forêt de Chaux areas. They are characterized

Figure 10: Results of regional heavy mineral analysis. Note the occurrence of unstable heavy minerals such as staurolite and epidote in all samples from the Doubs Valley (sample 2-6). These samples clearly reveal similarities with the Sundgau-Forêt de Chaux Gravels (SFC). The samples do not indicate a relation to those from the Ognon catchment sourced by the Vosges Mountains. The inset in the lower right shows a segment of the longitudinal river profile of the Doubs (see also Figure 9) onto which the base of the continuous gravel plane of the Sundgau and Forêt de Chaux areas and the gravel remnants from the Doubs Valley were projected. The remnants are elevated with respect to the hypothetical base of the Middle Pliocene gravel plain which testifies a post-Pliocene relative rock uplift. B: Besançon; BG: Bresse Graben; BZ: Besançon Zone; FB: Faisceau Bisontin; M:Montbéliard

sample	X	Y	altitude m. a.s.l.	geological formation	sediment type	Age	garnet	epidote	alterite	hornblende	pyroxene	Al-metamorph	tourmaline	zircon	rutile	anatase	apatite	exotics	sum	opaque	staurolite	disthene	sillimanite	chloritoide	titanite	monazite	xenotime	sample treatment
1	953002	2290171	380	SFC gravels	gravel matrix	Mid-Pliocene	5	63	9	10		2	3	5	1	2			100	42	1	1						
2	930088	2285077	341	Doubs terrace	overbank deposit	Pleistocene	2	18	4	5		9	14	35	2	8		3	100	70	7	1	1		2		1	HCl
3	891277	2262430	362	undefined	carst fissure	Pleistocene presumed	7	18	6	7	3	5	10	27	4	8		5	100	58	5				5			HCl
4	883438	2258964	244	Doubs terrace	overbank deposit	Holocene presumed	7	13	6	29	7	4	8	20		3	3		100	96	3	1						
5	878609	2253827	347	undefined	colluvium	Pleistocene presumed	11	13	1	9	2	3	20	34		2		5	100	58	3				5			HCl
6	876596	2252377	253	Doubs terrace	oxbow deposit	Pleistocene	6	19	13	25	2	6	9	17		1		2	100	89	6			1	1			
7	871198	2248092	263	SFC gravels	gravel matrix	Mid-Pliocene		18	1	1	2	12	7	44	5	8	1	1	100	82	5	4	3				1	
8	851147	2236394	244	SFC gravels	sand lense	Mid-Pliocene	3	64	10	2		3	1	14	1	2			100	36	1	1	1					
9	851100	2236379	240	SFC gravels	gravel matrix	Mid-Pliocene	3	53	7			15	6	13	1	2			100	81	13	2						
10	902802	2284136	273	Keuper	marl	Upper Triassic	13	2		5		1	33	37	2	3	3	1	100	98	1						1	HCl
11	902440	2285134	284	Ognon terrace	gravel matrix	Pleistocene presumed							8	74	2	12		4	100	44					1	3		
12	895984	2280255	240	Ognon terrace	gravel matrix	Late Pleistocene		5	4	35	16		10	16	1	12	1		100	80								
13	889589	2273176	227	Ognon terrace	gravel matrix	Late Pleistocene presumed	1	2	1	39	16		11	16		3	10	1	100	74						1		M
14	874393	2265929	211	Ognon terrace	overbank deposit	Holocene	2	3	3	36	6		2	39		5	3	1	100	51					1			
15	881089	2266196	243	Ognon terrace	sand lense	Pleistocene presumed	1	7					33	36	2	16		5	100	70						4	1	
16	875057	2263661	228	Ognon terrace	sand lense	Pleistocene presumed		8					43	38	3	8			100	48								
17	861988	2259364	230	Ognon terrace	gravel matrix	Pleistocene presumed	1	1	2	42			16	29	2	6		1	100	85						1		M
18	854744	2258817	227	Ognon terrace	sand lense	Late Pleistocene	1	10	4	57			16	10	1	1			100	63								
19	872453	2262765	242	Ognon terrace	overbank deposit	Pleistocene presumed							5	78	2	11		4	100	55						4		

Table 1: Results of heavy mineral analyses. Sample numbers refer to Figure 10. HCl: Chemical treatment; M: Magnetic Separation; SFC: Sundgau-Forêt de Chaux Gravels:

by relatively high percentage of unstable minerals, particularly epidote, but also contain significant amounts of hornblende and garnet. Most notably, staurolite occurs in all of these samples.

Unlike the samples from the Sundgau area, the samples form the Doubs Valley are also rich in zircon and tourmaline These differences in the heavy minerals spectra can be explained by a downstream increasing contribution of tributaries from the Vosges Mountains to the SFC braided river system (Théobald et al., 1976). This resulted in an increasing contribution of sediments derived from the Triassic cover of the Vosges Mountains, and consequently a dilution of the original "Alpine" heavy mineral spectra. Sediments derived from Triassic series are characterized by high amounts of stable minerals, such as zircon and tourmaline (Hagedorn, 2004; Hagedorn and Boenigk, 2008). This is evident from sample 10 that was taken from the Late Triassic Keuper Formation. This interpretation is constrained by the observation that the samples from the Doubs Valley as well as those of the Forêt de Chaux area show slightly higher amounts of zircon and tourmaline in comparison to the Sundgau area further upstream.

In addition, the effects of weathering of fluvial remnants must be considered, though these are probably only of minor importance. Higher weathering resistance of stable heavy minerals (Boenigk 1983) presumably led to a relative enrichment in samples of reworked sediments. Systematic heavy mineral analyses of weathering profiles carried out in the Sundgau area have shown that garnet is often depleted from the spectrum relative to the amount of epidote when strong weathering occurred (Boenigk, 1982; Boenigk, 1987). In carbonate rich sediments however, weathering of garnet is reduced (Sindowski, 1949). This is compatible with the fact that the carbonate-rich samples from the Doubs Valley (e.g. sample 3-5; see Figure 10 and Table 1) show higher amounts of garnet in comparison to the samples from the Sundgau and the Forêt de Chaux that are poor in carbonate.

Despite slight differences, the similarities between the heavy mineral spectra of remnants of fluvial deposits along the Doubs Valley and that of the SFC Gravels are obvious, particularly concerning the high amounts of epidote and the occurrence of staurolite. Therefore, these remnants were not exclusively derived from the Vosges Mountains but bear a distinct signature of Alpine provenance. Thus, the results of heavy mineral analyses clearly indicate that these deposits are not directly related to the Late Miocene Bois de Raube formation but represent reworked SFC Gravels.

5.6. Discussion

5.6.1. Paleo-topographic reconstruction of the Sundgau-Forêt de Chaux gravel base and implications for post-Pliocene relative rock uplift

The results of the heavy mineral analyses permit to attribute the remnants of fluvial sediments along the Doubs Valley to the eroded Middle Pliocene Sundgau-Forêt de Chaux (SFC) Gravels. The

elevation of these remnants marks the minimum altitude of the base of the SFC gravel sheet and therefore the Middle Pliocene paleo-topography. The inset of Figure 10 shows a segment of the longitudinal river profile of the Doubs that connects the continuous SFC gravel plains of the Sundgau and Forêt de Chaux areas. The base of the SFC gravel plain, as well as the elevation of SFC remnants detected during this study by heavy mineral analysis were projected orthogonally onto the longitudinal river profile. The stippled line marks the presumed undeformed base of the former SFC gravel plain linking the Sundgau and the Forêt de Chaux areas.

The remnants of SFC gravels detected in the Doubs Valley are located up to 170m above the extrapolated gravel base. The maximum thickness of the SFC gravels of 30-65 meters cannot account for this difference in elevation. This indicates that erosion of the SFC gravels in the area between the Sundgau and the Forêt de Chaux resulted from relative rock uplift, as was already proposed by Campy (1984). Biostratigraphic constraints on the age of deposition of the SFC gravels (4.2-2.9 Ma; Petit et al., 1996; Fejfar et al., 1998) indicate that this uplift occurred during latest Pliocene to Pleistocene times, presumably after thin-skinned deformation of the Jura fold-and-thrust belt ceased. Furthermore, these age constraints indicate a minimum latest Pliocene to recent uplift rate of 0.05 +/- 0.02 mm/yr. This rate is in good agreement with result from neighboring areas (Müller et al., 2002; Giamboni et al., 2004b; Ustaszewski and Schmid, 2007). At the site of Deluz (Figure 10 inset) SFC gravel remnants are located 240 meters above the active channel of the Doubs. This yields a minimum incision rate of 0.08 +/- 0.02 mm/yr that slightly exceeds the regional rock uplift rate.

Based on the highest elevations at which SFC gravel remnants occur and on the results of heavy mineral analyses, we reconstructed the Middle Pliocene palaeo-topography of the RBTZ using ArcGIS standard interpolation methods (Figure 11). Taking into account sedimentological and geomorphic observations in neighboring areas (Liniger, 1966; Bonvalot, 1974; Giamboni et al., 2004a) we considered the undeformed SFC gravel sheet to reflect a rather flat, i.e. low gradient surface. Well constrained data points for the interpolation are provided by the base of the Sundgau and Forêt de Chaux gravel sheets and the elevated SFC remnants preserved along the Doubs Valley. The highest elevated remnants determine the minimum elevation of the eroded gravel base at a certain position. As SFC remnants are scarce in the area, we also considered the results of heavy mineral analysis to better constrain the paleogeographic extent of the SFC braided river system.

The reconstructed channel of the Paleo-Aare that deposited the SFC gravels follows the ENE-WSW striking structural trend of the region (Figure 11). This channel is flanked to the NW by the thrusted Chailluz anticline and to the SE by the Faisceau Bisontin, both of which forming part of the thin-skinned Jura fold-and-thrust belt (Figure 1, 3). Whilst the SE boundary of the channel is well constrained and coincides with the deformation front of the Faisceau Bisontin, its width and extent to the NW is ill defined. The model shown in Figure 11 assumes that the width of the braided Paleo-Aare River was more or less constant. The maximum channel width of the Paleo-Aare did not extent into

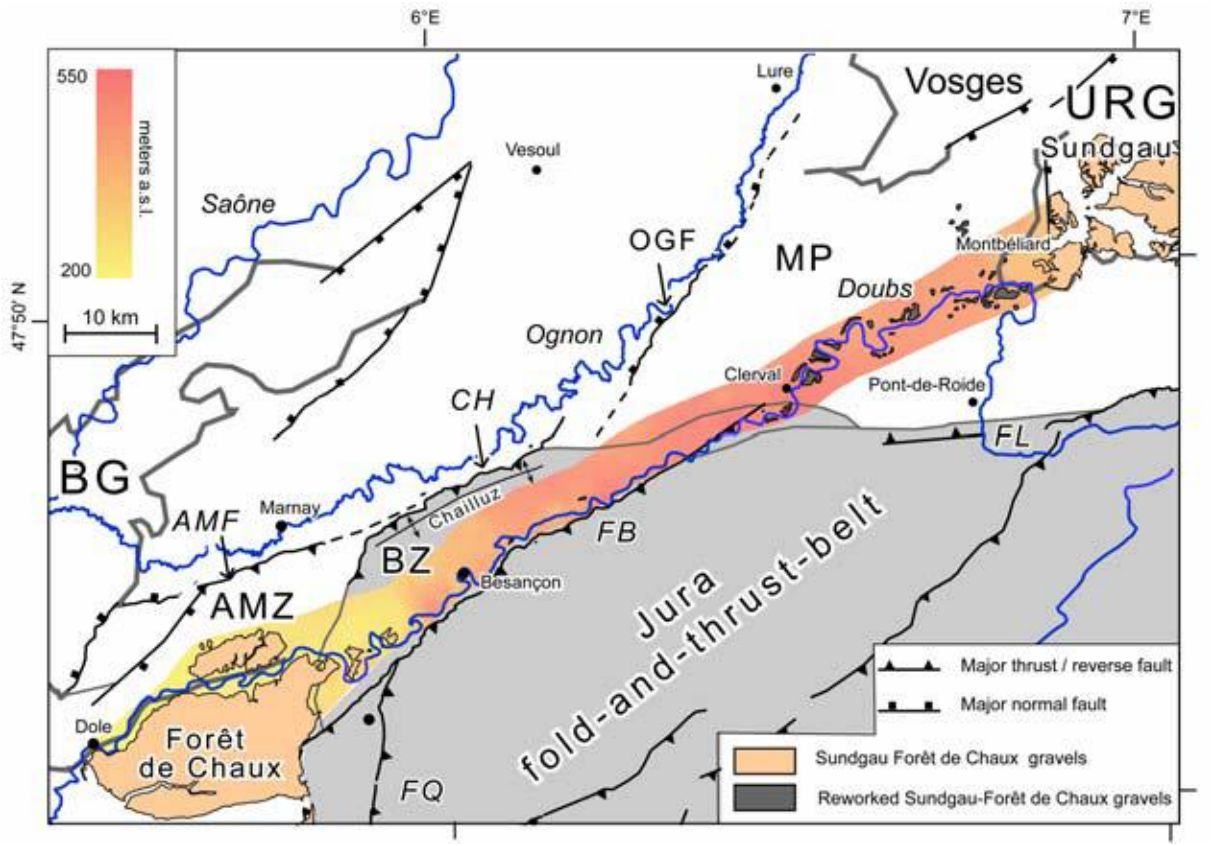

Figure 11: Paleo-topographic reconstruction of the eroded Paleo-Aare channel from the detection of elevated Sundgau-Forêt de Chaux gravel remnants along the Doubs Valley. The extent of the channel is poorly constrained. It did not extend beyond the Chailluz Anticline into the Lower Ognon Valley.

the Lower Ognon Valley. This is constrained by the observation that heavy mineral analyses of alluvial deposits from that area are devoid of Alpine-derived sediments (Figure 10). Hence, the Ognon Valley formed a separate drainage basin that was only sourced by the Vosges Mountains and their foothills already in Middle Pliocene times. This is in agreement with regional paleogeographic concepts (Sissingh, 1998).

During the Middle Pliocene, the Chailluz Anticline (Figure 1, 3, 10, 11) that is related to a low angle thrust fault formed the divide between the drainage basins of the Paleo-Aare and the precursor of the Ognon River. This hypothesis is in keeping with the fact that during the post-Pliocene uplift of the area no reworked SFC Gravels were shed into the Ognon Valley in the area north of the Chailluz Anticline. Some reworked SFC Gravel may, however, have been transported around the SW plunge of the Chailluz Anticline and shed into the lowermost Ognon Valley, leading to the deposition of fine grained gravels in the Fouchères area southeast of Marnay (Figure 3, 10). Dreyfuss and Kuntz (1969) interpreted these sediments as being related to the SFC gravels based on the presence of Alpine detritus (Figure 3). As this concept could not be confirmed by our heavy mineral analyses (Figure 10, Table 1, samples 2, 7-9, 17), we consider these deposits as forming part of the Latest Pliocene to

Pleistocene alluvial fill of the Ognon Valley, which was derived from the foothills of the Vosges Mountains and which also builds the Upper Ognon terraces (see interpretation in Figures 6 and 10).

5.6.2. Response of Pleistocene to recent drainage basins

Post-Pliocene uplift along the northwestern Jura fold-and-thrust belt was highly differential, as is evidenced by its effects on the Pleistocene morphological evolution of the Ognon and Doubs drainage basins.

5.6.2.1 The Ognon Valley

The morphologic and sedimentological record of the Ognon Valley points to the existence of a complex-response terrace system (Bull, 1990). Such a system is characterized by alternating phases of sediment aggradation and degradation during terrace formation. The conceptual reconstruction of the valley evolution shown in Figure 12 summarizes the results of our study.

The basal sedimentary sequence consists of a thick succession of clays that were deposited in a lacustrine environment (Chauve et al., 1983). These clays are covered by aggrading Plio-Pleistocene alluvial sediments, derived from the foothills of the Vosges Mountains and composed of mostly Triassic sediments. This varied alluvial succession reaches thicknesses of up to 50 m (Dreyfuss and Kuntz, 1969; Chauve et al., 1983). The sandy to gravely deposits that build up the uppermost Ognon terraces were most likely shed by a braided to anastomosing river system.

The onset of this phase of alluvial sedimentation is poorly constrained. Recent dating attempts of the uppermost Ognon terrace deposits by means of Optical Stimulated Luminescence (OSL) dating indicated minimum ages 300 kyr (work in preparation). As this age stems from the uppermost terraces it most likely marks the minimum age of the onset of river incision and formation of complex-response fill-cut terraces.

A second aggradational phase affected the Ognon Valley in Late Pleistocene times again indicated by the results of OSL dating (work in preparation). During this phase reddish gravels were deposited that were derived from the central Vosges Mountains composed of crystalline rocks (Figure 7, 10, 12). Sediment accumulation only affected the lower elevated parts of the valley implying that the Ognon River had already incised into its uppermost terraces. Aggradation of the red gravels was most likely driven by the Late Pleistocene deglaciation of the Vogses Mountains (Mercier and Jeser, 2004).

This reconstruction shows that the Ognon Valley was at best mildly affected by the processes that led to the more or less contemporaneous post-Pliocene degradation of the SFC-gravels further to the south. The Ognon Valley is characterized by continuous latest Pliocene and Pleistocene sediment accumulation that was mostly climatically controlled.

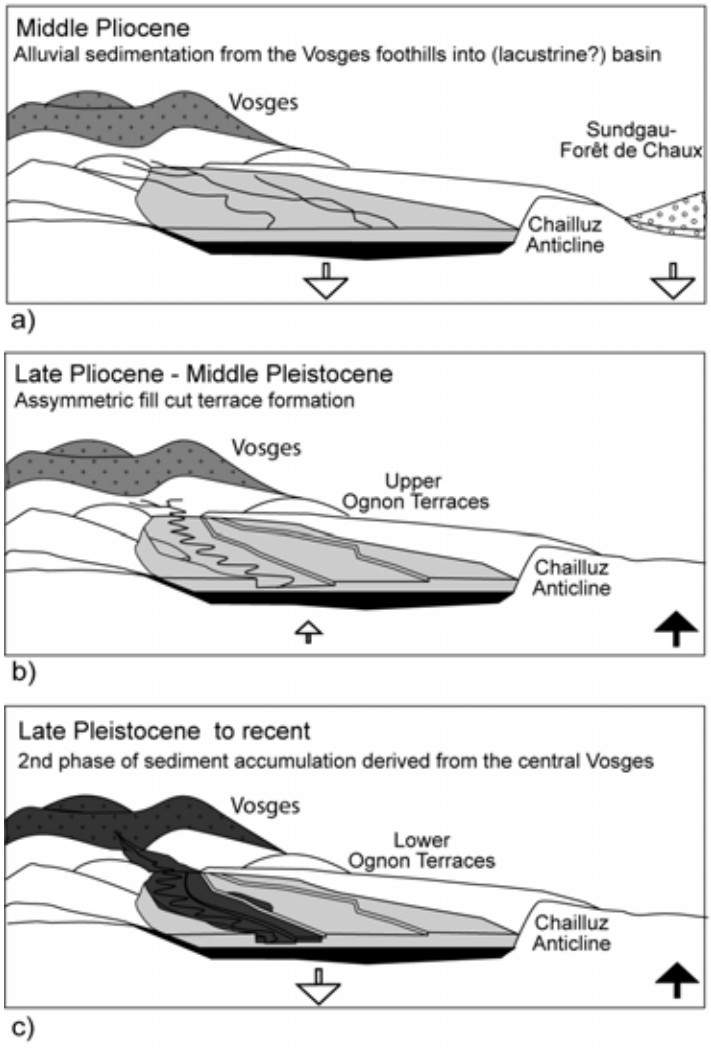

Figure 12: Plio-Pleistocene evolution of the Ognon Valley.
a) Lacustrine to alluvial sediment accumulation. Sediment was supplied from the foothills of the Vosges Mountains.
b) River incision and formation of asymmetric complex-response fill-cut terraces that started by the Middle Pleistocene at the very latest
c) Second major phase of aggradation with sediment supplied from the central Vosges Mountains.

Due to the scarce age information and complex development of the Ognon terraces a correlation of the terraces along the course of the Ognon was not attempted in this study. Tectonic effects on the valley evolution may be deduced from the terrace distribution, the incision pattern and the drainage geometry. A relation of these parameters with the prominent Ognon Normal Fault is evident (Figure 6, 7) The Vf ratio rises significantly once the river crosses the fault and moderately incises into its hanging wall forming up to 5 terrace levels. This clearly indicates a mild inversion of the Ognon Normal Fault.

The terrace distribution along the Ognon Valley is asymmetric as is inferred from the independent investigations of the northern and southern valley sides respectively (Figure 6, 7). Also Campy (1984) made this observation and interpreted it as the result of northward directed lateral deflection of the Ognon River in response to tectonic uplift along the southward adjacent front of the Jura fold-and-thrust belt and the Avant-Monts Fault. Presumably this deflection caused the preferential erosion of terraces along the northern side of the valley.

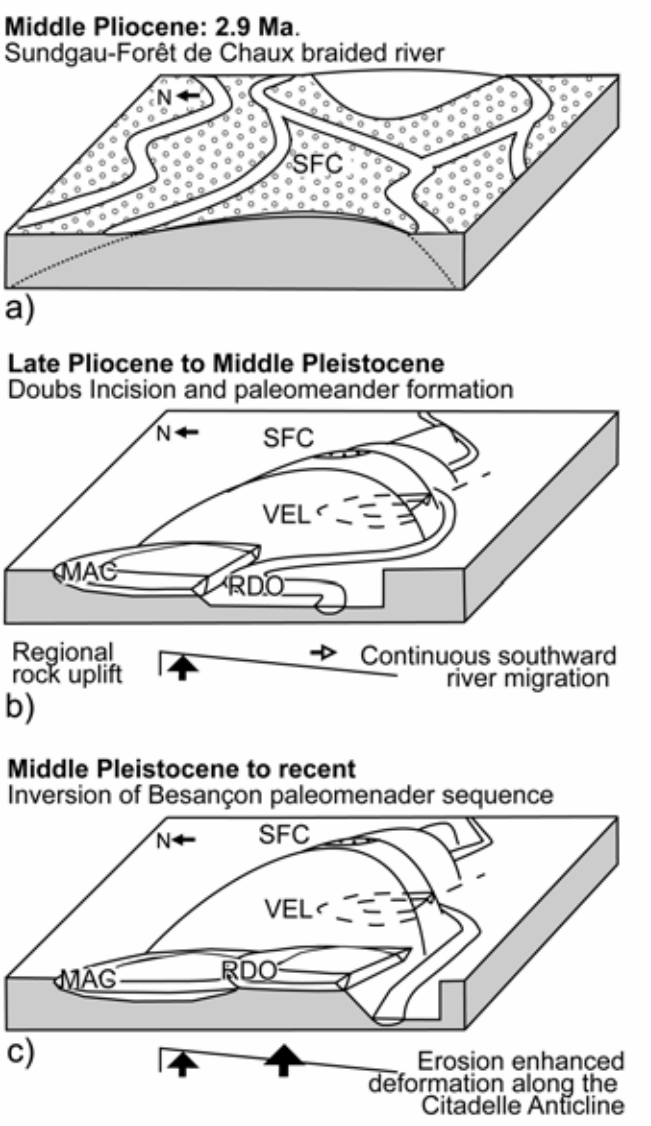

Figure 13: Plio-Pleistocene evolution of the lower Doubs Valley in the area of the the Citadelle Anticline (Figure 14a)

a) The fold structure that probably formed during the Late Miocene to Early Pliocene, is buried by the Middle Pleistocene Sundgau-Forêt de Chaux gravels.

b) Post-Pliocene regional relative rock uplift along the RBTZ induces the degradation of the SFC gravel plane and incision of the Doubs during which paleo-meanders are formed.

c) Pleistocene fold growth occurs localized and in response to erosion and is associated with relatively high local uplift rates. MAC: Malcombe meander; RDO: Roche d'Or meander; SFC: Sundgau-Forêt de Chaux gravels; VEL: Velotte meander.

5.6.2.2. The Lower Doubs Valley

The Doubs River occupied the braided river channel of the Paleo-Aare after it was rerouted into the Upper Rhine Graben in Late Pliocene times (Figure 4b, 4c, 13a). During latest Pliocene and Pleistocene times the Doubs River cut through the Middle Pliocene gravel sheet and deeply incised the underlying Jurassic limestones (Figure 13b). As hardly any Plio-Pleistocene sediment aggradation occurred, the strath terraces predominate. During its incision the Doubs River appears to have slightly shifted southward, as is evident from the symmetric orientation of paleo-meanders along the valley. This indicates a mild southward tilt of the valley (Figure 13b).

Whilst the Doubs received considerably less sediment supply from Pleistocene glaciers (Buoncristiani and Campy, 2004; Mercier and Jeser, 2004) than the Ognon, its incision and depositional patterns show a clear relation with the outlines of the tectonic units (Figure 6, 9). Upon its re-entry of the Jura fold-and-thrust belt at the Clerval water gap incision significantly intensifies (Figure 6, 9).

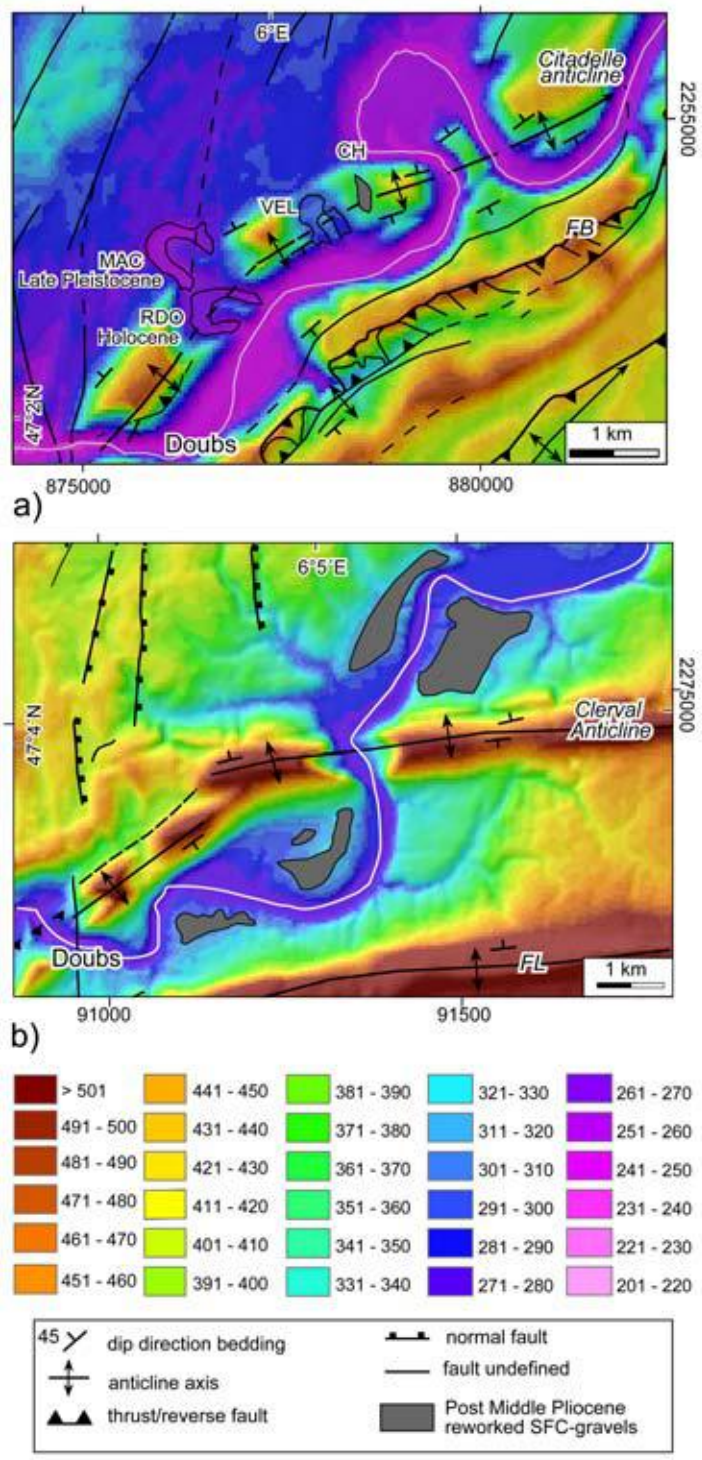

Figure 14: Examples of erosion related Post-Pliocene folding along the Doubs Valley (see Figure 6 for location)

a) The Citadelle Anticline shows evidence of Pleistocene fold growth from the differential uplift of paleo-meanders along the axis of the fold. Note that the Pliocene Sundgau-Forêt de Chaux (SFC) Gravels were detected in the wind gap of Chaudanne (see also Figure 9, 13). Modified after Madritsch et al. (2008 submitted)

b) The Clerval Anticline is dissected by the Doubs in an antecedent manner. Coarse SFC Gravels, most likely reworked by the Doubs, are found to the north and south of the anticline which suggests that fold growth occurred after the deposition of the gravels.

CH: Chaudanne wind gap; FB: Faisceau Bisontin; FL: Faisceau du Lomont; MAC: Malcombe paleo-meander; RDO: Roche d'Or paleo-meander; VEL: Velotte paleo-meander.

Apparently, at some point the incision of the Doubs River was structurally focused. This happened when the river became locked between the fault related folds of the Faisceau Bisontin. This process of focused incision was further amplified in places where the river reached easily erodable Late Triassic to Early Jurassic marls and clays that crop out in the cores of the anticlines.

Enhanced river incision throughout the uplifted area evidently triggered localized active deformation throughout the Besançon Zone, as was recently demonstrated along the Citadelle

Anticline (Madritsch et al., 2008 submitted) (Figure 14a). This structure, which presumably was pre-formed in Early Pliocene times and during the formation of the thin-skinned fold-and-thrust belt, was buried by the Middle Pliocene SFC gravels (Figure 13a). This is evidenced by gravel remnants detected in the Chaudanne wind gap (CH in Figure 14a) and others located at even greater elevations further upstream at Deluz (Figure 10). Paleo-meanders that were differentially up-warped along the axis of the Citadelle Anticline testify to its ongoing activity during the Pleistocene (Figure 13c, 14a) (Madritsch et al., 2008 submitted). Constraints on local fold-induced local relative uplift rates were obtained from OSL dating of oxbow sediments. The oxbow lake sediments of the Malcombe meander (MAC in Figures 13, 14a) revealed an age of around 30 kyr (Madritsch et al., 2008 submitted).By the time of sedimentation the abandoned meander was presumably still connected to the active channel. At present these deposits are cut off from the active channel and located some 5 meters lower than the bedrock elevation of the uplifted Roche d'Or paleo-meander (RDO in Figures 13, 14a) (Madritsch et al., 2008 submitted). This suggests a minimum relative uplift of 5 meters since 30 kyr and a related uplift rate of 0.17 +/-0.03 mm/yr. As this rate is significantly higher than the Latest Pliocene to recent regional uplift rate determined from the paleo-topographic reconstruction of the SFC gravel plain (0.05mm/yr), it appears that deformation had locally increased in response to intense Pleistocene erosion related to river incision (Figure 13c).

6.3. Tectonic implications

Post-Pleistocene differential uplift along the RBTZ is evident from the geomorphic observations discussed above. The uplift pattern and the different incision histories of the Doubs and Ognon rivers can be correlated to structural units and are thus partly controlled by tectonic processes.

A zone of late-stage differential uplift can be identified in the area of the RBTZ, deduced from differential erosion of the SFC Gravels, laterally bounded to the NE and SW by the Upper Rhine and Bresse Grabens, respectively. In the areas within and flanking these grabens the SFC Gravels are still well preserved (Figure 3, 6). Thus, the central RBTZ was relatively uplifted during the latest Pliocene and Pleistocene in respect to the Upper Rhine and Bresse grabens, parts of which subsided during this time interval (Ziegler and Dèzes, 2007).

A schematic NW-SE trending structural cross-section through a part of the study area, roughly parallel to the orientation of the present day maximum horizontal stress (Becker, 2000; Kastrup et al., 2004; Reinecker et al., 2005), is presented in Figure 15. This cross-section through the Besançon Zone and its foreland displays the part of the Jura fold-and-thrust belt that encroached onto the pre-existing normal fault system of the RBTZ and the underlying Burgundy Trough (Madritsch et al., 2008 in press) Along this section the evolution of the Ognon and Doubs Valley record the character of the relative rock uplift (Campy, 1984).

During the Middle Pliocene (Figure 12a, 13a, 15a) the Lower Ognon Valley and the southward precursor of the Doubs Valley were characterized by sediment aggradation. The Ognon Valley developed along the Ognon Normal Fault and as such occupied the site of a preexisting Eo-Oligocene graben structure (Theobald et al., 1977; Chauve et al., 1983; Madritsch et al., 2008, submitted). As shown in Figure 15 the Ognon Valley also borders the southward adjacent front of the Jura-fold-and-thrust belt formed by the Chailluz Anticline, related to the shallow Chailluz Thrust (Figures 1, 3, 6, 10) and the basement rooted Avant-Monts Fault (Figure 1, 3, 6, Madritsch et al., 2008 in press).

The Lower Ognon Valley formed a basin that received local sediment supply from the foothills of the Vosges Mountains. South of the Chailluz Anticline the Paleo-Aare occupied the area of the later Doubs Valley where the Middle Pliocene SFC Gravels were deposited (Figures 6, 10, 11, 15a). Sediment supply for the Paleo-Aare was provided by increased sediment discharge from the Alps and the immediately adjacent Molasse basin (Kuhlemann et al., 2002) that witnessed large-scale uplift and erosion during the Pliocene (Cederbom et al., 2004).

The paleogeographic considerations outlined above indicate that the Chailluz Anticline largely already pre-existed during that time and thus formed a structurally controlled drainage divide between the Lower Ognon Valley and the Paleo-Aare gravel plain. This is the reason to postulate that the Chailluz Anticline most likely initially formed during the main phase of thin-skinned deformation (10.5- 4.2 Ma; Ustaszewski and Schmid, 2006) and hence largely predates the onset of the Middle Pliocene SFC Gravel deposition. Most probably the same accounts for the deformation front of the Faisceau Bisontin that formed the southern boundary of the SFC gravel plain (Figure 15a).

At around 2.9 Ma (Late Pliocene Figure 15b) the Paleo-Aare was deflected into the Rhine-Graben. The study area was cut off from Alpine sediment supply and deposition of SFC gravels ceased. The former valley of the Paleo Aare now became occupied by the precursor of the Doubs River (Figure 4, 13a). At the same time the SFC gravels were uplifted with respect to the adjacent Upper Rhine and Bresse Grabens in the area of the RBTZ, leading to differential erosion of the SFC gravels (Figure 3, 6, 15b).

While degradation of the Middle Pliocene SFC gravel sheet can partly be explained by base level fall in response to subsidence of the Upper Rhine and Bresse Grabens, it also coincides with the onset of thick-skinned tectonics throughout the RBTZ (Giamboni et al., 2004a; Ustaszewski and Schmid, 2007; Madritsch et al., 2008 in press) (Figure 15b). Within our study area this type of deformation is best documented along the Avant-Monts Fault (AMF in Figure 15b, Madritsch et al., 2008 in press). Thick-skinned shortening most likely involves compressive to dextrally transpressive reactivation of various normal faults that characterize the RBTZ, including the underlying Permo-Carboniferous Burgundy Trough System (Giamboni et al., 2004a; Ustaszewski and Schmid, 2007; Madritsch et al., 2008 in press). Hence, basement rooted inversion tectonics are also held responsible for having

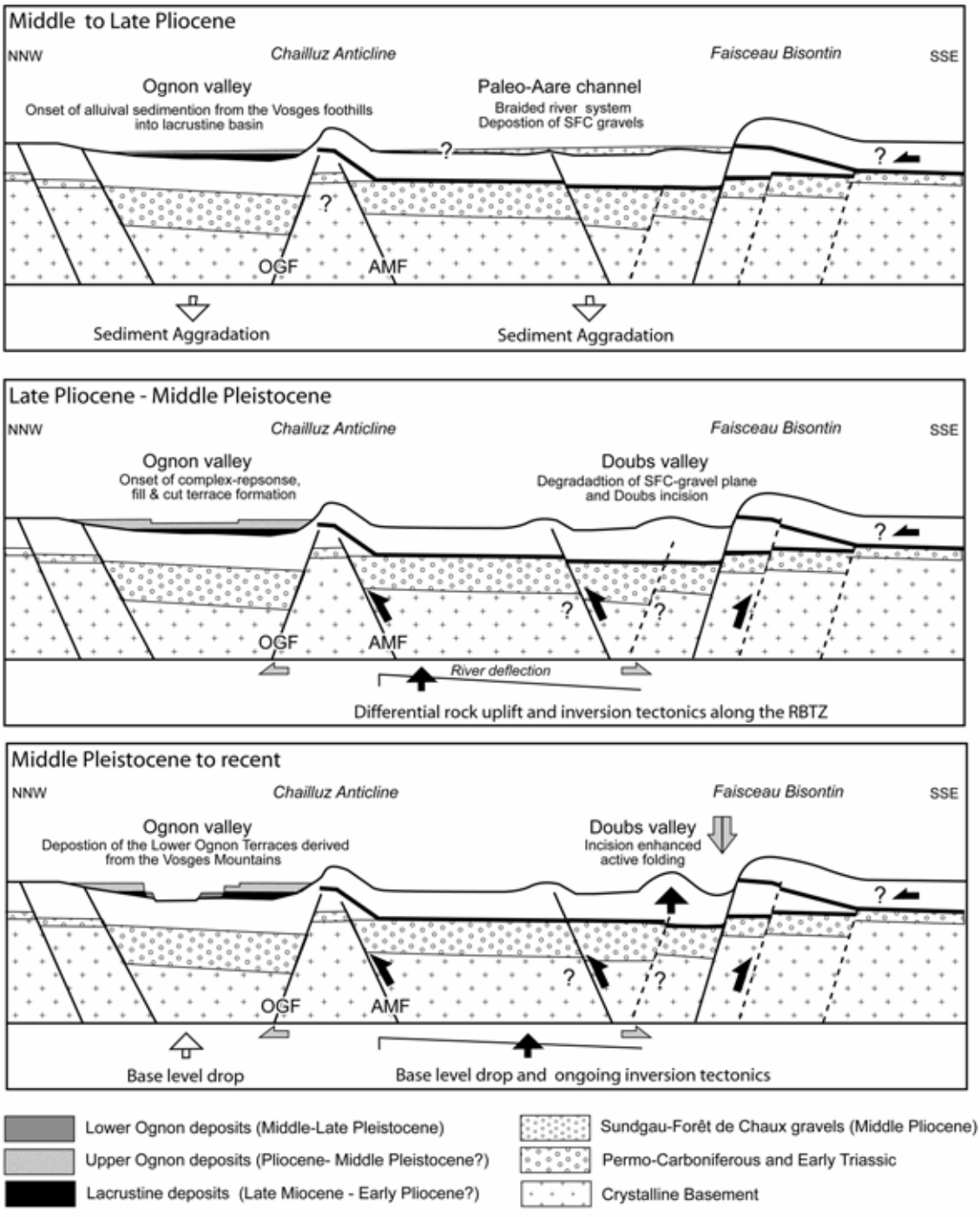

Figure 15: Schematic cross section across the central part of the study area illustrating the tectono-geomorphic evolution of the area during Plio-Pleistocene times a) Middle Pliocene aggradation of the Sundgau-Forêt de Chaux (SFC) Gravels. The main structures related to the thin-skinned Jura fold-and-thrust belt represent previously established define drainage basin boundaries. b) Late Pliocene contractional thick-skinned deformation results in differential rock uplift throughout the Besançon Zone and the erosion of the SFC gravel plain. The Ognon migrates towards the north in response to southward adjacent uplift (Campy 1984). c) Enhanced incision of the Doubs in response to relative rock uplift induces localized active folding in the internal parts of the Jura fold-and-thrust belt.

contributed to the differential post-Pliocene uplift along the RBTZ and the erosion of the SFC Gravels. This hypothesis is constrained from morphologic observation along the Ognon Valley. The Ognon River had the same base level as the precursor of the Doubs River, namely the Saône River occupying the Bresse Graben (Figure 3). Nevertheless, the Ognon drainage basin was characterized by only mild river incision and ongoing sediment accumulation and subsidence that took place contemporaneously to the degradation of the southward adjacent SFC gravel plain (Figure 15b).

The asymmetric terrace distribution along the Ognon Valley was already related to tectonically induced differential uplift south of the valley by Campy (1984). Our data suggest that the observed morphology is due to thick-skinned inversion tectonics reactivating Paleozoic to Paleogene normal faults rather than propagation of the thin-skinned thrust belt (Figure 15b). This is constrained by seismic reflection data from the Avant-Monts Fault and the inversion of the Ognon Normal Fault (Figure 1, 3, 6 7; Madritsch et al., 2008 in press). Along the front of the Besançon Zone such thick-skinned deformation most likely resulted in further amplification of the pre-existing décollement-related Chailluz Anticline. Note that reverse faulting along the thick-skinned Avant-Mont Fault also well explains the diverging migration of the Ognon and Doubs to the north and south, respectively, a feature that is hard to explain by invoking ongoing thin-skinned fold and thrust belt propagation.

Deformation within the Besançon Zone continued beyond 2.9 Ma as is documented by remnants of Middle Pliocene SFC Gravels that are involved into folding at several locations (Figure 14, 15c). Near the town of Clerval alluvial terraces composed of coarse, probably reworked SFC Gravels are found to the north and south of the Clerval Anticline that is dissected by the Doubs in an antecedent manner (Figure 14b) (Contini et al., 1973; Madritsch et al., 2008 in press). This strongly suggests that folding continued after the deposition of the SFC gravels into Pleistocene times at this location. Along the Citadelle Anticline near Besançon, folding even continued into Pleistocene times as recorded by the inversion of a paleo-meander sequence of the Doubs River (Dreyfuss and Glangeaud, 1950; Madritsch et al., 2008 submitted).

These observations that document post 2.9 Ma deformation within the internal parts of the thin-skinned Jura fold-and-thrust belt are in contrast to the northwestern front of the Jura Mountains where such activity was only recorded outside the fold-and-thrust belt proper (Niviere and Winter, 2000, Ustaszewski and Schmid, 2007). The active folding detected is apparently localized and enhanced by erosion (Dreyfuss and Glangeaud, 1950; Madritsch et al., 2008 submitted). The mechanical conditions for such positive feedbacks as defined by numerical models suggest that deformation is caused by buckling in response to regional horizontal compression that occurs at the same time as river incision and thus during the Pleistocene (Simpson, 2004; Zeilinger et al., 2005). Hence our field observations imply that Pleistocene shortening of the Mesozoic cover sequence within the Besançon Zone is, at least locally, decoupled from the basement and that ongoing thin-skinned deformation in this part of the fold-and-thrust belt cannot be entirely excluded.

The apparent back-stepping of the active fold-and-thrust belt front (Figure 15c) could be interpreted in terms of the critical tapered wedge theory and the related cyclic evolution of fold-and-thrust belt wedges (Davis et al., 1983; DeCelles and Mitra, 1995). Regional Plio-Pleistocene uplift and erosion may have transferred the critically tapered wedge of the Jura fold-and-thrust belt that stalled around the Early Pliocene into a sub critical stage, initiating renewed out of sequence deformation within the fold-and-thrust belt. This hypothesis is supported by analogue models (Smit et al., 2002).

On the other hand seismicity of the region (Baer et al., 2005; Baer et al., 2007) implies that at present deformation in the area is thick-skinned and involves the underlying basement. Thus, the active shortening of the cover sequence is more likely caused by basement fault reactivation in the nearby Alpine foreland (e.g. the Molasse basin or the Rhine-Bresse Transfer Zone itself; Piffner et al., 1997; Mosar, 1999; Ustaszewski and Schmid, 2007; Madritsch et al., 2008 in press) rather than rooted in the Central Alps as it was during the formation of the thin-skinned Jura fold-and-thrust belt in Late Miocene to Early Pliocene times (e.g. “Fernschub”; Laubscher, 1961).

7. Conclusion

Paleo-topographic reconstruction of the Middle Pliocene Sundgau-Forêt de Chaux gravels indicates large-scale post-Pliocene relative rock uplift along the northwestern front of the Jura Mountains. The uplifted area consists of the most external segment of the Jura fold-and-thrust belt as well as northerly adjacent parts of the intra-continental Rhine-Bresse Transfer Zone.

Relative uplift of this area, amounting to a maximum of 170 m (Deluz) translates into a minimum uplift rate of 0.05+/- 0.02 mm/yr. This is in good agreement with the results of geomorphic studies in adjacent areas. The Plio-Pleistocene evolution of the Ognon and Doubs River drainage basins indicates that it differential uplifts was at least partly driven by tectonic contraction that post-dates the main deformation phase of the thin-skinned Jura fold-and-thrust belt.

Two different types of post-Pliocene deformation were identified. Firstly, basement-involving, thick-skinned deformation, documented by reflection-seismic data and resulting in partial inversion of the Rhine-Bresse Transfer Zone by transpression. This type of deformation is still active today as shown by the seismicity of the region. Secondly, there is geomorphic evidence for localized active folding within the Besançon Zone. This deformation is associated with relatively high local uplift rates (e.g. 0.17 +/- 0.03 mm/yr along the Citadelle Anticline) and apparently enhanced by focused Pleistocene river incision that occurs in response to the regional relative rock uplift. According to numerical models this observation suggests that the Mesozoic cover sequence is shortened under regional horizontal compression simultaneously with river incision and thus during the Pleistocene. Thereby deformation of the Mesozoic cover is most likely decoupled from the immediately underlying basement. Hence our observations suggest Pleistocene, apparently aseismic deformation along the same Triassic evaporite horizon that was active during the formerly thin-skinned Jura fold-and-thrust

belt. Although ongoing thin-skinned tectonics cannot be excluded in this area the recorded décollement related deformation is more likely of local nature in that it roots into a basement fault nearby and hence does not necessarily indicate ongoing distant push from the Alps. As a consequence apparently aseismic shallow folding and thrusting is locally superimposed on basement rooted, seismogenic inversion tectonics within the Besancon Zone.

Our results show a variety of positive feedbacks between uplift, erosion and active deformation during the Plio-Peistocene evolution of the Jura fold-and-thrust belt and its foreland. Uplift and erosion, at least partly in response to basement involving inversion tectonics, localized active deformation within the internal parts of the Jura fold-and-thrust belt.

Acknowledgements

The first authors would like to thank the past and present EUCOR URGENT team in Basel especially his neotectonic fate-mates Marielle Fraefel and Stephane Kock. Matthias Tischler provided heavy mineral sample preparation experience which saved tremendous amounts of time. Vincent Bichet, Michel Campy, Fritz Schlunegger, Michael Schnellmann, Tim Vietor and Andreas Wetzel are very much thanked for sharing field trips and discussions.

References

Andel van, T.H., 1950. Provenance, transport and deposition of Rhine sediments. Wageningen, (Veenman & Zonen), 129p.

Baer, M. et al., 2007. Earthquakes in Switzerland and surrounding regions during 2006. Swiss Journal of Geosciences, 100: 517-528.

Baer, M. et al., 2005. Earthquakes in Switzerland and surrounding regions during 2004. Eclogae geol. Helv., 98(3): 407-418.

Becker, A., 2000. The Jura Mountains - an active foreland fold-and-thrust belt? Tectonophysics, 321: 381-406.

Berger, J.P. et al., 2005. Paleogeography of the Upper Rhine Graben (URG) and the Swiss Molasse Basin (SMB) from Eocene to Pliocene. International Journal of Earth Sciences, 94: 697-710.

Bergerat, F. and Chorowicz, J., 1981. Etude des images Landsat de la zone tranformante Rhin-Saône (France). Geologische Rundschau, 70(1): 354-367.

Boenigk, W., 1982. Der Einfluss des Rheingraben-Systems auf die Flussgeschichte des Rheins. Z. Geomorph. N. F., 42: 167-175.

Boenigk, W., 1983. Schwermineralanalyse. Enke, Stuttgart, 158 pp.

Boenigk, W., 1987. Petrographische Untersuchungen juntertiärer und quartärer Sediments am linken Oberrhein. Jber. u. Mitt. oberrh. geol. Ver., 69: 357-394.

Boigk, H. and Schöneich, H., 1970. Die Tiefenlage der Permbasis im nördlichen Teil des Oberrheingrabens. In: J.H. Illies and S. Mueller (Editors), Graben Problems. Proceedings of an International Rift Symposium held in Karlsruhe 1968, International Upper Mantle Project. E. Schweitzerbart'sche, Stuttgart, pp. 45-55.

Bonvalot, J., 1974. Les cailloutis de la Forêt de Chaux (Jura): leurs rapports avec les matériaux détritiques de Sundgau et du Nord de la Bresse, Université de Dijon, Dijon, 89pp.

Bourgeois, O., Ford, M., Diraison, C., Le Carlier de Veslud, M. and Gerbault, R., Pik, N., 2007. Separation of rifting and lithospheric folding signatures in the NW-Alpine foreland. International Journal of Earth Sciences, 2007(6): 1003-1031.

Bull, W., B., 1990. Stream-terrace genesis: implications for soil development. Geomorphology, 3: 351-367.

Bull, W.B. and McFadden, L.D., 1977. Tectonic Geomorphology north and south of Garlock fault, California. In: D.O. Doehring (Editor), Geomorphology in arid regions. Proceedings of the 8th Annual Geomorphology Symposium. Universtiy of New York, Binghampton, pp. 115-138.

Buoncristiani, J.-F. and Campy, M., 2004. The paleogeography of the last two glacial episodes in France: the Alps and Jura. In: J. Ehlers and P.L. Gibbard (Editors), Quaternary glaciations - extent and chronology. Part 1: Europe. Elsevier, pp. 113-118.

Burkhard, M., 1990. Aspects of the large-scale Miocene deformation in the most external part of the Swiss Alps (Subalpine Molasse to Jura fold belt). Eclogae Geologicae Helvetiae, 83(3): 559-583.

Burkhard, M. and Sommaruga, A., 1998. Evolution of the western Swiss Molasse basin: structural relations with the Alps and the Jura belt. In: A. Mascle, C. Puidgefàbregas, H.P. Luterbacher and M. Fernàndez (Editors), Cenozoic Foreland Basins of Western Europe. Geological Society, London, pp. 279-298.

Campy, M., 1984. Signification dynamique et climatique des formations et terrasses fluviatiles dans un environnement de moyenne montagne. Bulletin de l'Association française pour l'Etude du Quaternaire, 1: 87-92.

Cederbom, C.E., Sinclair, H.D., Schlunegger, F. and Rahn, M., 2004. Climate-induced rebound and exhumation of the European Alps. Geology, 32(8): 709-712, doi: 10.1130/G20491.1.

Chauve, P., Campy, M., Pernin, C. and Morre-Biot, N., 1983. Carte géolog. France (1/50000), feuille Pesmes, XXXII-23, BRGM.

Chauve, P., Enay, R., Fluck, P. and Sittler, C., 1980. L'Est de la France (Vosges, Fossé Rhénan, Bresse, Jura). Annales scientifiques de l'Université de Besançon, 4(1): 3-80.

Chauve, P., Kerrien, Y. and Pernin, C., 1979. Carte géolog. France (1/50000), feuille Dole XXXII-24, BRGM.

Contini, D. et al., 1973. Carte géolog. France (1/50000), feuille Montebeliard, XXXV-22, BRGM.

Contini, D. and Theobald, N., 1974. Relations entre le Fossé rhenan et le Fossé de la Saône. Tectonique des régions sous vosgiennes et prejurrassiennes. In: J.H. Illies and K. Fuchs (Editors), Approaches to Taphrogenesis. Sc. Report., Stuttgart, pp. 310-321.

Coromina, G. and Fabbri, O., 2004. Late Palaeozoic NE-SW ductile-brittle extension in the La Serre horst, eastern France. Comptes Rendus Geosciences, 336(1): 75-84.

Davis, D., Suppe, J. and Dahlen, F.A., 1983. Mechanics of fold-and-thrust-belts and accretionary wedges. Journal of Structural Geology, 88: 1153-1172.

Debrand-Passard, S. and Courbouleix, S. (Editors), 1984. Synthèse Géologique du Sud-Est de la France, volume 2: Atlas comprenant 64 planches en couleurs. Mémoire du Bureau de recherches géologiques et minières, 126. BRGM, 614 pp.

DeCelles, P.G. and Mitra, G., 1995. History of the Sevier orogenic wedge in terms of critical taper models, northeast Utah and southwest Wyoming. Geological Society of America Bulletin, 107(4): 454-462.

Dèzes, P., Schmid, S.M. and Ziegler, P.A., 2004. Evolution of the European Cenozoic Rift System: interaction of the Alpine and Pyrenean orogens with their foreland lithosphere. Tectonophysics, 389(1-2): 1-33.

Dreyfuss, M. and Glangeaud, L., 1950. La valée de Doubs et l'évolution morphotectonique de la région bisontine. Annales scientifiques de l'Université de Besançon, 5: 2.

Dreyfuss, M. and Kuntz, G., 1969. Carte géolog. France (1/50000), feuille Besancon, XXXII-23, BRGM.

Dreyfuss, M. and Kuntz, G., 1970. Carte géolog. France (1/50000), feuille Gy, XXXIII-22, BRGM.

Dreyfuss, M. and Théobald, N., 1972. Carte géolog. France (1/50000), feuille Baume-les-Dames, XXXIV-22, BRGM.

Fejfar, O., Heinrich, W.-D. and Lindsay, E.H., 1998. Updating the Neogene rodent biochronology in Europe. Mededelingen Nederlands Instituut voor Toegepaste Geowetenschappen, TNO 60: 533-554.

Giamboni, M., Ustaszewski, K., Schmid, S.M., Schumacher, M.E. and Wetzel, A., 2004a. Plio-Pleistocene Transpressional Reactivation of Paleozoic and Paleogene Structures in the Rhine-Bresse transform Zone (northern Switzerland and eastern France). International Journal of Earth Sciences, 93(2): 207–223, DOI: 10.1007/s00531-003-0375-2.

Giamboni, M., Wetzel, A., Niviere, B. and Schumacher, M., 2004b. Plio-Pleistocene folding in the southern Rhinegraben recorded by the evolution of the drainage network (Sundgau area: northwestern Switzerland and France). Eclogae Geol Helv, 97: 17-31.

Goguel, J. and Dreyfuss, M., 1965. Carte géolog. France (1/50000), feuille Vercel, XXXIV-23, BRGM.

Hagedorn, E.M., 2004. Sedimentpetrographie und Lithofazies der jungtertiären und quartären Sedimente im Oberrheingebiet. unpublished PhD-Thesis Thesis, University of Cologne, 310 pp.

Hagedorn, E.M. and Boenigk, W., 2008. The Pliocene and Quaternary sedimentary and fluvial history in the Upper Rhine Graben based on heavy mineral analyses. Netherlands Journal of Geosciences, 87(1): 21-31.

Hinsken, S., Ustaszewski, K. and Wetzel, A., 2007. Graben width controlling syn-rift sedimentation: the Palaeogene southern Upper Rhine Graben as an example. International Journal of Earth Sciences, 96(6): 979-1002.

Illies, J.H., 1972. The Rhinegraben rift system - plate tectonics and transform faulting. Geophysical Surv., 1: 27-60.

Kälin, D., 1997. Litho- und Biostratigraphie der mittel- bis obermiozänen Bois de Raube-Formation (Nordwestschweiz). Eclogae Geologicae Helvetiae, 90(1): 97-114.

Kastrup, U. et al., 2004. Stress field variations in the Swiss Alps and the northern Alpine foreland derived from inversion of fault plane solutions. J. Geophys. Res., 109(B01402): doi:10.1029/2003JB002550.

Kuhlemann, J., Frisch, W., Szekely, B., Dunkl, I. and Kazmer, M., 2002. Post-collisional sediment budget history of the Alps: Tectonic versus climatic control. International Journal of Earth Sciences, 91: 818-837.

Lacombe, O., Angelier, J., Byrne, D. and Dupin, J., 1993. Eocene-Oligocene tectonics and kinematics of the Rhine-Saone continental transform zone (Eastern France). Tectonics, 12(4): 874-888.

Laubscher, H., 1961. Die Fernschubhypothese der Jurafaltung. Eclogae Geologicae Helvetiae, 54(1): 222-282.

Laubscher, H., 1970. Grundsätzliches zur Tektonik des Rheingrabens. In: J.H. Illies and S. Mueller (Editors), Graben Problems. Proceedings of an International Rift Symposium held in Karlsruhe 1968, International Upper Mantle Project. E. Schweitzerbart'sche, Stuttgart, pp. 79-86.

Laubscher, H., 1972. Some overall aspects of Jura dynamics. American Journal of Science, 272: 293-304.

Liniger, H., 1966. Das Plio-Altpleistozäne Flussnetz der Nordschweiz. Regio Basil., 7: 158-177.

Liniger, H., 1967. Pliozän und Tektonik des Jura Gebirges. Eclogae Geol Helv, 60(2): 407-490.

Liniger, H. and Hofmann, P., 1965. Das Alter der Sundgauschotter westlich von Basel. Eclogae Geol Helv, 58(1): 215-230.

Madritsch, H., Kounov, A., Schmid, S.M. and Fabbri, O., 2008, submitted. Multiple fault reactivation within the intracontinental Rhine-Bresse Transfer Zone (La Serre Horst, Eastern France).

Madritsch, H. et al., 2008 submitted. Incision boosted buckling: Field evidence from an active fold at the front of the Jura mountains. Geology.

Madritsch, H., Schmid, S.M. and Fabbri, O., 2008 in press. Interactions of thin- and thick-skinned tectonics along the northwestern front of the Jura fold-and-thrust-belt (Eastern France). Tectonics.

Martin, J. and Mercier, E., 1996. Héritage distensif et structuration chevauchante dans une chaîne de couverture : apport de l`équilibrage par modélisation géométrique dans le Jura nord-occidental. Bull. Soc. Géol. France, 167(1): 101-110.

Matte, P., 1986. Tectonics and plate tectonics model for the Variscian belt of Europe. Tectonophysics, 126(2-4): 329-374.

Mayer-Rosa, D. and Cadiot, B., 1979. Review of the 1356 Basel earthquake: basic data. Tectonophysics, 53: 325-333.

Mercier, J.L. and Jeser, N., 2004. The glacial history of the Vosges Mountains. In: J. Ehlers and P.L. Gibbard (Editors), Quaternary glaciations - extent and chronology. Part 1: Europe. Elsevier, pp. 113-118.

Meyer, B., Lacassin, R., Brulhet, J. and Mouroux, B., 1994. The Basel 1356 earthquake: which fault produced it? Terra Nova, 6: 54-63.

Mosar, J., 1999. Present-day and future tectonic underplating in the western Swiss Alps: reconciliation of basement/wrench-faulting and décollement folding of the Jura and Molasse basin in the Alpine foreland. Earth and Planetary Science Letters, 173, 143-155.

Müller, W.H., Naef, H. and Graf, H.R. (Editors), 2002. Geologische Entwicklung der Nordschweiz, Neotektonik und Langzeitszenarien, Zürcher Weinland. NAGRA Technischer Bericht, 99-08. NAGRA, Wettingen, 226 pp.

Nivière, B. and Marquis, G., 2000. Evolution of terrace risers along the Upper Rhine Graben inferred from morphologic dating methods: evidence of climatic and tectonic forcing. Geophysical Journal International, 141(3): 577-594.

Nivière, B. and Winter, T., 2000. Pleistocene northwards fold propagation of the Jura within the southern Upper Rhine Graben: seismotectonic implications. Global and Planetary Change, 27: 263–288.

Peters, G. and van Balen, R.T., 2007. Tectonic geomorphology of the noertern Upper Rhine Graben, Germany. Global and Planetary Change, 58: 310-334.

Petit, C., Campy, M., Chaline, J. and Bonvalot, J., 1996. Major palaeohydrographic changes in Alpine foreland during the Pliocene-Pleistocene. Boreas, 25: 131-143.

Pfiffner, O.A., Erard, P. and Stäuble, M., 199t. Two cross sections through the Swiss Molasse Basin (lines E4-E6, W1, W7-W10). In: O.A. Pfiffner, P. Lehner, P. Heitzmann, S. Mueller and A. Steck (Editors), Deep structure of the Swiss Alps. Results of NRP 20. Birkhäuser, pp. 64-72.

Reinecker, J., Heidbach, O., Tingay, M., Sperner, B. and Mueller, B., 2005. The 2005 release of the World Stress Map (available online at www.world-stress-map.org).

RéNaSS, R.N.d.S.S., 2007. Réseau National de Surveillance Sismique, http://renass.u-strasbg.fr/. In: E.e.O.d.S.d.l.T.d. Strasbourg (Editor).

Rotstein, Y. and Schaming, M., 2004. Seismic Reflection evidence for thick-skinned tectonics in the northern Jura. Terra Nova, 16: 250-256.

Ruhland, M., 1959. Une dislocation majeure du socle Vosgien dans la haute Vallée de l' Ognon. Bull. Serv. Carte Géol. Als. Lorr., 12: 61-64.

Schmid, S.M., Pfiffner, O.A., Froitzheim, N., Schönborn, G. and Kissling, E., 1996. Geophysical-geological transect and tectonic evolution of the Swiss-Italian Alps. Tectonics, 15: 1036-1064.

Schumacher, M.E., 2002. Upper Rhine Graben: Role of preexisting structures during rift evolution. Tectonics, 21(1): 6-1-6-17.

Simpson, G., 2004. Role of river incison in enhancing deformation. Geology, 32(4): 341-344.

Sindowski, K.H., 1949. Results and problems of heavy mineral analysis in Germany; a review of sedimentary-petrological papers, 1936-148. J. sedim. Petrol., 19: 3-25.

Sissingh, W., 1998. Comparative Tertiary stratigraphy of the Rhine Graben, Bresse Graben and Molasse Basin: correlation of Alpine foreland events. Tectonophysics, 300: 249-284.

Smit, J.H.W., Brun, J.P. and Sokoutis, D., 2002. Deformation of brittle-ductile thrust wedges in experiments and nature. Journal of Geophysical Research, 108, NO. B10, 2480, doi:10.1029/2002JB002190.

Sommaruga, A., 1997. Geology of the Central Jura and the Molasse Basin: New insights into an evaporite-based foreland fold and thrust belt, Schweizerische Akademie der Naturwissenschaften, Neuchatel, 176 pp.

Tesauro, M., Hollenstein, C., Egli, R., Geiger, A. and Kahle, H.-G., 2005. Continuous GPS and broad-scale deformation across the Rhine Graben and the Alps. International Journal of Earth Sciences, 94: 525-537.

Théobald, N., Schweitzer, M. and Hudeley, H., 1976. Carte Géologique de la France à 1/50 000 Mulhouse, feuille XXXVII-XXXVIII-20. Ministère de l'industrie et de la recherche, Service Géologique National, Orléans.

Theobald, N., Vogt, H. and Wittmann, O., 1977. Néotectonique de la partie méridionale du bloc rhénan. Bull. B.R.G.M., 2(4): 121-140.

Thiebaut, J., Theobald, N. and Hudeley, H., 1974. Carte géolog. France (1/50000), feuille Giromagny, XXXV-22, BRGM.

Ustaszewski, K. and Schmid, S.M., 2006. Control of preexisting faults on geometry and kinematics in the northernmost part of the Jura fold-and-thrust belt. Tectonics, 25.

Ustaszewski, K. and Schmid, S.M., 2007. Latest Pliocene to recent thick-skinned tectonics at the Upper Rhine Graben - Jura Mountains junction. Swiss Journal of Geosciences, 100(2): 293-312.

Zeilinger, G., Schlunegger, F. and Simpson, G., 2005. The Oxaya anticline (northern Chile): a buckle enhanced by river incision? Terra Nova, 17: 368-375.

Ziegler, P. and Dèzes, P., 2007. Cenozoic uplift of Variscian Massifs in the foreland of the Alpine foreland: Timing and controlling mechanisms. Global and Planetary Change, 58: 237-269.

Ziegler, P.A., 1990. Geological Atlas of Western and Central Europe. Shell Internationale Petroleum Maatschappij B.V., Den Haag, 1-238 pp.

Ziegler, P.A., 1992. European Cenozoic rift system. Tectonophysics, 208: 91-111.

Ziegler, P.A., Bertotti, G. and Cloetingh, S.A.P.L., 2002. Dynamic processes controlling foreland development - roke of mechanical (de)coupling of orogenic wedges and forelands. In: B. Bertotti, K. Schulmann and S.A.P.L. Cloetingh (Editors), Continental collision and the tectono-sedimentary evolution of forelands. EUG Stephan Mueller Publication Series, pp. 17-56.

Ziegler, P.A. and Fraefel, M., 2008 submitted. Response of drainage systems to Neogene evolution of Jura fold-thrust belt and Upper Rhine Graben. Swiss Journal of Geosciences.

Ziegler, P.A., Schumacher, M.E., Dèzes, P., van Wees, J.-D. and Cloetingh, S., 2004. Post-Variscan evolution of the lithosphere in the Rhine Graben area: constraints from subsidence modelling. In: M. Wilson (Editor), Permo-Carboniferous magmatism and rifting in Europe. Geological Society of London Special Publications. Geological Society, pp. 289-317.

Chapter 6
Summary and conclusions

This PhD study sheds new light on the structural evolution and neotectonics of the Rhine-Bresse Transfer Zone that coincides with the outermost front of the Alpine orogen formed by the Jura fold-and-thrust belt. As such this area represents a natural field laboratory that allows investigating the the progressive evolution of this continental collisional foreland and also drawing conclusions on the present day geodynamics of the northwestern front of the Alpine orogenic system. In the following we summarize the most important results and conclusions of the thesis with reference to the relevant chapters. Furthermore the needs for future research are outlined.

6.1 Structural evolution of the Rhine-Bresse Transfer Zone

The structural evolution of the Rhine Bresse Transfer Zone, as documented during this investigation may be subdivided into 7 time slices:

6.1.1. Late Carboniferous to Late Permian

During a latest stage of NE-SW directed crustal extension related to Post-Variscian orogenic collapse, the Burgundy Trough formed along a transcontinental shear zone. The La Serre Horst Structure represents an internal basement high within this graben system that includes a pre-existing metamorphic core complex **(Chapter 2)** (Coromina and Fabbri 2004). The horst and graben structures and related extensional faults were later sealed by the Early Triassic sandstones of Buntsandstein formation.

6.1.2. Middle Jurassic to Early Cretaceous

The zircon fission track data obtained during this investigation **(Chapter 2)** indicates that the area around the La Serre Horst was affected by a heating event during Middle Jurassic to Early Cretaceous. This heating event has also been recorded in neighbouring parts of the European Cenozoic Rift System such as the Southern Upper Rhine Graben (Timar-Geng et al. 2006) and seems to be a regional phenomenon. It may indicate enhanced hydrothermal activity during a phase of crustal extension along the continental margin of the Alpine Tethys (Wetzel et al. 2000). This extension possibly also involved minor reactivation of the pre-existing Paleozoic fault system.

6.1.3. Middle Cretaceous to Late Paleocene

It is unclear what happened within the area of the future Rhine-Bresse Transfer Zone during that time span. Fission track data suggests slow cooling of the Paleozoic basement and its Permo-Triassic cover at a high geothermal gradient until the end of the Eocene **(Chapter 2)**. While this cooling may be related to thermal relaxation following the Middle Jurassic to Early Cretaceous heating event it could also indicate large scale uplift and erosion that is widely recognized throughout the north-western Alpine foreland by a regional unconformity and was probably induced by a phase of N-S directed intraplate compression (Ziegler 1986).

6.1.4 Middle-Late Eocene to Oligocene

The Eo-Oligocene formation of the RBTZ as part of the European Cenozoic Rift System was analyzed in detail by a combination of thermochronological, subsurface structural and kinematic methods **(Chapter 2).** Fission track data indicate a significant cooling between 38 to 32 Ma around the La Serre Horst Structure. This suggests that this Late Paleozoic structural high experienced substantial reactivation during Eo-Oligocene extension that contributed to the formation of the La Serre Horst and its exhumation. This was furthermore constrained by subsurface investigation using seismic reflection data that illustrated the extensional reactivation of the Late Paleozoic Burgundy Trough System during the formation of the Rhine-Bresse Transfer Zone.

The structural inheritance from the Late Paleozoic Trough System resulted in complex fault patterns and local stress field perturbations especially in the surroundings of the pre-existing Paleozoic horst structure. Significant extension along the RBTZ was achieved by ENE-WSW striking normal faults, oriented parallel to the pre-existing Late Paleozoic graben. These structures are highly oblique to a second but subordinate set of normal faults striking NNE-SSW and oriented parallel to the dominant strike of the Rhine and Bresse Graben rifts. Hence, reactivation of Paleozoic structures in the RBTZ is of extensional rather than of strike-slip character and resulted in the formation of an oblique rift segment under overall WNW-ESE extension. These observations demonstrate the significance of pre-existing structures for rift localization and kinematics.

6.1.5. Early to Middle Miocene

In Early Miocene large scale uplift caused the exhumation of the graben flanks of the Southern Upper Rhine Graben. The uplift has has been interpreted as reflecting the outward migration of the Alpine flexural fore-bulge (Laubscher, 1992) or as being the effect of collision-related compressional deformation involving lithospheric folding (Dèzes et al., 2004) and most likely also affected the Rhine-Bresse Transfer Zone. The fission track data obtained during this study indicate that the

Paleozoic basement of the La Serre Horst and its Permo-Triassic cover already reached temperatures lower than the partial annealing zone of apatite prior to the Early Miocene onset of uplift **(Chapter 2)**. Hence, the uplift could not be detected thermochronologically. Nevertheless it is documented by the widely erosion of almost all Oligocene rift sediments throughout that area.

6.1.6. Late Miocene to Early Pliocene

Neogene NW-SE directed foreland contraction, due to the latest stages of Alpine collision, induced two different styles of deformation in the area of the Rhine-Bresse Transfer Zone: (i) the formation of the thin-skinned Jura fold-and-thrust belt that was decoupled from the underlying non-deformed crystalline basement along a Triassic décollement layer, and (ii) basement rooted thick-skinned tectonics associated with the reactivation and inversion of pre-existing Late Paleozoic and Paleogene normal faults of the Rhine-Bresse Transfer zone and thus rooted within the underlying crystalline basement **(Chapter 3)**.

The northwestern most segment of the thin-skinned Jura fold-and-thrust belt, defined as the Besançon Zone, encroached onto the pre-existing Late Paleozoic to Paleogene normal faults belonging to the RBTZ during Late Miocene to Early Pliocene. Internal fold-and thrust bundles and the propagation front of this fold-and-thrust belt segment were sketched out by these pre-existing faults. During fold-and-thrust belt propagation the direction of maximum shortening fanned out from N-S in the east to E-W in the west.

Thick-skinned inversion tectonics started in Late Pliocene times (4.2 Ma) at the earliest and resulted in partial inversion of the RBTZ and basement rooted re-deformation of structures that formed during thin-skinned deformation. This type of deformation is best documented along the prominent Avant-Monts Fault that represents the outermost inverted fault structure in the northwestern Alpine foreland yet reported. It also coincides with the outermost thrust fault of the Jura fold-and-thrust belt (the Chailluz Thrust). Following the definition of Lacombe and Mouthereau (1999) the trace of the Avant-Monts fault thus forms the northwestern mountain and reactivation front of the Alpine orogen.

These results vividly illustrate the spatial and temporal interplay between thin- and thick-skinned tectonics during foreland deformation. In case of the northwestern Jura front initial thin-skinned tectonics were later overprinted by thick-skinned inversion tectonics (Ustaszewski and Schmid, 2007). Since both deformation processes – thin- and thick-skinned - were largely controlled by pre-existing fault geometries this investigation particularly stresses the importance of a solid knowledge about the pre-collisional tectonic history of the study area. The combination of subsurface, micro-tectonic and geomorphic data proved to be particularly powerful when investigating the spatial and temporal relationships between different tectonic styles and when elucidating the foreland deformation sequence.

6.1.7. Late Pliocene to recent

Geomorphic methods were applied to study the Late Pliocene to recent tectonic history of the Rhine-Bresse Transfer Zone **(Chapter 4, 5).** In this context Pliocene and Pleistocene alluvial sediments and the evolution of paleo- and recent drainage system that controlled their deposition were used as geomorphic marker horizons that recorded slow, long term deformation. A first marker was provided by the paleo-topographic reconstruction of the Middle Pliocene Sundgau - Forêt de Chaux Gravels shed by a braided river system that was part of the Aare-Doubs drainage system (Liniger, 1967; Giamboni et al., 2004) Comparing the Plio-Pleistocene valley evolution related to the Ognon and Doubs drainage areas, based on the sedimentological and geomorphic record, provided a second geomorphic marker.

Relative rock uplift was recorded along the Rhine-Bresse Transfer Zone on a regional scale by post-2.9 Ma differential erosion of the Sundgau - Forêt de Chaux Gravels. Uplifted gravels remnants, identified by heavy mineral analysis, permitted to determine the paleo-topography and establish a latest Pliocene to recent minimum regional rock uplift rate of 0.05 +/- 0.02 mm/yr. Relative rock uplift and erosion of the Sundgau-Forêt de Chaux Gravels throughout the area was most likely caused by a combination of subsidence in the Rhine and Bresse Grabens and thick-skinned inversion of the Rhine-Bresse Transfer Zone. The uplift also substantially affected the Pleistocene evolution of the modern drainage basins of the Ognon and Doubs and hence appears to have continued into Pleistocene times.

Differential up warping of a sequence of paleo-meanders of the Doubs River along the axis of the Citadelle Anticline near Besançon provided the first example for active folding within the internal parts of the Jura fold-and-thrust belt **(Chapter 4)**. Post Middle to Late Pleistocene folding has been found to occur contemporaneously with localized along strike river incision. This process is associated with relatively higher local rock uplift rates that reach 0.17 +/- 0.02 mm/yr and is apparently aseismic. Detailed, multidisciplinary investigations that applied structural, geophysical, geodetic and geochronological methods led to the conclusion that river incision localized and enhanced the observed active deformation. This unique field example thus allowed for demonstrating feedback processes between active folding and erosion that were theoretically predicted by numerical modeling.

6.2. Neotectonic scenario of the Rhine Bresse Transfer Zone and implications for the present-day geodynamics of the northwestern Alpine front

The present day tectonic activity of the Rhine-Bresse Transfer Zone is only vaguely defined by surveys of seismicity and by mid-term geodetic investigations. Combination of this data with the structural and geomorphic results obtained during this study allowed for a much more precise characterization **(Chapters 3, 4, 5)**.

The analysis of focal depths of earthquakes of the study area and its surroundings clearly shows that the present day deformation of the region also involves the crystalline basement. Throughout the central Jura fold-and-thrust belt and the Rhine-Bresse Transfer Zone, earthquakes are mostly found far below the supposed thin-skinned décollement horizon. Focal mechanisms of these deep earthquakes underneath the formerly thin-skinned Jura fold-and-thrust belt mostly feature strike-slip regimes. In contrast to the neighboring Rhine Graben area, which is characterized by a higher seismicity and earthquake focal mechanism that indicate a strike-slip or transtensional tectonic regime (Kastrup et al. 2004), the deep earthquakes observed within the Rhine-Bresse Transfer Zone also reveal pure to oblique thrust faulting mechanisms (Baer et al., 2005). The direction of the maximum principal stress ($\sigma 1$) is mostly within a western or northern quadrant and approximately strikes NW-SE. Therefore the seismotectonics of the region suggest that present-day deformation is thick-skinned. The compressive to dextral transpressive inversion of the Rhine-Bresse Transfer Zone and the underlying Permo-Carboniferous Burgundy Trough is potentially ongoing. This process may reflect presently active tectonic underplating in the northwestern Alpine foreland (Mosar, 1999) and is possibly responsible for significant past and future earthquakes (Meyer et al. 1994).

The uplifted Pleistocene paleo-meanders along the Citadelle Anticline represent the first evidence for active folding within the internal parts of the Jura fold-and-thrust belt (e.g. the Besançon Zone) whose present day tectonic activity is a matter of long lasting scientific debates (Becker, 2000). This fold structure also presents a unique field example that vividly illustrates the positive feedbacks between tectonic deformation and erosional surface processes. The mechanical conditions for such process coupling as defined by numerical models (Simpson, 2004) suggest that deformation is caused by buckling in response to regional horizontal compression. Moreover positive feedbacks have only been observed whenever horizontal compression occurs at the same time as river incision. Therefore our field observations imply that Pleistocene compression and shortening of the Mesozoic cover sequence within the Besançon Zone is ongoing at present and, at least locally, decoupled from the underlying basement. The decoupling horizon is most likely formed by the same Triassic evaporites that enabled the formation of the formerly thin-skinned Jura fold-and-thrust belt. Thus, ongoing décollement tectonics within the Besançon Zone cannot be entirely excluded. However considering the structural and seismotectonics observations outlined above the recorded décollement related and erosion controlled deformation is more likely of local nature in that it is induced by basement fault reactivation in the nearby Alpine foreland (e.g. the Rhine-Bresse Transfer Zone itself or the Molasse basin Piffner et al., 1997) rather than rooted in Central Alps as it was during classical thin-skinned Jura tectonics in Late Miocene to Early Pliocene times (e.g. “Fernschub”; Laubscher, 1961).

In summary the neotectonic scenario in the Rhine-Bresse Tranfer Zone is characterized by two superimposed processes that take place at different deformation rates and are hence locally decoupled from each other: seismogenic deformation within the basement and erosion controlled - apparently aseismic - deformation of the Mesozoic cover. It appears that while the evolution of the RBTZ was

largely controlled by the repeated reactivation of pre-existing structures, its present tectonic activity is to some extent also controlled by surface processes and involves positive feedbacks between large-scale post-Pliocene rock uplift, enhanced Pleistocene erosion and active deformation.

6.3. Future research perspectives

While the results of this PhD study yield answers to some questions they raise plenty of new ones that should be addressed during future investigations. Some of these are briefly outlined below:

The Neogene cooling and exhumation history of the La Serre Horst could not be sufficiently well constrained by this study. The question remains open as to what extent Early Miocene uplift, which is recorded in the area of the Southern Upper Rhine Graben, affected this basement high. Low temperature thermochronology (e.g. zircon/apatite (U-Th)/He) could possibly help to clarify this question.

Within the area of investigation, the Middle Pliocene Sundgau-Forêt de Chaux gravels do not define the front of the thin-skinned Jura fold-and-thrust belt as inferred further to the east and west but were deposited and deformed within its most external thrust segment (e.g. the Besançon Zone). Thus, the timing of the end of thin-skinned deformation and the transition to thick-skinned tectonics is still only vaguely defined for this area and needs further research.

The Citadelle Anticline represents a unique field example to study the interaction between active folding and erosion. OSL dating performed by this study provided first age constraints regarding the timing of river incision and deformation. Further OSL dating from deeper levels of the alluvial meander deposits could help to better constrain and eventually refine these ages. Moreover, several caves along the Doubs could potentially provide possibilities to reconstruct the incision history of this river by means of U-Th dating of speleothems and/or calcite crusts. Such an approach could be useful to determine incision rates within different tectonic units along the river course and thus detect areas of active deformation. This should be complemented by revised bedrock terrace mapping on the basis of digital elevation models of higher resolution.

References:

Baer, M., Deichmann, N., Braunmiller, J., Husen, S., Fäh, D., Giardini, D., Kästli, P., Kradolfer, U. and Wiemer, S., 2005. Earthquakes in Switzerland and surrounding regions during 2004. Eclogae Geologicae Helvetiae, 98, 407-418.

Becker, A., 2000. The Jura Mountains - an active foreland fold-and-thrust belt? Tectonophysics, 321: 381-406.

Coromina, G. and Fabbri, O., 2004. Late Palaeozoic NE-SW ductile-brittle extension in the La Serre horst,eastern France. Comptes Rendus Geosciences, 336(1): 75-84.

Dèzes, P., Schmid, S.M. and Ziegler, P.A., 2004. Evolution of the European Cenozoic Rift System: interaction of the Alpine and Pyrenean orogens with their foreland lithosphere. Tectonophysics, 389(1-2): 1-33.

Giamboni, M., Ustaszewski, K., Schmid, S.M., Schumacher, M.E. and Wetzel, A., 2004. Plio-Pleistocene Transpressional Reactivation of Paleozoic and Paleogene Structures in the Rhine-Bresse transform Zone (northern Switzerland and eastern France). Int. J. Earth Sci., 93(2): 207–223.

Kastrup, U., Zoback, M.L., Deichmann, N., Evans, K.F., Giardini, D. and Michael A.J., 2004. Stress field variations in the Swiss Alps and the northern Alpine foreland derived from inversion of fault plane solutions. J. Geophys. Res., 109, doi:10.1029/2003JB002550.

Lacombe, O. and Mouthereau, F., 1999. Qu'est-ce que le front des orogènes? L´exemple de l´orogène pyrénéen. C.R. Acad. Sci. Paris, Science de la terre et des planètes, 329: 889-896.

Laubscher, H., 1961. Die Fernschubhypothese der Jurafaltung. Eclogae Geologicae Helvetiae, 54, 222-282.

Laubscher, H., 1992. Jura kinematics and the Molasse Basin. Eclogae Geologicae Helvetiae, 85(3): 653-675.

Liniger, H., 1967. Pliozän und Tektonik des Jura Gebirges. Eclogae Geologicae Helvetiae, 60(2): 407-490.

Meyer, B., Lacassin, R., Brulhet, J. and Mouroux, B., 1994. The Basel 1356 earthquake: which fault produced it? Terra Nova, 6: 54-63.

Mosar, J., 1999. Present-day and future tectonic underplating in the western Swiss Alps: reconciliation of basement/wrench-faulting and décollement folding of the Jura and Molasse basin in the Alpine foreland. Earth and Planetary Science Letters, 173, 143-155.

Pfiffner, O.A., Erard, P. and Stäuble, M., 1997. Two cross sections through the Swiss Molasse Basin (lines E4-E6, W1, W7-W10). In: O.A. Pfiffner, P. Lehner, P. Heitzmann, S. Mueller and A. Steck (Editors), Deep structure of the Swiss Alps. Results of NRP 20. Birkhäuser, pp. 64-72.

Simpson, G., 2004. Role of river incison in enhancing deformation. Geology, 32(4): 341-344.

Timar-Geng, Z., Fügenschuh, B., Wetzel, A. and Dresmann, H. 2006. Low-temperature thermochronology of the flanks of the southern Upper Rhine Graben. Int. J. Earth Sci. 95: 685-702.

Ustaszewski, K. and Schmid, S.M., 2007. Latest Pliocene to recent thick-skinned tectonics at the Upper Rhine Graben - Jura Mountains junction. Swiss Journal of Geosciences, 100(2): 293-312.

Wetzel, A., Allenbach, R. and Allia, V., 2003. Reactivated basement structures affecting the sedimentary facies in tectonically "quiescent" epicontinental Basin: an example from NW Switzerland. Sedimentary Geology 157: 153-172.

Ziegler, P., 1986. Geodynamic model for the Paleozoic crustal consolidation of Western and Central Europe. Tectonophysics, 126(2-4): 303-328.

List of references

Affolter, T. and Gratier, J.P., 2004. Map view retrodeformation of an arcuate fold-and-thrust belt: The Jura case. J. Geophys. Res., 109(B03404): doi:10.1029/2002JB002270.

Alvarez, W., 1999. Drainage on evolving fold-thrust belts: A study of transverse canyons in the Apennines. Basin Research, 11: 267-284.

Andel van, T.H., 1950. Provenance, transport and deposition of Rhine sediments. Wageningen, (Veenman & Zonen), 129p.

Anderson, E.M., 1942. The dynamics of faulting. Olivier and Boyed, pp. 206.

Angelier, J., 1989. From orientation to magnitudes in paleostress determinations using fault slip data. Journal of Structural Geology, 11(1-2): 37-50.

Angelier, J., 1990. Inversion of field data in fault tectonics to obtain the regional stress - III. A new rapid direct inversion method by analytical means. Geophysical Journal International, 103(2): 363-376.

Angelier, J. and Mechler, P., 1977. Sur une méthode graphique de recherche des contraintes principales également utilisable en tectonique et en seismologie: la méthode des dièdres droits. Bull. Soc. géol. France, 19(6): 1309-1318.

Baer, M. et al., 2007. Earthquakes in Switzerland and surrounding regions during 2006. Swiss Journal of Geosciences, 100: 517-528.

Baer, M. et al., 2005. Earthquakes in Switzerland and surrounding regions during 2004. Eclogae geol. Helv., 98(3): 407-418.

Barbarand, J., Lucazeau, F., Pagel, M. and Sérrane, O., 2001. Burial and exhumation history of the south eastern Massif Central (France) constrained by apatite fission-track thermochronology. Tectonophysics, 335: 275-290.

Beaumont, C., Fullsack, P. and Hamilton, J., 1992. Erosional control of active compressional orogens. In: K.R. McClay (Editor), Thrust Tectonics. Chapman Hall, London, pp. 1-18.

Becker, A., 2000. The Jura Mountains - an active foreland fold-and-thrust belt? Tectonophysics, 321: 381-406.

Becker, A. and Werner, D., 1995. Neotectonic state of stress in the Jura mountains. Geodinamica Acta, 8(2): 99-111.

Berger, J.P. et al., 2005. Paleogeography of the Upper Rhine Graben (URG) and the Swiss Molasse Basin (SMB) from Eocene to Pliocene. International Journal of Earth Sciences, 94: 697-710.

Bergerat, F., 1977. La fraturaction de l'avant-pays jurassien entre les fossés de la Saône et du Rhin. Analyse et essai d'interpretation dynamique. Revue de Géographie physique et de Géologie dynamique (2), 14(4): 325-338.

Bergerat, F., 1985. Deformations cassantes et champs de constrainte tertiares de la platforme carbonatée européene. Thèse de Doctorat-es-Sciences, Mém. Sci. Terre, Univ.P. et M. Curie, No. 85-87, Paris 315 pp.

Bergerat, F., 1987. Stress Fields in the European Platform at the time of Africa-Eurasia Collision. Tectonics, 6(2): 99-132.

Bergerat, F. and Chorowicz, J., 1981. Etude des images Landsat de la zone tranformante Rhin-Saône (France). Geologische Rundschau, 70(1): 354-367.

Bergerat, F. et al., 1990. Extensional tectonics and subsidence of the Bresse basin: an interpretation from ECORS data. In: F. Roure, P. Heitzmann and R. Polino (Editors), Deep Structure of the Alps. Vol. spec. Soc. Geol. It. Mémoire de la Société géologique de la Suisse, Zürich, pp. 145-156.

Boenigk, W., 1982. Der Einfluss des Rheingraben-Systems auf die Flussgeschichte des Rheins. Z. Geomorph. N. F., 42: 167-175.

Boenigk, W., 1983. Schwermineralanalyse. Enke, Stuttgart, 158 pp.

Boenigk, W., 1987. Petrographische Untersuchungen juntertiärer und quartärer Sediments am linken Oberrhein. Jber. u. Mitt. oberrh. geol. Ver., 69: 357-394.

Boigk, H. and Schöneich, H., 1970. Die Tiefenlage der Permbasis im nördlichen Teil des Oberrheingrabens. In: J.H. Illies and S. Mueller (Editors), Graben Problems. Proceedings of an International Rift Symposium held in Karlsruhe 1968, International Upper Mantle Project. E. Schweitzerbart'sche, Stuttgart, pp. 45-55.

Bolliger, T., Engesser, B. and Weidmann, M., 1993. Première découverte de mammifères pliocènes dans le Jura neuchâtelois. Eclogae geol. Helv., 86 (3): 1031-1068.

Bonjer, K.-P. et al., 1984. Seismicity and dynamics of the Upper Rhine Graben. J. Geophys., 55: 1-12.

Bonte, A., 1975. Carte géolog. France (1/50000), feuille Quingey, XXXIII-24, BRGM.

Bonvalot, J., 1974. Les cailloutis de la Forêt de Chaux (Jura): leurs rapports avec les matériaux détritiques de Sundgau et du Nord de la Bresse, Université de Dijon, Dijon, 89pp.

Bourgeois, O., Ford, M., Diraison, C., Le Carlier de Veslud, M. and Gerbault, R., Pik, N., 2007. Separation of rifting and lithospheric folding signatures in the NW-Alpine foreland. International Journal of Earth Sciences, 2007(6): 1003-1031.

Brandon, M.T., Roden-Tice, M.K. and Garver, J.I., 1998. Late Cenozoic exhumation of the Cascadia accretionary wedge in the Olympic Mountains, northwest Washington State. GSA Bulletin, 110: 985-1009.

Brockamp, O. and Zuther, M., 1983. Das Uranvorkommen Müllenbach/Baden-Baden, eine epigenetisch-hydrothermale Imrägnationslagerstätte in Sedimenten des Oberkarbon, Teil II: Das Nebengestein. Neus Jahrb. Mineral. Abh., 148: 22-33.

Brudy, M., Zoback, M.D., Fuchs, K., Rumel, F. and Baumgärtner, J., 1997. Estimation of the complete stress tensors to 8km depth in the KTB scientific drilling holes: implications for crustal strengh. J. Geophys. Res., 102: 18453-18475.

Buck, W.R. et al., 2007. Group Report: Surface enviromental effects on and of faulting. In: M. Handy, G. Hirth and N. Hovius (Editors), Tectonic faults, agents of change on a dynamic earth. Dahlem workshop reports. MIT press, Massachusetts.

Bull, W., B., 1990. Stream-terrace genesis: implications for soil development. Geomorphology, 3: 351-367.

Bull, W.B. and McFadden, L.D., 1977. Tectonic Geomorphology north and south of Garlock fault, California. In: D.O. Doehring (Editor), Geomorphology in arid regions. Proceedings of the 8th Annual Geomorphology Symposium. Universtiy of New York, Binghampton, pp. 115-138.

Buoncristiani, J.-F. and Campy, M., 2004. The paleogeography of the last two glacial episodes in France: the Alps and Jura. In: J. Ehlers and P.L. Gibbard (Editors), Quaternary glaciations - extent and chronology. Part 1: Europe. Elsevier, pp. 113-118.

Burbank, D., Meigs, A. and Brozovic, N., 1996a. Interactions of growing folds and coeval depositional systems. Basin Research, 8: 199-223.

Burbank, D.W. et al., 1996b. Bedrock incision, rock uplift and threshold hillslopes in the western Himalaya. Nature, 379: 505-510.

Burkhard, M., 1990. Aspects of the large-scale Miocene deformation in the most external part of the Swiss Alps (Subalpine Molasse to Jura fold belt). Eclogae Geologicae Helvetiae, 83(3): 559-583.

Burkhard, M. and Sommaruga, A., 1998. Evolution of the western Swiss Molasse basin: structural relations with the Alps and the Jura belt. In: A. Mascle, C. Puidgefàbregas, H.P. Luterbacher and M. Fernàndez (Editors), Cenozoic Foreland Basins of Western Europe. Geological Society, London, pp. 279-298.

Burtner, L.R., Nigrini, A. and Donelik, R.A., 1994. Thermochronology of Lower cretaceous source rocks in the Idaho-Wyoming thrust belt. AAPG Bulletin, 78: 1613-1636.

Buxtorf, A., 1907. Geologische Beschreibung des Weissenstein Tunnels und seiner Umgebung. Beiträge der Geologischen Karte der Schweiz(21).

Calabrò, R.A., Corrado, S., Di Bucci, D., Robustini, P. and Tornaghi, M., 2003. Thin-skinned vs. thick-skinned tectonics in the Matese Massif, Central Southern Appennines. Tectonophysics, 337(3-4): 269-297.

Campy, M., 1984. Signification dynamique et climatique des formations et terrasses fluviatiles dans un environnement de moyenne montagne. Bulletin de l'Association française pour l'Etude du Quaternaire, 1: 87-92.

Carlson, D.W., Donelick, R.A. and Ketcham, R.A., 1999. Variability of apatite fission-track annealing kinetics, I. Experimental results. American Mineralogist, 84: 1213-1223.

Cederbom, C.E., Sinclair, H.D., Schlunegger, F. and Rahn, M., 2004. Climate-induced rebound and exhumation of the European Alps. Geology, 32(8): 709-712, doi: 10.1130/G20491.1.

Chapple, W.M., 1978. Mechanics of thin-skinned fold-and-thrust belts. Geological Society of American Bulletin, 89: 1189-1198.

Chauve, P., Campy, M., Pernin, C. and Morre-Biot, N., 1983. Carte géolog. France (1/50000), feuille Pesmes, XXXII-23, BRGM.

Chauve, P., Enay, R., Fluck, P. and Sittler, C., 1980. L'Est de la France (Vosges, Fossé Rhénan, Bresse, Jura). Annales scientifiques de l'Université de Besançon, 4(1): 3-80.

Chauve, P., Kerrien, Y. and Pernin, C., 1979. Carte géolog. France (1/50000), feuille Dole XXXII-24, BRGM.

Choulet, F., Faure, M., Fabbri O., 2007. The Autun Shear zone: age, kinematics, significance and regional correlations. In: "Mechanism of Variscan Orogeny : A modern view on orogenic research", Proceedings Special Meeting of the French and Czech Geological Societies, Géologie de la France, 2, p. 82.

Conroux, Y., Fabbri, O., Lebourg, T., Bichet, V. and Petit, C., 2004. Geological and geophysical investigations along a late Variscan fault exposed near the 23/02/2004 Besancon earthquake epicentral area. Abstract Volume, RST-GV Strasbourg.

Contini, D. et al., 1973. Carte géolog. France (1/50000), feuille Montebeliard, XXXV-22, BRGM.

Contini, D. and Theobald, N., 1974. Relations entre le Fossé rhenan et le Fossé de la Saône. Tectonique des régions sous vosgiennes et prejurrassiennes. In: J.H. Illies and K. Fuchs (Editors), Approaches to Taphrogenesis. Sc. Report., Stuttgart, pp. 310-321.

Coromina, G. and Fabbri, O., 2004. Late Palaeozoic NE-SW ductile-brittle extension in the La Serre horst, eastern France. Comptes Rendus Geosciences, 336(1): 75-84.

Corrigan, J.D., 1993. Apatite fission-track analysis of Oligocene strata in South Texas, USA; testing annealing models. Chemical Geology, 104: 227-249.

Costa, E. and Vendeville, B.C., 2002. Experimental insights on the geometry and kinematics of fold-and-thrust belts above weak, viscious evaporitic décollement. Journal of Structural Geology, 24: 1729-1739.

Coulon, M. and Frizon De Lamotte, D., 1988. Les extensions céneozoiques dans l'Est du bassin de Paris. C. R. Acad. Sc. Paris, 307: 1111-1119.

Coward, 1983. Thrust tectonics, thin skinned or thick skinned, and the continuation of thrusts to deep in the crust. Journal of Structural Geology, 5(2): 113-123.

Davis, D., Suppe, J. and Dahlen, F.A., 1983. Mechanics of fold-and-thrust-belts and accretionary wedges. Journal of Structural Geology, 88: 1153-1172.

Debrand-Passard, S. and Courbouleix, S. (Editors), 1984. Synthèse Géologique du Sud-Est de la France, volume 2: Atlas comprenant 64 planches en couleurs. Mémoire du Bureau de recherches géologiques et minières, 126. BRGM, 614 pp.

DeCelles, P.G. and Mitra, G., 1995. History of the Sevier orogenic wedge in terms of critical taper models, northeast Utah and southwest Wyoming. Geological Society of America Bulletin, 107(4): 454-462.

Deichmann, N., Ballarin Dolfin, D. and Kastrup, U., 2000. Seismizität der Nord- und Zentralschweiz. NAGRA Technischer Bericht, 00-05. NAGRA, Wettingen, 94 pp.

Dèzes, P., Schmid, S.M. and Ziegler, P.A., 2004. Evolution of the European Cenozoic Rift System: interaction of the Alpine and Pyrenean orogens with their foreland lithosphere. Tectonophysics, 389(1-2): 1-33.

Diebold, P. and Naef, H., 1990. Der Nordschweizer Permokarbontrog. Nagra informiert, 2: 29-36.

Diebold, P. and Noack, T., 1997. Late Palaeozoic troughs and Tertiary Structures in the eastern Folded Jura. In: O.A. Pfiffner, P. Lehner, P. Heitzmann, S. Mueller and A. Steck (Editors), Deep structure of the Swiss Alps. Results of NRP 20. Birkhäuser, pp. 59-63.

Dorel, J. et al., 1983. Focal mechanism in metropolitan France and the lesser Antilles. Annales Geophysicae, 1(4-5): 299-306.

Dreyfuss, M. and Glangeaud, L., 1950. La valée de Doubs et l'évolution morphotectonique de la région bisontine. Annales scientifiques de l'Université de Besançon, 5: 2.

Dreyfuss, M. and Kuntz, G., 1969. Carte géolog. France (1/50000), feuille Besancon, XXXII-23, BRGM.

Dreyfuss, M. and Kuntz, G., 1970. Carte géolog. France (1/50000), feuille Gy, XXXIII-22, BRGM.

Dreyfuss, M. and Théobald, N., 1972. Carte géolog. France (1/50000), feuille Baume-les-Dames, XXXIV-22, BRGM.

Dumitru, T.A., 1995. A new computer automated microscope stage system for fission track analysis. Nuclear Tracks Radiation Measurements, 21: 575-580.

Echtler, H. and Malavielle, J., 1990. Extensional basement uplift and Stephano-Permian collapse basin in a late Variscian metamorphic core complex (Montagne Noire, Southern Massif Central). Tectonophysics, 177: 125-138.

Echtler, H.P. and Chauvet, A., 1991-1992. Carboniferous convergence and subsequent crustal extension in the southern Schwarzwald (SW Germany). Geodinamica Acta, 5(1): 37-49.

Eisbacher, G., Lüschen, E. and Wickert, F., 1989. Crustal scale thrusting and extension in the Hercynian Schwarzwald and Vosges, Central Europe. Tectonics, 8(1): 1-21.

Elmohandes, S.-E., 1981. The Central European Graben System: Rifting imitated by Clay Modelling. Tectonophysics, 73: 69-78.

Fejfar, O., Heinrich, W.-D. and Lindsay, E.H., 1998. Updating the Neogene rodent biochronology in Europe. Mededelingen Nederlands Instituut voor Toegepaste Geowetenschappen, TNO 60: 533-554.

Ford, M., Le Carlier de Veslud, C. and Bourgeois, O., 2007. Kinematic and geometric analysis of fault related folds in a rift setting: The Dannemarie basin, Upper Rhine Graben, France. Journal of Structural Geology, 29: 1811-1830.

Fügenschuh, B. and Schmid, S.M., 2003. Late stages of deformation and exhumation of an orogen constrained by fission-track data: A case study in the Western Alps. Geol. Soc. Am. Bull., 115: 1425-1440.

Galbraith, R.F. and Laslett, G.M., 1993. Statistical models for mixed fission-track ages. Nuclear Tracks and Radiation Measurements, 21: 459-470.

Gallagher, K., 1995. Evolving temperature histories from apatite fission-track data. Earth and Planetary Sciences Letters, 136: 421-435.

Giamboni, M., Ustaszewski, K., Schmid, S.M., Schumacher, M.E. and Wetzel, A., 2004a. Plio-Pleistocene Transpressional Reactivation of Paleozoic and Paleogene Structures in the Rhine-Bresse transform

Zone (northern Switzerland and eastern France). International Journal of Earth Sciences, 93(2): 207–223, DOI: 10.1007/s00531-003-0375-2.

Giamboni, M., Wetzel, A., Niviere, B. and Schumacher, M., 2004b. Plio-Pleistocene folding in the southern Rhinegraben recorded by the evolution of the drainage network (Sundgau area: northwestern Switzerland and France). Eclogae Geol Helv, 97: 17-31.

Glangeaud, L., 1949. Les caractères structuraux du Jura. Bull. Soc. Geol France, 19: 669-688.

Gleadow, A.J.W., Duddy, I.R., Green, P.F. and Hegarty, K.A., 1986. Fission track length in the apatite annealing zone and interpretation of mixed ages. Earth and planetary Science Letters, 78: 245-254.

Goguel, J. and Dreyfuss, M., 1965. Carte géolog. France (1/50000), feuille Vercel, XXXIV-23, BRGM.

Green, P.F., 1981. A new look at statistics in fission track dating. Nuclear Tracks and Radiation Measurements, 5: 77-86.

Green, P.F. and Duddy, I.R., 1989. Some comments on paleotemperature estimation from apatite fission track analysis. Journal of Petroleum Geology, 12: 111-114.

Green, P.F., Duddy, I.R., Gleadow, A.J.W. and Tingate, P.R., 1985. Fission-track annealing in apatite: track length measurements and the form of the Arrhenius plot. Nuclear Tracks and Radiation Measurements, 10: 323-328.

Green, P.F., Duddy, I.R., Gleadow, A.J.W., Tingate, P.R. and Laslett, G.M., 1986. Thermal annealing of fission tracks in apatite, 1. A qualitative description. Chemical Geology, 59: 237-253.

Guellec, S., Mugnier, J.L., Tardy, M. and Roure, F., 1990. Neogene evolution of the western Alpine foreland in the light of ECORS data and balanced cross-sections. In: F. Roure, P. Heitzmann and R. Polino (Editors), Deep Structure of the Alps. Vol. spec. Soc. Geol. It. Mémoire de la Société géologique de la Suisse, Zürich, pp. 165-184.

Hagedorn, E.M., 2004. Sedimentpetrographie und Lithofazies der jungtertiären und quartären Sedimente im Oberrheingebiet. unpublished PhD-Thesis Thesis, University of Cologne, 310 pp.

Hagedorn, E.M. and Boenigk, W., 2008. The Pliocene and Quaternary sedimentary and fluvial history in the Upper Rhine Graben based on heavy mineral analyses. Netherlands Journal of Geosciences, 87(1): 21-31.

Hindle, D. and Burkhard, M., 1999. Strain, displacement and rotation associated with the formation of curvature in fold belts; the example of the Jura arc. Journal of Structural Geology, 21: 1089-1101.

Hinsken, S., Ustaszewski, K. and Wetzel, A., 2007. Graben width controlling syn-rift sedimentation: the Palaeogene southern Upper Rhine Graben as an example. International Journal of Earth Sciences, 96(6): 979-1002.

Homberg, C., Bergerat, F., Philippe, Y., Lacombe, O. and Angelier, J., 2002. Structural inheritance and cenozoic stress fields in the Jura fold-and-thrust belt (France). Tectonophysics, 357: 137– 158.

Homberg, C., Hu, J., Angelier, J., Bergerat, F. and Lacombe, O., 1997. Characterization of stress perturbations near major fault zones: insights from 2-D distinct-element numerical modelling and field studies (Jura mountains). Journal of Structural Geology, 19(5): 703-718.

Homberg, C., Lacombe, O., Angelier, J. and Bergerat, F., 1999. New constraints for indentation mechanisms in arcuate belts from the Jura Mountains, France. Geology, 27(9): 827-830.

Hurford, A.J. and Green, P.F., 1983. The zeta age calibration of fission-track dating. Chemical Geology, 41: 285-317.

Illies, J.H., 1972. The Rhinegraben rift system - plate tectonics and transform faulting. Geophysical Surv., 1: 27-60.

Illies, J.H. and Greiner, G., 1978. Rhine Graben and Alpine System. Geological Society of America Bulletin, 89: 770-782.

Jowett, E.C., 1991. Post-collisional formation of the Alpine foreland rifts. Annales Geological Society of Poland, 61: 37-59.

Kälin, D., 1997. Litho- und Biostratigraphie der mittel- bis obermiozänen Bois de Raube-Formation (Nordwestschweiz). Eclogae Geologicae Helvetiae, 90(1): 97-114.

Kastrup, U. et al., 2004. Stress field variations in the Swiss Alps and the northern Alpine foreland derived from inversion of fault plane solutions. J. Geophys. Res., 109(B01402): doi:10.1029/2003JB002550.

Koons, P.O., Zeitler, P.K., Chamberlain, C.P., Craw, D. and Melzer, A.S., 2002. Mechanical links between river erosion and metamorphism in Nanga Parbat, Pakistan, Himalaya. American Journal of Science, 302: 749-773.

Kuhlemann, J., Frisch, W., Szekely, B., Dunkl, I. and Kazmer, M., 2002. Post-collisional sediment budget history of the Alps: Tectonic versus climatic control. International Journal of Earth Sciences, 91: 818-837.

Kulig, G., 2005. Erstellung einer Auswertesoftware zur Altersbestimmung mittels Lumineszenzverfahren unter spezieller Berücksichtigung des Einflusses radioaktiver Ungleichgewichte in der 238U-Zerfallsreihe. Bsc. Thesis, University of Freiberg.

Lacombe, O., Angelier, J., Laurent, P., Bergerat, F. and Tourneret, C., 1990. Joint analyses of calcite twins and fault slips as a key for deciphering polphase tectonics: Burgundy as a case study. Tectonophysics, 182: 279-300.

Lacombe, O., Angelier, J., Byrne, D. and Dupin, J., 1993. Eocene-Oligocene tectonics and kinematics of the Rhine-Saone continental transform zone (Eastern France). Tectonics, 12(4): 874-888.

Lacombe, O. and Mouthereau, F., 1999. Qu'est-ce que le front des orogènes? L´exemple de l´orogène pyrénéen. C.R. Acad. Sci. Paris, Science de la terre et des planètes, 329: 889-896.

Lacombe, O. and Mouthereau, F., 2002. Basement-involved shortening and deep detachment tectonics in forelands of orogens: Insights from recent collision belts (Taiwan, Western Alps, Pyrenees). Tectonics, 21(4).

Lacombe, O., Mouthereau, F., Angelier, J., Chu, H.-T. and Lee, J.-C., 2003. Frontal curvature and oblique ramp development at an oblique ramp development at an obliquely collided irregular margin: Geometry and kinematics of the NW Taiwan fold-thrust belt. Tectonics 22 TC2003, doi:10.1029/2002TC001436.

Lacombe, O., Mouthereau, F., Kargar, S. and Meyer, B., 2006. Late Cenozoic and modern stress fields in the western Fars (Iran): implications for the tectonic and kinematic evolution of Central Zagros. Tectonics, 25: TC1003, doi:10.1029/2005TC001831.

Lacombe, O. and Obert, D., 2000. Héritage structural et déformation de couverture: plissement et fracturation tertiares dans l'Ouest du Bassin de Paris. C. R. Acad. Sc. Paris, 330, II: 793-798.

Lancelot, J., Briqueu, L., Respaut, J.P. and Clauer, N., 1995. Géochimie isotopique des systèmes U-Pb/Pb-Pb et évolution polyphasée des gîtes d'uranium du Lodévois et du sud du Massif central. Chron. Rech. Min., 521: 3-18.

Larroque, J. and Laurent, P., 1988. Evolution of the stress field pattern in the south of the Rhine Graben from the Eocene to the present. Tectonophysics, 148: 41-58.

Laubscher, H., 1961. Die Fernschubhypothese der Jurafaltung. Eclogae Geologicae Helvetiae, 54(1): 222-282.

Laubscher, H., 1970. Grundsätzliches zur Tektonik des Rheingrabens. In: J.H. Illies and S. Mueller (Editors), Graben Problems. Proceedings of an International Rift Symposium held in Karlsruhe 1968, International Upper Mantle Project. E. Schweitzerbart'sche, Stuttgart, pp. 79-86.

Laubscher, H., 1972. Some overall aspects of Jura dynamics. American Journal of Science, 272: 293-304.

Laubscher, H., 1978. Foreland folding. Tectonophysics, 47: 325-337.

Laubscher, H., 1983. Überschiebungen im Jura. Jber. u. Mitt. oberrh. geol. Ver., 65: 181-189.

Laubscher, H., 1986. The eastern Jura: Relations between thin-skinned and basement tectonics, local and regional. Geologische Rundschau, 75(3): 535-553.

Laubscher, H., 1987. Die tektonische Entwicklung der Nordschweiz. Eclogae Geologicae Helvetiae, 80: 287-303.

Laubscher, H., 1992. Jura kinematics and the Molasse Basin. Eclogae Geologicae Helvetiae, 85(3): 653-675.

Letouzey, J., 1986. Cenozoic paleo-stress pattern in the Alpine Foreland and structural interpretation in a platform basin. Tectonophysics, 132: 215-231.

Liniger, H., 1966. Das Plio-Altpleistozäne Flussnetz der Nordschweiz. Regio Basil., 7: 158-177.

Liniger, H., 1967. Pliozän und Tektonik des Jura Gebirges. Eclogae Geol Helv, 60(2): 407-490.

Liniger, H. and Hofmann, P., 1965. Das Alter der Sundgauschotter westlich von Basel. Eclogae Geol Helv, 58(1): 215-230.

Locke, M.H. and Barker, R.D., 1995. Least-Squares deconvolution of apparant resistivity pseudosections. Geophysics, 60(6): 1682-1690.

Lopes Cardozo, G.G.O. and Granet, M., 2003. New insight in the tectonics of the southern Rhine Graben-Jura region using local earthquake seismology. Tectonics, 22(6): 1078, doi:10.1029/ 2002TC001442.

Macquar, J.-C., 1984. Minéralisation triasiques en Pb, Zn, Ba (Cu, Fe) du Bassin subalpin: typologie, chronologie, contrôles et modèles. In: S. Debrand-Passard, S. Courbouleix and L. M.J. (Editors), Synthèse géologique du Sud-Est de la France- stratigraphie et paléogéographie, Mém. Bur. Rech. Géol. Min 125, 112-118.

Marrett, R. and Allmendinger, R.W., 1990. Kinematic analysis of fault-slip data. Journal of Structural Geology, 12(8): 973-986.

Marrett, R. and Peacock, D.C.P., 1999. Strain and stress. Journal of Structural Geology, 21: 1057-1063.

Martin, J. and Mercier, E., 1996. Héritage distensif et structuration chevauchante dans une chaîne de couverture : apport de l`équilibrage par modélisation géométrique dans le Jura nord-occidental. Bull. Soc. Géol. France, 167(1): 101-110.

Matte, P., 1986. Tectonics and plate tectonics model for the Variscian belt of Europe. Tectonophysics, 126(2-4): 329-374.

Mayer-Rosa, D. and Cadiot, B., 1979. Review of the 1356 Basel earthquake: basic data. Tectonophysics, 53: 325-333.

McCann, T. et al., 2006. Post-Variscan (end Carboniferous-Early Permian) basin evolution in Western and Central Europe. In: D.G. Gee and R.A. Stephenson (Editors), European Lithosphere Dynamics, Geological Society of London Memoirs, 32, pp. 355-388, London.

Mercier, J.L. and Jeser, N., 2004. The glacial history of the Vosges Mountains. In: J. Ehlers and P.L. Gibbard (Editors), Quaternary glaciations - extent and chronology. Part 1: Europe. Elsevier, pp. 113-118.

Merle, O. and Michon, L., 2001. The formation of the West European rift: A new model as exemplified by the Massif Central area. Bull. Soc. Geol France, 172(2): 213-221.

Merrits, D.J., Vincent, K.R. and Wohl, E.E., 1994. Long river profiles, tectonism and eustasy: a guide to interpreting fluvial terraces. Journal of Geophysical Research, 99 (B7): 14301-14050.

Meschede, M. and Decker, K., 1993. Störungsflächenanalyse entlang des Nordrandes der Ostalpen - ein methodischer Vergleich. Z. dt. Geol. Ges., 144: 419-433.

Meyer, B., Lacassin, R., Brulhet, J. and Mouroux, B., 1994. The Basel 1356 earthquake: which fault produced it? Terra Nova, 6: 54-63.

Michon, L. and Merle, O., 2001. The evolution of the Massif Central Rift: spatio-temporal distribution of the vulcanism. Bull. Soc. Geol France, 172(2): 69-80.

Michon, L. and Merle, O., 2005. Discussion on "Evolution of the European Cenozoic Rift System: interaction of the Alpine and Pyrenean orogens with their foreland lithosphere by P. Dèzes, S.M. Schmid and P.A. Ziegler, Tectonophysics 389 (2004) 1-33. Tectonophysics, 401: 251-256.

Michon, L. and Sokoutis, D., 2005. Interaction between structural inheritance and extension direction during graben formation: An experimental approach. Tectonophysics, 409: 125-146.

Molinaro, M., Leturmy, J.-C., Guezou, D., Frizon De Lamotte, D. and Eshraghi, S.A., 2005. The structure and kinematics of the southeastern Zagros fold-thrust belt Iran: From thin-skinned to thick-skinned tectonics. Tectonics, 24: TC3007, doi:10.1029/2004TC001633.

Montgomery, D.R. and Stolar, D.B., 2006. Reconsidering Himalayan river anticlines. Geomorphology, 82: 4-15.

Morre, N. and Thiebaut, J., 1961. Etude petrographique des roches cristallines decouvertes par sondage profonds entre Vosges et Morvan. Extrait des Annales scientifiques de l'Univeristé de Besançon, 14: 73-83.

Morre-Biot, N. and Storet, J., 1967. Sur l'âge absolu du granite de la Serre (Jura). C. R. Acad. Sc. Paris, 265(Ser.D.): 1869-1870.

Mosar, J., 1999. Present-day and future tectonic underplating in the western Swiss Alps: reconciliation of basement/wrench-faulting and décollement folding of the Jura and Molasse basin in the Alpine foreland. Earth and Planetary Science Letters, 173: 143-155.

Mouthereau, F. et al., 2007. Tertiary sequence of deformation in a thin-skinned / thick-skinned collision belt: The Zagros Folded Belt (Fars, Iran). Tectonics, 26 TC5006, doi:10.1029/2004TC001633.

Müller, W.H., Naef, H. and Graf, H.R. (Editors), 2002. Geologische Entwicklung der Nordschweiz, Neotektonik und Langzeitszenarien, Zürcher Weinland. NAGRA Technischer Bericht, 99-08. NAGRA, Wettingen, 226 pp.

Neugebauer, H.J., 1978. Crustal doming and mechanism of rifting: Part 1, Rift formation. Tectonophysics, 45: 159-186.

Nicloas, M., Santoire, M. and Delpech, P.Y., 1990. Intraplate seismicity: new seimotectonic data in Western Europe. Tectonophysics, 179(1/2): 27-54.

Nivière, B. and Marquis, G., 2000. Evolution of terrace risers along the Upper Rhine Graben inferred from morphologic dating methods: evidence of climatic and tectonic forcing. Geophysical Journal International, 141(3): 577-594.

Nivière, B. and Winter, T., 2000. Pleistocene northwards fold propagation of the Jura within the southern Upper Rhine Graben: seismotectonic implications. Global and Planetary Change, 27: 263–288.

Oberlander, T.M., 1985. Origin of drainage transverse to structures in orogens. In: M. Morisawa and J.T. Hack (Editors), Tectonic Geomorphology. Allen and Unwin, Boston, pp. 155-182.

Pavoni, N., 1961. Faltung durch Horizontalverschiebung. Eclogae Geologicae Helvetiae, 54(2): 515-534.

Pavoni, N., 1987. Zur Seismotektonik der Nordschweiz. Eclogae Geol Helv, 80(2): 461-472.

Peters, G. and van Balen, R.T., 2007. Tectonic geomorphology of the noertern Upper Rhine Graben, Germany. Global and Planetary Change, 58: 310-334.

Petit, C., Campy, M., Chaline, J. and Bonvalot, J., 1996. Major palaeohydrographic changes in Alpine foreland during the Pliocene-Pleistocene. Boreas, 25: 131-143.

Petit, J.P., 1987. Criteria for the sense of movement on fault surfaces in brittle rocks. Journal of Structural Geology, 9(5-6): 597-608.

Pfiffner, O.A., 2006. Thick-skinned and thin-skinned styles of continental contraction. In: S. Mazzoli and R.W.H. Butler (Editors), Styles of Continental Contraction: Geological Society of America Special Papers, pp. 153-177.

Pfiffner, O.A. and Burkhard, M., 1987. Determination of paleo-stress axes orientations from fault, twin and earthquake data. Annales Tectonicae, 1(1): 48-57.

Pfiffner, O.A., Erard, P. and Stäuble, M., 1997. Two cross sections through the Swiss Molasse Basin (lines E4-E6, W1, W7-W10). In: O.A. Pfiffner, P. Lehner, P. Heitzmann, S. Mueller and A. Steck (Editors), Deep structure of the Swiss Alps. Results of NRP 20. Birkhäuser, pp. 64-72.

Philippe, Y., Colletta, B., Deville, E. and Mascle, A., 1996. The Jura fold-and-thrust belt: a kinematic model based on map-balancing. In: P. Ziegler and F. Horvath (Editors), Peri-Tethys Memoir 2: Structure and prospects of Alpine Basins and Forelands. Mem. Mus. natn. Hist. nat., Paris, pp. 235-261.

Pinter, N. and Brandon, M.T., 1997. How erosion builds mountains. Scientific Am., 276(4): 74-79.

Plenefisch, T. and Bonjer, K., 1997. The stress field in the Rhine Graben area inferred from earthquake focal mechanisms and estimation of frictional parameters. Tectonophysics, 275: 71-97.

Pollard, D.D., Saltzer, S.D. and Rubin, A.M., 1993. Stress inversion methods : are they based on faulty assumption? Journal of Structural Geology, 15(8): 1045-1054.

Preusser, F., 2004. Towards a chronology of the Late Pleistocene in the northern Alpine foreland. Boreas, 33: 195-210.

Rat, P., 1976. Structures et phases de structuration dans les plateaux bourguignons et le Nord Ouest du fossé bressan (France). Geologische Rundschau, 65: 101-126.

Reinecker, J., Heidbach, O., Tingay, M., Sperner, B. and Mueller, B., 2005. The 2005 release of the World Stress Map (available online at www.world-stress-map.org).

Reiter, F. and Acs, P., 1996-2000. TectonicsFP, Innsbruck, pp. Computer Software for Structural Geology, version 2.0 PR. http://www.tectonicsfp.com/.

RéNaSS, R.N.d.S.S., 2007. Réseau National de Surveillance Sismique, http://renass.u-strasbg.fr/. In: E.e.O.d.S.d.l.T.d. Strasbourg (Editor).

Rey, P., Burg, J.-P. and Caron, J.-M., 1991-1992. Middle and Late Carboniferous extension in the Variscian Belt: structural and petrological evidences from the Vosges massif (Eastern France). Geodinamica Acta, 5(1-2): 17-36.

Rocher, M., Chevalier, F., Petit, C. and Guiraud, M., 2003. Tectonics of the Northern Bresse region (France) during the Alpine cycle. Geodinamica Acta, 16(2-6): 131-147.

Rocher, M., Cushing, M., Lemeille, F., Lozac'h, Y. and Angelier, J., 2004. Intraplate paleostresses reconstructed with calcite twining and faulting: improved method and application to the eastern Paris Basin (Lorrainne, France). Tectonophysics, 387: 1-21.

Rotstein, Y. and Schaming, M., 2004. Seismic Reflection evidence for thick-skinned tectonics in the northern Jura. Terra Nova, 16: 250-256.

Rotstein, Y., Schaming, M. and Rousse, S., 2005. Structure and Tertiary Tectonic history of the Mulhouse High, Upper Rhine Graben: Block faulting modified by changes in the Alpine stress regime. Tectonics, 24, TC1012 doi:10.1029/2004TC001654.

Ruhland, M., 1959. Une dislocation majeure du socle Vosgien dans la haute Vallée de l' Ognon. Bull. Serv. Carte Géol. Als. Lorr., 12: 61-64.

Schaltegger, U., Schneider, J.L., Maurin, J.C. and Corfu, F., 1996. Precise U-Pb chronometry of 345-340 Ma old magmatism related to syn-convergence extension in the southern Vosges (Central Variscian Belt). Earth and Planetary Science Letters, 144: 403-419.

Schmid, S.M., Pfiffner, O.A., Froitzheim, N., Schönborn, G. and Kissling, E., 1996. Geophysical-geological transect and tectonic evolution of the Swiss-Italian Alps. Tectonics, 15: 1036-1064.

Schumacher, M.E., 2002. Upper Rhine Graben: Role of preexisting structures during rift evolution. Tectonics, 21(1): 6-1-6-17.

Sengör, A.M.C., 1976. Collision of irregular continental margins: implications for foreland deformation of Alpine-type orogens. Geology, 4: 779-782.

Seward, D., 1989. Cenozoic basin histories determined by fission track dating of basement granites, South Island, New Zealand. Chemical Geology, 79: 31-48.

Simpson, G., 2004. Role of river incison in enhancing deformation. Geology, 32(4): 341-344.

Simpson, G. and Schlunegger, F., 2003. Topographic evolution and morphology of surfaces evolving in response to coupled fluvial and hillslope sediment transport. Journal of Geophysical Research, 108(ETG7-1-7-16).

Sindowski, K.H., 1949. Results and problems of heavy mineral analysis in Germany; a review of sedimentary-petrological papers, 1936-148. J. sedim. Petrol., 19: 3-25.

Sissingh, W., 1998. Comparative Tertiary stratigraphy of the Rhine Graben, Bresse Graben and Molasse Basin: correlation of Alpine foreland events. Tectonophysics, 300: 249-284.

Sissingh, W., 2001. Tectonostratigraphy of the West Alpine Foreland: correlation of Tertiary sedimentary sequences, changes in eustatic sea-level and stress regimes. Tectonophysics, 333: 361-400.

Smit, J.H.W., Brun, J.P. and Sokoutis, D., 2002. Deformation of brittle-ductile thrust wedges in experiments and nature. Journal of Geophysical Research, 108, NO. B10, 2480, doi:10.1029/2002JB002190.

Sommaruga, A., 1997. Geology of the Central Jura and the Molasse Basin: New insights into an evaporite-based foreland fold and thrust belt, Schweizerische Akademie der Naturwissenschaften, Neuchatel, 176 pp.

Sommaruga, A. and Burkhard, M., 1997. Jura Mountains. In: O.A. Pfiffner, P. Lehner, P. Heitzmann, S. Mueller and A. Steck (Editors), Deep structure of the Swiss Alps. Results of NRP 20. Birkhäuser, pp. 45-53.

Spang, J., 1972. Numerical Method for Dynamic Analysis of Calcite Twin Lamellae. Geological Society of America Bulletin, 83(2): 467-472.

Sperner, B., Ratschbacher, L. and Ott, R., 1993. Fault-Striae Analysis: a Turbo Pascal Program Package for Graphical Representation and Reduced Stress Tensor Calculation. Computers & Geosciences, 19(9): 1361-1388.

Steininger, F.F. et al., 1996. Circum-Mediterranean Neogene (Miocene and Pliocene) marine-continental chronologic correlations of European Mammal Units. In: R.L. Bernor, V. Fahlbusch and H.-W. Mittmann (Editors), The Evolution of Western Eurasian Neogene Mammal Faunas. Columbia University Press, New York, pp. 7-46.

Suppe, J., 1983. Geometry and kinematics of fault-bend folding. American Journal of Science, 283: 684-721.

Surma, F. et al., 2003. Microstructures d'un gres affecte par une faille normale; anisotropie de connectivite et de permeabilite. Bull. Soc. Geol France, 174(3): 295-303.

Swiss Seismological Service, E.T.H.Z., 2007. Regional Moment Tensor catalogue, http://www.seismo.ethz.ch/mt/.

Tagami, T. and Dumitru, T.A., 1996. Provenance and history of the Franciscan accretionary complex: Constraints from zircon fission track thermochronology. J. Geophys. Res., 101: 8345-8255.

Tagami, T., Galbraith, R.F., Yamada, R. and Laslett, G.M. (Editors), 1998. Revised annealing kinetics of fission tracks in zircon and geological implications. Advances in Fission-Track Geochronology. Solid Earth Sci. Libr. Kluwer Acad., Norwell, Mass., 10, 99-112 pp.

Tesauro, M., Hollenstein, C., Egli, R., Geiger, A. and Kahle, H.-G., 2005. Continuous GPS and broad-scale deformation across the Rhine Graben and the Alps. International Journal of Earth Sciences, 94: 525-537.

Théobald, N., Schweitzer, M. and Hudeley, H., 1976. Carte Géologique de la France à 1/50 000 Mulhouse, feuille XXXVII-XXXVIII-20. Ministère de l'industrie et de la recherche, Service Géologique National, Orléans.

Theobald, N., Vogt, H. and Wittmann, O., 1977. Néotectonique de la partie méridionale du bloc rhénan. Bull. B.R.G.M., 2(4): 121-140.

Thiebaut, J., Theobald, N. and Hudeley, H., 1974. Carte géolog. France (1/50000), feuille Giromagny, XXXV-22, BRGM.

Timar-Geng, Z., Fügenschuh, B., Schaltegger, U., and Wetzel, A., 2004. The impact of the Jurassic hydrothermal activity on zircon fission track data from the southern Upper Rhine Graben area. Schweizerische Mineralogische und Petrographische Mitteilungen, 84: 257-269.

Timar-Geng, Z., Fügenschuh, B., Wetzel, A., Dresmann, H. 2006. Low-temperature thermochronology of the flanks of the southern Upper Rhine Graben. Int J Earth Sci 95: 685-702.

Tozer, R.S.J., Butler, R.W.H. and Corrado, S., 2001. Comparing thin- and thick-skinned thrust tectonic models of the Central Apennines, Italy. In: B. Bertotti, K. Schulmann and S.A.P.L. Cloetingh (Editors), Continental collision and the tectono-sedimentary evolution of forelands. European Geoscience Union Stephan Mueller Special Publication Series, 1, 181-194.

Twidal, C.R., 2004. River patterns and their meaning. Earth Science Reviews, 67/3-4: 159-219.

Twiss, R., J. and Unruh, J., R., 1998. Analysis of fault slip inversions: Do they constrain stress or strain rate? Journal of Geophysical Research, 103: NO. B6, 12205-12222.

Ustaszewski, K. and Schmid, S.M., 2006. Control of preexisting faults on geometry and kinematics in the northernmost part of the Jura fold-and-thrust belt. Tectonics, 25.

Ustaszewski, K. and Schmid, S.M., 2007. Latest Pliocene to recent thick-skinned tectonics at the Upper Rhine Graben - Jura Mountains junction. Swiss Journal of Geosciences, 100(2): 293-312.

Ustaszewski, K., Schumacher, M.E. and Schmid, S.M., 2005a. Simultaneous normal faulting and extensional flexuring during rifting - an example from the southernmost Upper Rhine Graben. International Journal of Earth Sciences, 94(4).

Ustaszewski, K., Schumacher, M.E., Schmid, S.M. and Nieuwland, D., 2005b. Fault reactivation in brittle-viscous wrench systems - dynamically scaled analogue models and application to the Rhine-Bresse Transfer Zone. Quaternary Science Reviews, 24(3-4): 363-380, doi:10.1016/j.quascirev.2004.03.015.

Wallace, R.E., 1951. Geometry of shearing stress and relation to faulting. J. Geol., 59: 118-130.

Wetzel, A., Allenbach, R. and Allia, V., 2003. Reactivated basment structures affecting the sedimentary facies in a tectonicallally "quiescent" epicontinental Basin: an example from NW Switzerland. Sedimentary Geology, 157: 153-172.

Whipple, K.X., Hancock, G.S. and Anderson, R.S., 2000. River incision into bedrock: Mechanic and relative efficacy of plucking, abrasion and cavitation. Geological Society of America Bulletin, 112: 490-503.

Wintle, A.G. and Murray, A.S., 2006. A review of quartz optically stimulated luminescence characteristics and their relevance in single aliquot regeneration dating protocols. Radiation Measurements, 41: 369-391.

Yamada, R., Tagami, T., Nishimura, S. and Ito, H., 1995. Annealing kinetics of fission tracks in zircon: an experimental study. Chemical Geology, 122: 249-248.

Zeilinger, G., Schlunegger, F. and Simpson, G., 2005. The Oxaya anticline (northern Chile): a buckle enhanced by river incision? Terra Nova, 17: 368-375.

Ziegler, P., 1986. Geodynamic model for the Paleozoic crustal consolidation of Western and Central Europe. Tectonophysics, 126(2-4): 303-328.

Ziegler, P. and Dèzes, P., 2007. Cenozoic uplift of Variscian Massifs in the foreland of the Alpine foreland: Timing and controlling mechanisms. Global and Planetary Change, 58: 237-269.

Ziegler, P.A., 1990. Geological Atlas of Western and Central Europe. Shell Internationale Petroleum Maatschappij B.V., Den Haag, 1-238 pp.

Ziegler, P.A., 1992. European Cenozoic rift system. Tectonophysics, 208: 91-111.

Ziegler, P.A., Bertotti, G. and Cloetingh, S.A.P.L., 2002. Dynamic processes controlling foreland development - roke of mechanical (de)coupling of orogenic wedges and forelands. In: B. Bertotti, K. Schulmann and S.A.P.L. Cloetingh (Editors), Continental collision and the tectono-sedimentary evolution of forelands. EUG Stephan Mueller Publication Series, pp. 17-56.

Ziegler, P.A. and Fraefel, M., 2008 submitted. Response of drainage systems to Neogene evolution of Jura fold-thrust belt and Upper Rhine Graben. Swiss Journal of Geosciences.

Ziegler, P.A., Schumacher, M.E., Dèzes, P., van Wees, J.-D. and Cloetingh, S., 2004. Post-Variscan evolution of the lithosphere in the Rhine Graben area: constraints from subsidence modelling. In: M. Wilson (Editor), Permo-Carboniferous magmatism and rifting in Europe. Geological Society of London Special Publications. Geological Society, pp. 289-317.

Acknowledgements

The present thesis would not have been possible and much more difficult to finalize without the help, support and distraction by numerous people.

First of all I would like to thank my two main supervisors, Stefan Schmid and Olivier Fabbri. Stefan taught me a lot during intense scientific discussions, especially about the importance and the strength of precise argumentation and how to handle criticism. He always promoted me and my work and gave me the feeling that I do something important which, in turn, gave me a lot of self confidence. Olivier was not only an indispensable logistic local French support but also a partner in crime during some tough field days when things seemed absolutely "hopeless". I will always remember his modesty and the hospitality of his entire family, but especially the sharing of cigars and the French wine.

Peter Ziegler, in his function as EUCOR URGENT initiator was always a driving force behind this study. Constant interest in my research and stimulating discussion during his Wednesday visits to the institute were very motivating. His enthusiasm and passion are outstanding to me.

Frank Preusser introduced me to the red-light district of Bern and opened me the door to a non tectonic but yet very exiting branch of geologic research. Franks "drive" and vigor pushed me a lot, which is probably the reason for all the broken glass in the lab…

It was great to work with Alexandre Kounov, who was never tired of long lasting discussion and my even longer sentences. I very much enjoyed discussions on the meaning of fission track ages as well as those on the credibility of Peter Gabriel and the quality of Led Zeppelin's drummer.

During my research and the writing process I experienced essential cooperation and support by Vincent Bichet (Besançon), Eva-Maria Hagedorn (Leverkusen) and Fritz Schlunegger (Bern). Fruitful discussion in the field and the office with many colleagues but especially Michel Campy, Nico Deichmann, Ruth Drescher, Patrick Rolin, Michi Schnellmann, Kamil Ustaszewski, Tim Vietor, Andreas Wetzel and Erich Zechner were very helpful in shaping the ideas presented in the thesis. I'm very thankful for the generosity and efforts of Francois Deronzier (GAZ de France), Frederic Simien (BEPH), Jean Claude Ringenbach and Francois Roure (TOTAL) who enabled access to seismic reflection data. The "Freie Akademische Gesellschaft Basel" is very much thanked for providing me additional financial support.

I furthermore would like to thank of my colleagues as well as the entire staff of the Geological and Mineralogical Institute of Basel especially all past and present members of the EUCOR-URGENT team. Special thanks go out to my room mates Horst, Marielle, Pierre, Sebastian and Stephane for collegiality and tolerance towards my occasional manic manners, Senecio for lending me his almost indestructible car, Matthias for advice in heavy mineral separation and Quake4, and Heike and Corrine who taught me how to handle toxic liquors. Bruno and Francois from Franche Comté University are also very much thanked for helping with grave digging. In Bern, Sally and Damian

taught me the fine art of OSL sample preparation (and by that probably prevented more lab damage…) while Kamil and Micha provided me Austrian hospitality during overnight stays. All other unnamed colleagues and friends in Basel, Innsbruck and back home in Lienz are thanked for sharing, coffee, beer, “rock musik”, ropes, peaks, geological and not so geological excursions during the last years. I guess they prefer to stay anonymous….

Very, very special thanks go out to my “Highstreet” flat mates Jan, Tabea, Monique Andy, Simon, Sandy and Mirko who build (and maintained) a pleasant refuge from the “braincell” that saved me from the mouth of madness. I had and awesome and unforgettable time. Thank you.

Finally I would like to express my deep gratitude for the infinite support of my family and last but never least Lissi for her understanding, patience and love.

... and thanks for all the fish

CURRICULUM VITAE

Herfried Madritsch

PERSONAL DATA

DATE OF BIRTH 23rd January 1979
PLACE OF BIRTH Lienz
NATIONALITY Austria

EDUCATION

04 2005 - 06 2008 PhD-studies:
joint study (co-tutelle) between the the Universities of Basel (Switzerland) and Franche Comté (France)
- PhD-thesis title: "Structural evolution and neotectonics of the Rhine-Bresse Transfer Zone (Eastern France)"
- Supervision: Prof. Dr. Stefan Schmid and Prof. Dr. Olivier Fabbri
- Thesis defense: 27th June 2008 ("summa cum laude")

10 1998 - 06 / 2004 Diploma studies in Earth Sciences
University of Innsbruck (Austria)
- Master thesis title: "Geology and hydrogeology of deep seated gravitational slope deformations within the Innsbruck Quartzphyllite Complex and their significance for groundwater management. Watterntal, Tyrol" (in German)
- Supervision: Ao. Prof. Dr. Karl Krainer and Dr. Gerhard Poscher

1989-1997 High school (Bundesrealgymnasium) Lienz
- Emphasis: natural sciences

ADDITIONAL UNIVERSITY EDUCATION

02 / 2008 Seismic stratigraphy and facies analysis
(ETH Zürich / Universiy of Miami: Prof. Dr. G. Eberli)

03 / 2007 Structural modelling with GoCAD
(University of Vienna: Dr. U. Exner)

10 / 2005 Field course: Applied Geophysics
(ETH Zürich: Prof. Dr. H. Maurer et al.)

07 / 2003 Field course: brittle deformation
(University of Vienna: PD. Dr. K. Decker)

PROFESSIONAL EXPIERIENCE

04-2005 - 06 2008	teaching assistant Institute of Geology, University of Basel (Switzerland) field courses and lectures in structural geology and sedimentology
07 2004 -04 2005	research assistant (with Prof. Dr. Rainer Brandner) Geological Institute, University of Innsbruck (Austria) Project: Geological prospecting for the Brenner Base Tunnel
10 2002	working contract: geological mapping National Geological Survey of Austria
08- 09 2001	working contract: hydrogeology Austrian Research Centers, Seibersdorf, Vienna (Austria)

PRACTICAL TRAINING

08- 09 2003 & 06- 08 2002	practical work and master thesis ILF Consulting Engineers, Innsbruck, Austria
09 2002 & 07 2001	practical work Regional government of Tyrol, Division: geodesy and geology, Innsbruck (Austria)
2000/ 2001	laboratory assistant Mineralogical Institute, University of Innsbruck (Austria)

PUBLICATIONS IN JOURNALS WITH REVIEW PROCEDURE

Madritsch, H., Schmid, S.M. & Fabbri, O. (2008): Interactions between thin- and thick-skinned tectonics at the northwestern Jura front (eastern France), Tectonics in press.

Madritsch, H. & Millen B.M.J. (2007): Hydrogeological evidence for a continuous basal shear zone within a deep seated gravitational slope deformation (Eastern Alps, Tyrol, Austria). Landslides, 4/2, 149-162, Springer, Kyoto.

PUBLICATIONS IN JOURNALS AND PROCEEDINGS WITHOUT REVIEW PROCEDURE

Madritsch, H. (2005): Bericht 2004 über geologische Aufnahmen im Tarntal-Mesozoikum auf Blatt 149 Lanersbach. – Jb. d. Geol. B-A., 145, 3/4, 343-44. (in German).

Madritsch, H. & Riedl, F. (2005): Erhebung der Massenbewegungen Vorderes Wattental unter Berücksichtigung geotechnischer und hydrogeologischer Aspekte. Tagungsband Geoforum Umhausen (Tirol), Bd. 3/4.(in German).

Madritsch, H. & Riedl, F. (2004): Bericht 2003 über geologische Aufnahmen im Innsbrucker Quarzphyllit im Vorderen Wattental südlich von Wattens auf Blatt 149 Lanersbach. - Jb. d. Geol. B- A., 144, 3/4, 390-91. (in German)